A MASS BALANCE, BIOGEOCHEMICAL FRAMEWORK FOR ASSESSING FOREST BIOMASS HARVEST SUSTAINABILITY

by

Joshua Noseworthy

BScF., University of New Brunswick, 2009

A Thesis Submitted in Partial Fulfilment of
the Requirements for the Degree of

Masters of Science in Forestry

In the Faculty of Forestry and Environmental Management

Supervisors:	Paul Arp, PhD, FOREM, UNB
Examining Board:	Dr. Muhammad Afzal, PhD, FOREM Dr. Emmanuel Stefanakis, PhD, GGE

This thesis is accepted by the
Dean of Graduate Studies

THE UNIVERSITY OF NEW BRUNSWICK

August, 2011

© Joshua Noseworthy, 2011

ABSTRACT

A computational framework was developed to calculate and map long-term forest biomass harvest sustainability across Nova Scotia, Canada, based on forest mensurational, biochemical and mass-balance principles. Processes that would affect sustainability refer to primary nutrient supplies (N, Ca, Mg, and K via atmospheric deposition and soil weathering) and losses (forest harvesting, soil leaching). The effects of biomass harvesting were represented by way of four harvest scenarios: no harvesting, stem only, full-tree brown (no foliage) and full-tree green (with foliage), for each forest stand based on current tree compositions. All model calculations were done within a geospatial context using the current data layers for atmospheric deposition, climate, digital elevation, bedrock geology, forest inventory, and soil distribution, all consistent with recent updates for wetlands, flow channels, floodplains, and coastlines. The framework contains a dynamic link between the geospatial layers to a spreadsheet-based evaluator, to allow for realistic stand-by-stand sustainable harvest-scenario analyses and designs.

TABLE OF CONTENTS

Page

ABSTRACT ii

TABLE OF CONTENTS iii

LIST OF TABLES viii

LIST OF FIGURES xiii

ACKNOWLEDGMENTS xxiv

CHAPTER 1 1

General Introduction. Background and Objective 1

Subject Matter 3

Literature Cited 4

CHAPTER 2. Concepts and Applications 6

Sustainable Biomass Harvesting 6

Critical Loads 7

Primary Element Sources 10

Parent Material Weathering 10

Atmospheric Deposition 12

Primary Element Sinks 14

Base-cation Depletion 14

Biomass Harvesting 15

Literature Cited 17

CHAPTER 3. Forest Biomass Projections I: A comparison of Two Current Published Stem Biomass Equation Sets with a Newly Recommended Method of Obtaining Stem Biomass 24

Introduction 24

Methodology 25

Results and Discussion 26

Literature Cited....40

CHAPTER 4. Forest Biomass Projection II: Diameter-based Bark, Branch, Stem-wood and Foliage Biomass Projections....42

Introduction....42

Methodology....42

Results and Discussion....43

Literature Cited....65

CHAPTER 5. Forest Biomass Projections III: A Review of Species-specific Nutrient Concentrations (N, K, Ca, Mg) in Tree Bark, Branch, Stem-wood and Foliage Biomass Compartments....66

Introduction....66

Data Sources....67

Tree Chemistry Database (TCD)....67

Acid Rain Network Early Warning System (ARNEWS)....67

Nova Scotia Forest Biomass Nutrient Project (NS-FBNP)....68

Methods....69

Results....69

Box plots by Data Source....69

Relationships between Data Sources, by Biomass Compartment and Nutrient concentrations....75

NS-FBNP Validation....82

Relationships between Nutrients....84

Nutrient Concentration Lookup-Tables....89

Discussion....91

Sampling....91

Tree Nutrition....92

Conclusion....94

Literature Cited....95

CHAPTER 6. Spatial and Aspatial Review of Nova Scotia Physical & Chemical Soil Properties 97
Introduction 97
Aspatial Methods 98
Mineral Soil Texture 99
Coarse Fragment Content 100
Loss-on-Ignition, Organic Matter and Organic Carbon Contents 100
Total Nitrogen 103
Cation Exchange Capacity 104
Exchangeable Base Cations 106
Base Saturation 110
Rooted Depth 110
Bulk Density 110
Final Soil Model Inputs 112
Spatial Methods 113
Spatial Alignment 113
Soil Attribute Amendments 116
Upland - Lowland Soil Delineation 119
Literature Cited 120
CHAPTER 7. Mass Balance: Primary element input and export methodology 123
Introduction 123
Parent Material Weathering 123
Aspatial Methods 123
Spatial Methods 126
Atmospheric Deposition 129
Biomass Harvesting 132
Nutrient Deficiencies 134
Base-cation Leaching 135

Harvest Operability and Sustainable MAI 137
Literature Cited.....138
CHAPTER 8. Biomass Decision Support Tool Specifications 141
Introduction 141
Model Components 141
Ecounit Layer.....141
Biomass Lookup Table 142
Forest Inventory.....142
BDST Model Structure.....143
Spatial Model.....143
Aspatial Model.....145
BDST Model Specifications.....145
Model Inputs 145
Model Outputs 146
Potential Model Scenarios 147
Model Validation 147
Model Platforms.....147
Literature Cited.....147
CHAPTER 9. Generated Results, Validation and Sensitivity Analyses.....148
Introduction 148
Provincial Results and Validation 148
Parent Material Weathering 148
Critical Acid Loads and Exceedances.....150
Base-cation Depletions 152
Sustainable Operability.....154
Kejimkujik Spatial Results.....155
Parent Material Weathering 157
Critical Acid Loads and Exceedances.....160

Base-cation Depletion 165
Sustainable Operability 168
Sensitivity Analyses 176
Sensitivity Scenarios 177
Sensitivity Results 178
Literature Cited 187
CHAPTER 10. Thesis Summary, Original Contributions, Recommendations and Conclusion 189
Thesis Summary 189
Original Contribution 191
Recommendations 192
Conclusion 197
Literature Cited 197
Appendix (I). Common Name, Latin Name and Species Code for tree species within the Nova Scotia Forest Inventory 200
Appendix (II). Ker's species-specific biomass compartment parameters 202
Appendix (III). Lambert's species-specific biomass compartment parameters 204
Appendix (IV). Species-specific Stem-wood Densities 206
Appendix (V). Tree Chemistry Database Search Criteria 208
Appendix (VI). Species-specific biomass compartment nutrient concentrations (%) for the 40 species within the Nova Scotia forest inventory 210
Appendix (VII). Chronological Listing of Nova Scotia Soil Surveys 213
Appendix (VIII). Nova Scotia Ecological Land Classification Bedrock Unit Substrate Classes 215
Appendix (IX). Landform Dependent Soil Parent Material Weathering Classes 217
Appendix (X). Biomass Compartment and Nutrient Concentration Look-up Table 219
Vita ..... **Error! Bookmark not defined.**

LIST OF TABLES

Table Page

3.1. Common name, Latin name and species code of the 17 tree species within this study. 26

3.2. Species-specific volume-diameter relationship parameter values (a and b; Eq. 3.4), error values (±), and r^2 values. 27

4.1. Derived species-specific parameter values (A and B; Eq. 4.5 and 4.6 respectively), for each of the biomass compartment ratio equations adapted from Lambert et al., (2005). 46

4.2. Derived species-specific parameter values (A and B; Eq. 4.7 and 4.8 respectively), for each of the biomass compartment ratio equations adapted from Ker, (1980a; 1980b). 46

5.1. Summary of the ARNEWS regression equations y = a + bx, for each biomass compartment nutrient concentration (%) as they relate to the corresponding TCD values; r^2 is the adjusted indication of fit between variables; *n* is the sample number fitting (all $P < 0.001$). 76

5.2. Summary of the NS-FBNP regression equations y = a + bx, for each biomass compartment nutrient concentration (%) as they relate to the corresponding TCD values; r^2 is the adjusted indication of fit between variables; *n* is the sample number fitting (all $P < 0.001$). 77

5.3. Summary of the NS-FBNP regression equations y = a + bx, for each biomass compartment nutrient concentration (%) as they relate to the corresponding ARNEWS values; r^2 is the adjusted indication of fit between variables; *n* is the sample number fitting (all $P < 0.001$). 78

5.4. Comparing the NS-FBNP and ARNEWS datsets with the TCD dataset by nutrient (N, K, Ca, Mg) by way of simple linear or power regression equations (superscripts 1 and 2, respectively); r^2 is the adjusted indication of fit between variables; *n* is the sample number fitting (all $P < 0.001$). 82

5.5. Relating the total nutrients (%) of NS-FBNP, ARNEWS and Freedman datasets to the TCD dataset through simple linear regression (y = a + b x); r^2 is the adjusted indication of fit between variables; *n* is the sample number fitting (all $P < 0.001$). 83

5.6. Relating NS-FBNP, ARNEWS and TCD datsets by nutrient (N, K, Ca, Mg) as they relate to the Freedman dataset through simple linear regression (y = a + bx); r^2 is the adjusted indication of fit between variables; *n* is the sample number fitting (all $P < 0.001$). 84

5.7. Relating the paired nutrient ratios among N, K, Ca, Mg, as they relate to one another for the combined TCD, ARNEWS, NS-FBNP datasources through simple linear regression (y = a + bx); r^2 is the adjusted indication of fit between variables; *n* is the sample number fitting ($P < 0.001$ unless assigned *, which indicates $P = 0.003$). 85

5.8. Relating the Ca concentrations to the N, K and Mg concentrations in foliage and stem-wood for the combined datasources (TCD, ARNEWS, NS-FBNP), by simple linear regression (y = a + bx); r^2 is the adjusted indication of fit between variables; *n* is the sample number fitting ($P < 0.001$). 88

5.9. Determing the 85% upper and lower envelope limits of the Ca concentrations to the N, K and Mg concentrations in bark and branches for the combined datasources (TCD, ARNEWS, NS-FBNP) by simple linear regression (y = a + bx); *n* is the sample number, and *% Cap* details the percentage of data points captured within the envelope. 88

5.10. TCD bark nutrient concentrations (%) for the 16 tree species of this study. 89

5.11. TCD stem-wood nutrient concentrations (%) for the 16 tree species of this study. 90

5.12. TCD branch nutrient concentrations (%) for the 16 tree species of this study. 90

5.13. TCD foliage nutrient concentrations (%) for the 16 tree species of this study. 91

6.1 Physical and chemical soil properties tallied within the Nova Scotia soil database. 98

6.2. Average sand, silt and clay content for the missing soil texture classes within the Nova Scotia Soil Inference System, 2009. 99

6.3. Descriptive statistics of organic carbon contents (%) in each of the soil horizon categories, including the LFH layer, within the Nova Scotia Soil Inference System. 102

6.4. Descriptive statistics of total LFH nitrogen contents (%), by landform within the Nova Scotia Soil Inference System. 104

6.5. Descriptive statistics for exchangeable Ca^{2+} (me $100g^{-1}$), by soil horizon, within the Nova Scotia Soil Inference System. 107

6.6. Descriptive statistics of exchangeable Mg^{2+} (me $100g^{-1}$), by soil horizon within the Nova Scotia Soil Inference System. 108

6.7. Descriptive statistics of exchangeable K^{+} (me $100g^{-1}$), by soil horizon within the Nova Scotia Soil Inference System. 109

7.1. Multipliers representing dry deposition across Nova Scotia for base cations and acid compounds, adapted from Yanni (1996).....132

9.1. Descriptive statistics for base-cation weathering rates (eq ha^{-1} yr^{-1}), by substrate acidity class, across Nova Scotia.....149

9.2. Descriptive statistics for critical acid loads (eq ha^{-1} yr^{-1}), by harvest scenario, across Nova Scotia. 150

9.3. Descriptive statistics for critical acid load exceedances (eq ha^{-1} yr^{-1}), by harvest scenario, across Nova Scotia.....151

9.4. Descriptive statistics for base-cation depletions (eq ha^{-1} yr^{-1}), by harvest scenario, across Nova Scotia. 152

9.5. Descriptive statistics for observed base-cation leachate estimates (Yanni *et al.,* 2000; eq ha^{-1} yr^{-1}) and predicted base cation leachate estimates for the no harvest, stem-only, full-tree brown and full--tree green harvest scenarios, across Kejimkujik National Park, Nova Scotia. 154

9.6. Descriptive statistics for base-cation weathering rates (eq ha^{-1} yr^{-1}), by substrate acidity class, across Kejimkujik National Park, Nova Scotia. 159

9.7. Descriptive statistics for critical acid loads (eq ha^{-1} yr^{-1}), by harvest scenario, across Kejimkujik National Park, Nova Scotia. 161

9.8. Descriptive statistics for critical acid load exceedances (eq ha^{-1} yr^{-1}), by harvest scenario, across Kejimkujik National Park, Nova Scotia. 163

9.9. Descriptive statistics for base-cation depletions (eq ha^{-1} yr^{-1}), by harvest scenario, across Kejimkujik National Park, Nova Scotia.....166

9.10. Descriptive statistics for sustainable harvest rates (m^3 ha^{-1} yr^{-1}), with and without base -cation depletion, across Kejimkujik National Park, Nova Scotia.....175

9.11. Descriptive statistics for critical acid loads under baseline and increased substrate acidity class estimates (eq ha^{-1} yr^{-1}), by harvest scenario, across Kejimkujik National Park, Nova Scotia. 179

9.12. Descriptive statistics for critical acid load exceedances under baseline and increased substrate acidity class estimates (eq ha^{-1} yr^{-1}), by harvest scenario, across Kejimkujik National Park, Nova Scotia. 179

9.13. Descriptive statistics for base-cation depletions under baseline and increased substrate acidity class estimates (eq ha^{-1} yr^{-1}), by harvest scenario, across Kejimkujik National Park, Nova Scotia. 180

9.14. Descriptive statistics for sustainable harvest rates under baseline and increased substrate acidity class estimates (m^3 ha^{-1} yr^{-1}) for harvesting, with and without base cation-depletion, across Kejimkujik National Park, Nova Scotia. 180

9.15. Descriptive statistics for parent material weathering (eq ha^{-1} yr^{-1}) under the baseline, 1°C increase in average annual temperature, and 4.5°C increase in average annual temperature estimates, across Kejimkujik National Park, Nova Scotia. 181

9.16. Descriptive statistics for parent material weathering (eq ha^{-1} yr^{-1}) under baseline, 25cm increase in soil rooting depth, and 25cm decrease in soil rooting depth estimates, across Kejimkujik National Park, Nova Scotia. 182

9.17. Descriptive statistics for critical acid load exceedances (eq ha^{-1} yr^{-1}) under baseline, decreased acid deposition and increased acid deposition estimates, for each harvest scenario, across Kejimkujik National Park, Nova Scotia. 183

9.18. Descriptive statistics for base-cation depletions (eq ha^{-1} yr^{-1}) under baseline, decreased acid deposition and increased acid deposition estimates, for each harvest scenario, across Kejimkujik National Park, Nova Scotia. 184

9.19. Descriptive statistics for sustainable harvest rates under baseline, decreased acid deposition and increased acid deposition estimates (m^3 ha^{-1} yr^{-1}) for harvesting, with and without base-cation depletion, across Kejimkujik National Park, Nova Scotia. 185

9.20. Descriptive statistics for base-cation depletions (eq ha^{-1} yr^{-1}) under baseline, K-exchange ratio of 5 and K-exchange ratio of 15 estimates, for each harvest scenario, across Kejimkujik National Park, Nova Scotia. 186

9.21. Descriptive statistics for sustainable harvest rates under baseline, 20cm DBH and 60cm DBH estimates (m^3 ha^{-1} yr^{-1}) for harvesting, with and without base-cation depletion, across Kejimkujik National Park, Nova Scotia. 187

LIST OF FIGURES

Figure Page

2.1. The Goldich Stability Series, adapted from Goldich, 1938 11

3.1. Beech stem density (tonnes/m^3) over volume (m^3) using biomass equations by Lambert *et al.*, (2005) and Ker (1980a; 1980b), as well as published density by Gonzalez (1990). 28

3.2. Balsam Fir stem density (tonnes/m^3) over volume (m^3) using biomass equations by Lambert *et al.*, (2005) and Ker (1980a; 1980b), as well as published density by Gonzalez (1990). 29

3.3. Black Spruce stem density (tonnes/m^3) over volume (m^3) using biomass equations by Lambert *et al.*, (2005) and Ker (1980a; 1980b), as well as published density by Gonzalez (1990). 29

3.4. Eastern Hemlock stem density (tonnes/m^3) over volume (m^3) using biomass equations by Lambert *et al.*, (2005) and Ker (1980a; 1980b), as well as published density by Gonzalez (1990). 29

3.5. Eastern Larch stem density (tonnes/m^3) over volume (m^3) using biomass equations by Lambert *et al.*, (2005) and Ker (1980a; 1980b), as well as published density by Gonzalez (1990). 30

3.6. Eastern White Cedar stem density (tonnes/m^3) over volume (m^3) using biomass equations by Lambert *et al.*, (2005) and Ker (1980a; 1980b), as well as published density by Gonzalez (1990). 30

3.7. Eastern White Pine stem density (tonnes/m^3) over volume (m^3) using biomass equations by Lambert *et al.*, (2005) and Ker (1980a; 1980b), as well as published density by Gonzalez (1990). 30

3.8. Jack Pine stem density (tonnes/m^3) over volume (m^3) using biomass equations by Lambert *et al.*, (2005) and Ker (1980a; 1980b), as well as published density by Gonzalez (1990). 31

3.9. Red Maple stem density (tonnes/m^3) over volume (m^3) using biomass equations by Lambert *et al.*, (2005) and Ker (1980a; 1980b), as well as published density by Gonzalez (1990). 31

3.10. Red Pine stem density (tonnes/m^3) over volume (m^3) using biomass equations by Lambert *et al.*, (2005) and Ker (1980a; 1980b), as well as published density by Gonzalez (1990). 31

3.11. Red Spruce stem density (tonnes/m^3) over volume (m^3) using biomass equations by Lambert *et al.*, (2005) and Ker (1980a; 1980b), as well as published density by Gonzalez (1990). 32

3.12. Sugar Maple stem density (tonnes/m^3) over volume (m^3) using biomass equations by Lambert *et al.*, (2005) and Ker (1980a; 1980b), as well as published density by Gonzalez (1990). 32

3.13. Trembling Aspen stem density (tonnes/m^3) over volume (m^3) using biomass equations by Lambert *et al.*, (2005) and Ker (1980a; 1980b), as well as published density by Gonzalez (1990). 32

3.14. White Ash stem density (tonnes/m^3) over volume (m^3) using biomass equations by Lambert *et al.*, (2005) and Ker (1980a; 1980b), as well as published density by Gonzalez (1990). 33

3.15. White Birch stem density (tonnes/m^3) over volume (m^3) using biomass equations by Lambert *et al.*, (2005) and Ker (1980a; 1980b), as well as published density by Gonzalez (1990). 33

3.16. White Spruce stem density (tonnes/m^3) over volume (m^3) using biomass equations by Lambert *et al.*, (2005) and Ker (1980a; 1980b), as well as published density by Gonzalez (1990). 33

3.17. Yellow Birch stem density (tonnes/m^3) over volume (m^3) using biomass equations by Lambert *et al.*, (2005) and Ker (1980a; 1980b), as well as published density by Gonzalez (1990). 34

3.18. Beech stem biomass (tonnes) over stem DBH (cm) using biomass equations of Lambert *et al.*, (2005) and Ker (1980a, b), as well as the generated method in this paper. 34

3.19. Balsam Fir stem biomass (tonnes) over stem DBH (cm) using biomass equations of Lambert *et al.*, (2005) and Ker (1980a, b), as well as the generated method in this paper. 34

3.20. Black Spruce stem biomass (tonnes) over stem DBH (cm) using biomass equations of Lambert *et al.*, (2005) and Ker (1980a, b), as well as the generated method in this paper. 35

3.21. Eastern Hemlock stem biomass (tonnes) over stem DBH (cm) using biomass equations of Lambert *et al.*, (2005) and Ker (1980a, b), as well as the generated method in this paper. 35

3.22. Eastern Larch stem biomass (tonnes) over stem DBH (cm) using biomass equations of Lambert *et al.*, (2005) and Ker (1980a, b), as well as the generated method in this paper. 35

3.23. Eastern White Cedar stem biomass (tonnes) over stem DBH (cm) using biomass equations of Lambert *et al.*, (2005) and Ker (1980a, b), as well as the generated method in this paper. 36

3.24. Eastern White Pine stem biomass (tonnes) over stem DBH (cm) using biomass equations of Lambert *et al.*, (2005) and Ker (1980a, b), as well as the generated method in this paper. 36

3.25. Jack Pine stem biomass (tonnes) over stem DBH (cm) using biomass equations of Lambert *et al.*, (2005) and Ker (1980a, b), as well as the generated method in this paper. 36

3.26. Red Maple stem biomass (tonnes) over stem DBH (cm) using biomass equations of Lambert *et al.*, (2005) and Ker (1980a, b), as well as the generated method in this paper. 37

3.27. Red Pine stem biomass (tonnes) over stem DBH (cm) using biomass equations of Lambert *et al.*, (2005) and Ker (1980a, b), as well as the generated method in this paper. 37

3.28. Red Spruce stem biomass (tonnes) over stem DBH (cm) using biomass equations of Lambert *et al.*, (2005) and Ker (1980a, b), as well as the generated method in this paper. 37

3.29. Sugar Maple stem biomass (tonnes) over stem DBH (cm) using biomass equations of Lambert *et al.*, (2005) and Ker (1980a, b), as well as the generated method in this paper. 38

3.30. Trembling Aspen stem biomass (tonnes) over stem DBH (cm) using biomass equations of Lambert *et al.*, (2005) and Ker (1980a, b), as well as the generated method in this paper. 38

3.31. White Ash stem biomass (tonnes) over stem DBH (cm) using biomass equations of Lambert *et al.*, (2005) and Ker (1980a, b), as well as the generated method in this paper. 38

3.32. White Birch stem biomass (tonnes) over stem DBH (cm) using biomass equations of Lambert *et al.*, (2005) and Ker (1980a, b), as well as the generated method in this paper. 39

3.33. White Spruce stem biomass (tonnes) over stem DBH (cm) using biomass equations of Lambert *et al.,* (2005) and Ker (1980a, b), as well as the generated method in this paper. 39

3.34. Yellow Birch stem biomass (tonnes) over stem DBH (cm) using biomass equations of Lambert *et al.,* (2005) and Ker (1980a, b), as well as the generated method in this paper. 39

4.1. Relationship between Beech compartment ratios (compartment mass / stem mass) and DBH (cm) using the published equations by Lambert *et al.,* (2005). 47

4.2. Relationship between Beech compartment ratios (compartment mass / stem mass) and DBH (cm) using the published equations by Ker, (1980a). 47

4.3. Relationship between Balsam Fir compartment ratios (compartment mass / stem mass) and DBH (cm) using the published equations by Lambert *et al.,* (2005). 48

4.4. Relationship between Balsam Fir compartment ratios (compartment mass / stem mass) and DBH (cm) using the published equations by Ker, (1980b). 48

4.5. Relationship between Black Spruce compartment ratios (compartment mass / stem mass) and DBH (cm) using the published equations by Lambert *et al.,* (2005). 49

4.6. Relationship between Black Spruce compartment ratios (compartment mass / stem mass) and DBH (cm) using the published equations by Ker, (1980b). 49

4.7. Relationship between Eastern Hemlock compartment ratios (compartment mass / stem mass) and DBH (cm) using the published equations by Lambert *et al.,* (2005). 50

4.8. Relationship between Eastern Hemlock compartment ratios (compartment mass / stem mass) and DBH (cm) using the published equations by Ker, (1980a).....50

4.9. Relationship between Eastern Larch compartment ratios (compartment mass / stem mass) and DBH (cm) using the published equations by Lambert *et al.,* (2005). 51

4.10. Relationship between Eastern Larch compartment ratios (compartment mass / stem mass) and DBH (cm) using the published equations by Ker, (1980b). 51

4.11. Relationship between Eastern White Cedar compartment ratios (compartment mass / stem mass) and DBH (cm) using the published equations by Lambert *et al.,* (2005). 52

4.12. Relationship between Eastern White Cedar compartment ratios (compartment mass / stem mass) and DBH (cm) using the published equations by Ker, (1980a). 52

4.13. Relationship between Eastern White Pine compartment ratios (compartment mass / stem mass) and DBH (cm) using the published equations by Lambert *et al.,* (2005). 53

4.14. Relationship between Eastern White Cedar compartment ratios (compartment mass / stem mass) and DBH (cm) using the published equations by Ker, (1980a). 53

4.15. Relationship between Jack Pine compartment ratios (compartment mass / stem mass) and DBH (cm) using the published equations by Lambert *et al.,* (2005). 54

4.16. Relationship between Jack Pine compartment ratios (compartment mass / stem mass) and DBH (cm) using the published equations by Ker, (1980b). 54

4.17. Relationship between Red Maple compartment ratios (compartment mass / stem mass) and DBH (cm) using the published equations by Lambert *et al.,* (2005). 55

4.18. Relationship between Red Maple compartment ratios (compartment mass / stem mass) and DBH (cm) using the published equations by Ker, (1980b). 55

4.19. Relationship between Red Pine compartment ratios (compartment mass / stem mass) and DBH (cm) using the published equations by Lambert *et al.,* (2005). 56

4.20. Relationship between Red Pine compartment ratios (compartment mass / stem mass) and DBH (cm) using the published equations by Ker, (1980b). 56

4.21. Relationship between Red Spruce compartment ratios (compartment mass / stem mass) and DBH (cm) using the published equations by Lambert *et al.,* (2005). 57

4.22. Relationship between Red Spruce compartment ratios (compartment mass / stem mass) and DBH (cm) using the published equations by Ker, (1980b). 57

4.23. Relationship between Sugar Maple compartment ratios (compartment mass / stem mass) and DBH (cm) using the published equations by Lambert *et al.*, (2005). 58

4.24. Relationship between Sugar Maple compartment ratios (compartment mass / stem mass) and DBH (cm) using the published equations by Ker, (1980a).....58

4.25. Relationship between Trembling Aspen compartment ratios (compartment mass / stem mass) and DBH (cm) using the published equations by Lambert *et al.*, (2005). 59

4.26. Relationship between Trembling Aspen compartment ratios (compartment mass / stem mass) and DBH (cm) using the published equations by Ker, (1980b). 59

4.27. Relationship between White Ash compartment ratios (compartment mass / stem mass) and DBH (cm) using the published equations by Lambert *et al.*, (2005). 60

4.28. Relationship between White Ash compartment ratios (compartment mass / stem mass) and DBH (cm) using the published equations by Ker, (1980a).....60

4.29. Relationship between White Birch compartment ratios (compartment mass / stem mass) and DBH (cm) using the published equations by Lambert *et al.*, (2005). 61

4.30. Relationship between White Birch compartment ratios (compartment mass / stem mass) and DBH (cm) using the published equations by Ker, (1980b). 61

4.31. Relationship between White Spruce compartment ratios (compartment mass / stem mass) and DBH (cm) using the published equations by Lambert *et al.*, (2005). 62

4.32. Relationship between White Spruce compartment ratios (compartment mass / stem mass) and DBH (cm) using the published equations by Ker, (1980b). 62

4.33. Relationship between Yellow Birch compartment ratios (compartment mass / stem mass) and DBH (cm) using the published equations by Lambert *et al.*, (2005). 63

4.34. Relationship between Yellow Birch compartment ratios (compartment mass / stem mass) and DBH (cm) using the published equations by Ker, (1980a).....63

4.35. Process flow-chart illustrating stand level biomass estimations for each of the three harvest scenarios.....64

5.1. Box plots of N concentrations (%) in bark, branch, stem-wood and foliage compartments, by tree species, for the TCD dataset; the corresponding entries from the ARNEWS and NS-FBNP data sources are shown by the line symbols. Box plots show the 10^{th}, 50^{th}, and 90^{th} percentiles, and outliers below the 10^{th} and above the 90^{th} percentiles.....71

5.2. Box plots of K concentrations (%) in bark, branch, stem-wood and foliage compartments, by tree species, for the TCD dataset; the corresponding entries from the ARNEWS and NS-FBNP data sources are shown by the line symbols. Box plots show the 10^{th}, 50^{th}, and 90^{th} percentiles, and outliers below the 10^{th} and above the 90^{th} percentiles.....72

5.3. Box plots of Mg concentrations (%) in bark, branch, stem-wood and foliage compartments, by tree species, for the TCD dataset; the corresponding entries from the ARNEWS and NS-FBNP data sources are shown by the line symbols. Box plots show the 10^{th}, 50^{th}, and 90^{th} percentiles, and outliers below the 10^{th} and above the 90^{th} percentiles.....73

5.4. Box plots of Ca concentrations (%) in bark, branch, stem-wood and foliage compartments, by tree species, for the TCD dataset; the corresponding entries from the ARNEWS and NS-FBNP data sources are shown by the line symbols. Box plots show the 10^{th}, 50^{th}, and 90^{th} percentiles, and outliers below the 10^{th} and above the 90^{th} percentiles.....74

5.5. Comparing the nitrogen and calcium concentrations (%) for the NS-FBNP and ARNEWS datasets. The dashed lines represent a 1:1 ratio; r^2 is the adjusted indication of fit between variables.....80

5.6. Comparing the potassium and magnesium concentrations (%) for the NS-FBNP and ARNEWS datasets. The dashed lines represent a 1:1 ratio; r^2 is the adjusted indication of fit between variables. 81

5.7. Comparing total nutrient concentrations (N, K, Mg, Ca) for the NS-FBNP, ARNEWS and Freedman datasets in relation to the TCD dataset (see Table 5.4); r^2 is the adjusted indication of fit between variables.....83

5.8. Comparing how N, K, Mg and Ca relate to one another across all three datasets, by tree compartment, through simple linear regression analysis ($y = a + bx$); r^2 is the adjusted indication of fit between variables.....86

5.9. Relating N, K, and Mg concentrations to the Ca concentrations (%), by tree compartment for the combined datasets, using simple linear regression equations (y = a + bx) for stem-wood and foliage, and capturing 85% for the Ca data within the bark and branches using linear envelopes. 87

5.10. The hypothetical relationhsip between biomass compartment nutrient concentrations and tree growth, adapted from Chapman, 1967. 94

6.1. Box plots illustrating the range of organic carbon contents (%) for each of the 13 mineral soil horizons within the Nova Scotia Soil Inference System. Box plots show the 10^{th}, 50^{th}, and 90^{th} percentiles, and outliers below the 10^{th} and above the 90^{th} percentiles. 102

6.2. Reported nitrogen contents (%) for the A, B and C horizons versus best-fitted values (Eq. 6.6 - 6.8) within the Nova Scotia Soil Inference System. r^2 is the adjusted indication of fit between variables. 103

6.3. Box plots illustrating the range of LFH nitrogen contents (%) by landform within the Nova Scotia Soil Inference System. Box plots show the 10^{th}, 50^{th}, and 90^{th} percentiles, and outliers below the 10^{th} and above the 90^{th} percentiles.....104

6.4. Reported CEC (me $100g^{-1}$) values of the A, B and C layers versus best-fitted values (Eq. 6.11 - 6.13) within the Nova Scotia Soil Inference System. r^2 is the adjusted indication of fit between variables. 106

6.5. Box plots illustrating the range of exchangeable Ca^{2+} (me $100g^{-1}$), by soil horizon within the Nova Scotia Soil Inference System. Box plots show the 10^{th}, 50^{th}, and 90^{th} percentiles, and outliers below the 10^{th} and above the 90^{th} percentiles.....107

6.6. Box plots illustrating the range of exchangeable Mg^{2+} (me $100g^{-1}$), by soil horizon within the Nova Scotia Soil Inference System. Box plots show the 10^{th}, 50^{th}, and 90^{th} percentiles, and outliers below the 10^{th} and above the 90^{th} percentiles.....108

6.7. Box plots illustrating the range of exchangeable K^{+} (me $100g^{-1}$), by soil horizon within the Nova Scotia Soil Inference System. Box plots show the 10^{th}, 50^{th}, and 90^{th} percentiles, and outliers below the 10^{th} and above the 90^{th} percentiles.....109

6.8. Example illustration showing the two forms of disalignment within the soil county layers, both as slivers "inside" the provincial boundary (a), and "outside" the provincial boundary (b). 114

6.9. Example illustration showing the overlap of soil polygons between county soil layer borders. 115

6.10. Example illustration showing the spatial inaccuracy of the county soil layers water bodies, both in detail (such as islands and shorelines), as well as actual extent of the water bodies. 115

7.1. Spatial distribution of the four upland soil parent material weathering classes across Nova Scotia. 127

7.2. Average annual temperature across Nova Scotia based on Environment Canada's National Climate Archive, Canadian Daily Climate Data, averaged across 2004-2008 and interpolated using the Tension Spline method (Franke, 1982). 128

7.3. Potassium (K^+) wet deposition across Nova Scotia based on the National Atmospheric Chemistry Database and Analysis System dataset. 130

7.4. Calcium (Ca^{2+}) wet deposition across Nova Scotia based on the National Atmospheric Chemistry Database and Analysis System dataset. 130

7.5. Magnesium (Mg^{2+}) wet deposition across Nova Scotia based on the National Atmospheric Chemistry Database and Analysis System dataset. 131

7.6. Total nitrogen (NH_4^+ & NO_3^-) wet deposition across Nova Scotia based on the National Atmospheric Chemistry Database and Analysis System dataset. 131

7.7. Total sulphur (SO_4^{2-} & SO_x) wet deposition across Nova Scotia based on the National Atmospheric Chemistry Database and Analysis System dataset. 132

8.1. Model structure and the relationships between inputs, sub-models, and outputs for the Biomass Decision Support Tool. 144

9.1. Stream chemistry study areas in relation to mapped water features within the Kejimkujik National Park boundaries. 153

9.2. Substrate acidity classification for Kejimkujik National Park. 156

9.3. Dominant forest tree species across Kejimkujik National Park. 157

9.4. Box plots illustrating the range of base-cation weathering rates (eq ha^{-1} yr^{-1}), by substrate acidity class, across Kejimkujik National Park. Box plots show the 10^{th}, 50^{th}, and 90^{th} percentiles, and outliers below the 10^{th} and above the 90^{th} percentiles. 158

9.5. Spatial illustration of parent material weathering rates (eq ha^{-1} yr^{-1}) across Kejimkujik National Park. 159

9.6. Box plots illustrating the range of critical acid loads (eq ha^{-1} yr^{-1}), by harvest scenario across Kejimkujik National Park. Box plots show the 10^{th}, 50^{th}, and 90^{th} percentiles, and outliers below the 10^{th} and above the 90^{th} percentiles. 161

9.7. Spatial illustration of critical acid load estimations (eq ha^{-1} yr^{-1}) for each harvest scenario, within Kejimkujik National Park, Nova Scotia. 162

9.8. Box plots illustrating the range of critical acid load exceedances (eq ha^{-1} yr^{-1}), by harvest scenario across Kejimkujik National Park. Box plots show the 10^{th}, 50^{th}, and 90^{th} percentiles, and outliers below the 10^{th} and above the 90^{th} percentiles. 163

9.9. Spatial illustration of critical acid load exceedance estimations (eq ha^{-1} yr^{-1}) for each harvest scenario, within Kejimkujik National Park, Nova Scotia. 164

9.10. Box plots illustrating the range of base-cation depletions (eq ha^{-1} yr^{-1}), by harvest scenario across Kejimkujik National Park. Box plots show the 10^{th}, 50^{th}, and 90^{th} percentiles, and outliers below the 10^{th} and above the 90^{th} percentiles. 166

9.11. Spatial illustration of base-cation depletion estimations (eq ha^{-1} yr^{-1}) for each harvest scenario, within Kejimkujik National Park, Nova Scotia. 167

9.12. Deficiency-based area (%) predicted to be sustainably and not sustainably clear-cut harvested, across Kejimkujik National Park under the stem-only, full-tree brown and full-tree green harvest scenarios. 169

9.13. Deficiency- and depletion-based area (%) predicted to be sustainably and not sustainably clear-cut harvested, across Kejimkujik National Park under the stem-only, full-tree brown and full-tree green harvest scenarios. 169

9.14. Spatial illustration of the clear-cut operability calculator outputs for each harvest scenario, with and without base cation depletions, across Kejimkujik National Park, Nova Scotia. 170

9.15. Deficiency-based area (%) predicted to be N, K or Ca limited across Kejimkujik National Park under the stem-only, full-tree brown and full-tree green harvest scenarios. 172

9.16. Deficiency- and depletion-based area (%) predicted to be N, K or Ca limited across Kejimkujik National Park under the stem-only, full-tree brown and full-tree green harvest scenarios. 172

9.17. Spatial illustration of growth limiting nutrients for each harvest scenario, with and without base cation depletions, across Kejimkujik National Park, Nova Scotia. 173

9.18 Box plots illustrating the range of sustainable harvest rates (m^3 ha^{-1} yr^{-1}), for harvesting with and without base-cation depletions, across Kejimkujik National Park. Box plots show the 10^{th}, 50^{th}, and 90^{th} percentiles, and outliers below the 10^{th} and above the 90^{th} percentiles. 175

9.19. Spatial illustration of predicted sustainable harvest rates across Kejimkujik National Park for harvesting with and without base-cation depletions. 176

ACKNOWLEDGMENTS

The knowledge and experience that I have gained over the past 2 years could not have been possible without the guidance and expertise of Dr. Paul Arp. Thank you very much Dr. Arp for mentoring me, as well as providing opportunities for me to explore my interests outside the context of this project. I am very grateful to have worked with you and the entire Forest Watershed Research Centre team.

I would like to sincerely thank Jae Ogilvie and Mark Castonguay for all their support, both in technical nature, as well as making it enjoyable to come to work every day. Although we worked hard, we also had a lot of fun. Thank you.

To my secondary supervisors, Dr. Graham Forbes and Dr. Fan-Rui Meng, thank you very much for your time and expertise, as well as for providing perspective when I needed it.

Financial support for this study was received from the Nova Scotia Department of Natural Resources, of which, I am very thankful. Specifically, a great deal of thanks to Kevin Keys and Rob O'Keefe for all your technical advice, as well as for providing helpful comments and suggestions throughout the duration of this project.

Finally, I would like to thank everyone at the Forest Watershed Research Centre for the coffee break chats, Justin Chase for helping me review and edit this document when my eyes were blind to error, and to my parents, Jim and Betty Noseworthy, for their continued encouragement and support.

J.D.N

CHAPTER 1

GENERAL INTRODUCTION

BACKGROUND AND OBJECTIVE

Increased pressures to harvest forest biomass for energy production have led to the demand for sustainability models that predict the impacts of biomass harvesting on forest nutrient budgets. Although sustainability may be defined in a number of ways, the long-term sustainability of forest biomass is ultimately dependant on the availability of primary growth-limiting nutrient supplies (Ågren, 1985). Anthropogenic factors such as biomass harvesting and enhanced soil acidification due to acid precipitation are known to increase primary nutrient exports, thereby reducing the overall nutrient pool of forest sites (Tew *et al.*, 1986). If these exports exceed the primary nutrient supplies, then repeated harvesting may create long-term nutrient deficiencies, ultimately leading to a decline in forest health (Ouimet *et al.*, 2001). The import, export and retention of nutrients within forested ecosystems has been extensively studied under the general topic of biogeochemical cycling (Federer *et al.*, 1989; Johnson *et al.*, 1991; Merino *et al.*, 2005), but these studies are typically limited to sites for which the studies were conducted. Over-simplified or inaccurate estimates of nutrient input/output budgets may result when site-specific models are used outside the original site conditions of where they were generated (Bosman *et al.*, 2001; Augusto *et al.*, 2008; Arthur *et al.*, 2001). In general, nutrient input, retention and losses vary strongly across a landscape based on atmospheric deposition, soil type and vegetation type, thereby requiring a detailed analysis of primary nutrient supplies and losses in relation to the nutrient amounts already

stored in the vegetation and the underlying soil (Ranger & Turpault, 1999). Primary nutrient supplies refer to atmospheric deposition and soil weathering, whereas primary nutrient losses refer to base-cation depletion and forest biomass harvesting. The natural variability in biological, geological, hydrological and climatic conditions across forested landscapes suggest that the net implications of biomass harvesting will be the result of the unique combination of these conditions for any given site. The most accurate model projections of nutrient balances for management purposes will therefore be those that are able to account for environmental gradients. The net implications of biomass harvesting are assumed to be a function of:

1. The ability and degree to which specific tree species and tree compartments accumulate and store nutrients, as well as return nutrients to the soil during decomposition (Cornelissen, 1996; Thiffault, 2006).

2. The ability of specific soil types to retain nutrients based upon physical and chemical characteristics such as texture, depth and base saturation (McLaughlin, 1998).

3. The ability and degree to which soil parent material weathering replenishes the available base-cation supplies for plant uptake and acid buffering (Ouimet & Duchesne, 2005).

4. The degree to which atmospheric deposition supplies base cations to the soil, but can also lead to a gradual base-cation depletion due to atmospheric acid deposition causing soil acidification (Stutter *et al.,* 2003; Lovett, 1994).

This thesis focuses on nutrient mass balances across wide environmental gradients in order to relate these implications to the sustainability of forest biomass harvesting. The

overall objective is to provide the background computational framework for a geospatial, steady-state, mass balance biomass sustainability model, designed for tree species and site conditions specific to the province of Nova Scotia, Canada. Nova Scotia was chosen for this study due to: (i) the diversity of environmental conditions; (ii) the availability of pertinent geospatial data-layers at spatial resolutions sufficient for forest management planning; (iii) social pressure to evaluate the potential sustainability of forest biomass harvesting as affected by anthropogenic factors such as acid precipitation and climate change. Although Nova Scotia was chosen as the case study, the framework is likely generic depending on the availability of geospatial data and specie specific tree biomass functions and nutrient concentrations.

SUBJECT MATTER

Chapters 2: reviews the various concepts and applications pertinent to this thesis including biomass harvest sustainability and critical loads theory.

Chapters 3: introduces and describes 2 sets of published stem biomass equations and compares the results to a newly described method of projecting stem biomass.

Chapters 4: introduces and describes projections for bark, branch, stem-wood and foliage biomass compartments, prorated using stem biomass projections from Chapter 3.

Chapters 5: reviews and compares biomass compartment nutrient concentration data sources, discusses the relationships between nutrient concentrations, and illustrates the final nutrient values used within the model.

Chapters 6: introduces and describes the development of the Nova Scotia soil properties database and soil inference system, as well spatial soil alignment and upland-lowland soil delineation procedures.

Chapters 7: introduces, discusses and describes the methods used to quantify primary nutrient and acid inputs through atmospheric deposition and parent material weathering, as well as the primary nutrient outputs through biomass harvesting and acid leaching.

Chapters 8: details the specifications of the Biomass Decision Support Tool based on the two computer interfaces, with detailed descriptions of each component.

Chapters 9: presents the aspatial results and validation of the Biomass Decision Support Tool for the province of Nova Scotia, as well as spatial results and sensitivity analyses for Kejimkujik National Park.

Chapters 10: provides an overall summary of the thesis, a statement of original contributions, and recommendations for further development.

LITERATURE CITED

Ågren, G. (1985). Limits to plant production. *Journal of theoretical biology, 113*, 89-91.

Arthur, M., Hamburg, S., & Siccama, T. (2001). Validating allometric estimates of aboveground living biomass and nutrient contents of a northern hardwood forest. *Canadian Journal of Forest Research, 31*, 11-17.

Augusto, L., Meredieu, C., Bert, D., Trichet, P., Porte, A., Bosc, A., et al. (2008). Improving models of forest nutrient export with equations that predict the nutrient concentration of tree compartments. *Annals of Forest Science, 65*, 808p1 - 808p11.

Bosman, B., Remacle, J., & Carnol, M. (2001). Element removal in harvested tree biomass: scenarios for critical loads in Wallonia, South Belgium. *Water, Air, and Soil Pollution, 1,* 153-167.

Cornelissen, J. (1996). An Experimental Comparison of Leaf Decomposition Rates in a Wide Range of Temperate Plant Species and Types. *Journal of Ecology, 84,* 573-582.

Federer, C., Hornbeck, J., Tritton, L., Martin, C., Pierce, R., & Smith, C. (1989). Long-term depletion of calcium and other nutrients in eastern U.S. forests. *Environmental Management, 13,* 593-601.

Johnson, C., Johnson, A., & Siccama, T. (1991). Whole-tree clear-cutting effects on exchangeable cations and soil acidity. *Soil Science Society of America Journal, 55,* 502-508.

Lovett, G. (1994). Atmospheric Deposition of Nutrients and Pollutants in North America: An Ecological Perspective. *Ecological Applications, 4,* 630-650.

McLaughlin, D. (1998). A decade of forest tree monitoring in Canada: evidence of air pollution effects. *Environmental Reviews, 6,* 151-171.

Merino, A., Balboa, M., Rodriguez-Soalleiro, R., & Gonzalez, J. (2005). Nutrient exports under different harvesting regimes in fast-growing forest plantations in southern Europe. *Forest Ecology & Management, 207,* 325-339.

Ouimet, R., & Duchesne, L. (2005). Base-cation mineral weathering and total release rates from soils in three calibrated forest watersheds on the Canadian Boreal Shield. *Canadian Journal of Soil Science , 85,* 245-260.

Ouimet, R., Duchesne, L., Houle, D., & Arp, P. (2001). Critical loads and exceedances of acid deposition and associated forest growth in the northern hardwood and boreal coniferous forests in Quebec, Canada. *Water, Air, and Soil Pollution, 1,* 119-134.

Ranger, J., & Turpault, M. (1999). Input-output nutrient budgets as a diagnostic tool for sustainable forest management. *Firest Ecology and Management, 122,* 139-154.

Stutter, M., Langan, S., & Cresser, M. (2003). Weathering and atmospheric deposition signatures of base cations in upland soils of NE Scotland: their application to critical load assessment. *Geoderma, 116,* 301-324.

Tew, D., Morris, L., Allen, H., & Wells, C. (1986). Estimates of nutrient removal, displacement and loss resulting from harvest and site preparation of a Pinus taeda plantation in the Piedmont of North Carolina. *Forest Ecology and Management, 15,* 257-267.

CHAPTER 2

CONCEPTS AND APPLICATIONS

SUSTAINABLE BIOMASS HARVESTING

In light of concerns regarding climate change and the decline in fossil fuel availability, the demand for renewable and ecologically sustainable sources of energy have been steadily increasing. In 1978, the Canadian federal government established the Energy from the Forest program (ENFOR) in order to develop renewable energy sources using forest biomass (Boudewyn *et al.,* 2007). The concept of forest biomass has been used to represent a variety of organically derived energy sources, including both the above and belowground portion of living trees, deadwood material, herbaceous and woody plants, and wildlife (Townsend, 2008). Within Canada, a variety of direct and indirect methods of obtaining forest biomass have been established, including short rotation energy crops through high yield agroforestry (Yemshanov & McKenney, 2008), mill waste (Champagne, 2007), and collection of on-site harvest residues (Levin *et al.,* 2007). The majority of energy from biomass is produced directly through "hog fuel" combustion, although biomass chipping coupled with wood pelletization has resulted in the production of marketable biomass fuel, for local, regional and intercontinental transport and consumption. Driven by certification criteria for sustainable management, and also by accelerated demand for Carbon-creditable "green energy", it is therefore important to build a generalized framework to assess the long-term ramifications of biomass harvest sustainability within the context of stand-specific forest inventories and related nutrient constraints. Throughout this thesis, the term "biomass" will be used to

describe only the above ground portion (stem-wood, bark, branch and foliage compartments) of live, merchantable and unmerchantable trees (2- to 100-cm DBH).

Tree growth is assumed to be a function of the Sprengel-Liebig Law of the Minimum, derived from the universal principle of mass conservation, which states that plant growth is not controlled by the sum of available nutrients, but is entirely controlled by the availability of the most limiting nutrient (Ploeg, Böhm, & Kirkham, 1999). Using the Sprengel-Liebig Law, Sverdrup & Rosen (1998; p. 223) suggest that the basic principle of sustainable biomass harvesting is:

> "*...when the removal of nutrients with the harvest does not exceed the supply of the same nutrients represented by chemical weathering of rocks, atmospheric deposition and fertilisation*."

If soil fertility is lost due to soil acidification and/or current harvest practices, a decline in forest health may occur in the form of foliage discoloration, defoliation, and an overall decrease in growth rates (Sverdrup *et al.*, 2006). Although plant nutrition is dependent on a variety of factors such as available water, CO_2, micronutrients and macronutrients, it is assumed that long-term forest growth (and subsequent biomass removal) can only be sustained if the essential supply of Mg^{2+}, Ca^{2+}, K^{+} and N is not limited (Sverdrup & Rosen, 1998).

CRITICAL LOADS

The method of determining whether the removal of nutrients through biomass harvesting exceeds nutrient inputs is largely adapted from the critical loads concept.

Critical loads modelling was originally applied within Europe as a means of developing strategies to limit transboundary air pollution (Grennfelt *et al.,* 2001). The method has now been adopted throughout the world as a tool for calculating acceptable amounts of atmospherically derived acid compounds, as well as a method of identifying acid sensitive ecosystems. The critical load of an ecosystem is defined by Nilsson & Grennfelt (1988) as:

> "*The maximum deposition of (acidifying) compounds that will not cause chemical changes leading to long-term harmful effects on ecosystem structure and function*".

The concept is comprised of three main elements: (i) a biological indicator, (ii) a chemical criterion, and (iii) a critical chemical value (Løkke *et al.,* 1996). Within forested ecosystems, the biological indicator is primarily tree growth, the chemical criterion is the total amount of atmospherically derived acid compounds, and the critical chemical value refers to the total amount of acid deposited, below which no harmful effects will occur within the forest ecosystem. The critical load of forested ecosystems are most frequently determined using a steady-state, simple mass balance approach (SSMB) that calculates the difference between primary nutrient sources and sinks (Bosman *et al.,* 2001). Since this study focuses on long-term harvest sustainability, episodic factors such as natural disturbance dynamics, and secondary processes dealing with litterfall, decomposition, nutrient mineralization and re-uptake by vegetation, are not accounted for. Only primary nutrient supplies and losses are used to calculate the critical acid load (*CL*) of nitrogen (*N*) and sulphur (*S*), as set by:

$$CL = BC_{dep} + BC_{we} - BC_{up} + N_{im} + N_{up} + N_{de} + AC_{le,CL} \quad (2.1)$$

where *BC* denotes the soil base cations essential for plant growth (Mg^{2+}, Ca^{2+}, K^{+}), *N* denotes nitrogen, and *AC* denotes the soil acid cations (H^{+}, Al^{3+}). Subscripts *dep*, *we*, *up*, *im*, *de* and *le* refer to atmospheric deposition, soil weathering, uptake by vegetation, immobilisation, denitrification and leaching, respectively. Furthermore, $AC_{le,CL}$ is the rate of acid cation leaching when a zero base-cation depletion scenario is achieved (Eq. 7.12). All terms are expressed in eq ha^{-1} yr^{-1}. Soil acidification impacts from atmospheric deposition of Na^{+} and Cl^{-} are assumed to be negligible (Nasr *et al.,* 2010), as well as both nitrogen denitrification (N_{de}) and immobilisation (N_{im}). Nitrogen denitrification primarily occurs under anaerobic conditions such as in lowland hydric soils (Whitfield *et al.,* 2006a; Ouimet *et al.,* 2006), whereas this study focuses only on upland forest soils. Immobilisation of nitrogen is negligible under the assumption that soil N does not accumulate over the long-term due to various disturbance patterns such as canopy openings created by insect and wind damage, blow downs, and forest fires (Ouimet *et al.,* 2001). Therefore, the critical soil acidification load is generally defined by:

$$CL = BC_{dep} + BC_{we} - BC_{up} + N_{up} + AC_{le,CL} \quad (2.2)$$

Critical load exceedance for soil acidification (*EXC*) refers to the amount of atmospherically deposited N and S that exceeds the total critical acid load of an ecosystem, and is set as:

$$EXC = S_{dep} + N_{dep} - CL \quad (2.3)$$

The criterion for sustainable forest biomass harvesting needs to ensure that there will be no net decline in soil base saturation due to forest harvesting and the adverse effects of S

and N deposition. The sustainable forest biomass assessment model to be presented is formulated accordingly by addressing nutrient specific mass balances, species-specific biomass and nutrient contents within trees from immature to mature growth stages, and ion retention and exchange dynamics within soils.

PRIMARY ELEMENT SOURCES

Parent Material Weathering

The weathering of soil parent material is the primary source of soil base cations for plant growth (Werner & Spranger, 1996), as well as of long-term soil buffering capacity (Clayton, 1988). The dissolution of primary and secondary minerals from soil parent material is controlled by a number of factors such as mineral composition, soil temperature, soil moisture, soluble reactants, and soil physical characteristics (Sverdrup & Warfringe, 1993). Mineral structure and chemical composition dictate the resistance of minerals to weathering; granitic substrates composed of quartz and K-feldspars are highly resistant to weathering, whereas basaltic substrates containing olivine tend to weather rapidly (Goldich, 1938; Figure 2.1). Temperature and precipitation also affect the rate of weathering as elevated soil temperatures increase weathering rates (White *et al.*, 1999), and soil moisture acts as the primary driver of mineral dissolution and the dispersal of soluble products (Velbel, 1985). Soluble weathering reactants such as organic acids, CO_2, H^+, Al^{3+}, and base cations effect weathering depending on the relative concentrations of each within soil solution. Generally, organic acids, H^+ and CO_2 tend to increase the rate of weathering through hydrolysis reactions, whereas Al^{3+} and base cations tend to decrease the rate of weathering by replacing the acidifying agents on soil exchange sites.

Physical soil characteristics such as soil depth and bulk density dictate the total surface area available for weathering.

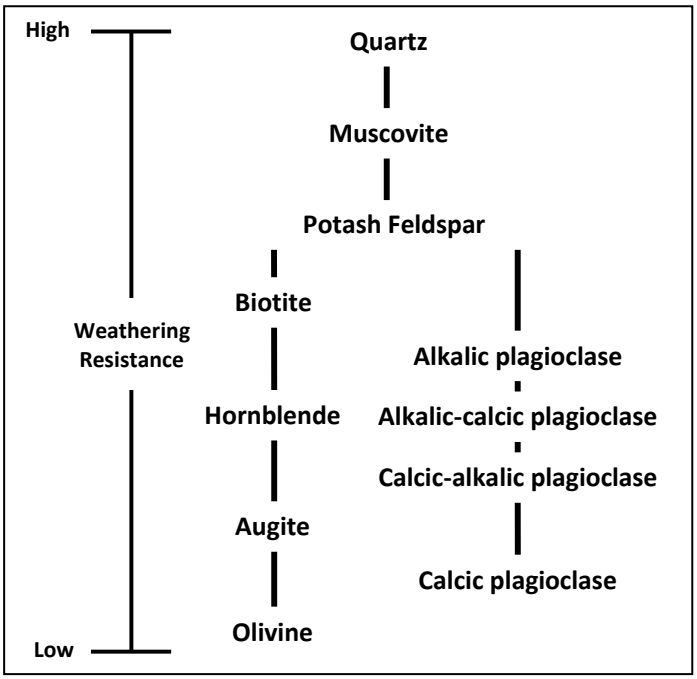


Figure 2.1. The Goldich Stability Series, adapted from Goldich, 1938

Parent material weathering rates are one of the most poorly understood soil processes due to the complex relationships between the various factors affecting weathering, with little quantitative data available (Ouimet & Duchesne, 2005; Løkke *et al.*, 1996). Rates of weathering are also the main source of uncertainty within critical load assessments (Li & McNulty, 2007). A variety of models have been developed in an attempt to quantify mineral weathering rates, including soil profile-based models such as Zirconium Depletion (Kirkwood & Nesbitt, 1991), PROFILE (Warfringe & Sverdrup, 1992) and Clay Content (Sverdrup *et al.*, 1990), as well as catchment-based models such as MAGIC (Cosby *et al.*, 1985) and Mass Balance Deficit (Clayton, 1979). Previous studies have shown significant variations in model outputs depending on parent material

mineralogy and soil acidity (Langan *et al.,* 1995; Whitfield *et al.,* 2006a; Koseva, Watmough & Aherne, 2010), and no single model has proven to be superior (Ouimet & Duchesne, 2005).

Within eastern Canada and United States, there is a growing body of evidence that suggests soils are experiencing base-cation depletions due to soil acid sensitivity (Federer *et al.,* 1989; Yanai *et al.,* 1999; Ouimet et al, 2001; Watmough & Dillon, 2001; Bélanger *et al.,* 2002). Nova Scotia soils have been documented as exceptionally acid sensitive due to the combination of small soil base-cation pools (Whitfield *et al.,* 2006a; 2006b), as well as low weathering rates due to considerable area being underlain by slates or granitic and felsic parent materials across the province (Clair *et al.,* 2002; Clair *et al.,* 2003; Ouimet *et al.,* 2006).

Atmospheric Deposition

Atmospheric deposition acts as both a primary source of nutrients to forested ecosystems, but also as a source of acidifying compounds through industrial and urban S and N emissions. Both acidifying compounds (SO_x, SO_4^{2-}, NO_3^-, NH_4^+) and base cations (Mg^{2+}, Ca^{2+}, K^+) are known to be deposited atmospherically in two main forms: wet and dry deposition (see Arp *et al.,* 2001). Wet deposition in the form of rain, snow, sleet, hail and fog is the result of atmospheric particles and gases being incorporated into cloud droplets. The subsequent form of precipitation that these droplets take, the total amount of precipitation received, and the concentration of ions within the droplets will dictate the amount of nutrient and acid deposited (Lovett, 1994). Dry deposition refers to the direct

sedimentation and diffusion of aerosol particles on vegetation and soil surfaces, the amount of which is mainly dictated by surface roughness (Hicks *et al.,* 1987).

SO_4^{2-} and SO_x deposition from anthropogenic emissions and marine salt influences are extensive across Nova Scotia (Underwood *et al.,* 1985), with SO_4^{2-} deposition considered the primary source of surface water acidification due to seasonal runoff within forested catchments (Kerekes *et al.,* 2004). Similarly, NO_3^- has been found to be a major constituent of wet deposition within eastern North America (Brydges & Summers, 1988). Although the accumulation of atmospherically derived NO_3^- and NH_4^+ have been linked to soil and water eutrophication throughout a number of forest regions (Hopkinson & Day, 1980; Prietzel & Kaiser, 2005), within eastern North America, this is not of concern as temperate forests are typically nitrogen limited (Vitousek & Howarth, 1991; McLauchlan *et al.,* 2007). The accumulation of N within upland forest soils that is not taken up by vegetation as an essential nutrient is therefore assumed to act solely as an acidifying agent caused by NO_3^- leaching (Brydges & Summers, 1988), and will not result in soil N-saturation and subsequent eutrophication. Base cations essential for plant growth (Mg^{2+}, Ca^{2+}, K^+) are known to be deposited both through industrial emissions (Hedin *et al.,* 1994), as well as from wind-blown dust particles, primarily in arid and semi-arid regions (Chang *et al.,* 1996). Although parent material weathering is generally considered the predominant input of soil base cations, many soils with acidic substrates rely on atmospheric deposition as the primary source of base cations to support vegetation (Draaijers *et al.,* 1997).

Within eastern North America, the New England Governors and Eastern Canadian Premiers Environmental Task Group on Forest Mapping developed a

nationwide protocol for modeling and mapping critical acid loads of atmospheric N and S (Carou *et al.*, 2008). The coarse resolution data suggests that acid deposition exceeds the buffering capacity of shallow forest soils within eastern Canada, by up to 500 eq ha^{-1} yr^{-1}, notably in southwest Nova Scotia (Ouimet *et al.*, 2001). Although, due to emission control strategies, there has been a noted decline of both acid and base-cation deposition within North America over the past decade (Lajtha & Jones, 2010), if current levels of acid deposition still exceed the soil buffering capacity, it may still pose a threat to forest soils across eastern Canada.

PRIMARY ELEMENT SINKS

Base-cation Depletion

Both the wet and dry accumulation of acidifying compounds within forest soils is known to cause leaching of essential base cations (DeHayes *et al.*, 1999), which can result in forest growth reduction, and overall forest decline (Duchesne *et al.*, 2002; McLaughlin, 1998). The leaching of base cations primarily occurs by allowing a toxic form of inorganic aluminum (Al^{3+}) to become mobile within soil solution due to a decrease in soil pH (Delhaize & Ryan, 1995). This form of aluminum, once soluble, has the ability to replace base cations on the soil cation exchange sites, thereby forcing base cations in solution, and thus more susceptible to leaching beyond the nutrient pool (i.e. depletion; Mossor-Pietraszewska, 2001). Quantifying Al^{3+} leaching, however, is difficult due to the complexity of Al speciation within soils (Mladkova *et al.*, 2005), as well as the inherent difficulties in addressing the relative toxicity levels of Al species between tree species and across soil layers (de Vries, 1991). However, since soil cation leaching tends

to be linearly related to atmospheric acid deposition loads (Dise & Wright, 1995), atmospheric N and S deposition rates can be used to quantify the extent of primary acid cation leaching (H^+, Al^{3+}) and base-cation leaching (Ca^{2+}, Mg^{2+}, K^+, Na^+)

Biomass Harvesting

As stated previously, the export of biomass from a forested site acts as a secondary sink, resulting in the removal of nutrients available for plant growth (Jorgenson *et al.*, 1975; Tew *et al.*, 1986). Although nutrient removal is linearly related to the mass of organic material being exported (Mann *et al.*, 1988; Federer *et al.*, 1989), there is a high degree of both spatial and temporal variation in aboveground nutrient pools. The amount of nutrients removed during a harvest event is dependent on: (i) the tree species composition, (ii) the biomass compartments being removed, relating to harvest type and seasonality, and (iii) the development stage of the trees at the time of harvest. Nutrient exports from harvesting are highly dependent on the relative proportions of tree species within the community due to differences in growth rates and nutrient demands between species (Augusto *et al.*, 2000; Hagen-Thorn *et al.*, 2004; Johnson & Cole, 2005). Generally, hardwoods require greater amounts of nutrients than conifers (Perala & Alban, 1982; Wilson & Grigal, 1995; Ste-Marie *et al.*, 2007), although significant differences within these two classes are also evident (Rochon *et al.*, 1998; Augusto *et al.*, 2000). These differences are directly related to the accumulation and storage of nutrients within individual biomass compartments. Foliage base-cation concentrations are generally greater in hardwoods (Augusto *et al.*, 2002), but even within individual trees, nutrient concentrations tend to follow the stem-wood < branches < bark

< foliage sequence (Pastor & Bockheim, 1984: Wang *et al.,* 1991; Mou *et al.,* 1993). The type of harvest implemented is therefore an important determining factor in the total export of nutrients from a forested site. Traditional stem-only harvesting is generally accepted as having a comparatively lower impact on forest nutrient pools than whole-tree removal in both conifer and hardwood communities (Olsson *et al.,* 1996 and Mroz *et al.,* 1985, respectively).

Numerous studies within Nova Scotia have suggested that whole-tree removal acts as a substantial export of primary nutrients due to branch and foliage compartments being relatively nutrient rich (Freedman, 1981; Freedman *et al.,* 1981; Freedman *et al.,* 1986). Stand development stage at the time of harvest also affects the amount of nutrients exported because younger stands accumulate nutrients more rapidly than older stands (Miller, 1995), with young trees having a greater portion of nutrient rich bark and foliage biomass than stem-wood and branches (Augusto *et al.,* 2000).

Within critical load methods, the removal of biomass and subsequent nutrient mass is expressed as uptake (BC_{up} and N_{up}; Eq. 2.2). Three harvest scenarios are used to represent the variation in biomass compartment removal depending on the type of harvest event: stem-only (stem-wood and bark compartments), full-tree brown (stem-wood, bark and branch compartments) and full-tree green (stem-wood, bark, branch and foliage compartments). Compartments that are not represented within the uptake equations under these three scenarios are assumed to remain within the nutrient pool of the forested site (see Bosman *et al.,* 2001). Although few studies have illustrated the impacts of biomass harvesting on soil critical acid loads, within southern Ontario, Watmough & Dillon (2003) found that critical acid loads generally were not exceeded within forested

catchments from base-cation depletion alone, but with the addition of a stem-only harvest scenario, all catchments were exceeded.

LITERATURE CITED

Arp, P. A., Leger, W., Moayeri, M., & Hurley, J. (2001). Methods for mapping forest sensitivity to acid deposition for northeastern North America. *Ecosystem Health, 7*, 35-47.

Augusto, L., Ranger, J., Binkley, D., & Rothe, A. (2002). Impact of several common tree species of European temperate forests on soil fertility. *Annals of Forest Science, 59*, 233-253.

Augusto, L., Ranger, J., Ponette, Q., & Rapp, M. (2000). Relationships between forest tree species, stand production and stand nutrient amount. *Annals of Forest Science, 57*, 313-324.

Bélanger, N., Courchesne, F., Côté, B., Fyles, J., Warfvingue, P., & Hendershot, W. (2002). Simulation of soil chemistry and nutrient availability in a forested ecosystem of southern Quebec. Part II. Application of the SAFE model. *Environmental Modelling & Software, 17*, 447-465.

Bosman, B., Remacle, J., & Carnol, M. (2001). Element removal in harvested tree biomass: scenarios for critical loads in Wallonia, South Belgium. *Water, Air, and Soil Pollution, 1*, 153-167.

Boudewyn, P., Song, X., Magnussen, S., & Gillis, M. (2007). *MODEL-BASED, VOLUME-TO-BIOMASS CONVERSION FOR FORESTED AND VEGETATED LAND IN CANADA.* Victoria, BC: Pacific Forestry Centre, Natural Resources Canada.

Brydges, T., & Summer, P. (1988). The acidifying potential of atmospheric deposition in Canada. *Water, Air, & Soil Pollution, 43*, 249-263.

Carou, S., Dennis, I., Aherne, J., Ouimet, R., Arp, P., Watmough, S., et al. (2008). *A NATIONAL PICTURE OF ACID DEPOSITION CRITICAL LOADS FOR FOREST SOILS IN CANADA.* CCME Acid Rain Task Group.

Champagne, P. (2007). Feasibility of producing bio-ethanol from waste residues: A Canadian perspective. *Resources, Conservation and Recycling, 50*, 211-230.

Chang, Y., Arndt, R., & Carmichael, G. (1996). Mineral base-cation deposition in Asia. *Atmospheric Environment, 30*, 2417-2427.

Clair, T., Dennis, I., Amiro, P., & Cosby, B. (2003). Probable changes in lake chemistry in Canada's Atlantic Provinces under proposed North American emission reductions. *Hydrology and Earth System Sciences Special Issue 7 , 7*, 574-583.

Clair, T., Ehrman, J., Ouellet, A., Brun, G., Lockerbie, D., & Ro, C. (2002). Changes in freshwater acidification trends in Canada's Atlantic Provinces: 1983-1997. *Water, Air, and Soil Pollution, 135*, 335-354.

Clayton, J. (1979). *Nutrient supply to soil by rock weathering. Impacts of Intensive Harvesting on Forest Nutrient Cycling.* Syracuse, NY: State University of New York.

Clayton, J. (1988). Some observations on the stoichiometry of feldspar hydrolysis in granitic soil. *Journal of Environmental Quality, 17*, 153-157.

Cosby, B., Hornberger, G., Galloway, J., & Wright, R. (1985). Modeling the effects of acid deposition: assessment of a lumped parameter model of soil water and streamwater chemistry. *Water Resources Research, 21*, 51-63.

de Vries, W. (1991). *METHODOLOGIES FOR THE ASSESSMENT AND MAPPING OF CRITICAL LOADS AND OF THE IMPACT OF ABATEMENT STRATEGIES ON FOREST SOILS.* Wageningen, The Netherlands: The Winand Staring Centre, Agricultural Research Department.

DeHayes, D., Schaberg, P., Hawley, G., & Strimbeck, R. (1999). Acid Rain Impacts on Calcium Nutrition and Forest Health: Alteration of membrane-associated calcium leads to membrane destabilization and foliar injury in red spruce. *BioScience, 49*, 789-800.

Delhaize, E., & Ryan, P. (1995). Aluminum Toxicity and Tolerance in Plants. *Plant Physiology, 107*, 315-321.

Draaijers, G., Van Leeuwen, E., De Jong, P., & Erisman, J. (1997). Base-cation deposition in Europe—part II. Acid neutralization capacity and contribution to forest nutrition. *Atmospheric Environment, 31*, 4159-4168.

Duchesne, L., Ouimet, R., & Houle, D. (2002). Basal Area Growth of Sugar Maple in Relation to Acid Deposition, Stand Health, and Soil Nutrients. *Journal of Environmental Quality, 31*, 1676-1683.

Federer, C., Hornbeck, J., Tritton, L., Martin, C., Pierce, R., & Smith, C. (1989). Long-term depletion of calcium and other nutrients in eastern U.S. forests. *Environmental Management, 13*, 593-601.

Freedman, B. (1981). *Intensive Forest Harvest: A REVIEW OF NUTRIENT BUDGET CONSIDERATIONS.* Fredericton, NB: Maritimes Forest Research Centre. Canadian Forest Service.

Freedman, B., Duinker, P., & Morash, R. (1986). Biomass and nutrients in Nova Scotian forests, and implications of intensive harvesting for future site productivity. *Forest Ecology and Management, 15*, 103-127.

Freedman, B., Morash, R., & Hanson, A. (1981). Biomass and Nutrient Removals by Conventional and Whole-tree Clear-cutting of a Red Spruce - Balsam Fir Stand in Central Nova Scotia. *Canadian Journal of Forest Research, 11*, 249-257.

Goldich, S. (1938). A Study in Rock-Weathering. *The Journal of Geology, 46*, 17-58.

Grennfelt, P., Moldan, F., Alveteg, M., Warfringe, P., & Sverdrup, H. (2001). Critical Loads - Is there need for a new concept? *Water, Air, and Soil Pollution, 1*, 21-27.

Hagen-Thorn, A., Armolaitis, K., Callesen, I., & Stjernquist, I. (2004). Macronutrients in tree stems and foliage: a comparative study of six temperate forest species planted at the same sites. *Annals of Forest Science, 61*, 489-498.

Hedin, L., Granat, G., Likens, T., Buishand, J., Galloway, T., & Rodhe, H. (1994). Steep declines in atmospheric base cations in regions of Europe and North America. *Nature, 367*, 351-354.

Hicks, B., Baldocchi, D., Meyers, T., Hosker, R., & Matt, D. (1987). A preliminary multiple resistance routine for deriving dry deposition velocities from measured quantities. *Water, Air, & Soil Pollution, 36*, 311-330.

Hopkinson, C., & Day, J. (1980). Modeling hydrology and eutrophication in a Louisiana swamp forest ecosystem. *Environmental Management, 4*, 325-335.

Johnson, D., & Cole, D. (2005). *NUTRIENT CYCLES IN CONIFER FORESTS (CH. 11),* taken from *ECOSYSTEMS OF THE WORLD, VOLUME 6: CONIFEROUS FORESTS.* The Netherlands: Elsevier B.V.

Jorgensen, J., Wells, C., & Metz, L. (1975). The Nutrient Cycle: Key to Continuous Forest Production. *Journal of Forestry, 73*, 400-403.

Kerekes, J., Beauchamp, S., Tordon, R., & Pollock, T. (2004). Sources of sulphate and acidity in wetlands and lakes in Nova Scotia. *Water, Air, & Soil Pollution, 31*, 207-214.

Kirkwood, D., & Nesbitt, H. (1991). Formation and evolution of soils from an acidified watershed: Plastic Lake, Ontario, Canada. *Geochimica et Cosmochimica, 55*, 1295-1308.

Koseva, I., Watmough, S., & Aherne, J. (2010). Estimating base-cation weathering rates in Canadian forest soils using a simple texture-based model. *Biogeochemistry, 101*, 183-196.

Lajtha, K., & Jones, J. (2010). Interactive effects of cations on multi-decade trends in sulfate and acid deposition in North America and Europe: a new look at an old problem. *American Geophysical Union*, Fall Meeting 2010, abstract #B12C-06.

Langan, S., Hodson, M., Bain, D., Skeffington, R., & Wilson, M. (1995). A preliminary review of weathering rates in relation to their method of calculation for acid sensitive soil parent materials. *Water, Air, & Soil Pollution, 85*, 1075-1081.

Levin, D., Zhu, H., Beland, M., Cicek, N., & Holbein, B. (2007). Potential for hydrogen and methane production from biomass residues in Canada. *Bioresource Technology, 98*, 654-660.

Li, H., & McNulty, S. (2007). Uncertainty analysis on simple mass balance model to calculate critical loads for soil acidity. *Environmental Pollution, 149*, 315-326.

Løkke, H., Bak, J., Falkengren-Grerup, U., Finlay, R., Ilvesniemi, H., & Nygaard, P. (1996). Critical loads of acidic deposition for forest soils: Is the current approach adequate? *Ambio, 25*, 510-516.

Lovett, G. (1994). Atmospheric Deposition of Nutrients and Pollutants in North America: An Ecological Perspective. *Ecological Applications, 4*, 630-650.

Mann, L., Johnson, D., West, D., Cole, D., Hornbeck, J., Martin, C., et al. (1988). Effects of whole-tree and stem-only clearcutting on postharvest hydrologic losses, nutrient capital and regrowth. *Forest Science, 34*, 412-428.

McLauchlan, K., Craine, J., Oswald, W., Leavitt, P., & Likens, G. (2007). Changes in nitrogen cycling during the past century in a northern hardwood forest. *PNAS, 104*, 7466-7470.

McLaughlin, D. (1998). A decade of forest tree monitoring in Canada: evidence of air pollution effects. *Environmental Reviews, 6*, 151-171.

Miller, H. (1995). The influence of stand development on nutrient demand, growth and allocation. *Plant and Soil, 168-169*, 225-232.

Mladkova, L., Boruvka, L., & Drabek, O. (2005). Soil Properties and Selected Aluminum Forms in Acid Forest Soils as Influenced by the Type of Stand Factors. *Soil Science and Plant Nutrition, 51*, 741-744.

Mossor-Pietraszewska, T. (2001). Effect of aluminium on plant growth and metabolism. *Acta Biochimica Polonica, 48*, 673-686.

Mou, P., Fahey, T., & Hughes, J. (1993). Effects of Soil Disturbance on Vegetation Recovery and Nutrient Accumulation Following Whole-Tree Harvest of a Northern Hardwood Ecosystem. *Journal of Applied Ecology, 30*, 661-675.

Mroz, G., Jurgenson, M., & Frederick, D. (1985). Soil nutrient changes following whole tree harvesting on three northern hardwood sites. Soil Science *Society of America Journal, 49*, 1552-1557.

Nasr, M., Castonguay, M., Ogilvie, J., Raymond, B., & Arp, P. (2010). Modelling and mapping critical loads and exceedances for the Georgia Basin, British Columbia, using a zero base-cation depletion criterion. *Journal of Limnology, 69*, 181-192.

Nilsson, J., & Grennfelt, P. (1988). *CRITICAL LOADS OF SULPHUR AND NITROGEN: REPORT FROM A WORKSHOP HELD AT SKOKLOSTER, SWEDEN, 19-24 MARCH, 1988.* Nordic Council of Ministers: Kobenhaven.

Olsson, B., Staaf, H., Lundkvist, H., Bengtsson, J., & Rosen, K. (1996). Carbon and nitrogen in coniferous forest soils after clear-felling and harvests of different intensity. *Forest Ecology & Management, 82*, 19-32.

Ouimet, R., & Duchesne, L. (2005). Base-cation mineral weathering and total release rates from soils in three calibrated forest watersheds on the Canadian Boreal Shield. *Canadian Journal of Soil Science, 85*, 245-260.

Ouimet, R., Arp, P., Watmough, S., Aherne, J., & Demerchant, I. (2006). Determination and mapping of critical loads of acidity and exceedances for upland forest soils in Eastern Canada. *Water, Air and Soil Pollution, 172*, 57-66.

Ouimet, R., Duchesne, L., Houle, D., & Arp, P. (2001). Critical loads and exceedances of acid deposition and associated forest growth in the northern hardwood and boreal coniferous forests in Quebec, Canada. *Water, Air, and Soil Pollution, 1*, 119-134.

Pastor, J., & Bockheim, J. (1984). Distribution andCycling of Nutrients in an Aspen-Mixed-Hardwood-Spodosol Ecosystem in Northern Wisconsin. *Ecology, 65*, 339-353.

Perala, D., & Alban, D. (1982). Biomass, nutrient distribution and litterfall in Populus, Pinus and Picea stands on two different soils in Minnesota. *Plant and Soil, 64*, 177-192.

Ploeg, R., Böhm, R. v., & Kirkham, M. (1999). On the origin of the theory of mineral nutrition of plants and the Law of the Minimum. *Soil Science Society of America, 63*, 1055 - 1062.

Prietzel, J., & Kaiser, K. (2005). De-eutrophication of a nitrogen-saturated Scots pine forest by prescribed litter-raking. *Journal of Plant Nutrition and Soil Science, 168*, 461-471.

Rochon, P., Pare, D., & Messier, C. (1998). Development of an improved model estimating the nutrient content of the bole for four boreal tree species. *Canadian Journal of Forest Research, 28*, 37-43.

Ste-Marie, C., Pare, D., & Gagnon, D. (2007). The Contrasting Effects of Aspen and Jack Pine on Soil Nutritional Properties Depend on Parent Material. *Ecosystems, 10*, 1299-1310.

Sverdrup, H., & Rosen, K. (1998). Long-term base-cation mass balances for Swedish forests and the concept of sustainability. *Forest Ecology and Management, 110*, 221-236.

Sverdrup, H., & Warfringe, P. (1993). Calculating field weathering rates using a mechanistic geochemical model PROFILE. *Applied Geochemistry, 8*, 273-283.

Sverdrup, H., DeVries, W., & Henriksen, A. (1990). *MAPPING CRITICAL LOADS: A GUIDELINE TO THE CRITERIA, CALCULATIONS, DATA COLLECTION, AND MAPPING OF CRITICAL LOADS.* Copenhagen: Miljoraport. Nordic Council of Ministers, NORD.

Sverdrup, H., Thelin, G., Robles, M., Stjernquist, I., & Sorenson, J. (2006). Assesing nutrient sustainability for forest production for different tree species considering Ca, Mg, K, N and P at Bjornstorp Estate, Sweden. *Biogeochemistry, 81*, 219-238.

Tew, D., Morris, L., Allen, H., & Wells, C. (1986). Estimates of nutrient removal, displacement and loss resulting from harvest and site preparation of a Pinus taeda plantation in the Piedmont of North Carolina. *Forest Ecology and Management, 15*, 257-267.

Townsend, P. (2008). *FOREST BIOMASS OF LIVING, MERCHANTABLE TREES IN NOVA SCOTIA.* Truro, NS: Nova Scotia Department of Natural Resources.

Underwood, J., Ogden, J., Kerekes, J., & Vaughan, H. (1985). Acidification of Nova Scotia Lakes. *Water, Air, & Soil Pollution, 32*, 77-88.

Velbel, M. (1985). Geochemical mass balances and weathering rates in forested watershed of the southern Blue Ridge. *American Journal of Science, 285*, 904-930.

Vitousek, P., & Howarth, R. (1991). Nitrogen Limitation on Land and in the Sea: How Can It Occur? *Biogeochemistry, 13*, 87-115.

Wang, D., Bormann, F., Lugo, A., & Bowden, R. (1991). Comparison of nutrient-use efficiency and biomass production in five tropical tree taxa. *Forest Ecology and Management, 46*, 1-21.

Warfringe, P., & Sverdrup, H. (1992). Calculating critical loads of acid deposition with PROFILE - a steady-state soil chemistry model. *Water, Air, and Soil Pollution, 63*, 119-143.

Watmough, S., & Dillon, P. (2003). 'Do critical load models adequately protect forests? A case study in south-central Ontario'. *Canadian Journal of Forest Research, 33*, 1544-1556.

Watmough, S., & Dillon, P. (2001). Base-cation losses from a coniferous catchment in Central Ontario, Canada. *Water, Air, and Soil Pollution, 1*, 507-524.

Werner, B., & Spranger, T. (1996). *MANUAL ON METHODOLOGIES AND CRITERIA FOR MAPPING CRITICAL LEVEL/LOADS AND GEOGRAPHICAL AREAS WHERE THEY ARE EXCEEDED.* Berlin, Germany: Federal Environmental Agency (Umweltbundesamt).

White, A., Blum, A., Bullen, T., Vivit, D., Schulz, M., & Fitzpatrick, J. (1999). The effect of temperature on experimental and natural chemical weathering rates of granitoid rocks. *Geochimica et Cosmochimica Acta, 63*, 3277-3291.

Whitfield, C., Aherne, J., Dillon, P., & Watmough, S. (2006b). Modelling acidification, recovery and target loads for headwater catchments in Nova Scotia, Canada. *Hydrology and Earth System Sciences Discussions, 3*, 3595-3627.

Whitfield, C., Watmough, S., Aherne, J., & Dillon, P. (2006a). A comparison of weathering rates for acid-sensitive catchments in Nova Scotia, Canada and their impacts on critical load calculations. *Geoderma, 136*, 899-911.

Wilson, D., & Grigal, D. (1995). Effects of pine plantations and adjacent deciduous forests on soil calcium. *Soil Science Society of America Journal, 59*, 1755-1761.

Yanai, R., Siccama, T., Arthur, M., Federer, C., & Friedland, A. (1999). Accumulations and depletion of base cations in forest floors in the northeastern United States. *Ecology, 80*, 2774-2787.

Yemshanov, D., & McKenney, D. (2008). Fast-growing poplar plantations as a bioenergy supply source for Canada. *Biomass and Bioenergy, 32*, 185-197.

CHAPTER 3

FOREST BIOMASS PROJECTIONS I: A COMPARISON OF TWO CURRENT PUBLISHED STEM BIOMASS EQUATION SETS WITH A NEWLY RECOMMENDED METHOD OF OBTAINING STEM BIOMASS

INTRODUCTION

The method of predicting individual tree biomass through allometric relationships between tree dimensions is termed "dimensional analysis" (Whittaker & Woodwell, 1968). This method is used to indirectly quantify forest biomass to determine sustainable harvest levels (Gronowska *et al.,* 2009), as well as a means of calculating forest carbon budgets (Kurz *et al.,* 2002). The following chapter discusses the various dimensional analyses conducted in order to predict stem biomass, for 17 commercial tree species within the Nova Scotia forest inventory[1]. A stem-wood density dependant method of projecting stem biomass will be compared to two published biomass equation sets, both of which were found to be generally limited to a 20- to 40-cm DBH range. This bias became apparent when combining the projected stem biomass with Honer's stem volume estimates (Honer *et al.,* 1983), and comparing the resulting wood density trends with published wood densities by Gonzalez, (1990). This problem also concurs with the conclusion drawn by Neumann & Jandl (2005), that parameter dependant biomass equations rarely account for the entire range of potential stem diameters, and may therefore limit the accuracy of stand level biomass estimations (see also Jenkins *et al.,* 2003).

[1] see Appendix I for the complete list of tree species within the Nova Scotia forest inventory.

METHODOLOGY

The two sets of published equations assessed were regional diameter based equations by Ker (1980a; 1980b), and national diameter based equations by Lambert *et al.*, (2005), respectively, as set by:

$$Stem_{Ker} = c \exp\left(\gamma_{stem1} + \gamma_{stem2} \ln\left(DBH\right)\right) \quad (3.1)$$

$$Stem_{Lambert} = \left(\beta_{wood1} \left(DBH\right)^{\beta_{wood2}}\right) + \left(\beta_{bark1} \left(DBH\right)^{\beta_{bark2}}\right) \quad (3.2)$$

where *Stem* refers to total stem biomass (kg) for both the *Ker* and *Lambert* equation sets, γ refers to Ker's species-specific biomass parameters (Appendix II), *c* denotes the correction factor used to remove bias from linear to logarithmic regression analyses, and β refers to Lambert's species-specific biomass parameters (Appendix III). The Ker studies were formulated for 17 commercial tree species, native to the Acadian forest region (see Rowe, 1972), and in order to maintain consistency, only those species common to both studies were reviewed (Table 3.1). Using both equation sets, oven-dry stem biomass was calculated for each species across a broad range of stem diameters (2- to 100-cm DBH). For simplicity, equation sets using only DBH as the predictive variable were used, and all equations were realized within the Modelmaker modeling framework (1999). Stem densities were calculated using the projected stem biomass estimates and Honer volumes, across the DBH range, for each species. The method of predicting stem biomass first involved allometrically relating stem diameter to volume, such that:

$$Volume = a\ DBH^{b} \quad (3.3)$$

where *Volume* refers to individual stem volume (m^3), and *a* and *b* are least-squares calibrated, species-specific parameter values, validated using Honer's volumes. Stem biomass was then calculated by setting:

$$M_{stem} = Volume\ D \quad (3.4)$$

where M_{stem} refers to stem biomass (tonnes), and *D* are the species-specific stem densities taken from Gonzalez (1990; tonnes m^{-3}; Appendix IV).

Table 3.1. Common name, Latin name and species code of the 17 tree species within this study.

Common Name	Latin Name	Species Code
Beech	*Fagus grandifolia*	BE
Balsam Fir	*Abies balsamea*	BF
Black Spruce	*Picea mariana*	BS
Eastern Hemlock	*Tsuga canadensis*	EH
Eastern Larch	*Larix laricina*	TL
Eastern White Cedar	*Thuja occidentalis*	EC
Eastern White Pine	*Pinus strobus*	WP
Jack Pine	*Pinus banksiana*	JP
Red Maple	*Acer rubrum*	RM
Red Pine	*Pinus resinosa*	RP
Red Spruce	*Picea rubens*	RS
Sugar Maple	*Acer saccharum*	SM
Trembling Aspen	*Populus tremuloides*	TA
White Ash	*Fraxinus americana*	WA
White Birch	*Betula papyrifera*	WB
White Spruce	*Picea glauca*	WS
Yellow Birch	*Betula alleghaniensis*	YB

RESULTS AND DISCUSSION

The diameter-volume relationship parameters (*a* and *b*) as they relate to Honer's volumes are found in Table 3.2, along with the error and r^2 values. The close correspondence between predicted and Honer's volumes suggests that volume can be directly calculated from tree diameters alone, with considerable confidence ($r^2 > 0.968$).

Table 3.2. Species-specific volume-diameter relationship parameter values (a and b; Eq. 3.4), error values (±), and r^2 values.

	a	±	b	±	r^2
BE	0.00062815	0.00000634	2.0059	0.0022	0.99995
BF	0.00061410	0.00015273	2.0201	0.0538	0.96863
BS	0.00060611	0.00015618	2.0146	0.0558	0.96863
EC	0.00046498	0.00013511	2.0108	0.0629	0.97723
EH	0.00052221	0.00011895	2.0419	0.0493	0.97733
JP	0.00063278	0.00013433	2.0110	0.0460	0.97746
RM	0.00056128	0.00012383	2.0049	0.0478	0.98175
RP	0.00063508	0.00010506	2.0299	0.0358	0.98395
RS	0.00060611	0.00015618	2.0146	0.0558	0.96863
SM	0.00060275	0.00011363	2.0097	0.0408	0.98404
TA	0.00069486	0.00012644	2.0113	0.0394	0.97998
TL	0.00069642	0.00010359	2.0109	0.0322	0.98660
WA	0.00056128	0.00012383	2.0049	0.0478	0.98175
WB	0.00056059	0.00009831	2.0025	0.0380	0.98872
WP	0.00058919	0.00002906	2.0723	0.0107	0.99827
WS	0.00058753	0.00002514	2.0369	0.0093	0.99903
YB	0.00057360	0.00001317	2.0096	0.0050	0.99979

Predicted and published wood densities are plotted for all 17 species in Figures 3.1 - 3.17, versus Honer's volumes. Generally, predicted densities were either under- or overestimated for small volume stems, and always overestimated for large volume stems for both the Ker and Lambert equation sets, with many species approaching or exceeding 1 tonne m^{-3}. The stem biomass predictions (Eq. 3.1, 3.2 and 3.4) are plotted across the DBH range for each species in Figures 3.18 - 3.34. Generally, estimates are comparable between studies within the first 40-cm DBH, although the Lambert equations tend to produce the highest biomass estimates for diameters >40cm, with few exceptions.

Although regression equations are generally the dominant method of predicting stem biomass (Crow & Schlaegel, 1988), a number of biomass and carbon studies have used wood-density corrected methods, particularly within tropical regions (Brown &

Lugo, 1984; Fearnside, 1997; Ketterings et al., 2001). Parresol & Thomas (1989) first introduced the concept of a density-integral approach for calculating stem biomass, and concluded that this approach gave more precise estimates than other predictive methods (see Parresol & Thomas, 1996; Thomas *et al.*, 1995). A study by Schroeder *et al.*, (1997), evaluating biomass expansion factors (BEF's), which were used to allometrically convert volume to total tree biomass, suggested that BEF's for calculating stem biomass alone would be equal to the average wood density of broadleaf stands within the northeast United States. The approach discussed within this chapter takes this concept one step further by applying species-specific volumes and wood densities as they relate to current stand compositions. In summary, due to the elevated wood densities projected from both parameter driven functions (Eq. 3.1 - 3.2), it is suggested that the revised function (Eq. 3.4) be used to calculate systematic, and wood-density correct biomass projections, and is the current approach used within this study.

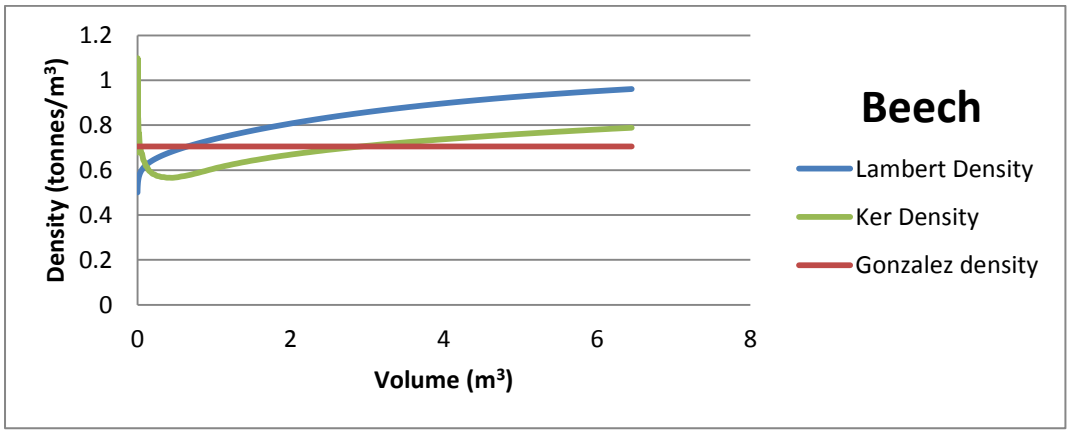


Figure 3.1. Beech stem density (tonnes/m^3) over volume (m^3) using biomass equations by Lambert *et al.*, (2005) and Ker (1980a; 1980b), as well as published density by Gonzalez (1990).

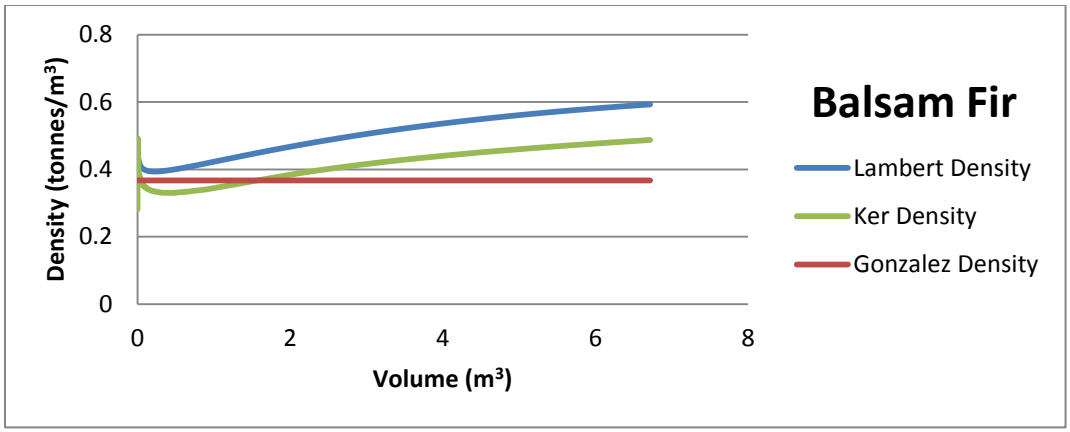


Figure 3.2. Balsam Fir stem density (tonnes/m^3) over volume (m^3) using biomass equations by Lambert *et al.*, (2005) and Ker (1980a; 1980b), as well as published density by Gonzalez (1990).

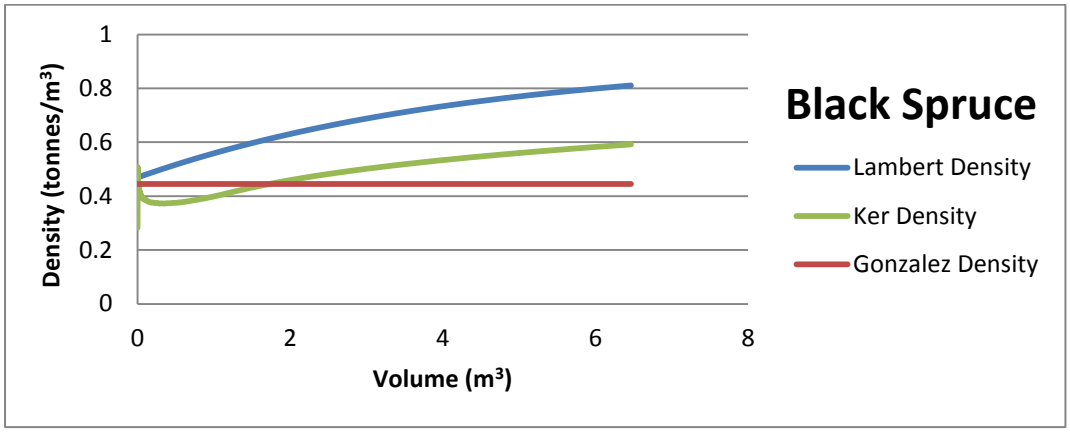


Figure 3.3. Black Spruce stem density (tonnes/m^3) over volume (m^3) using biomass equations by Lambert *et al.*, (2005) and Ker (1980a; 1980b), as well as published density by Gonzalez (1990).

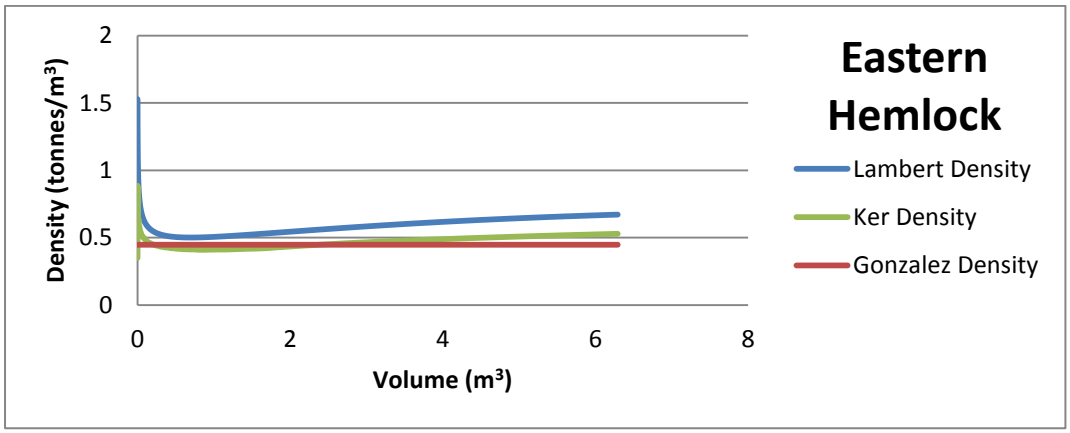


Figure 3.4. Eastern Hemlock stem density (tonnes/m^3) over volume (m^3) using biomass equations by Lambert *et al.*, (2005) and Ker (1980a; 1980b), as well as published density by Gonzalez (1990).

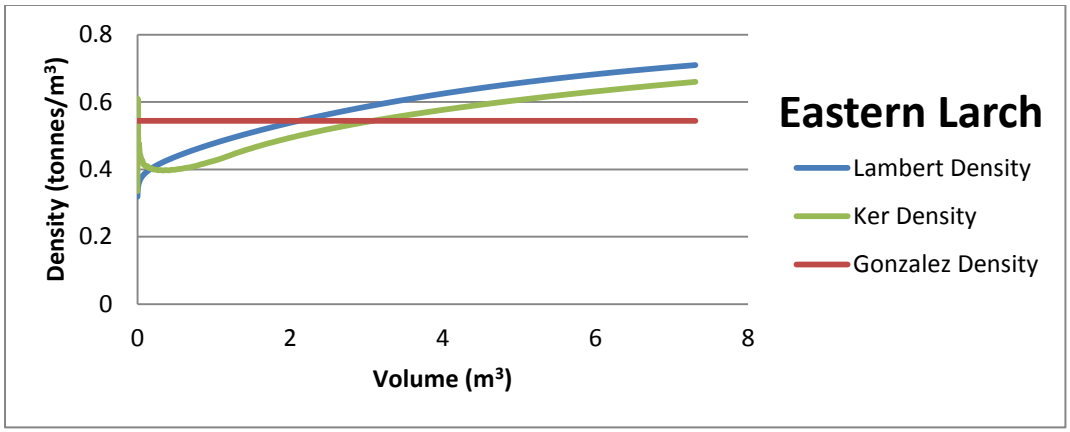


Figure 3.5. Eastern Larch stem density (tonnes/m^3) over volume (m^3) using biomass equations by Lambert *et al.*, (2005) and Ker (1980a; 1980b), as well as published density by Gonzalez (1990).

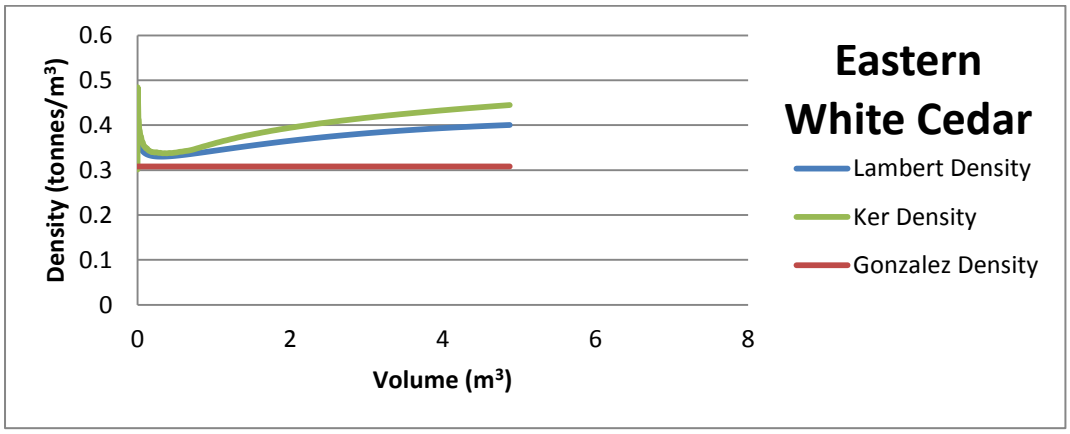


Figure 3.6. Eastern White Cedar stem density (tonnes/m^3) over volume (m^3) using biomass equations by Lambert *et al.*, (2005) and Ker (1980a; 1980b), as well as published density by Gonzalez (1990).

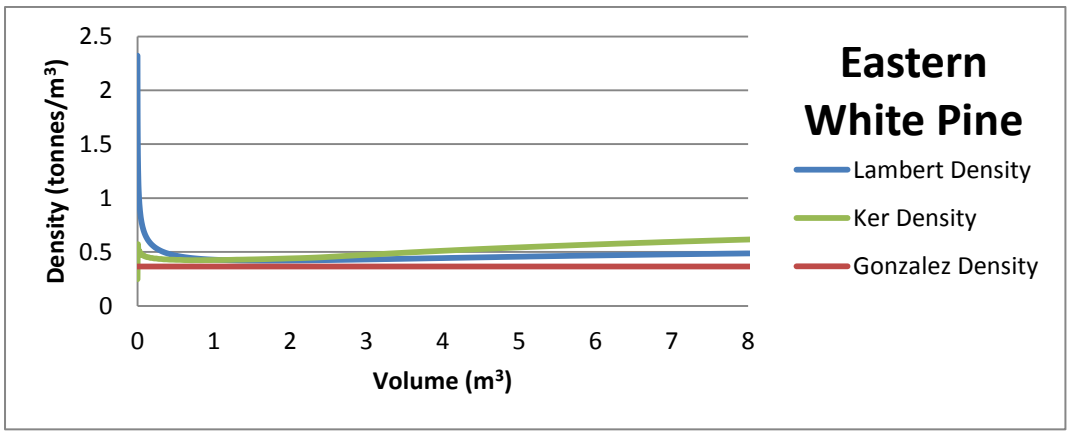


Figure 3.7. Eastern White Pine stem density (tonnes/m^3) over volume (m^3) using biomass equations by Lambert *et al.*, (2005) and Ker (1980a; 1980b), as well as published density by Gonzalez (1990).

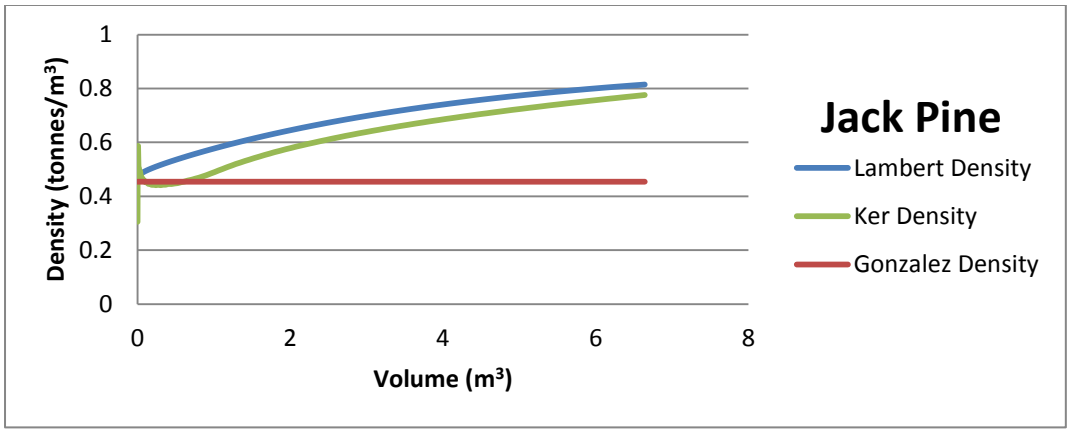


Figure 3.8. Jack Pine stem density (tonnes/m^3) over volume (m^3) using biomass equations by Lambert *et al.*, (2005) and Ker (1980a; 1980b), as well as published density by Gonzalez (1990).

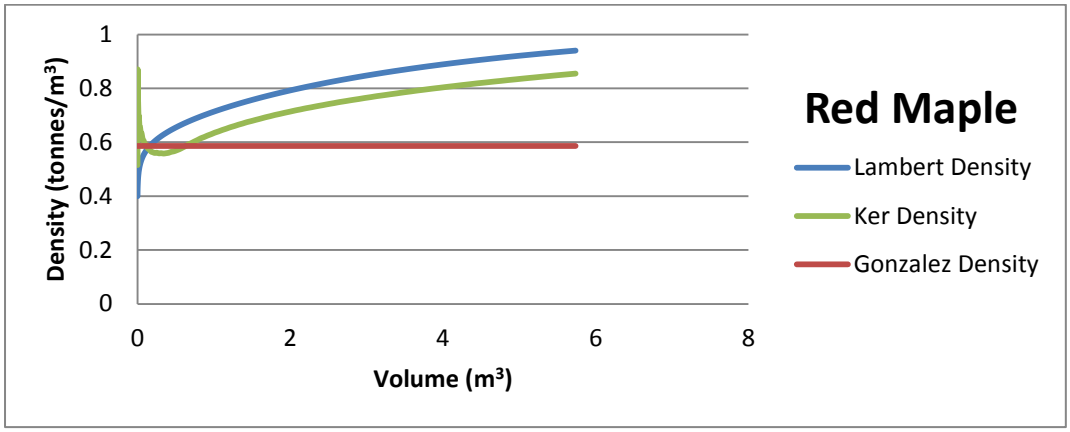


Figure 3.9. Red Maple stem density (tonnes/m^3) over volume (m^3) using biomass equations by Lambert *et al.*, (2005) and Ker (1980a; 1980b), as well as published density by Gonzalez (1990).

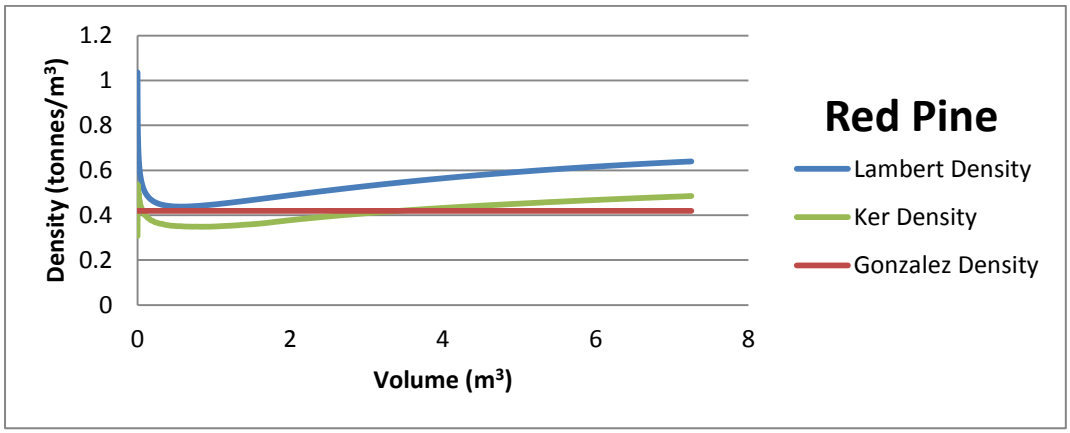


Figure 3.10. Red Pine stem density (tonnes/m^3) over volume (m^3) using biomass equations by Lambert *et al.*, (2005) and Ker (1980a; 1980b), as well as published density by Gonzalez (1990).

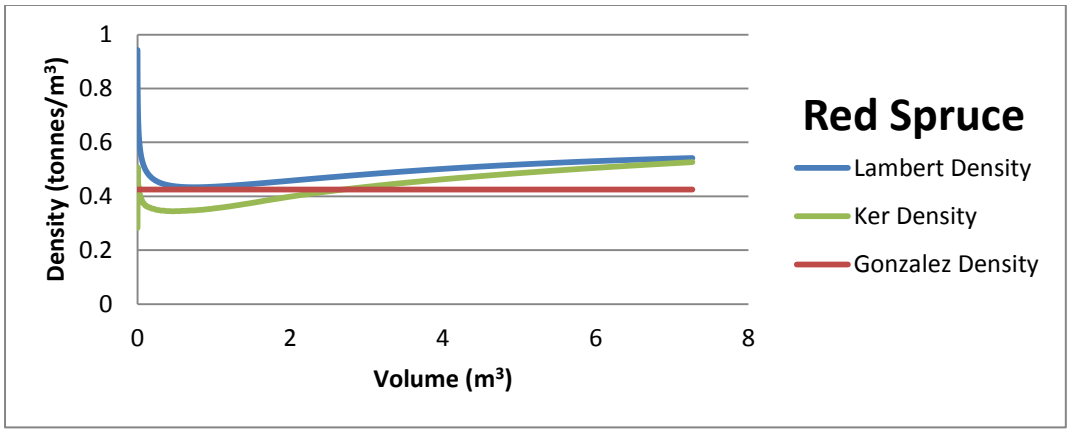


Figure 3.11. Red Spruce stem density (tonnes/m^3) over volume (m^3) using biomass equations by Lambert *et al.*, (2005) and Ker (1980a; 1980b), as well as published density by Gonzalez (1990).

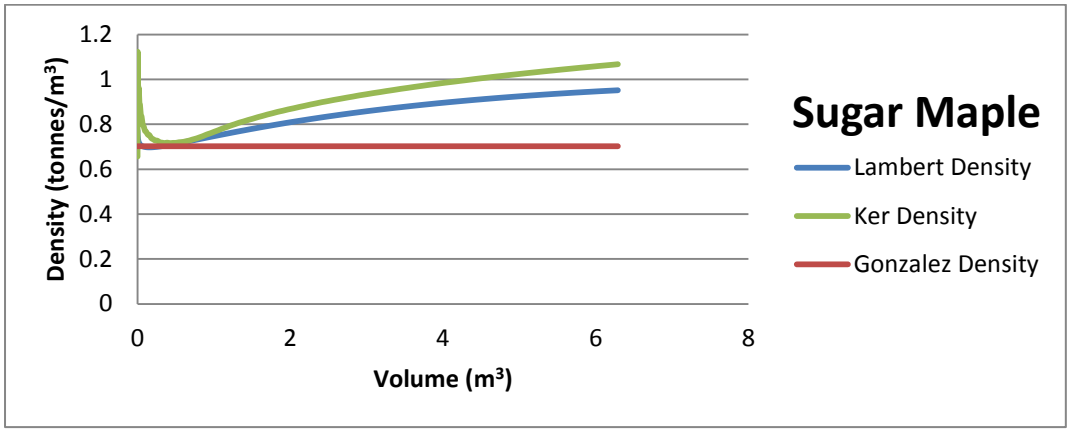


Figure 3.12. Sugar Maple stem density (tonnes/m^3) over volume (m^3) using biomass equations by Lambert *et al.*, (2005) and Ker (1980a; 1980b), as well as published density by Gonzalez (1990).

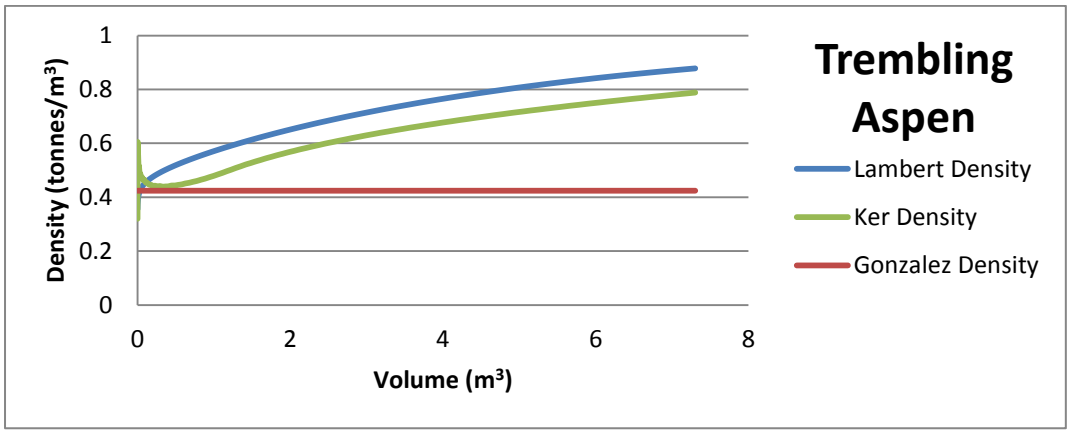


Figure 3.13. Trembling Aspen stem density (tonnes/m^3) over volume (m^3) using biomass equations by Lambert *et al.*, (2005) and Ker (1980a; 1980b), as well as published density by Gonzalez (1990).

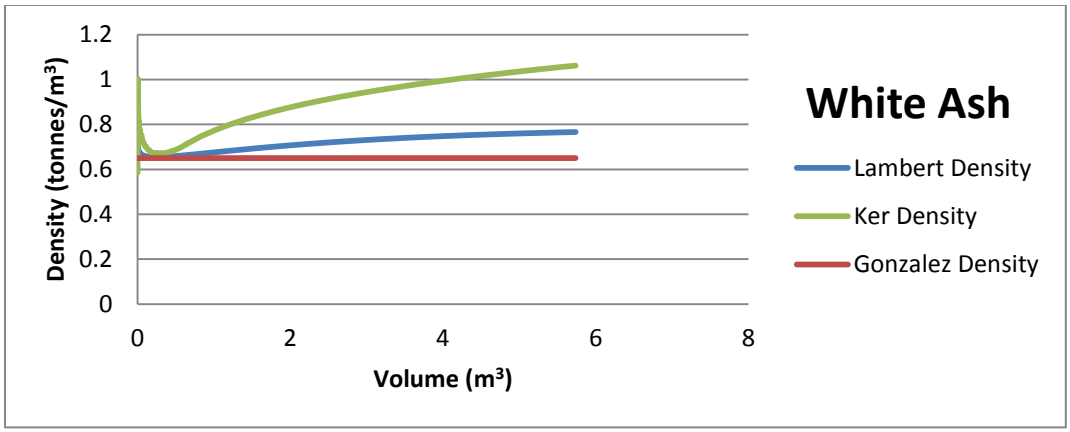


Figure 3.14. White Ash stem density (tonnes/m^3) over volume (m^3) using biomass equations by Lambert *et al.*, (2005) and Ker (1980a; 1980b), as well as published density by Gonzalez (1990).

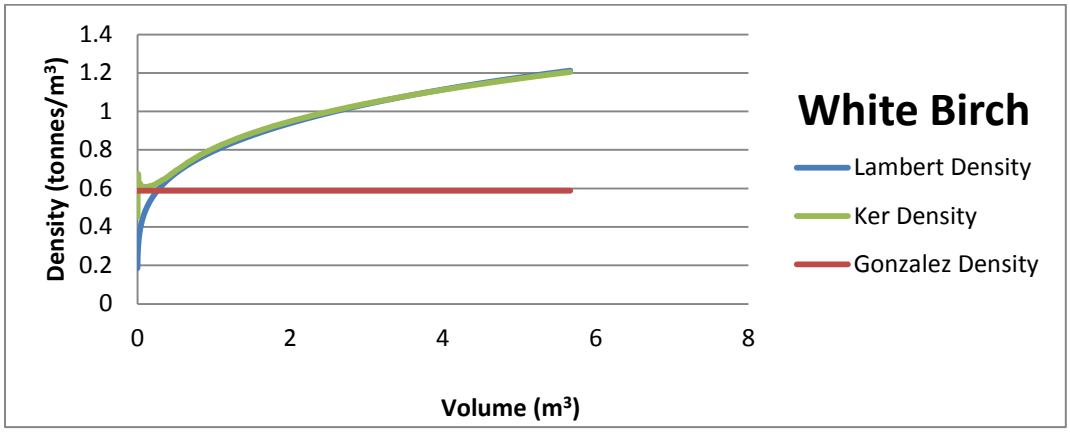


Figure 3.15. White Birch stem density (tonnes/m^3) over volume (m^3) using biomass equations by Lambert *et al.*, (2005) and Ker (1980a; 1980b), as well as published density by Gonzalez (1990).

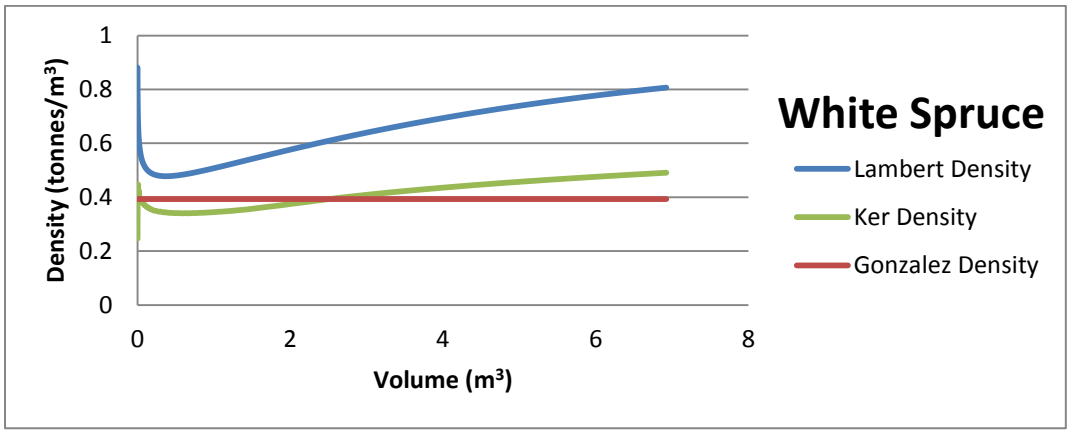


Figure 3.16. White Spruce stem density (tonnes/m^3) over volume (m^3) using biomass equations by Lambert *et al.*, (2005) and Ker (1980a; 1980b), as well as published density by Gonzalez (1990).

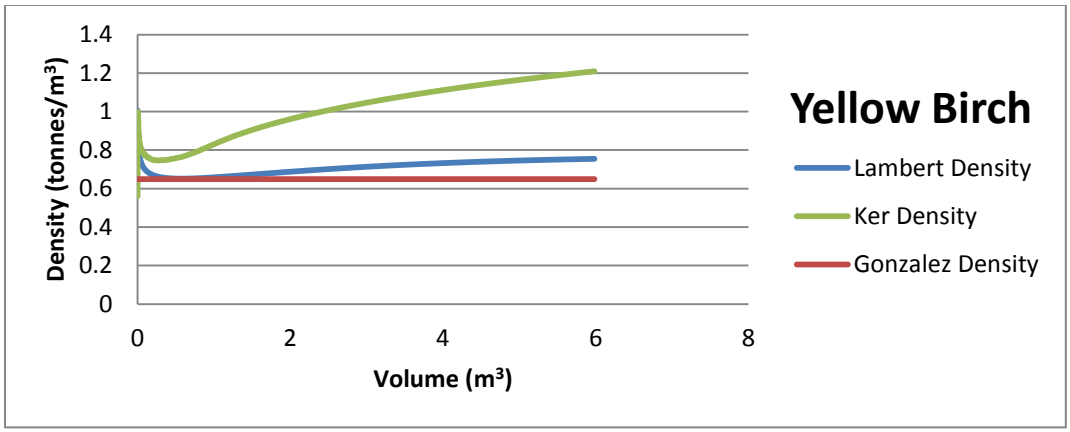


Figure 3.17. Yellow Birch stem density (tonnes/m^3) over volume (m^3) using biomass equations by Lambert *et al.*, (2005) and Ker (1980a; 1980b), as well as published density by Gonzalez (1990).

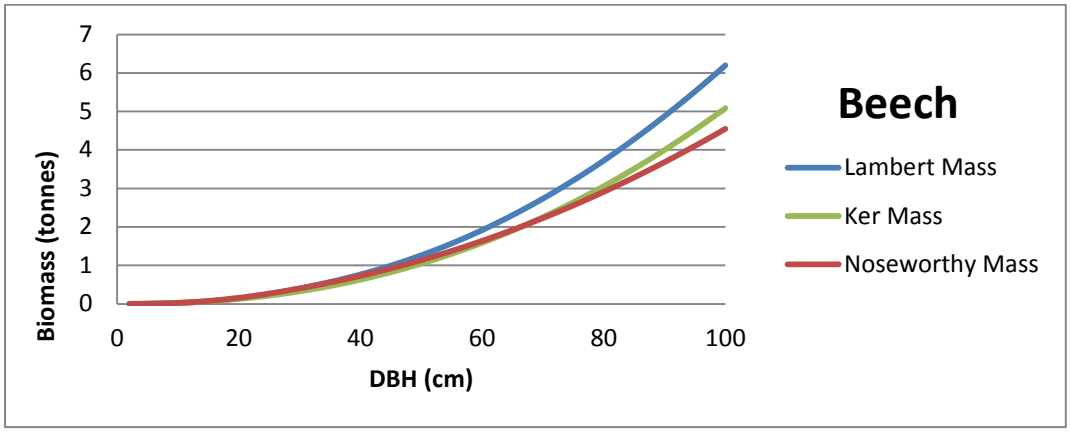


Figure 3.18. Beech stem biomass (tonnes) over stem DBH (cm) using biomass equations of Lambert *et al.*, (2005) and Ker (1980a, b), as well as the generated method in this paper.

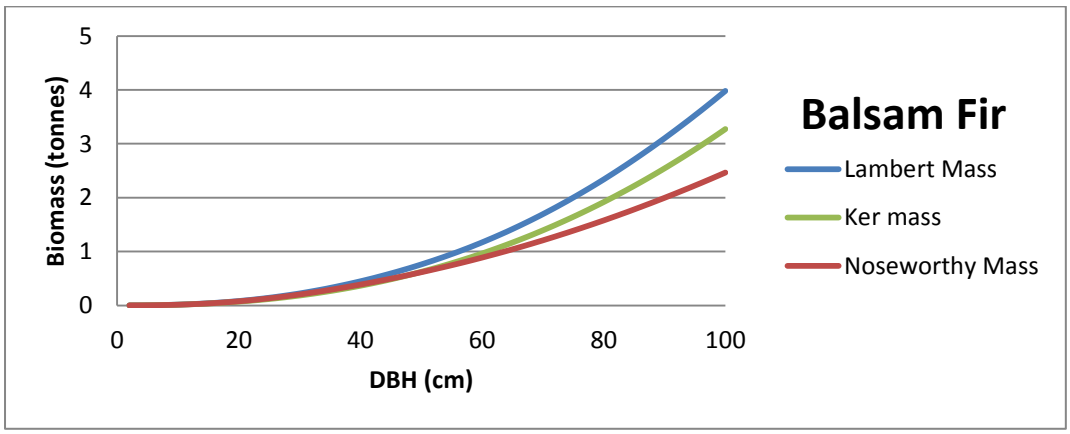


Figure 3.19. Balsam Fir stem biomass (tonnes) over stem DBH (cm) using biomass equations of Lambert *et al.*, (2005) and Ker (1980a, b), as well as the generated method in this paper.

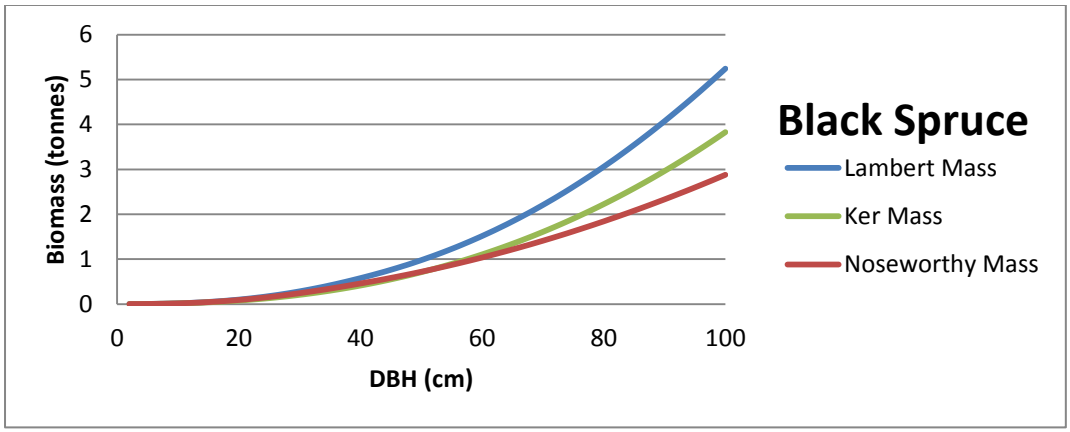


Figure 3.20. Black Spruce stem biomass (tonnes) over stem DBH (cm) using biomass equations of Lambert *et al.*, (2005) and Ker (1980a, b), as well as the generated method in this paper.

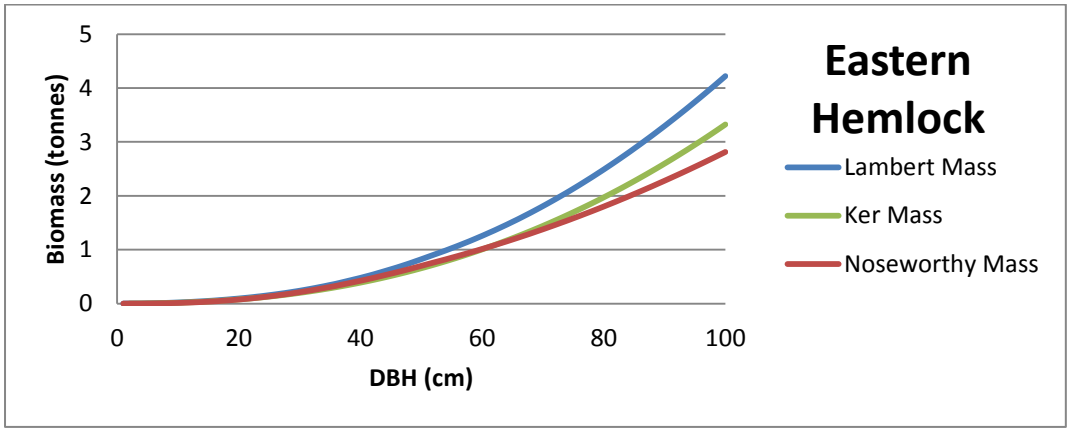


Figure 3.21. Eastern Hemlock stem biomass (tonnes) over stem DBH (cm) using biomass equations of Lambert *et al.*, (2005) and Ker (1980a, b), as well as the generated method in this paper.

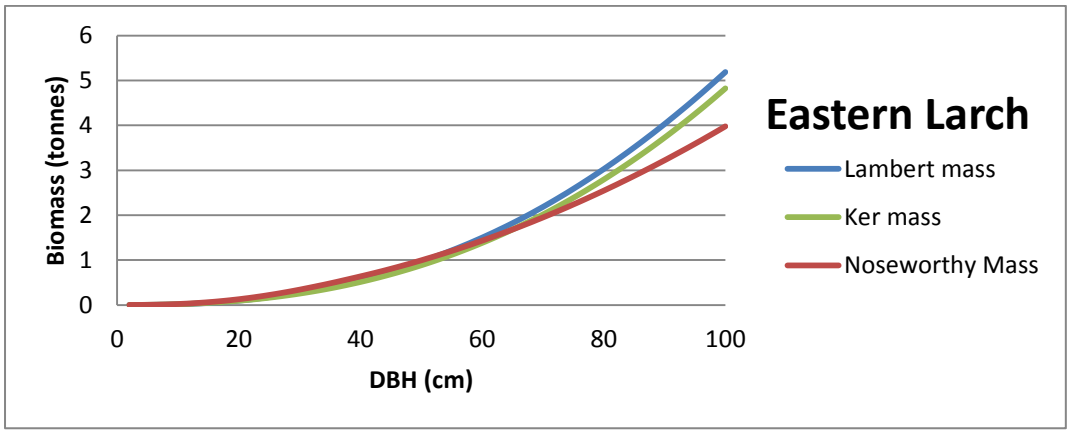


Figure 3.22. Eastern Larch stem biomass (tonnes) over stem DBH (cm) using biomass equations of Lambert *et al.*, (2005) and Ker (1980a, b), as well as the generated method in this paper.

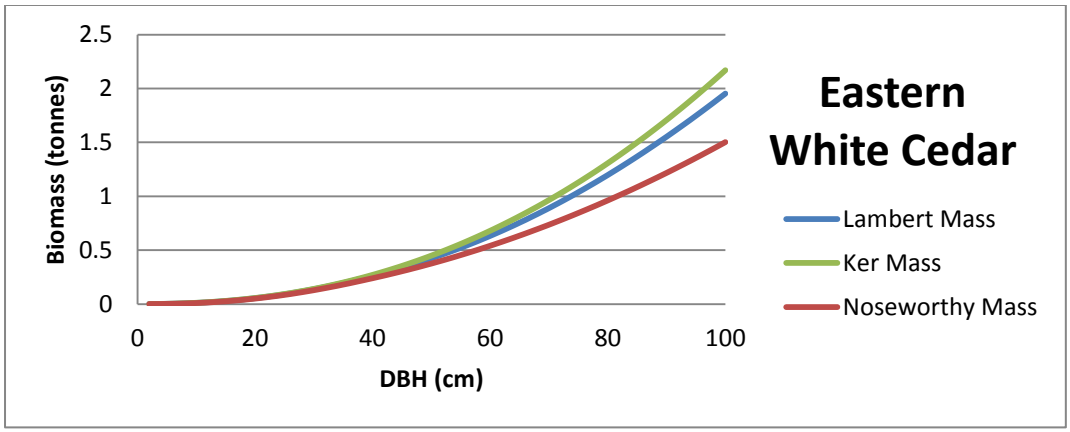


Figure 3.23. Eastern White Cedar stem biomass (tonnes) over stem DBH (cm) using biomass equations of Lambert *et al.*, (2005) and Ker (1980a, b), as well as the generated method in this paper.

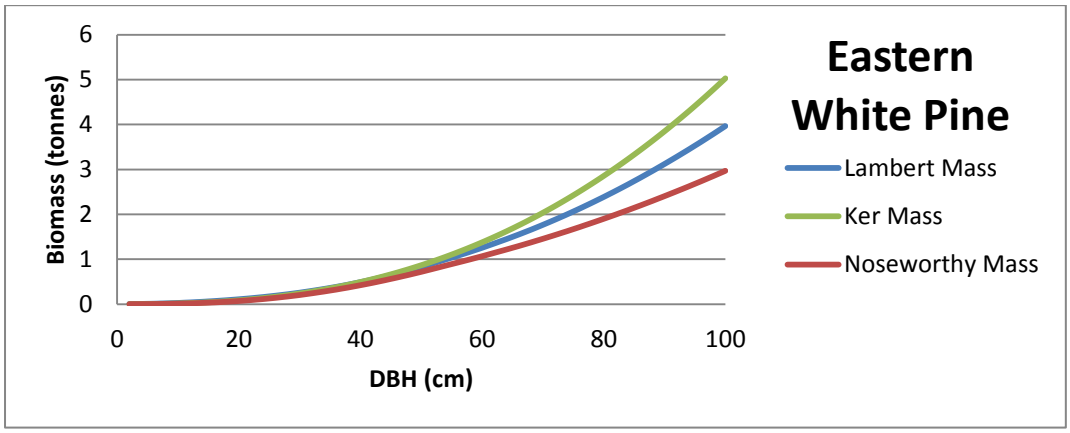


Figure 3.24. Eastern White Pine stem biomass (tonnes) over stem DBH (cm) using biomass equations of Lambert *et al.*, (2005) and Ker (1980a, b), as well as the generated method in this paper.

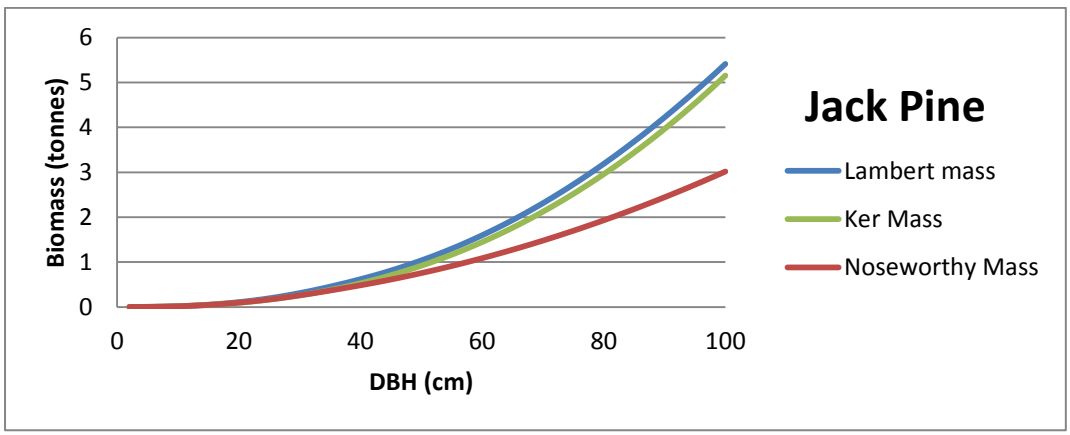


Figure 3.25. Jack Pine stem biomass (tonnes) over stem DBH (cm) using biomass equations of Lambert *et al.*, (2005) and Ker (1980a, b), as well as the generated method in this paper.

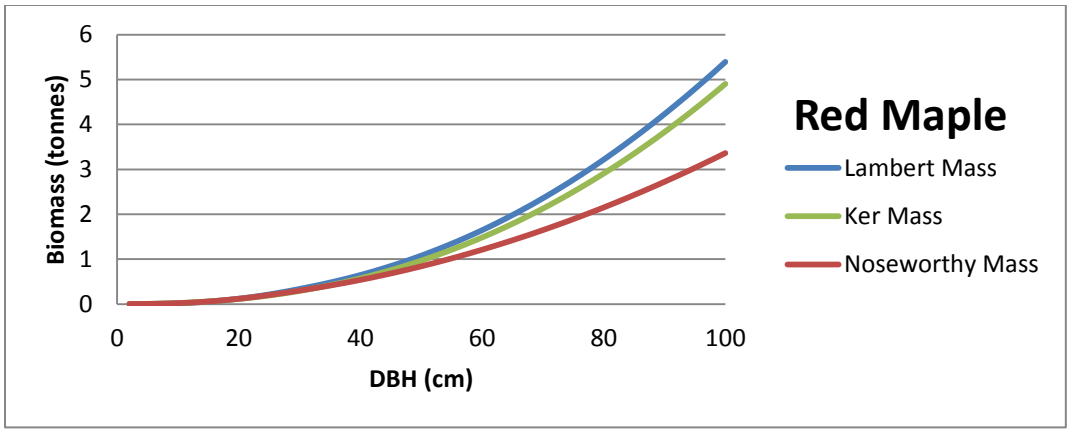


Figure 3.26. Red Maple stem biomass (tonnes) over stem DBH (cm) using biomass equations of Lambert *et al.*, (2005) and Ker (1980a, b), as well as the generated method in this paper.

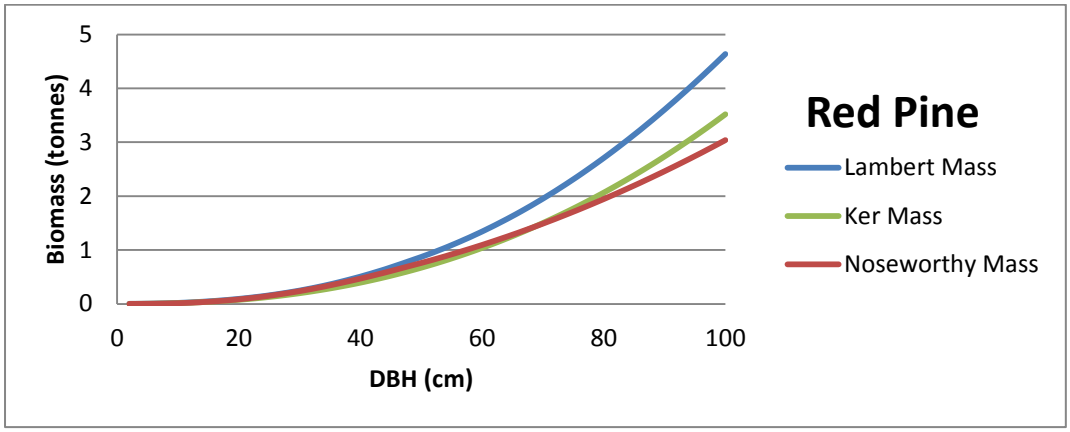


Figure 3.27. Red Pine stem biomass (tonnes) over stem DBH (cm) using biomass equations of Lambert *et al.*, (2005) and Ker (1980a, b), as well as the generated method in this paper.

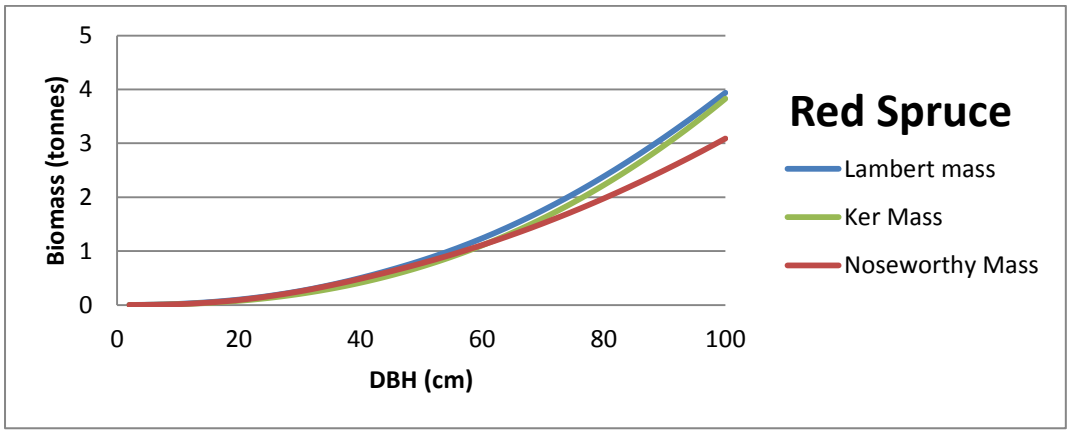


Figure 3.28. Red Spruce stem biomass (tonnes) over stem DBH (cm) using biomass equations of Lambert *et al.*, (2005) and Ker (1980a, b), as well as the generated method in this paper.

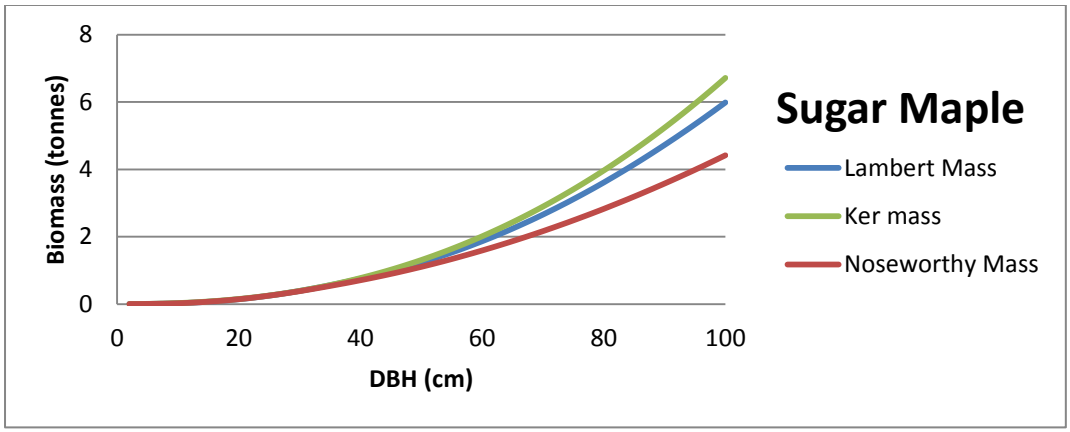


Figure 3.29. Sugar Maple stem biomass (tonnes) over stem DBH (cm) using biomass equations of Lambert *et al.*, (2005) and Ker (1980a, b), as well as the generated method in this paper.

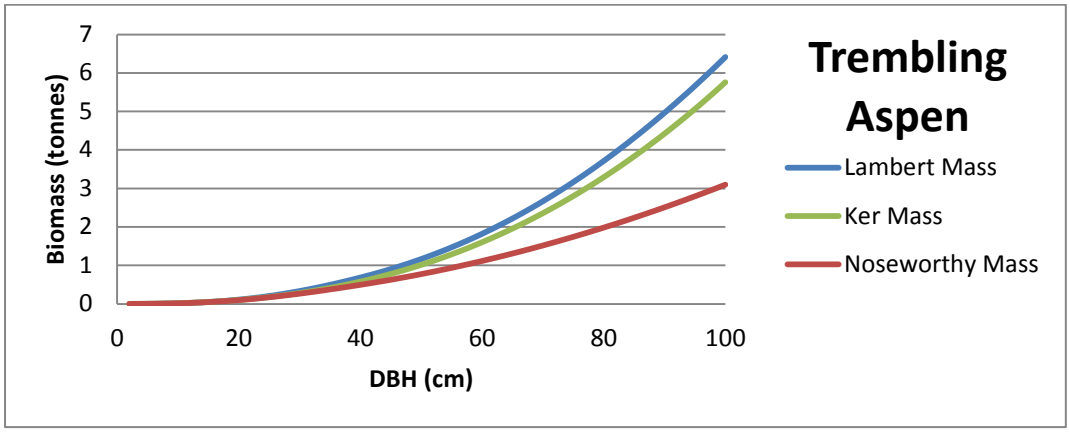


Figure 3.30. Trembling Aspen stem biomass (tonnes) over stem DBH (cm) using biomass equations of Lambert *et al.*, (2005) and Ker (1980a, b), as well as the generated method in this paper.

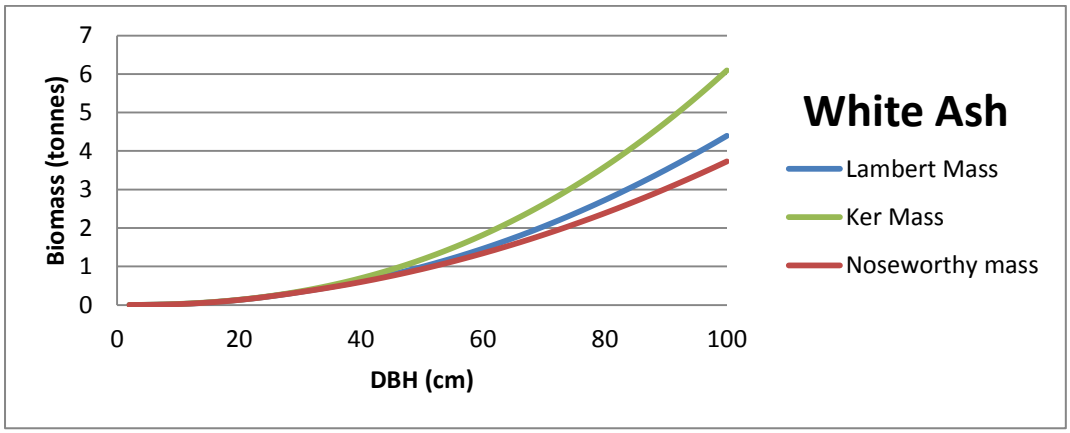


Figure 3.31. White Ash stem biomass (tonnes) over stem DBH (cm) using biomass equations of Lambert *et al.*, (2005) and Ker (1980a, b), as well as the generated method in this paper.

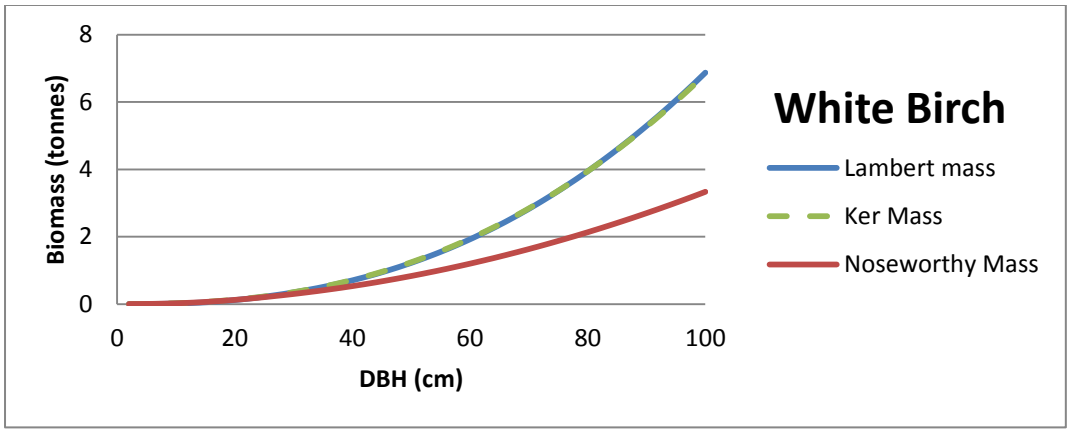


Figure 3.32. White Birch stem biomass (tonnes) over stem DBH (cm) using biomass equations of Lambert *et al.*, (2005) and Ker (1980a, b), as well as the generated method in this paper.

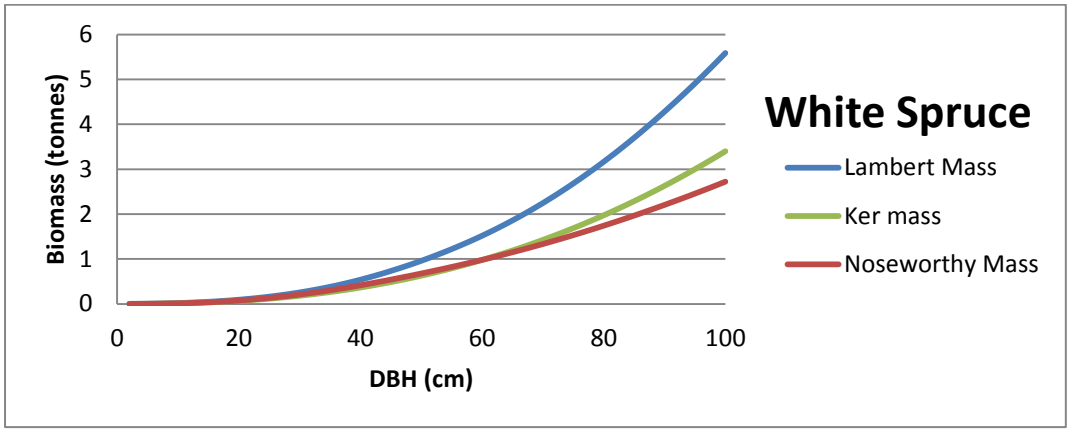


Figure 3.33. White Spruce stem biomass (tonnes) over stem DBH (cm) using biomass equations of Lambert *et al.*, (2005) and Ker (1980a, b), as well as the generated method in this paper.

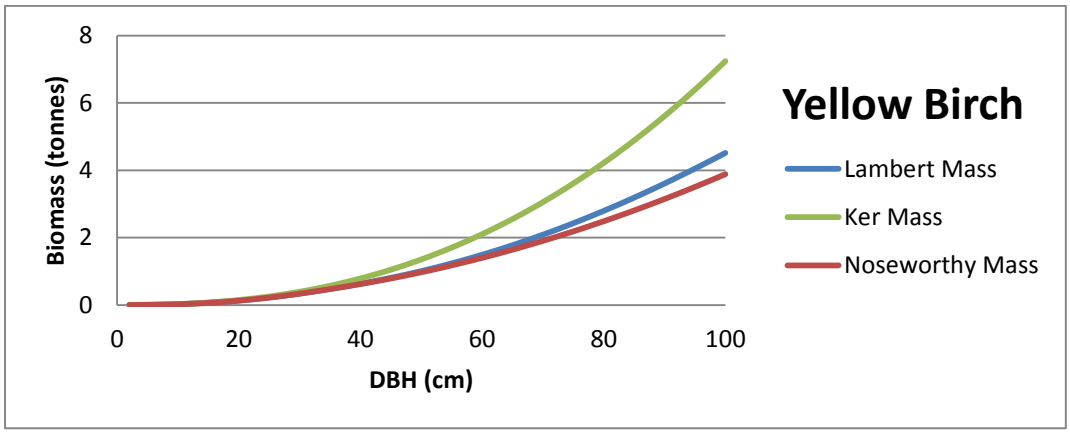


Figure 3.34. Yellow Birch stem biomass (tonnes) over stem DBH (cm) using biomass equations of Lambert *et al.*, (2005) and Ker (1980a, b), as well as the generated method in this paper.

LITERATURE CITED

Brown, S., & Lugo, A. (1984). Biomass of Tropical Forests: A New Estimate Based on Forest Volumes. *Science, 223*, 1290-1293.

Crow, T., & Schlaegal, B. (1988). A Guide to Using Regression Equations for Estimating Tree Biomass. *Northern Journal of Applied Forestry, 5*, 15-22.

Fearnside, P. (1997). Wood density for estimating forest biomass in Brazilian Amazonia. *Forest Ecology and Management, 90*, 59-87.

Gonzalez, J. (1990). *Wood density of Canadian tree species.* Edmonton, Alberta: Forestry Canada, Northwest Region, Northern Forestry Centre. Information Report NOR-X-315.

Gronowska, M., Joshi, S., & Maclean, H. (2009). A review of U.S. and Canadian biomass supply studies. *BioResources, 4*, 341-369.

Honer, T., Ker, M., & Alemdag, I. (1983). *Metric timber tables for the commercial tree species of central and eastern Canada.* Fredericton, N.B.: Maritime Forest Research Centre. Information Report M-X-140.

Jenkins, J., Chojnacky, D., Heath, L., & Birdsey, R. (2003). National-Scale Biomass Estimators for United States Tree Species. *Forest Science, 49*, 12-35(24).

Ker, M. (1980a). *Tree biomass equations for seven species in southwestern New Brunswick.* Fredericton, N.B.: Maritime Forest Research Centre. Information Report M-X-114.

Ker, M. (1980b). *Tree biomass equations for ten major species in Cumberland County, Nova Scotia.* Fredericton, N.B.: Maritime Forest Research Centre. Information Report M-X-108.

Ketterings, Q., Coe, R., Noordmijk, M., Ambagau, Y., & Palm, C. (2001). Reducing uncertainty in the use of allometric biomass equations for predicting above-ground tree biomass in mixed secondary forests. *Forest Ecology and Management, 146*, 199-209.

Kurz, W., Apps, M., Banfield, E., & Stinson, G. (2002). Forest carbon accounting at the operational scale. *Forestry Chronicle, 78*, 672-679.

Lambert, M., Ung, C., & Raulier, F. (2005). Canadian national tree aboveground biomass equations. *Canadian Journal of Forest Research, 35*, 1996-2018.

ModelMaker. (1999). [Computer Software]. Cherwell Scientific Ltd. Oxford, U.K.

Neumann, M., & Jandl, R. (2005). Derivation of locally valid estimators of the aboveground biomass of Norway spruce. *European Journal of Forest Research, 124*, 125-131.

Parresol, B., & Thomas, C. (1989). A density-integral approach to estimating stem biomass. *Forest Ecology and Management, 26*, 285-297.

Parresol, B., & Thomas, C. (1996). A simultaneous density-integral system for estimating stem profile and biomass: Slash pine and willow oak. *Canadian Journal of Forest Research, 26*, 773-781.

Rowe, J.S. (1972). *Forest Regions of Canada.* Canadian Forest Service. Publication No. 1300.

Schroeder, P., Brown, S., Mo, J., Birdsey, R., & Cieszewski, C. (1997). Biomass estimations for temperate broadleaf forests of the United States using inventory data. *Forest Science, 43*, 424-434.

Thomas, C., Parresol, B., & Le, K. (1995). Biomass and taper for trees in thinned and unthinned longleaf pine plantations. *Southern Journal of Applied Forestry, 19*, 29-35.

Whittaker, R., & Woodwell, G. (1968). Dimension and production relations of trees and shrubs in the Brookhaven forest, New York. *Journal of Ecology, 56*, 1-25.

CHAPTER 4

FOREST BIOMASS PROJECTION II: DIAMETER-BASED BARK, BRANCH, STEM-WOOD AND FOLIAGE BIOMASS PROJECTIONS

INTRODUCTION

The national Lambert equations (Lambert *et al.*, 2005) and regional Ker equations (Ker, 1980a; 1980b) introduced in the previous chapter provide a practical means of determining diameter-based, tree biomass in respect to above-ground compartments (no roots or stump). In the preceding chapter, it was shown that both the Lambert and Ker stem biomass equations were generally in good agreement with the expectations arising from multiplying stem volume with wood density, within a limited empirical range. Outside this range, the published stem biomass estimates were found to be exaggerated, and it is assumed that the wood-density correct projections provide better estimates of stem biomass. This chapter is a continuation of the previous, and describes the process of developing consistently viable stem-wood, foliage, branch and bark biomass projections by way of prorated biomass expansion factors (BEF), using the wood-density correct stem biomass projections from Chapter 3.

METHODOLOGY

Prorated BEF's of bark, branch, stem-wood and foliage were calculated across the DBH range for both the Lambert and Ker equation sets, such that:

$$R_{Tissue} = A\exp\left[B\ln\left(DBH\right)\right] \tag{4.1}$$

where *R* refers to the prorated ratio for each compartment. For the Lambert equation set, *A* and *B* were calculated as:

$$A_{Lambert} = \left(\frac{\beta_{X1}}{\beta_{Stem1}} \right) \tag{4.2}$$

$$B_{Lambert} = \left(\beta_{X2} - \beta_{stem2} \right) \tag{4.3}$$

where subscript *X* denotes one of the 4 aboveground tree biomass compartments and β refers to Lambert's species-specific parameters (1 and 2) per biomass compartment (see Appendix III). For the Ker model, a modified version of the above equations accounts for the correction factor used to remove bias from linear to logarithmic regression analysis (*c*), such that:

$$A_{Ker} = \left(\frac{c_X}{c_{stem}} \right) \exp\left(\gamma_{X1} - \gamma_{Stem1} \right) \tag{4.4}$$

$$B_{Ker} = \left(\gamma_{X2} - \gamma_{stem2} \right) \tag{4.5}$$

where γ refers to Ker's species-specific parameters per biomass compartment (see Appendix II). The above equations were realized within the Modelmaker modeling framework (1999). Final biomass compartment values are calculated by multiplying the stem biomass (M_{stem}; Eq. 3.4) with the prorated BEF ratio from Eq. 4.1.

RESULTS AND DISCUSSION

All species-specific biomass parameter values (*A* and *B*) are compiled in Tables 4.1 and 4.2 for the Lambert and Ker equation sets, respectively. Plotted biomass

compartment ratios for each tree species can be found in Figures 4.1 - 4.34, which alternate between the Lambert and Ker equation sets. Both equation set ratios were generally found to correlate well for hardwoods, but in the case of conifers, the Ker equations tend to overestimate the relative contribution of foliage and branch compartments to total biomass, particularly within small diameter classes. The only major discrepancy observed was the linear trend in Lambert's Red Spruce branch ratio. As seen in Appendix III, the branch β_1 parameter is significantly lower than all other species, and contradicts Ker's observation that both Black Spruce and Red Spruce have similar growth patterns (Ker, 1984). Since the resulting trends between the two studies are comparable, it is recommended that (i) the prorated Lambert parameters be used to calculate compartment-specific biomass due to greater species representation than the Ker studies, and (ii) that Lambert's Red Spruce branch parameter be substituted with the Black Spruce branch parameter, as suggested by Ker.

Due to the nature of regression equations for calculating tree biomass, compartment-specific projections would follow the same trend as the stem biomass projections, which as shown in Chapter 3, are limited to a narrow DBH range. It is therefore assumed that compartment-specific biomass can be determined with greater accuracy when the regression parameters are converted to DBH-dependant BEF ratios, and used in conjunction with density-corrected stem biomass estimates. The use of BEF's to calculate compartment-specific biomass from stem biomass projections has been applied extensively (Somogyi *et al.*, 2006; Brown *et al.*, 1999; Teobaldelli *et al.*, 2009), although previous approaches have typically used stem biomass regression equations as the basis for BEF's, which likely over- or underestimate stem biomass (see Chapter 3).

Although the stem biomass projections from Chapter 3 are shown to be volume and density dependant, stand-level stem biomass projections can be calculated by simply substituting individual stem volume with merchantable stand volume, per tree species. This method, in addition to using average stand diameters, allows for stand level biomass estimations to be calculated directly from forest inventory data. Biomass estimates can then be summed to represent differences in harvest scenarios (Figure 4.35), as discussed in further detail in Chapter 7.

Table 4.1. Derived species-specific parameter values (A and B; Eq. 4.5 and 4.6 respectively), for each of the biomass compartment ratio equations adapted from Lambert et al., (2005).

	Foliage		Bark		Branches		Stemwood		Total	
	A	B	A	B	A	B	A	B	A	B
BE	0.2357	-0.6786	0.0752	-0.0562	0.2320	0.0730	0.9267	0.0036	1.2714	0.0105
BF	0.8350	-0.7255	0.1778	-0.0466	0.1082	0.1456	0.8257	0.0080	1.3246	-0.0115
BS	2.8232	-1.0756	0.2621	-0.2470	0.4762	-0.4060	0.8172	0.0248	1.4357	-0.0594
EC	0.6528	-0.4764	0.1491	-0.0610	0.4382	-0.2675	0.8555	0.0079	1.6164	-0.0647
EH	1.0274	-0.6744	0.1840	-0.0457	0.2873	-0.1086	0.8195	0.0082	1.5207	-0.0479
JP	0.4255	-0.6576	0.2013	-0.3163	0.0864	0.0289	0.8795	0.0175	1.1869	-0.0128
RM	0.4206	-0.8024	0.2377	-0.2329	0.1429	0.1624	0.8281	0.0226	1.1587	0.0270
RP	0.3206	-0.3544	0.2843	-0.3707	0.0499	0.3281	0.8529	0.0231	1.1083	0.0326
RS	0.0564	0.1571	0.1881	-0.1734	0.0043	1.0108	0.8458	0.0172	0.5113	0.2421
SM	0.2379	-0.5871	0.3820	-0.3560	0.1998	0.0940	0.7962	0.0328	1.2501	0.0124
TA	0.3400	-0.8310	0.2188	-0.0665	0.1042	0.0600	0.7881	0.0136	1.1438	0.0002
TL	1.0990	-0.9390	0.2387	-0.3156	0.2689	-0.1613	0.8575	0.0210	1.3454	-0.0356
WA	0.5015	-0.9224	0.1841	-0.1555	0.2091	0.0790	0.8439	0.0164	1.2469	0.0103
WB	0.7582	-0.8548	0.1875	-0.0846	0.1875	0.0633	0.8234	0.0127	1.2726	-0.0013
WP	0.2400	-0.3249	0.1623	-0.0586	0.0473	0.3387	0.8426	0.0085	1.0718	0.0382
WS	3.6451	-1.0856	0.2641	-0.2504	0.6443	-0.4703	0.8174	0.0249	1.5246	-0.0715
YB	0.5310	-0.7686	0.0911	0.0816	0.1447	0.2385	0.9169	-0.0090	1.1211	0.0556

Table 4.2. Derived species-specific parameter values (A and B; Eq. 4.7 and 4.8 respectively), for each of the biomass compartment ratio equations adapted from Ker, (1980a; 1980b).

	Foliage		Bark		Branches		Stemwood		Total	
	A	B	A	B	A	B	A	B	A	B
BE	0.1768	-0.6506	0.1141	-0.1655	0.2217	0.0899	0.8901	0.0147	1.4174	-0.0271
BF	1.2107	-0.7195	0.2383	-0.1541	1.4152	-0.6139	0.7748	0.0296	3.0761	-0.2649
BS	1.5845	-0.7115	0.2414	-0.2506	1.2558	-0.4900	0.7810	0.0422	3.2794	-0.2544
EC	0.5828	-0.6500	0.1542	-0.0478	0.7946	-0.5272	0.8417	0.0098	1.8587	-0.1267
EH	0.6855	-0.6589	0.2068	-0.0758	0.8929	-0.4261	0.7993	0.0152	2.3942	-0.1882
JP	0.2732	-0.4371	0.3521	-0.4967	0.3534	-0.2440	0.7462	0.0695	2.0299	-0.1592
RM	0.1786	-0.6889	0.2219	-0.1999	0.1876	0.0088	0.7858	0.0377	1.3090	-0.0219
RP	0.2123	-0.2672	0.2698	-0.3191	0.1438	0.0739	0.7648	0.0526	1.4599	-0.0389
RS	1.5845	-0.7115	0.2414	-0.2506	1.2558	-0.4900	0.7810	0.0422	3.2794	-0.2544
SM	0.1257	-0.6613	0.1664	-0.0919	0.1516	0.0238	0.8092	0.0266	1.2644	-0.0227
TA	0.1854	-0.6641	0.2538	-0.1039	0.1417	0.0949	0.7726	0.0279	1.3012	-0.0219
TL	0.1102	-0.4682	0.2761	-0.3604	0.3065	-0.2745	0.7626	0.0578	1.5530	-0.0900
WA	0.1492	-0.6717	0.1794	-0.1887	0.2910	-0.1714	0.8327	0.0254	1.3659	-0.0436
WB	0.1822	-0.5859	0.2411	-0.1799	0.1580	0.0479	0.7748	0.0337	1.3182	-0.0281
WP	1.6690	-1.0707	0.3751	-0.3579	1.7973	-0.8274	0.7209	0.0619	3.9095	-0.3940
WS	0.8538	-0.5267	0.2484	-0.2823	0.7049	-0.3002	0.7746	0.0477	2.3056	-0.1463
YB	0.1687	-0.6959	0.1676	-0.1114	0.3123	-0.0615	0.8358	0.0169	1.4877	-0.0534

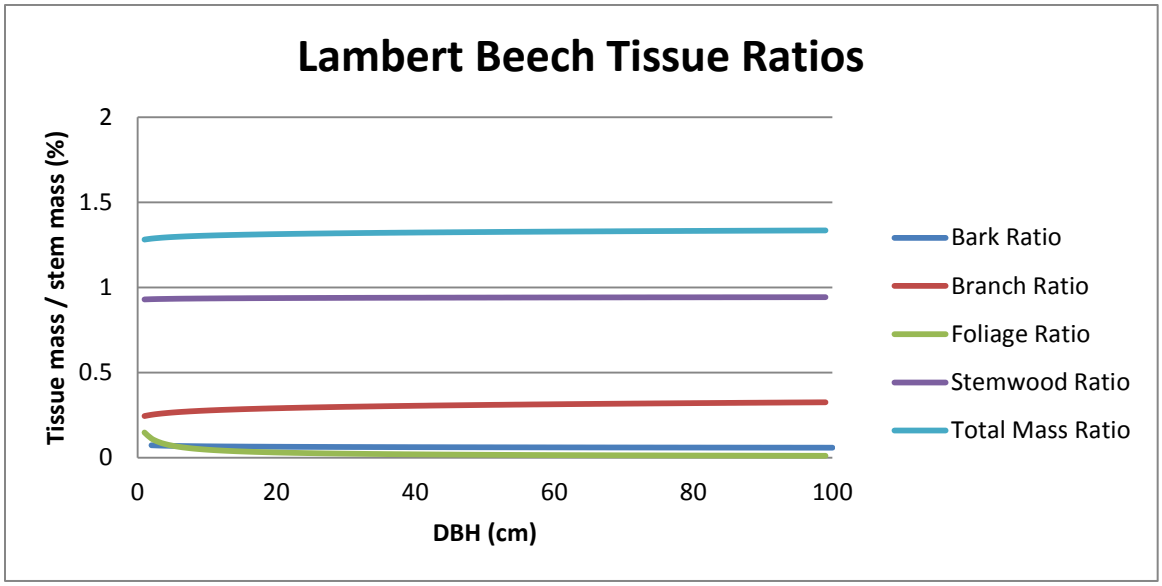


Figure 4.1. Relationship between Beech compartment ratios (compartment mass / stem mass) and DBH (cm) using the published equations by Lambert *et al.*, (2005).

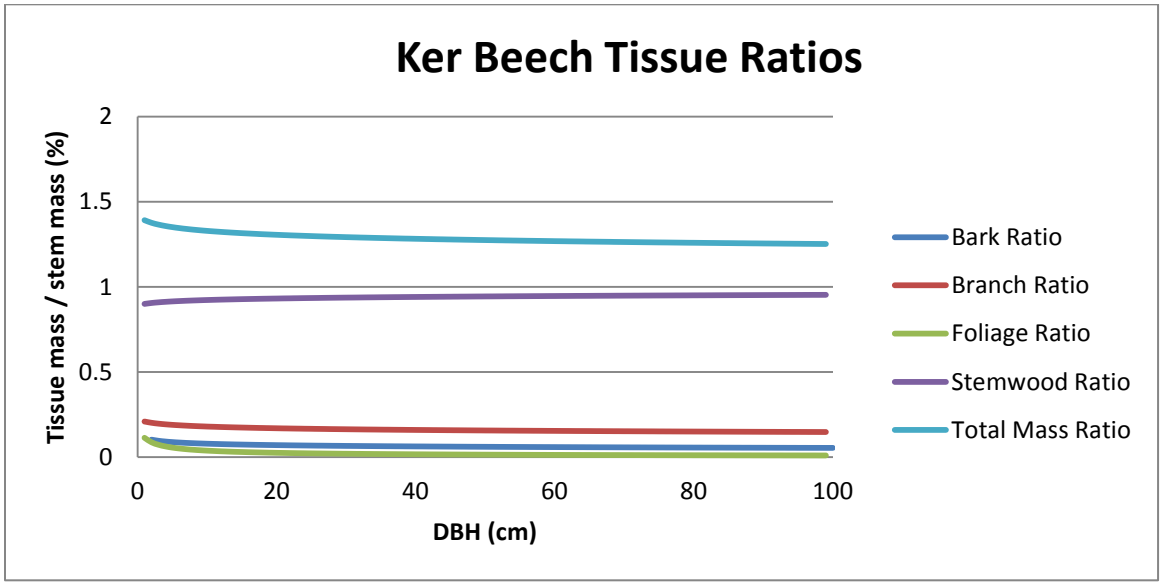


Figure 4.2. Relationship between Beech compartment ratios (compartment mass / stem mass) and DBH (cm) using the published equations by Ker, (1980a).

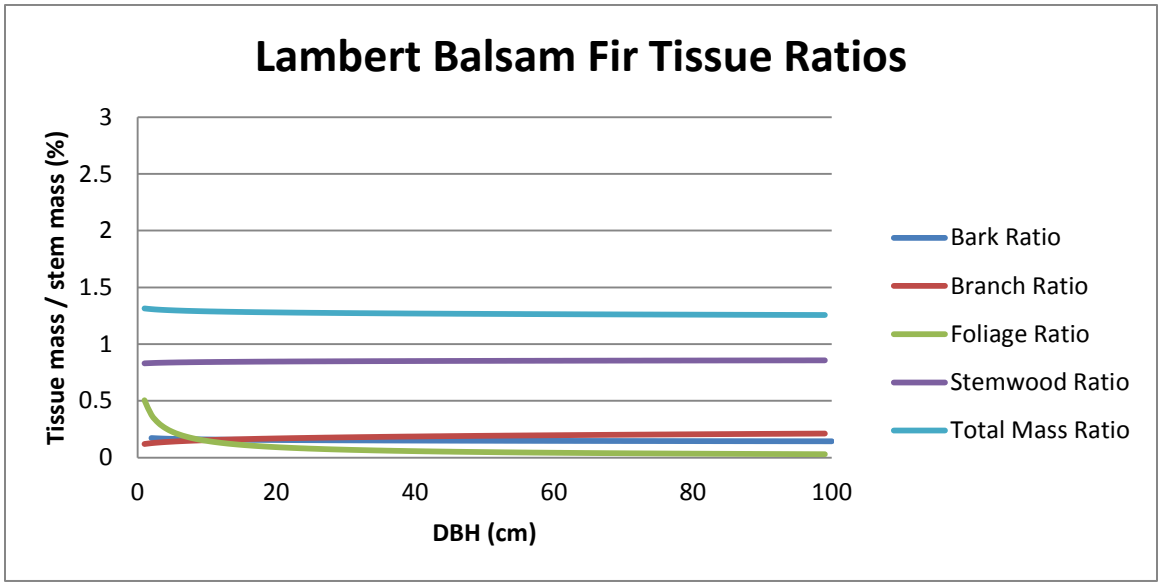


Figure 4.3. Relationship between Balsam Fir compartment ratios (compartment mass / stem mass) and DBH (cm) using the published equations by Lambert *et al.*, (2005).

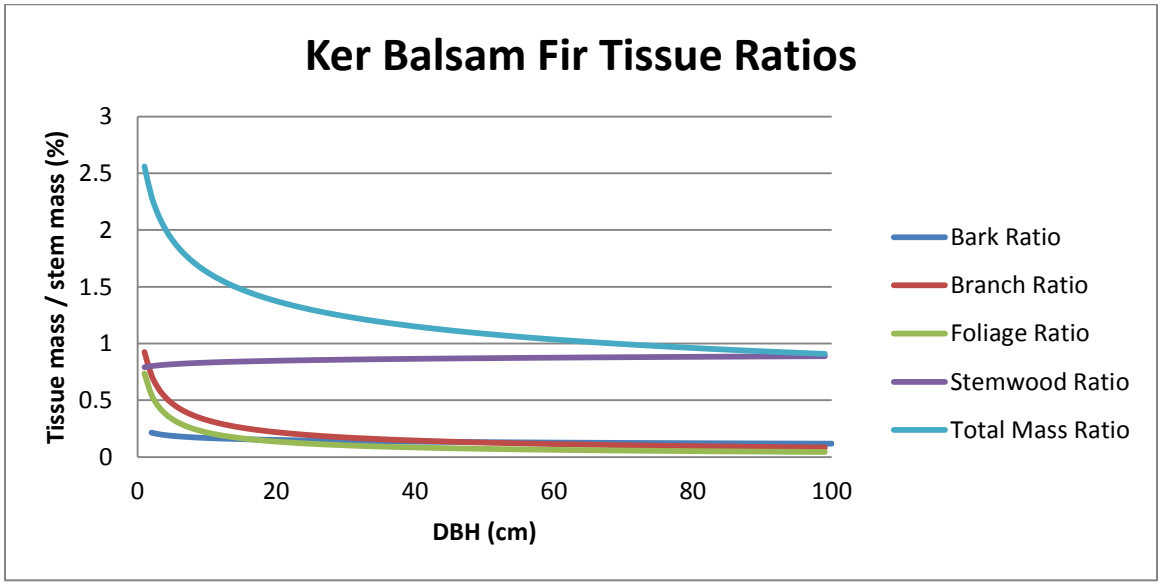


Figure 4.4. Relationship between Balsam Fir compartment ratios (compartment mass / stem mass) and DBH (cm) using the published equations by Ker, (1980b).

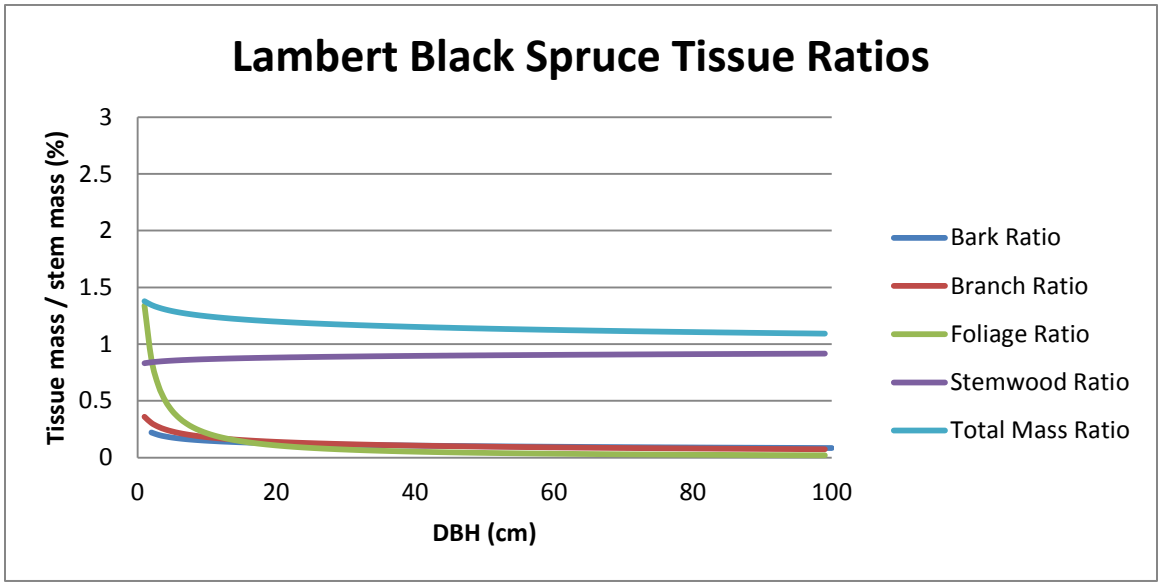


Figure 4.5. Relationship between Black Spruce compartment ratios (compartment mass / stem mass) and DBH (cm) using the published equations by Lambert *et al.*, (2005).

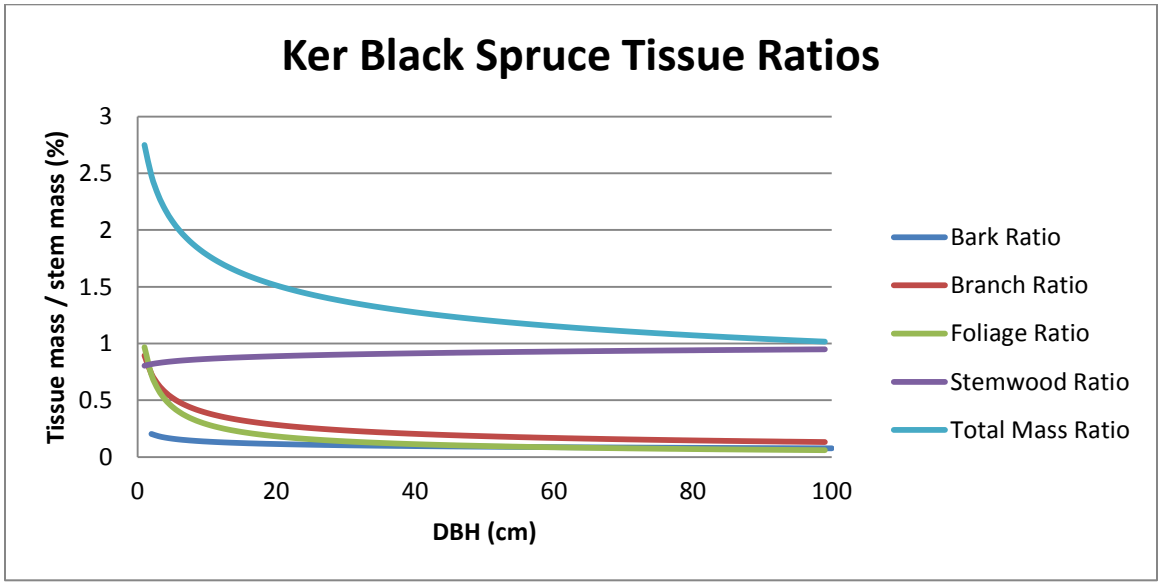


Figure 4.6. Relationship between Black Spruce compartment ratios (compartment mass / stem mass) and DBH (cm) using the published equations by Ker, (1980b).

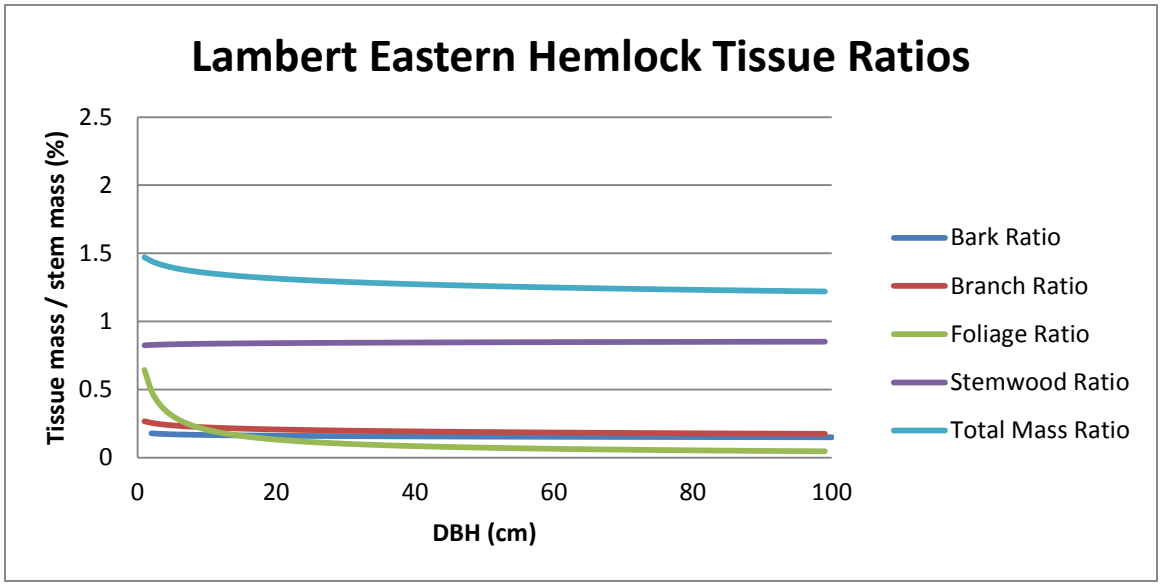


Figure 4.7. Relationship between Eastern Hemlock compartment ratios (compartment mass / stem mass) and DBH (cm) using the published equations by Lambert *et al.*, (2005).

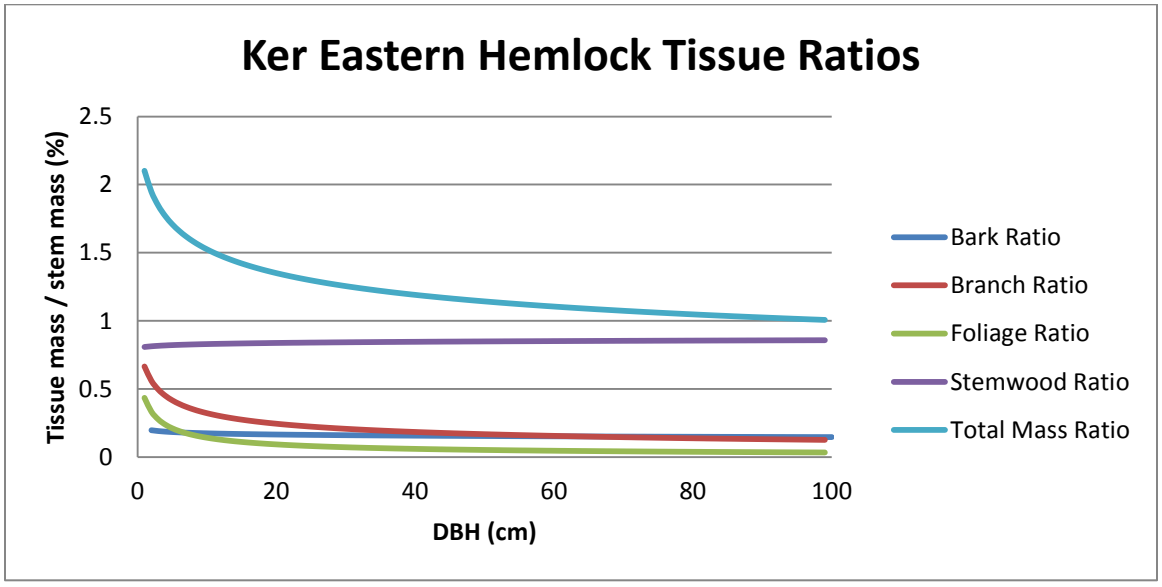


Figure 4.8. Relationship between Eastern Hemlock compartment ratios (compartment mass / stem mass) and DBH (cm) using the published equations by Ker, (1980a).

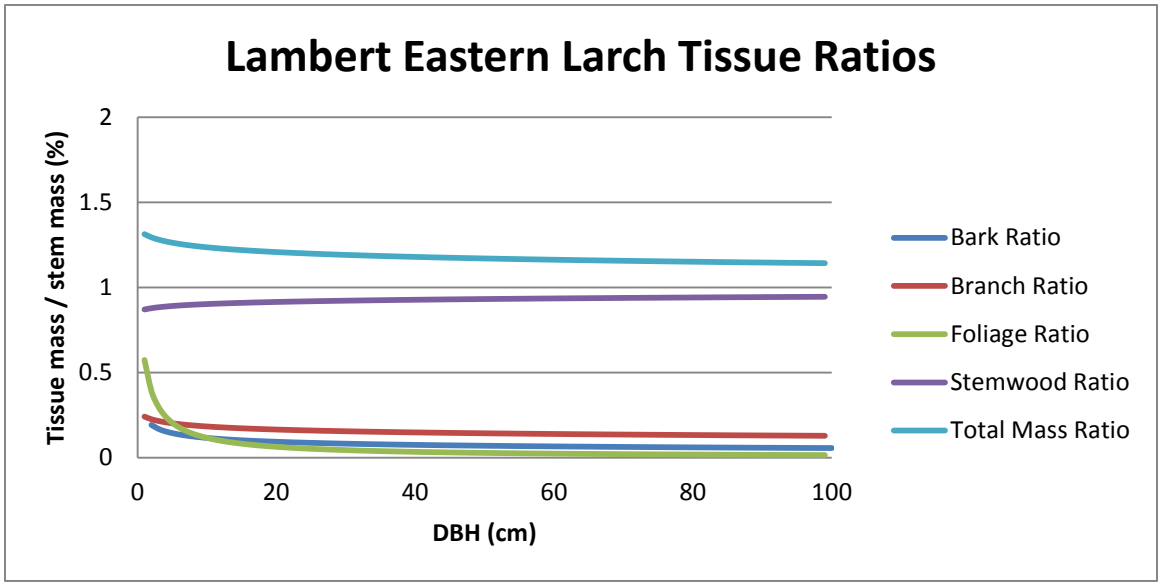


Figure 4.9. Relationship between Eastern Larch compartment ratios (compartment mass / stem mass) and DBH (cm) using the published equations by Lambert *et al.*, (2005).

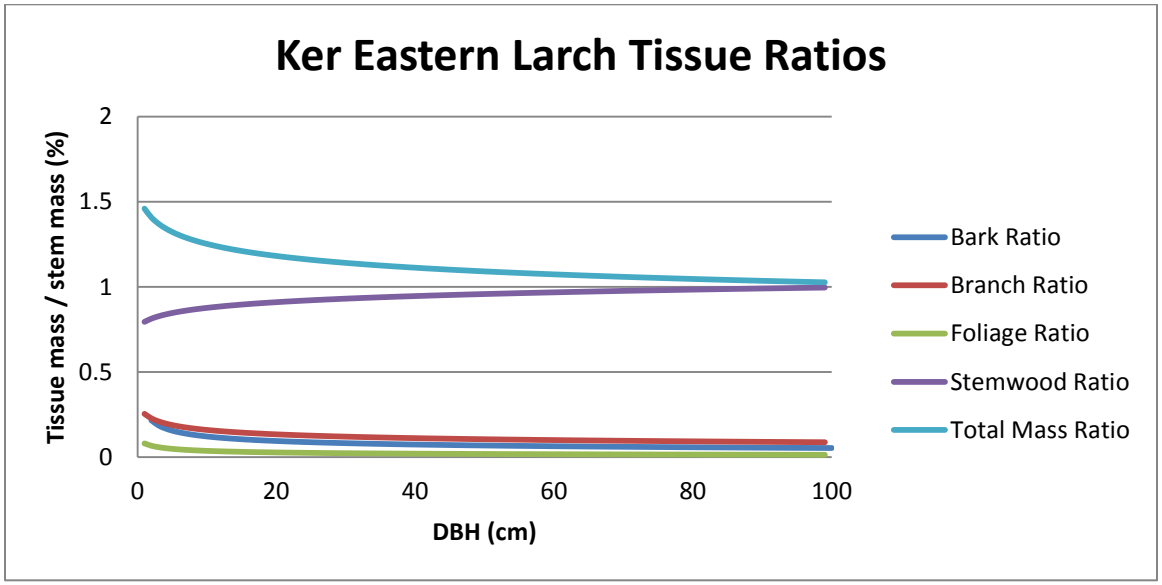


Figure 4.10. Relationship between Eastern Larch compartment ratios (compartment mass / stem mass) and DBH (cm) using the published equations by Ker, (1980b).

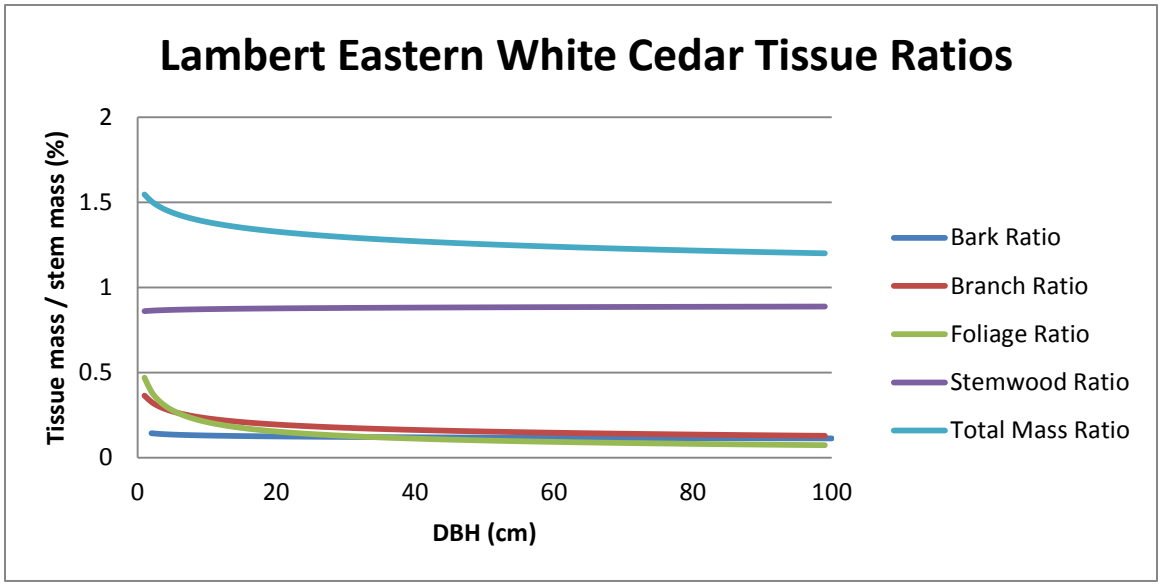


Figure 4.11. Relationship between Eastern White Cedar compartment ratios (compartment mass / stem mass) and DBH (cm) using the published equations by Lambert *et al.*, (2005).

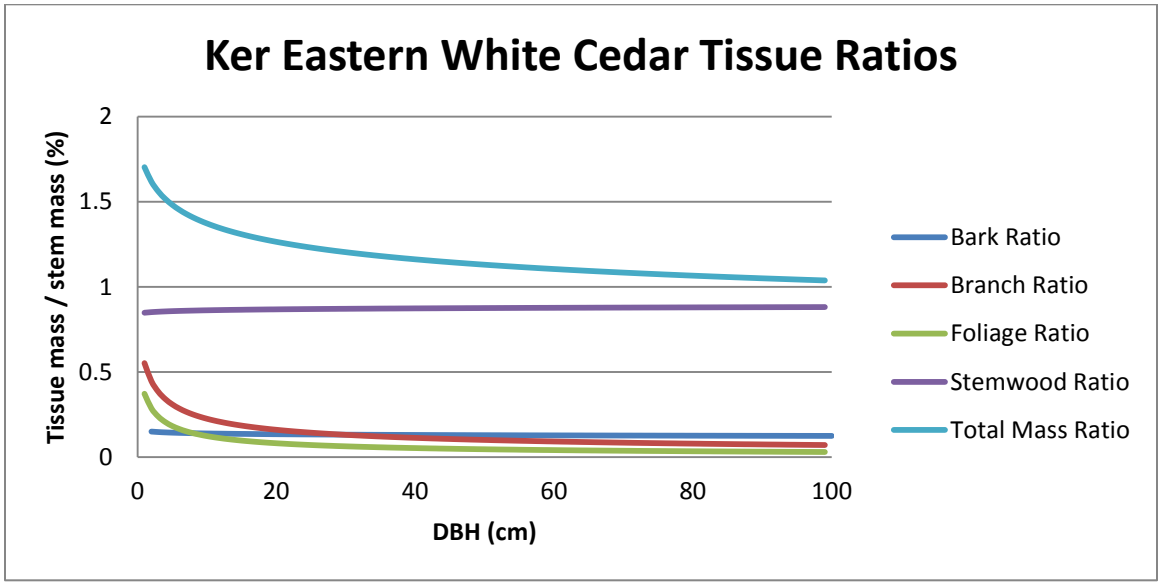


Figure 4.12. Relationship between Eastern White Cedar compartment ratios (compartment mass / stem mass) and DBH (cm) using the published equations by Ker, (1980a).

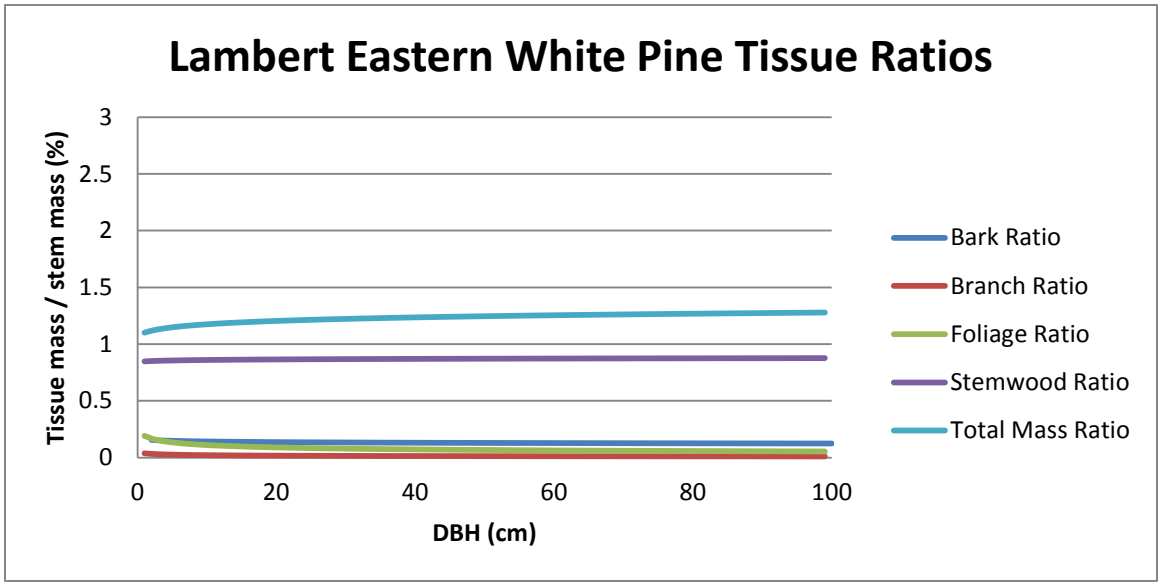


Figure 4.13. Relationship between Eastern White Pine compartment ratios (compartment mass / stem mass) and DBH (cm) using the published equations by Lambert *et al.*, (2005).

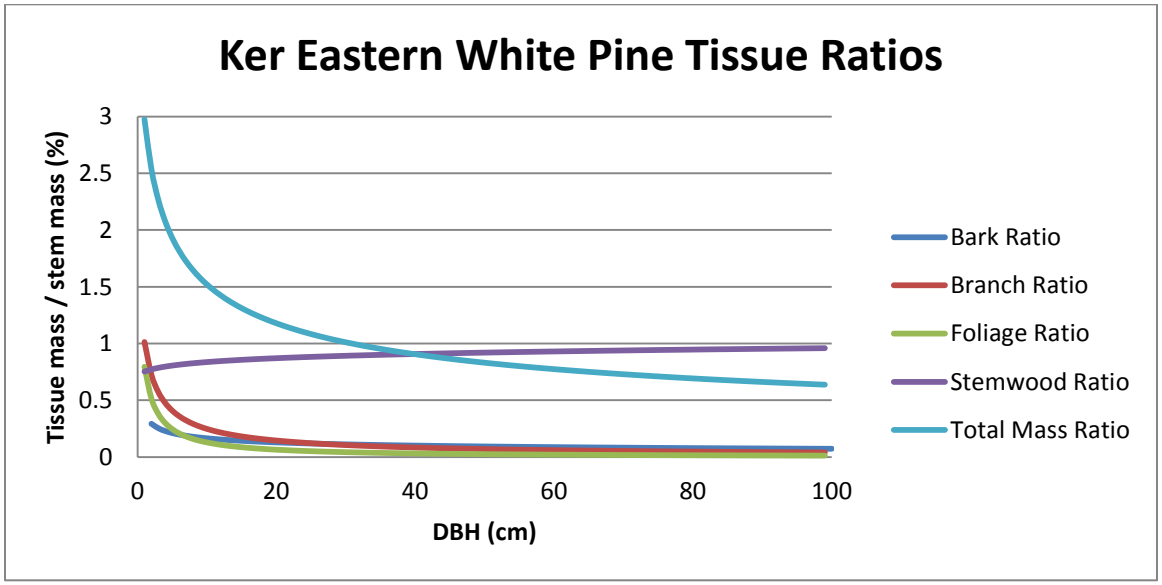


Figure 4.14. Relationship between Eastern White Cedar compartment ratios (compartment mass / stem mass) and DBH (cm) using the published equations by Ker, (1980a).

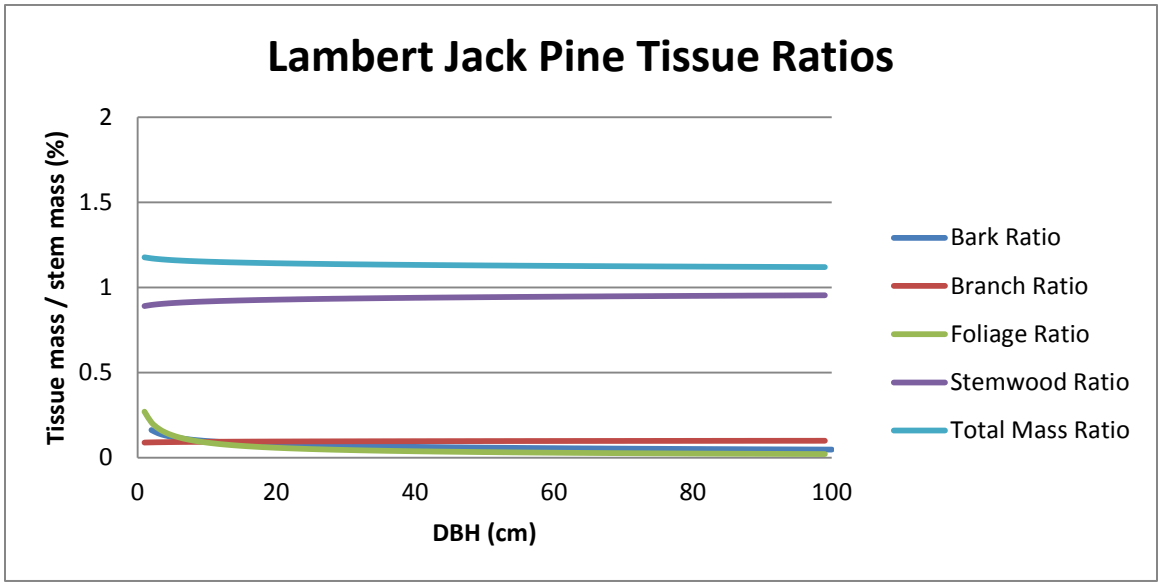


Figure 4.15. Relationship between Jack Pine compartment ratios (compartment mass / stem mass) and DBH (cm) using the published equations by Lambert *et al.*, (2005).

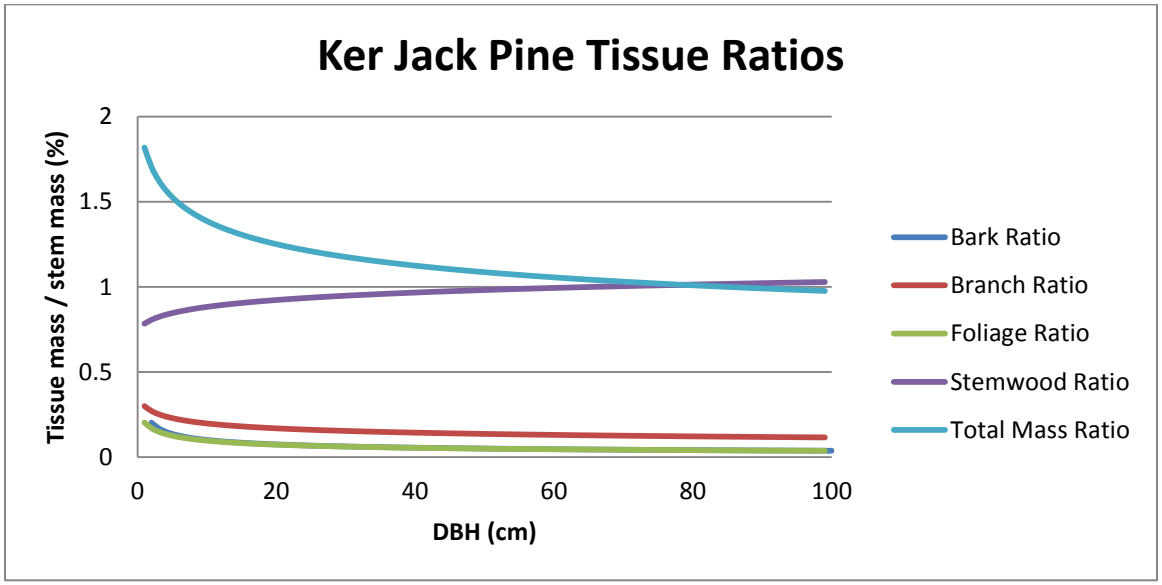


Figure 4.16. Relationship between Jack Pine compartment ratios (compartment mass / stem mass) and DBH (cm) using the published equations by Ker, (1980b).

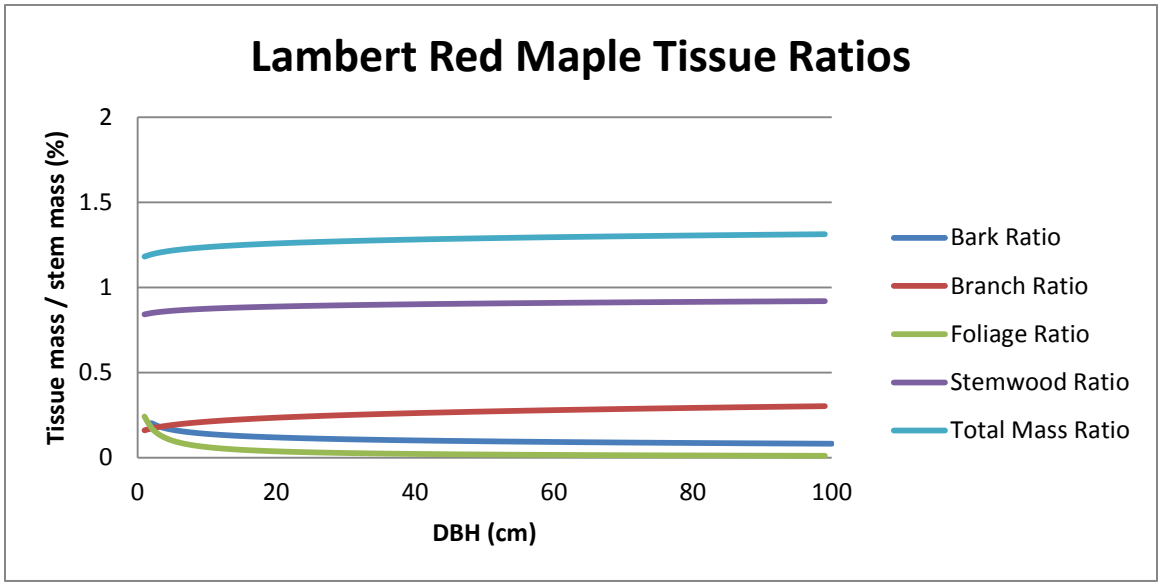


Figure 4.17. Relationship between Red Maple compartment ratios (compartment mass / stem mass) and DBH (cm) using the published equations by Lambert *et al.*, (2005).

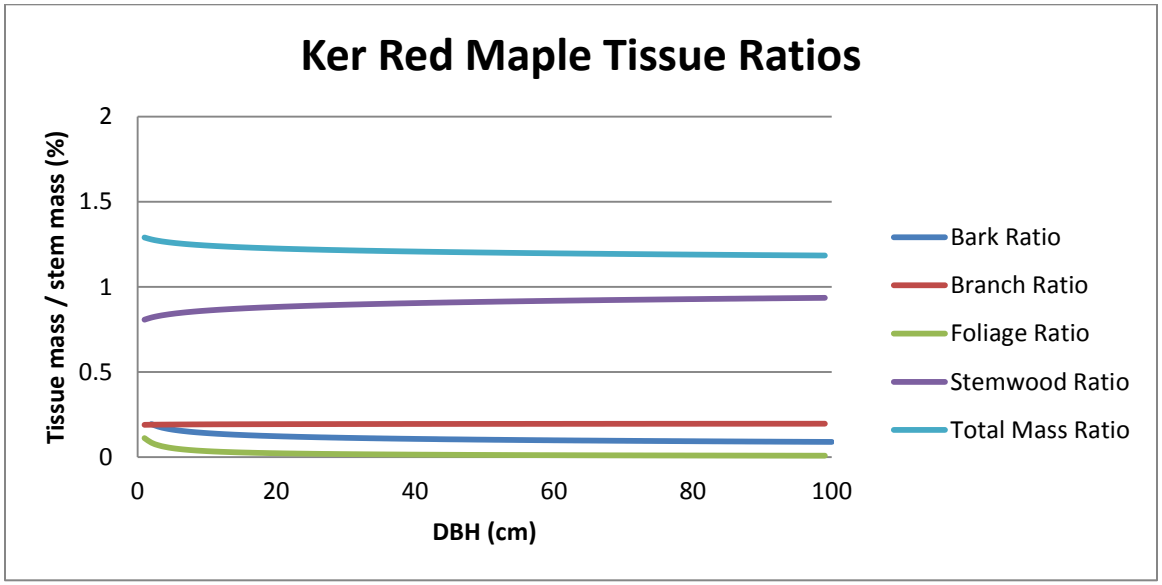


Figure 4.18. Relationship between Red Maple compartment ratios (compartment mass / stem mass) and DBH (cm) using the published equations by Ker, (1980b).

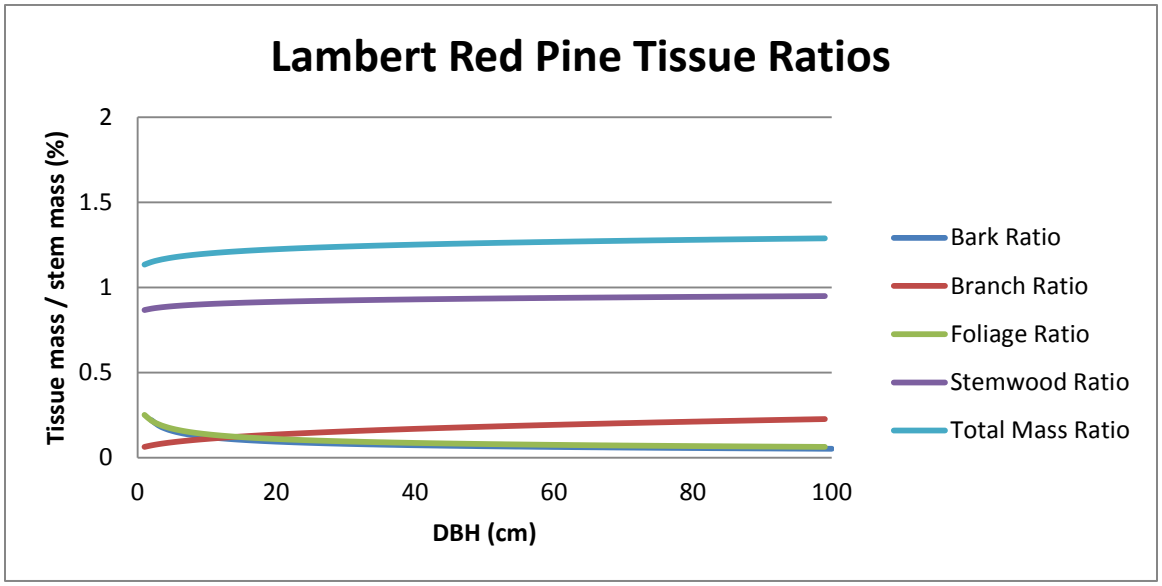


Figure 4.19. Relationship between Red Pine compartment ratios (compartment mass / stem mass) and DBH (cm) using the published equations by Lambert *et al.*, (2005).

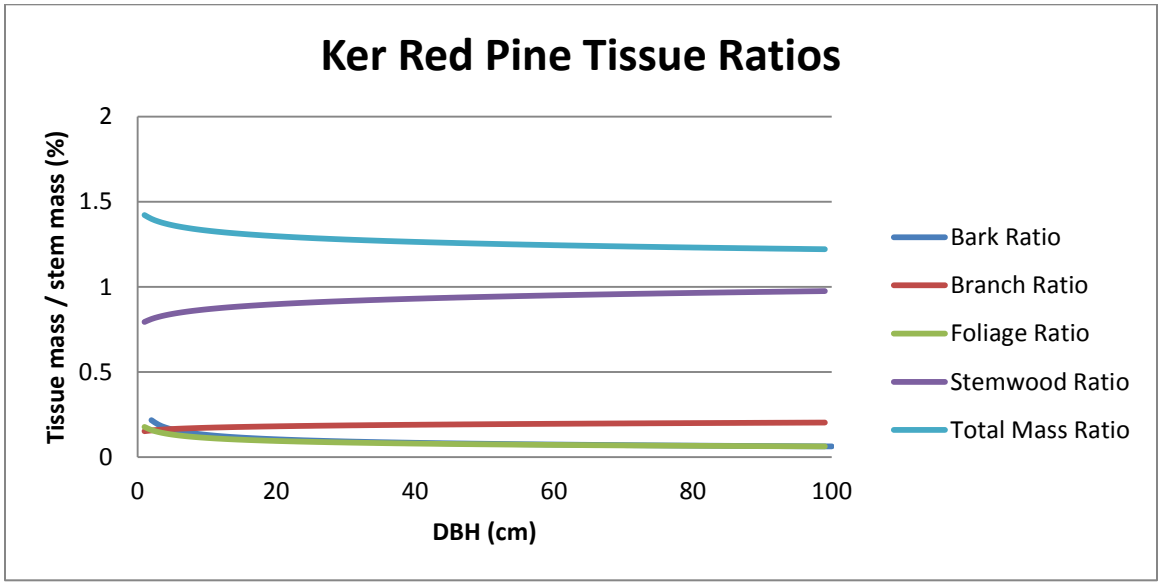


Figure 4.20. Relationship between Red Pine compartment ratios (compartment mass / stem mass) and DBH (cm) using the published equations by Ker, (1980b).

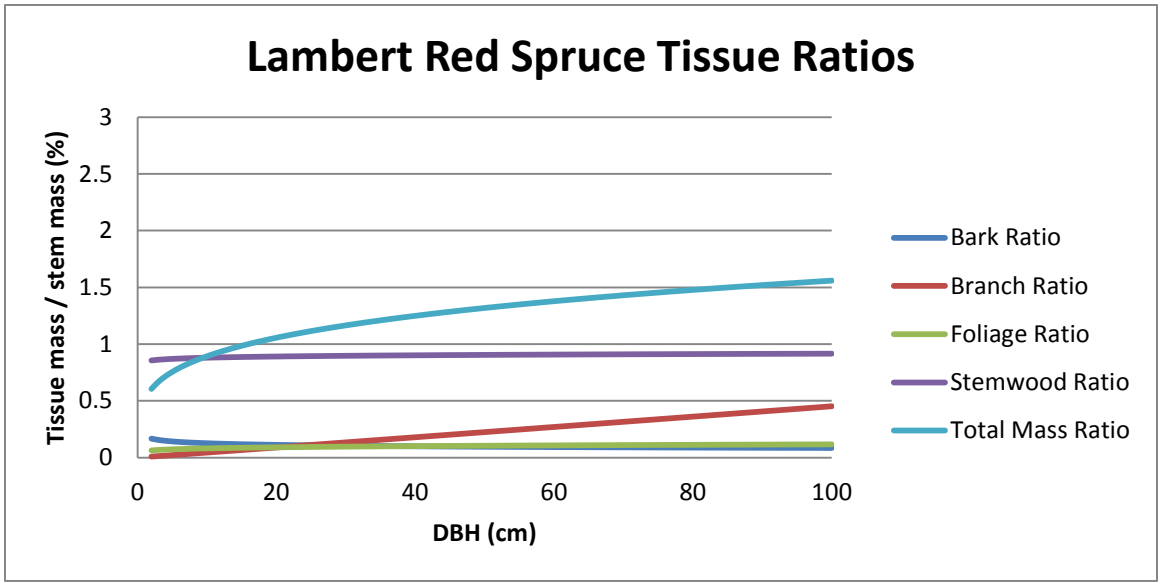


Figure 4.21. Relationship between Red Spruce compartment ratios (compartment mass / stem mass) and DBH (cm) using the published equations by Lambert *et al.*, (2005).

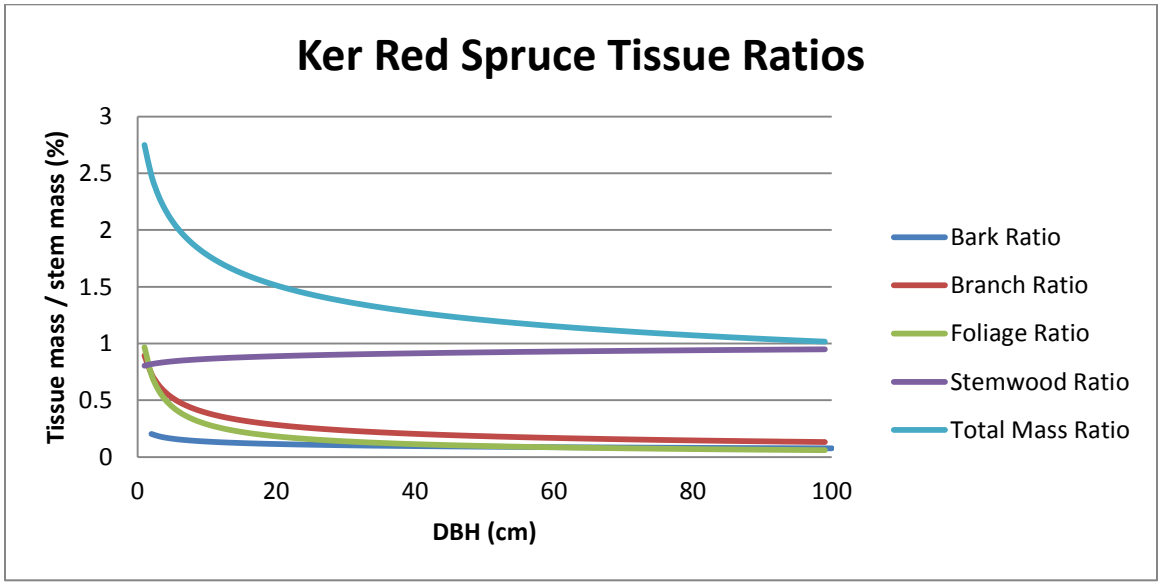


Figure 4.22. Relationship between Red Spruce compartment ratios (compartment mass / stem mass) and DBH (cm) using the published equations by Ker, (1980b).

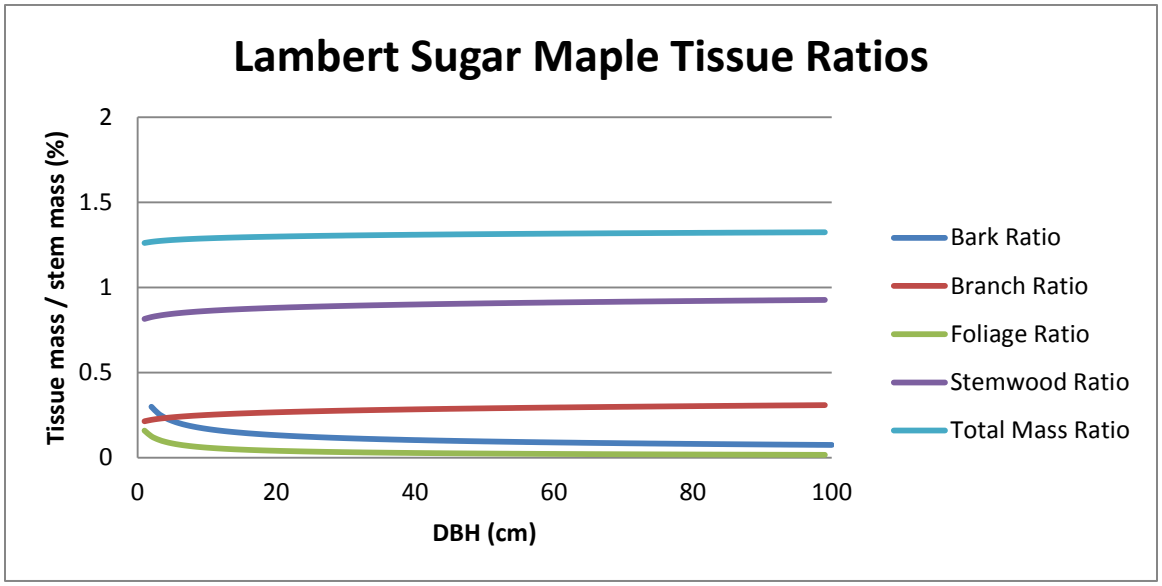


Figure 4.23. Relationship between Sugar Maple compartment ratios (compartment mass / stem mass) and DBH (cm) using the published equations by Lambert *et al.*, (2005).

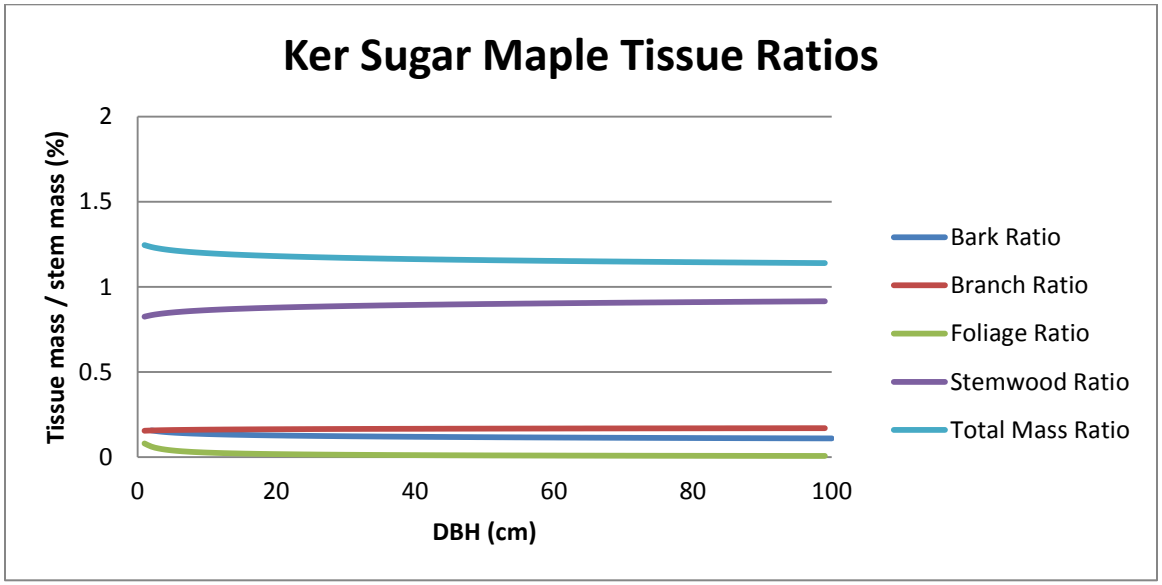


Figure 4.24. Relationship between Sugar Maple compartment ratios (compartment mass / stem mass) and DBH (cm) using the published equations by Ker, (1980a).

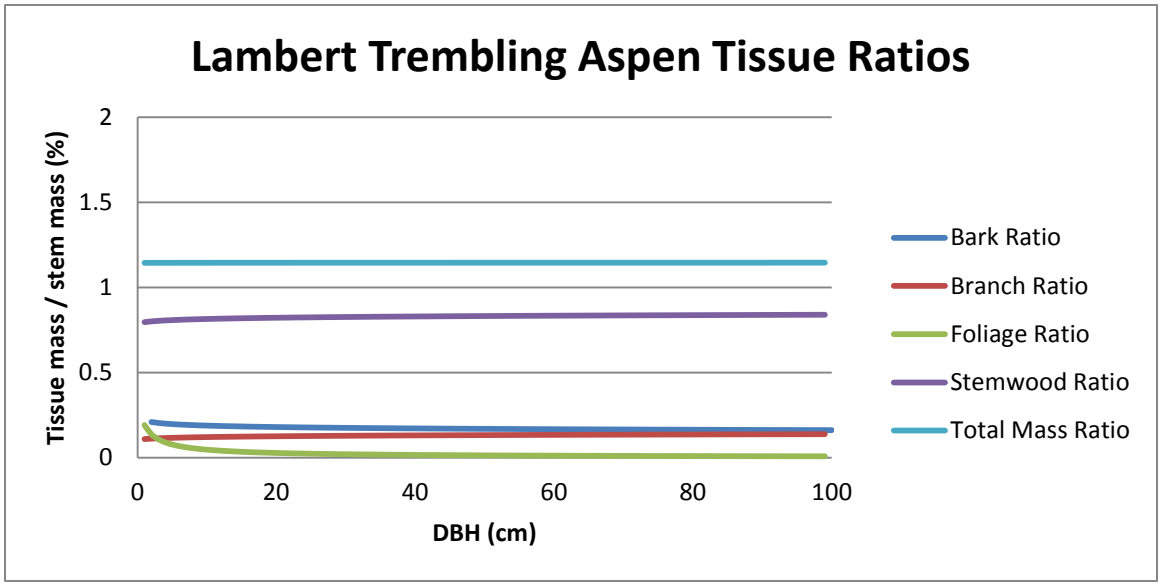


Figure 4.25. Relationship between Trembling Aspen compartment ratios (compartment mass / stem mass) and DBH (cm) using the published equations by Lambert *et al.*, (2005).

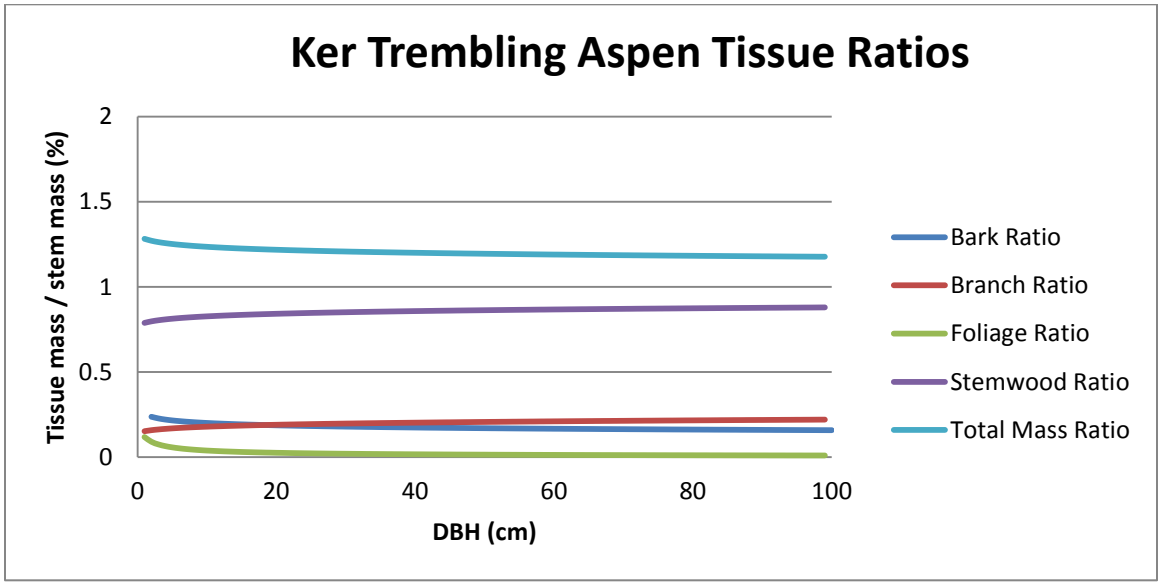


Figure 4.26. Relationship between Trembling Aspen compartment ratios (compartment mass / stem mass) and DBH (cm) using the published equations by Ker, (1980b).

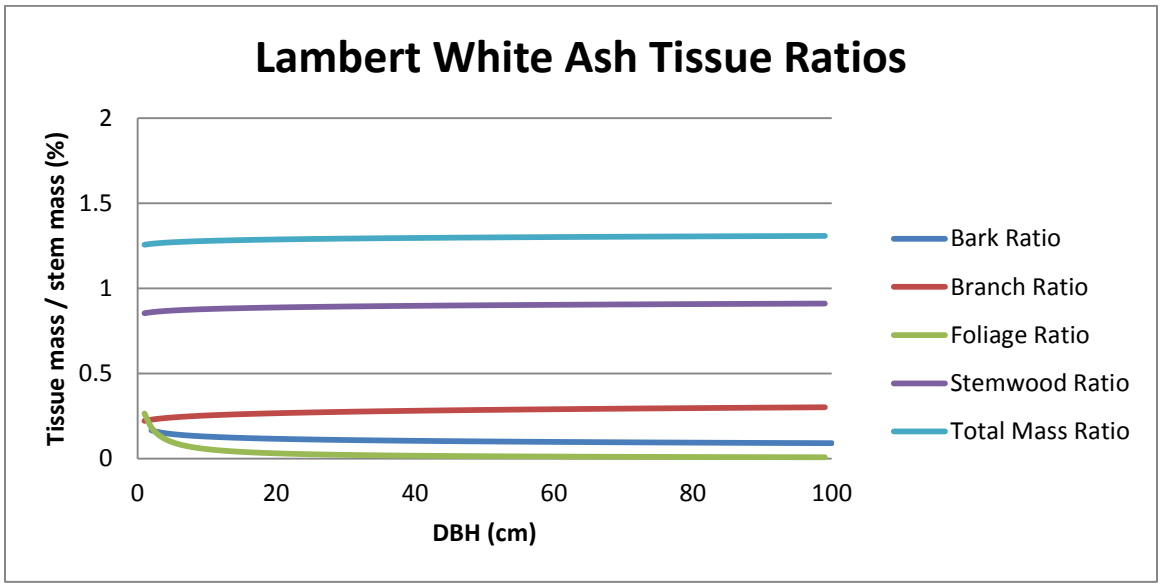


Figure 4.27. Relationship between White Ash compartment ratios (compartment mass / stem mass) and DBH (cm) using the published equations by Lambert *et al.*, (2005).

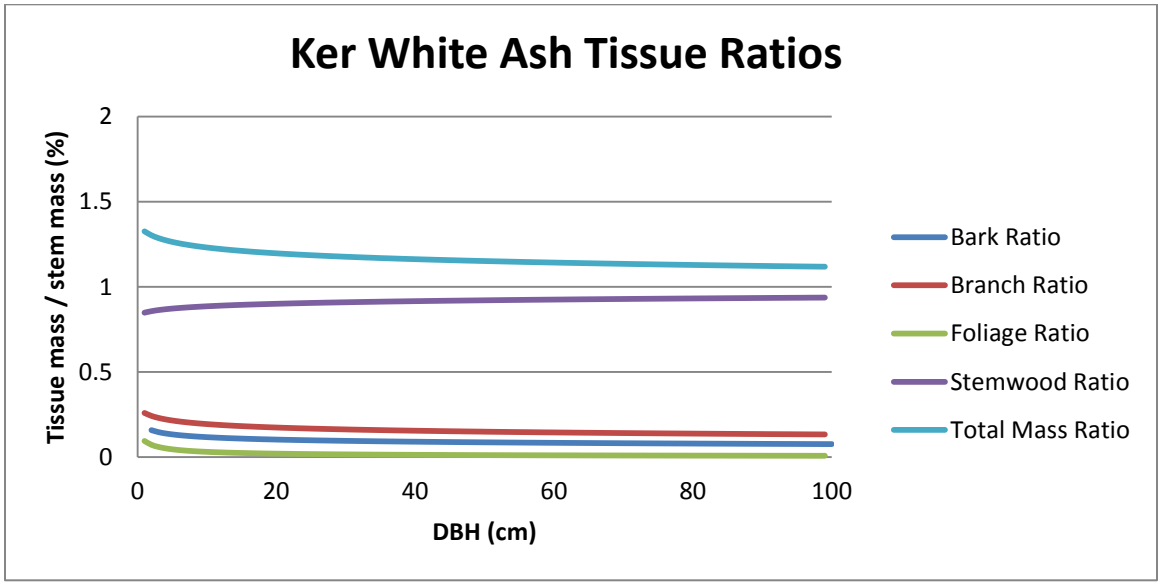


Figure 4.28. Relationship between White Ash compartment ratios (compartment mass / stem mass) and DBH (cm) using the published equations by Ker, (1980a).

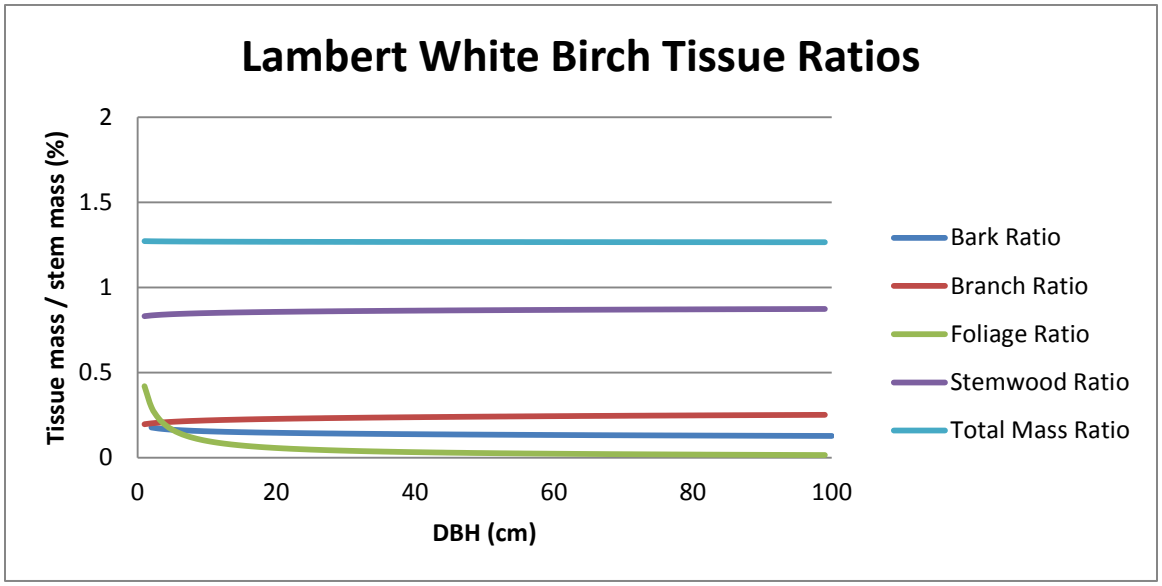


Figure 4.29. Relationship between White Birch compartment ratios (compartment mass / stem mass) and DBH (cm) using the published equations by Lambert *et al.*, (2005).

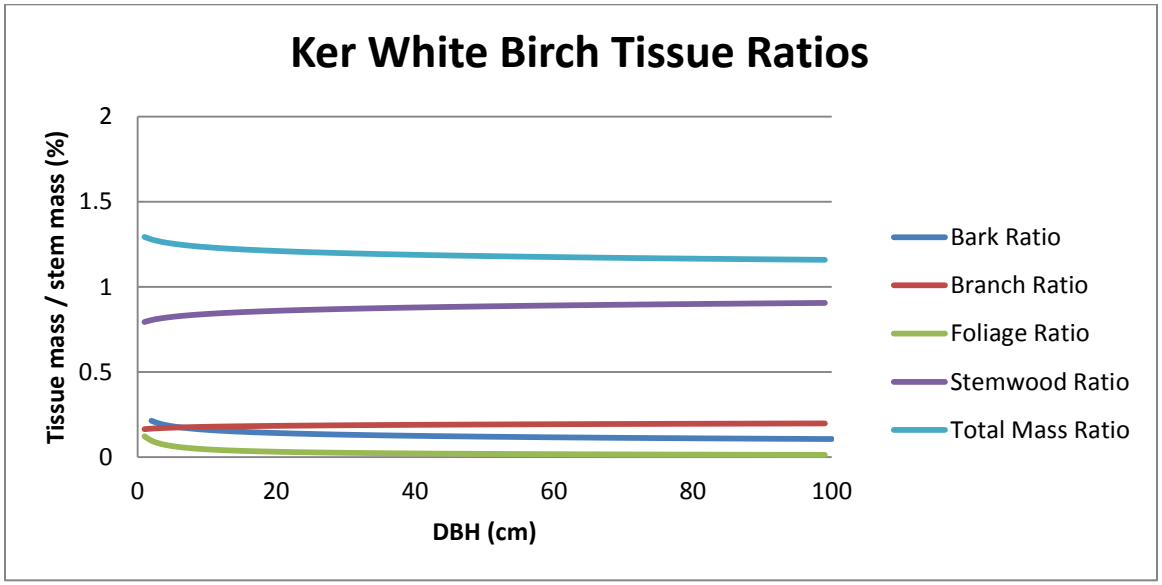


Figure 4.30. Relationship between White Birch compartment ratios (compartment mass / stem mass) and DBH (cm) using the published equations by Ker, (1980b).

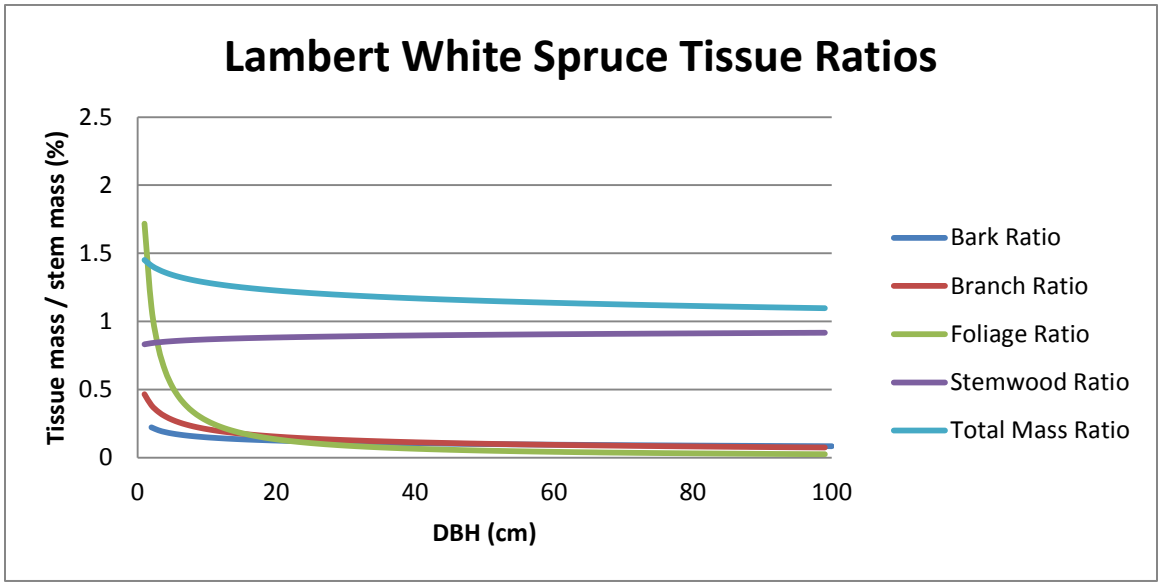


Figure 4.31. Relationship between White Spruce compartment ratios (compartment mass / stem mass) and DBH (cm) using the published equations by Lambert *et al.*, (2005).

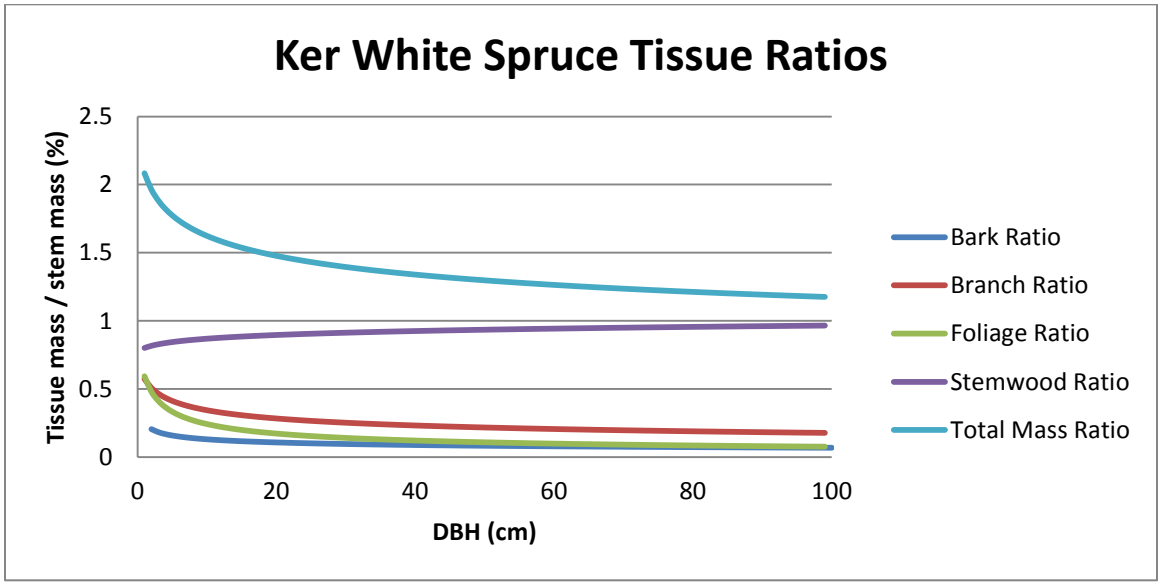


Figure 4.32. Relationship between White Spruce compartment ratios (compartment mass / stem mass) and DBH (cm) using the published equations by Ker, (1980b).

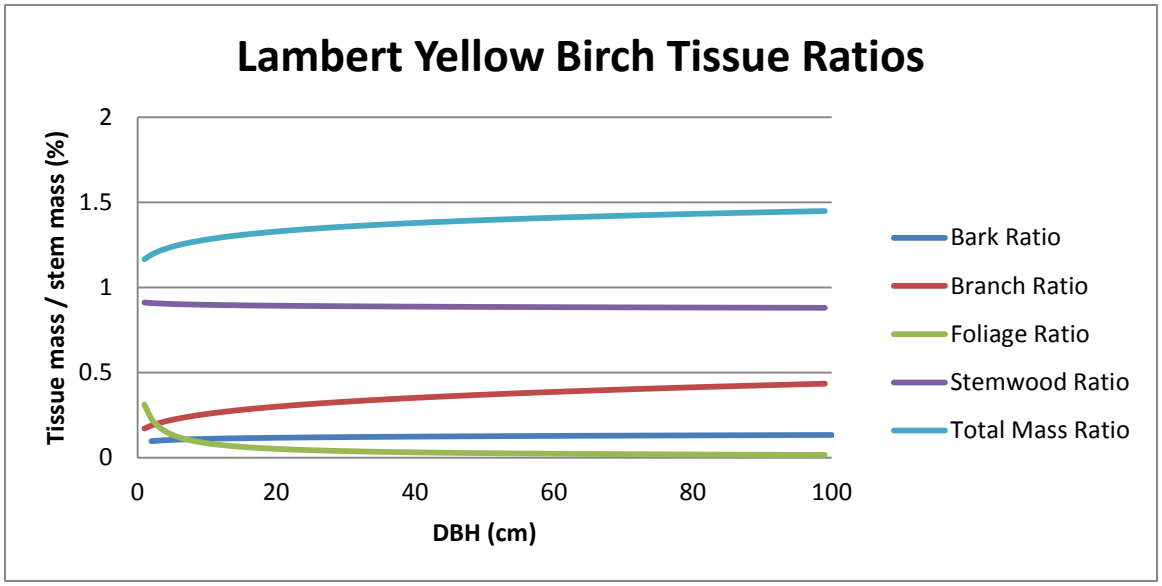


Figure 4.33. Relationship between Yellow Birch compartment ratios (compartment mass / stem mass) and DBH (cm) using the published equations by Lambert *et al.*, (2005).

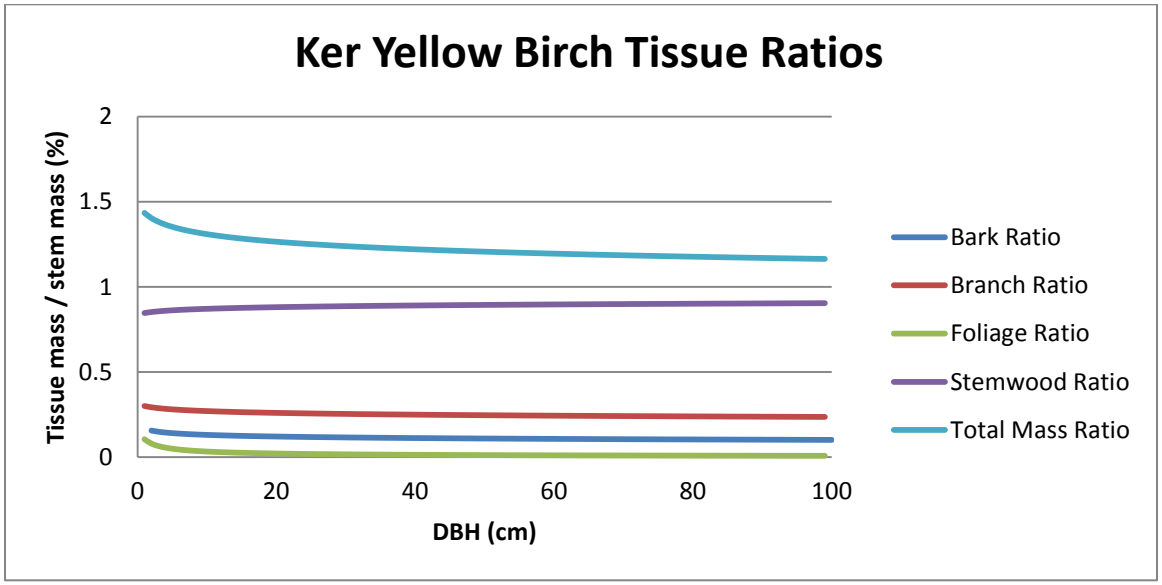


Figure 4.34. Relationship between Yellow Birch compartment ratios (compartment mass / stem mass) and DBH (cm) using the published equations by Ker, (1980a).

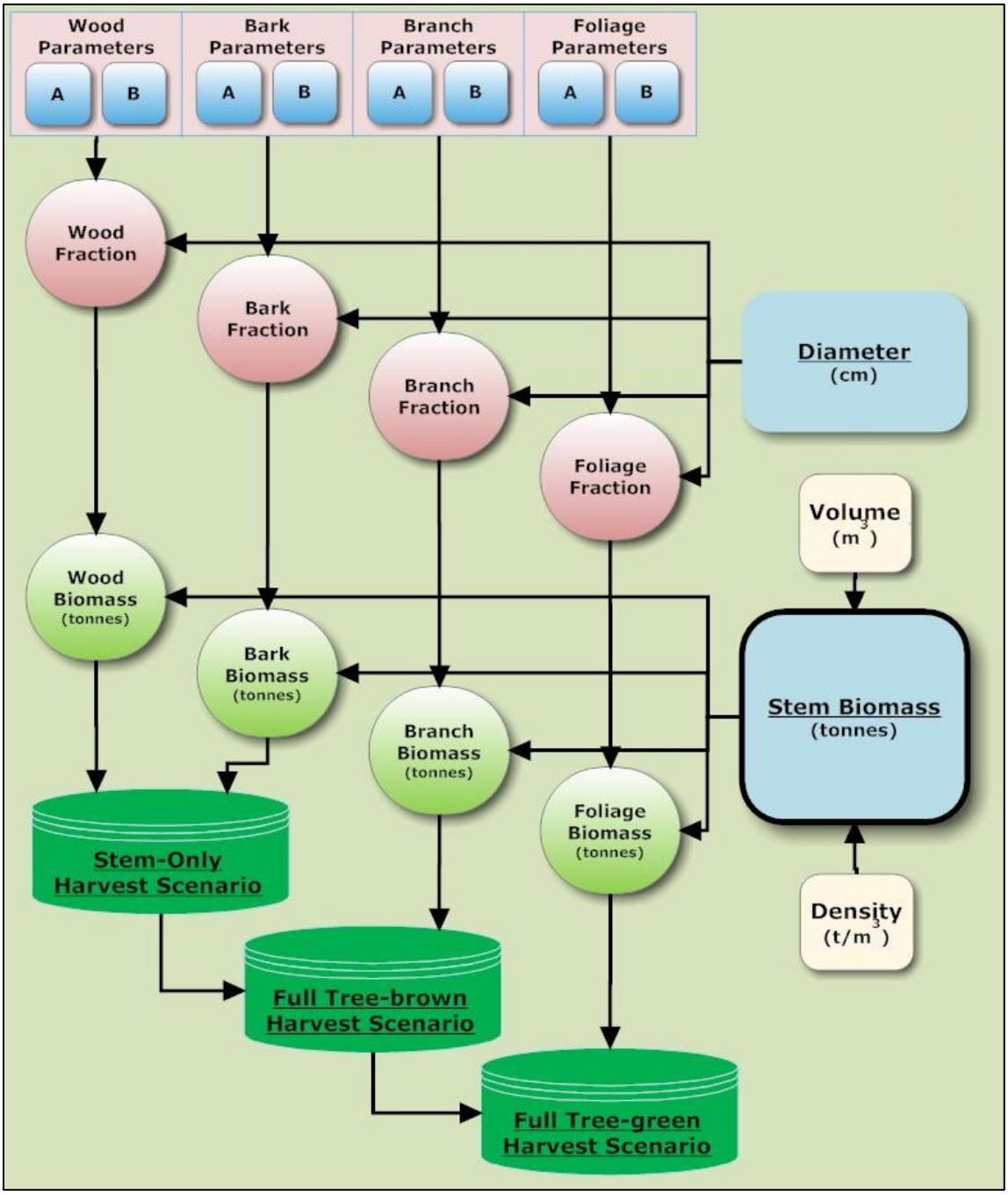


Figure 4.35. Process flow-chart illustrating stand level biomass estimations for each of the three harvest scenarios.

LITERATURE CITED

Brown, S., Schroeder, P., & Kern, J. (1999). Spatial distribution of biomass in forests of the eastern USA. *Forest Ecology and Management, 123*, 81-90.

Ker, M. (1984). *Biomass equations for seven major maritimes tree species.* Fredericton, N.B.: Maritime Forest Research Centre. Information Report M-X-148.

Ker, M. (1980a). *Tree biomass equations for seven species in southwestern New Brunswick.* Fredericton, N.B.: Maritime Forest Research Centre. Information Report M-X-114.

Ker, M. (1980b). *Tree biomass equations for ten major species in Cumberland County, Nova Scotia.* Fredericton, N.B.: Maritime Forest Research Centre. Information Report M-X-108.

Lambert, M., Ung, C., & Raulier, F. (2005). Canadian national tree aboveground biomass equations. *Canadian Journal of Forest Research, 35*, 1996-2018.

ModelMaker. (1999). [Computer Software]. Cherwell Scientific Ltd. Oxford, U.K.

Somogyi, Z., Cienciala, E., Mäkipää, R., Muukkonen, P., Lehtonen, A., & Weiss, P. (2007). Indirect methods of large-scale forest biomass estimation. *European Journal of Forest Research, 126*, 197-207.

Teobaldelli, M., Somogyi, Z., Migliavacca, M., & Usoltsev, V. (2009). Generalized functions of biomass expansion factors for conifers and broadleaved by stand age, growing stock and site index. *Forest Ecology and Management, 257*, 1004-1013.

CHAPTER 5

FOREST BIOMASS PROJECTIONS III: A REVIEW OF SPECIES-SPECIFIC NUTRIENT CONCENTRATIONS (N, K, CA, MG) IN TREE BARK, BRANCH, STEM-WOOD AND FOLIAGE BIOMASS COMPARTMENTS.

INTRODUCTION

The accumulation, retention and cycling of nutrients between trees and soil involve a suite of complex spatial and temporal factors that are not easily quantified (Boucher, 1999). This quantification is, however, essential for understanding the impacts of biomass removal on forest site productivity and sustainability (Freedman *et al.*, 1981; Ouimet *et al.*, 2006). The extent of post-biomass harvesting nutrient availability is directly dependent on the forest biomass that remains on site (Mann *et al.*, 1988), but the concentrations and distributions of nutrient elements tend to differ between tree species and biomass compartment (e.g., bark, branches, foliage, stem-wood, coarse and fine roots). Relating the concentrations and amounts of these nutrients within trees by species and compartment is therefore important for modelling stand-level nutrient budgets, and post-harvest nutrient availability. The objectives of this chapter are to: (i) compile nutrient concentrations of N, K, Ca and Mg, and review their relationships to one another, by above-ground biomass compartment (bark, branch, stem-wood, foliage), for 16 commercial Acadian Forest tree species[2] using three data sources; (ii) use the compiled data to establish a nutrient lookup table for each tree species and biomass compartment for use within the Nova Scotia Biomass Decision Support Tool.

[2] See Table 3.1, with the exception of White Ash, which was not available for comparison between data sources

DATA SOURCES

Tree Chemistry Database (TCD)

The TCD (v1.0) was developed by the United States Department of Agriculture, Forest Service, in order to support the development of regional critical acid loads and exceedances, by facilitating the linkage between biomass removal and nutrient exports (see Pardo *et al.*, 2004). The database contained over 200 publications, summarizing concentrations of C, N, P, K, Ca, Mg, Mn, and Al for above-ground tree-biomass bark, branch, stem-wood and foliage compartments. The TCD allowed for species-specific search criteria of trees native to the north-eastern United States and eastern Canada, by way of a Microsoft Access (2002) database (see Appendix V for detailed search criteria).

Acid Rain Network Early Warning System (ARNEWS)

The ARNEWS network was established by the Canadian Forest Service in 1984 as a means of detecting the impacts of air pollution on forest health across Canada (see D'Eon *et al.,* 1994). Concentrations of N, P, K, Ca and Mg were summarized for bark, branch, stem-wood and foliage components by Moayeri (2001), from over 95 nation-wide ARNEWS plots (ARNEWS CD-ROM, 2000, Veg-data folder). Originally, tree species were grouped into 5 categories based on community type: tolerant hardwood, intolerant hardwood, spruce, pine and fir. For the purpose of this study, a number of species were removed from the groupings in order represent only tree species native to eastern Canada. Additionally, the available data was expanded into 8 categories: (i) tolerant hardwood (Red Maple, Sugar Maple, Yellow Birch, Beech, Red Oak), (ii) intolerant hardwood (Large-tooth Aspen, Trembling Aspen), (iii) White Birch, (iv)

spruce (Red Spruce, Black Spruce), (v) White Spruce, (vi) pine (Red Pine, White Pine), (vii) Jack Pine, and (viii) Balsam Fir. Stem-wood and bark samples were collected from 125 trees during the summer of 1995. Total concentrations of N, P, K, Ca and Mg were analysed using the laboratory procedures described by Case *et al.*, (1996). Foliage element concentrations were taken from the Canadian Forest Service (ARNEWS CD-ROM, 2000, Nut-fol file) following the ARNEWS sampling procedures described by D'Eon *et al.*, (1994). Additionally, due to differences in sampling efforts, a series of predictive functions were developed by Moayeri (2001) for missing stem-wood, bark and foliage nutrient concentrations. Branch element concentrations were estimated through regression analyses using independent data by Maliondo *et al.,* (1990).

Nova Scotia Forest Biomass Nutrient Project (NS-FBNP)

The NS-FBNP was initiated in 2008 as a joint project between the Nova Scotia Department of Natural Resources and the University of New Brunswick in order to establish baseline information on nutrient contents within trees and soils for select upland forest locations across Nova Scotia (Keys & Arp, 2009). Eight unique soil-vegetation combinations were identified within 4 locations, each with a minimum of 2 plots, representing harvested and un-harvested conditions, for a total of 34 vegetation sampling plots. Twelve tree species were analyzed: White Ash, Balsam Fir, Black Spruce, Large-tooth Aspen, Red Oak, Red Maple, Red Spruce, Sugar Maple, White Birch, White Pine, White Spruce and Yellow Birch. Biomass compartments were sampled from live tree crowns for foliage, twigs, bark and wood, the latter two compartments being sampled from large diameter branches. Species composite samples of each biomass compartment

were stored at room temperature in plastic bags. Vegetation analyses consisted of total C, N, S, P, K, Ca, and Mg (%, od), total Mn, Fe, Zn, Al (ppm, od), stem-wood and bark density (g cm^{-3}), and moisture (%, od) for both pre- and post-harvest wood, bark, twig and foliage compartments following the organic matter digestion procedures described by Mckeague (1978).

METHODS

Total concentrations of N, K, Ca and Mg for bark, branch, foliage and stem-wood biomass compartments were summarized within box-plots, illustrating their variation by data source. In order to quantify data source variations, a series of regression analyses were conducted in order to (i) relate the TCD to both the ARNEWS and NS-FBNP for each biomass compartment and nutrient element, and (ii) compare the TCD with both the ARNEWS and NS-FBNP for the combined compartments, by nutrient. A second set of regression analyses were conducted in order to determine the relationships between nutrients using the combined data sources. All regression analyses were realized within Statview statistical software (v5.0; 1998).

RESULTS

Box plots by Data Source

Figures 5.1 - 5.4 illustrate box plots of N, K, Ca and Mg concentrations, respectively, for each species, by data source, separated by bark, branch, stem-wood and foliage compartments. Results from the figures are as follows:

1. Nutrient concentrations tend to follow a foliage > bark ≈ branch > stem-wood sequence, with the exception of calcium, which generally follows that bark > foliage > branch > stem-wood.

2. Nutrient concentrations tend to follow the tolerant hardwoods > intolerant hardwoods > conifers sequence.

3. For N, the NS-FBNP values are generally elevated above the 75th percentile of the TCD, with the exception of foliage. Conversely, the ARNEWS values tend to fall below the 25th percentile of the TCD dataset, with the exception of foliage. Foliage N concentrations are generally in good agreement across all species and data sources.

4. For K, the ARNEWS and NS-FBNP generally agree with the TCD for all biomass compartments, with the exception of the ARNEWS bark values, which are consistently below the 25th percentile of the TCD dataset.

5. For Mg, the ARNEWS values are in good agreement with the TCD, whereas the NS-FBNP bark, branch and stem-wood values are consistently elevated above the 75th percentile of the TCD dataset.

6. For Ca, both the ARNEWS and NS-FBNP are generally in agreement with the TCD, with the exception of the elevated ARNEWS tolerant hardwood bark and branch concentrations, and the NS-FBNP stem-wood concentrations.

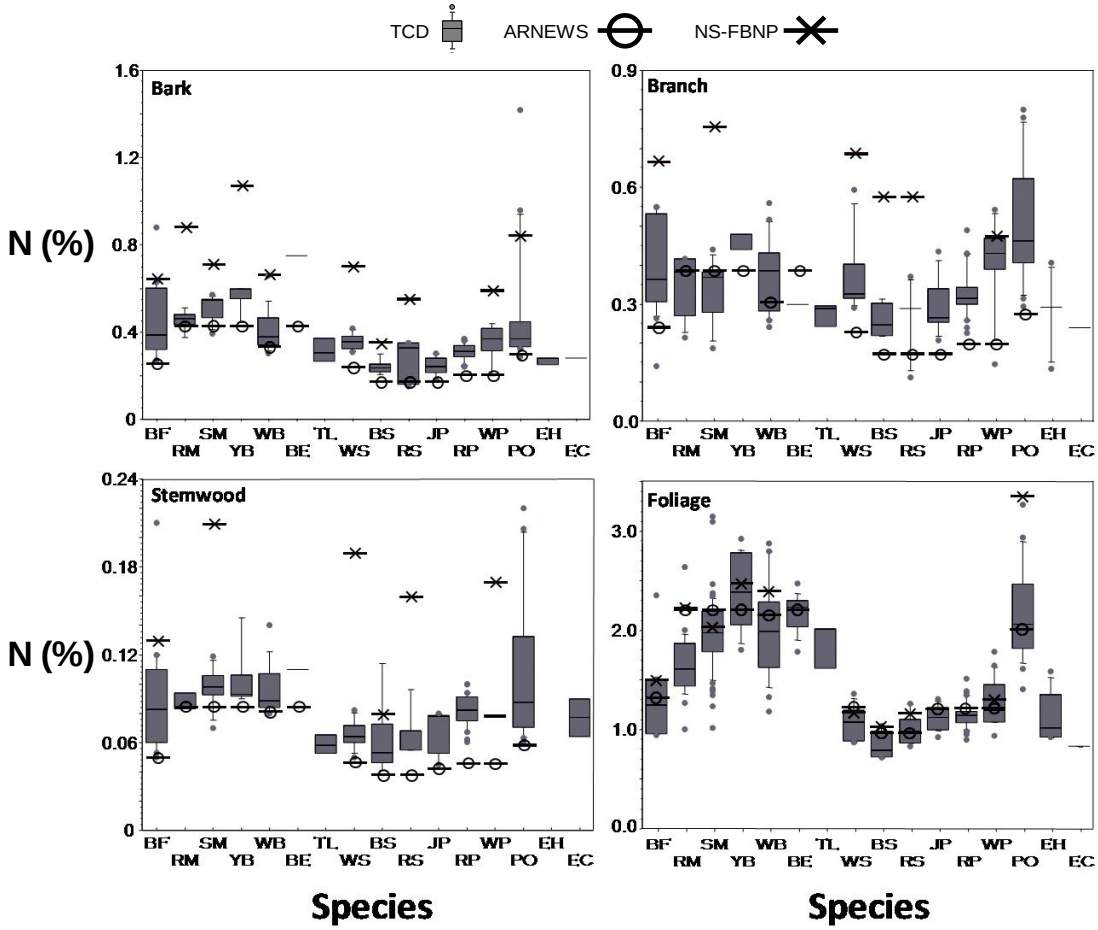


Figure 5.1. Box plots of N concentrations (%) in bark, branch, stem-wood and foliage compartments, by tree species, for the TCD dataset; the corresponding entries from the ARNEWS and NS-FBNP data sources are shown by the line symbols. Box plots show the 10th, 50th, and 90th percentiles, and outliers below the 10th and above the 90th percentiles.

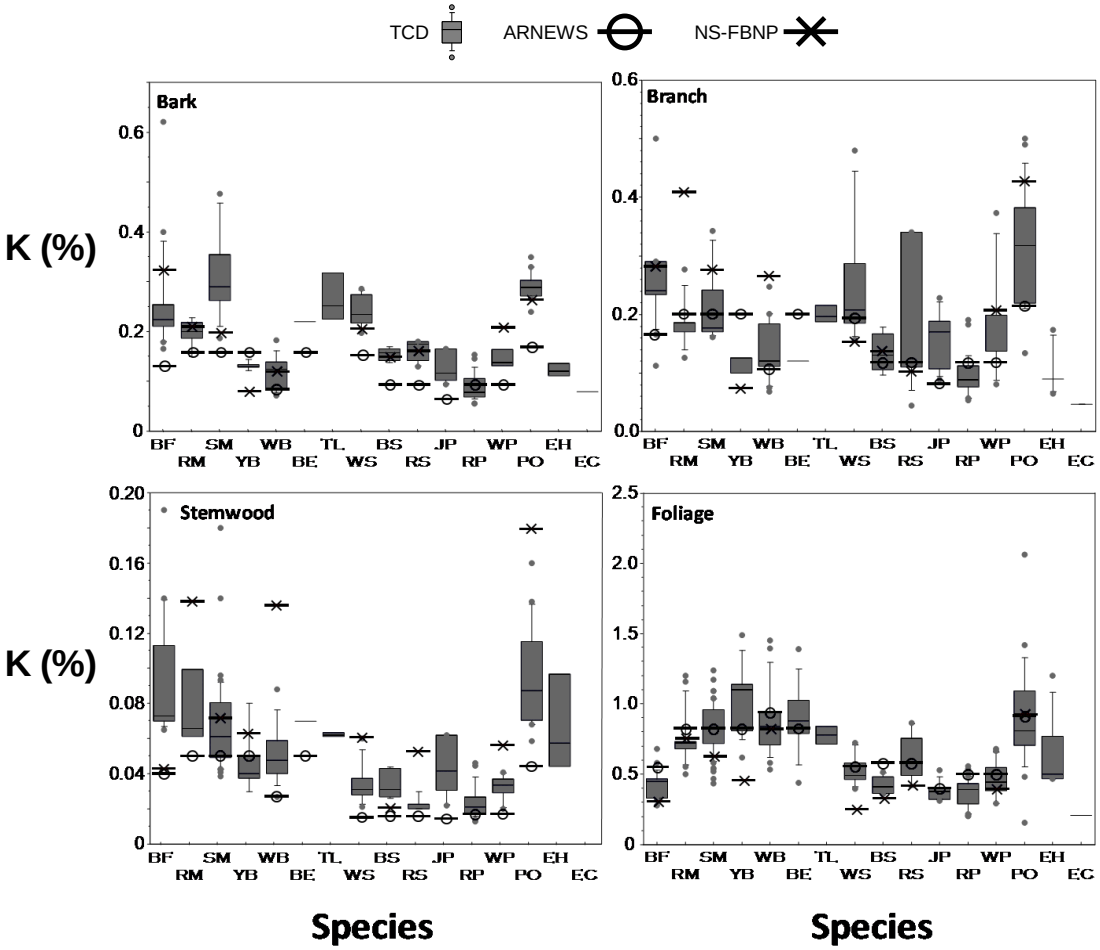


Figure 5.2. Box plots of K concentrations (%) in bark, branch, stem-wood and foliage compartments, by tree species, for the TCD dataset; the corresponding entries from the ARNEWS and NS-FBNP data sources are shown by the line symbols. Box plots show the 10th, 50th, and 90th percentiles, and outliers below the 10th and above the 90th percentiles.

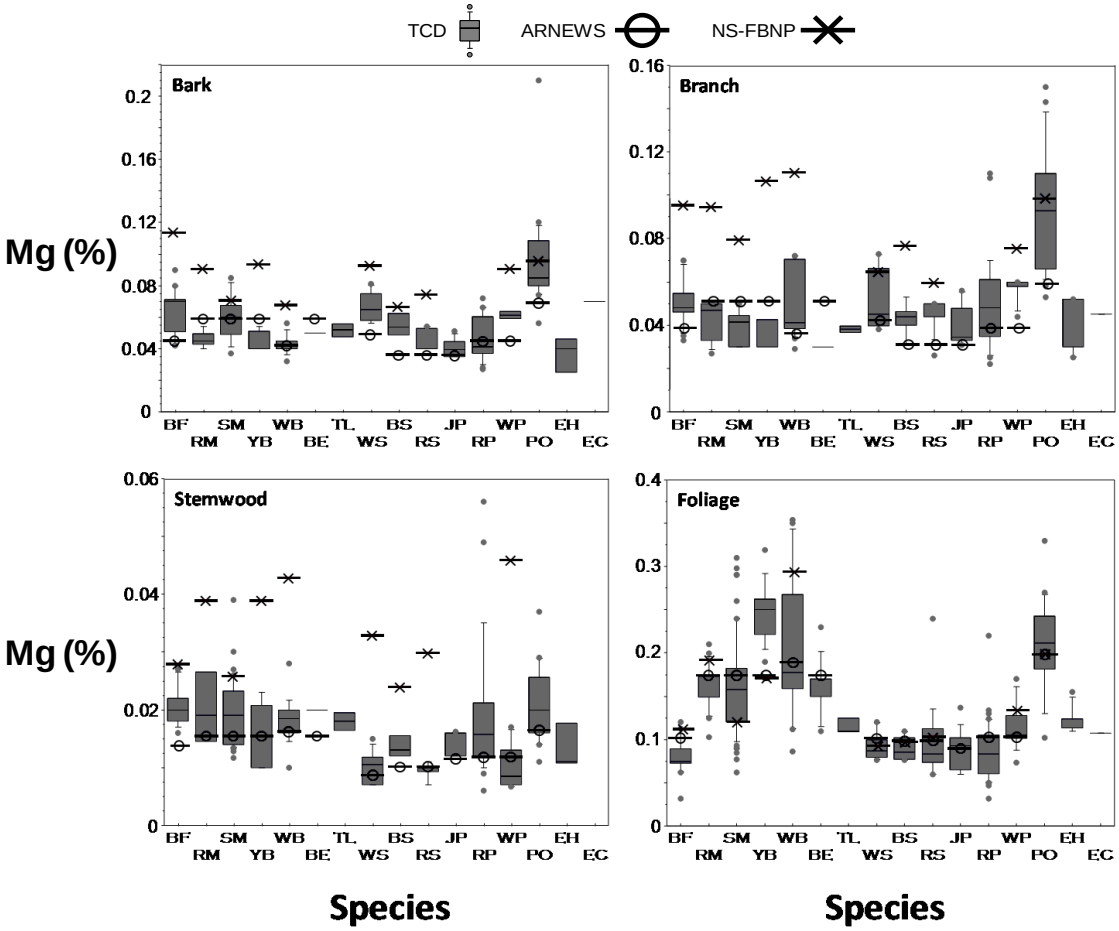


Figure 5.3. Box plots of Mg concentrations (%) in bark, branch, stem-wood and foliage compartments, by tree species, for the TCD dataset; the corresponding entries from the ARNEWS and NS-FBNP data sources are shown by the line symbols. Box plots show the 10th, 50th, and 90th percentiles, and outliers below the 10th and above the 90th percentiles.

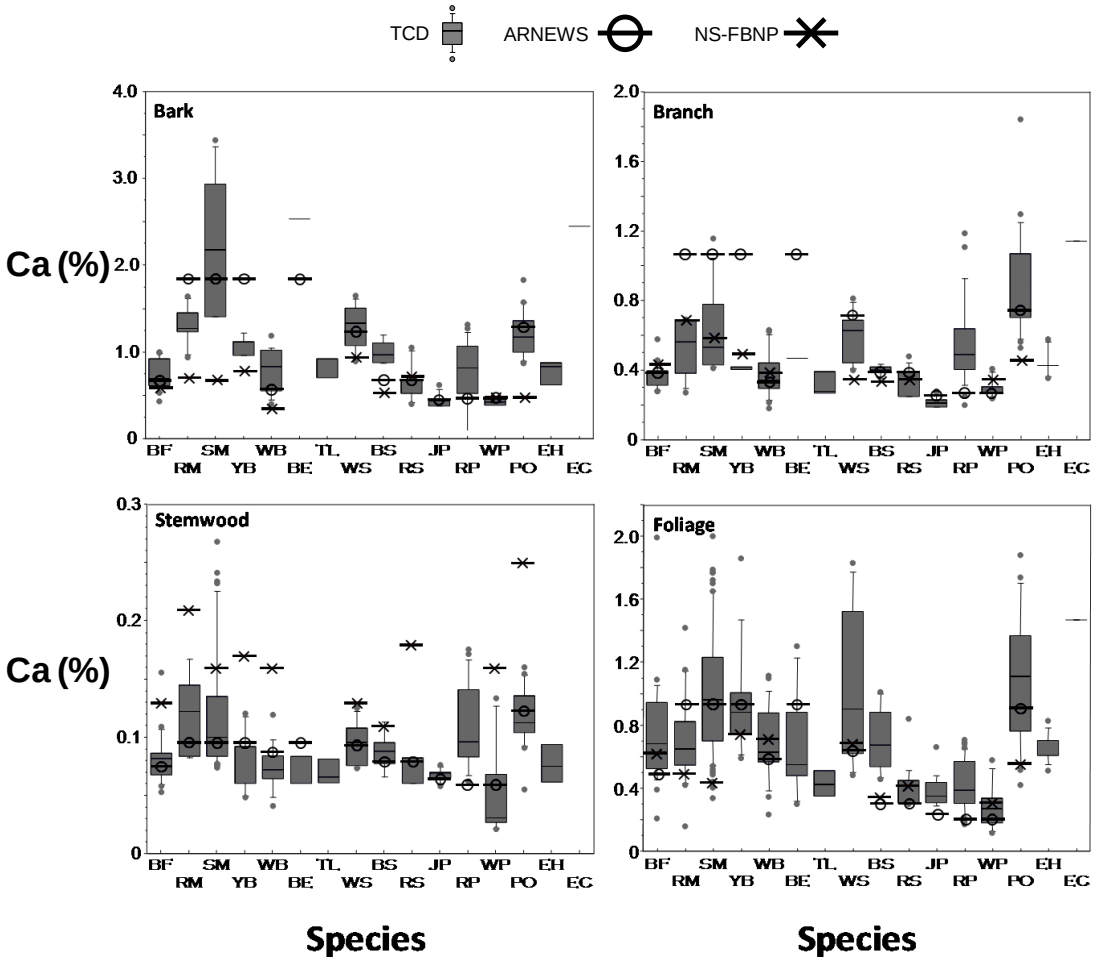


Figure 5.4. Box plots of Ca concentrations (%) in bark, branch, stem-wood and foliage compartments, by tree species, for the TCD dataset; the corresponding entries from the ARNEWS and NS-FBNP data sources are shown by the line symbols. Box plots show the 10th, 50th, and 90th percentiles, and outliers below the 10th and above the 90th percentiles.

Relationships between Data Sources, by Biomass Compartment and Nutrient concentrations

Regression equations for each nutrient element between the ARNEWS, TCD and NS-FBNP datasets, by tree biomass compartment, are shown in Tables 5.1 - 5.3. These tables show that:

1. the ARNEWS dataset are generally better correlated with the TCD than the NS-FBNP dataset, with the exception of branch N, K and Mg;

2. the general conformance between the ARNEWS, NS-FBNP and the TCD datasets improves, being best for foliage, and least for branches;

3. the conformance between the TCD and NS-FBNP nutrient concentrations is best for N and least for Mg, such that $N > K > Ca \geq Mg$ across all biomass compartments;

4. the conformance between the TCD and ARNEWS, by nutrient, does not appear to follow any sequence;

5. the conformance between the ARNEWS and NS-FBNP is generally best for foliage concentrations.

Table 5.1. Summary of the ARNEWS regression equations y = a + bx, for each biomass compartment nutrient concentration (%) as they relate to the corresponding TCD values; r^2 is the adjusted indication of fit between variables; *n* is the sample number fitting (all $P < 0.001$).

Tissue	Nutrient	*a*	*b*	r^2	*n*
Bark	N	0.067	0.64	0.698	13
	K	0.052	0.38	0.489	13
	Ca	0.227	0.76	0.614	13
	Mg	0.029	0.37	0.196	13
Branch	N	0.138	0.38	0.009	13
	K	0.103	0.30	0.094	13
	Ca	0.171	0.96	0.167	13
	Mg	0.034	0.18	0.007	13
Stemwood	N	-0.018	0.91	0.574	13
	K	0.005	0.50	0.577	13
	Ca	0.051	0.39	0.178	13
	Mg	0.006	0.48	0.566	13
Foliage	N	0.170	0.95	0.871	13
	K	0.208	0.73	0.856	13
	Ca	-0.040	0.90	0.566	13
	Mg	0.042	0.69	0.819	13

Table 5.2. Summary of the NS-FBNP regression equations y = a + bx, for each biomass compartment nutrient concentration (%) as they relate to the corresponding TCD values; r^2 is the adjusted indication of fit between variables; *n* is the sample number fitting (all $P < 0.001$).

Tissue	Nutrient	*a*	*b*	r^2	*n*
Bark	N	0.037	1.63	0.716	10
	K	0.049	0.71	0.442	10
	Ca	0.499	0.12	0.002	10
	Mg	0.064	0.39	0.059	10
Branch	N	0.137	1.71	0.284	10
	K	0.012	1.12	0.248	10
	Ca	0.329	0.24	0.030	10
	Mg	0.078	0.16	0.023	10
Stemwood	N	-0.287	6.15	0.514	10
	K	0.040	0.98	0.234	10
	Ca	0.104	0.70	0.061	10
	Mg	0.028	0.58	0.060	10
Foliage	N	-0.116	1.27	0.800	10
	K	0.017	0.77	0.455	10
	Ca	0.286	0.33	0.231	10
	Mg	0.032	0.81	0.537	10

Table 5.3. Summary of the NS-FBNP regression equations y = a + bx, for each biomass compartment nutrient concentration (%) as they relate to the corresponding ARNEWS values; r^2 is the adjusted indication of fit between variables; *n* is the sample number fitting (all $P < 0.001$).

Tissue	Nutrient	*a*	*b*	r^2	*n*
Bark	N	0.040	0.43	0.581	10
	K	0.103	0.14	0.080	10
	Ca	0.016	1.76	0.194	10
	Mg	0.028	0.27	0.023	10
Branch	N	0.069	0.27	0.377	10
	K	0.131	0.15	0.062	10
	Ca	-0.375	2.29	0.628	10
	Mg	0.023	0.24	0.090	10
Stemwood	N	0.046	0.06	0.078	10
	K	0.018	0.16	0.106	10
	Ca	0.044	0.27	0.355	10
	Mg	0.009	0.13	0.140	10
Foliage	N	0.514	0.61	0.667	10
	K	0.369	0.64	0.766	10
	Ca	0.126	0.94	0.158	10
	Mg	0.061	0.54	0.564	10

The conformance between the nutrient concentrations across the four biomass compartments is further illustrated in Figures 5.5 and 5.6 for the three datasets, and the corresponding least-squares fitted regression results are listed in Table 5.4. The following can be observed:

1. the ARNEWS data are highly correlated with the TCD across the four compartments ($r^2 > 0.916$). Among the four nutrients, Ca has the least cross-data correlations;

2. the NS-FBNP data also correlate best with the TCD as compared to the ARNEWS dataset;

3. the ARNEWS versus TCD correlations are best for N and least for Ca, such that N > K > Mg > Ca;

4. the NS-FBNP versus TCD correlations are also best for N and least for Ca, the goodness-of-fit decreases as follows: N > Mg > K > Ca;

5. the correlations generally follow linear 1:1 trends; the strongest deviation from the 1:1 trend occurred for the NS-FBNP-Ca versus TCD-Ca comparison.

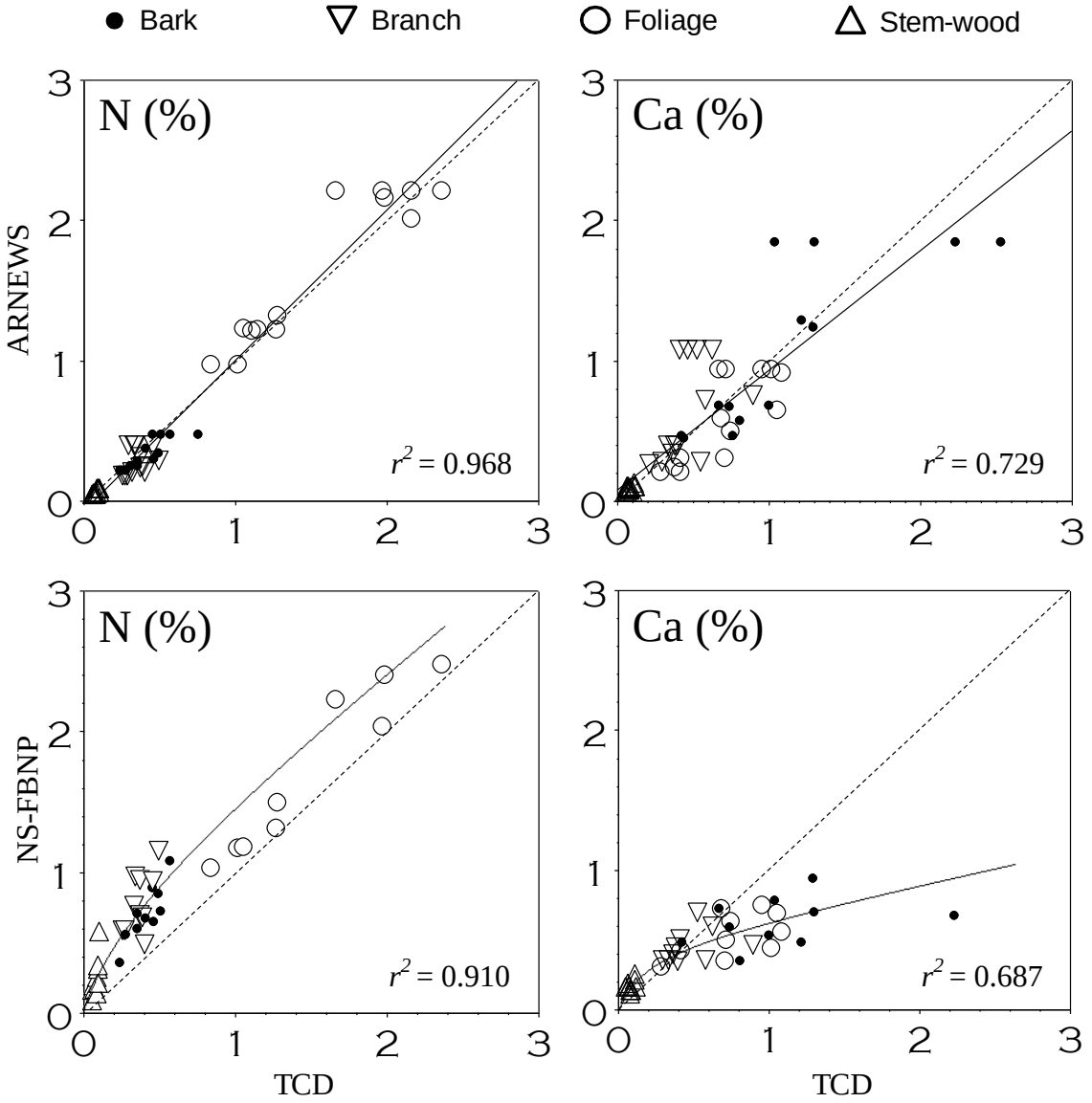


Figure 5.5. Comparing the nitrogen and calcium concentrations (%) for the NS-FBNP and ARNEWS datasets. The dashed lines represent a 1:1 ratio; r^2 is the adjusted indication of fit between variables.

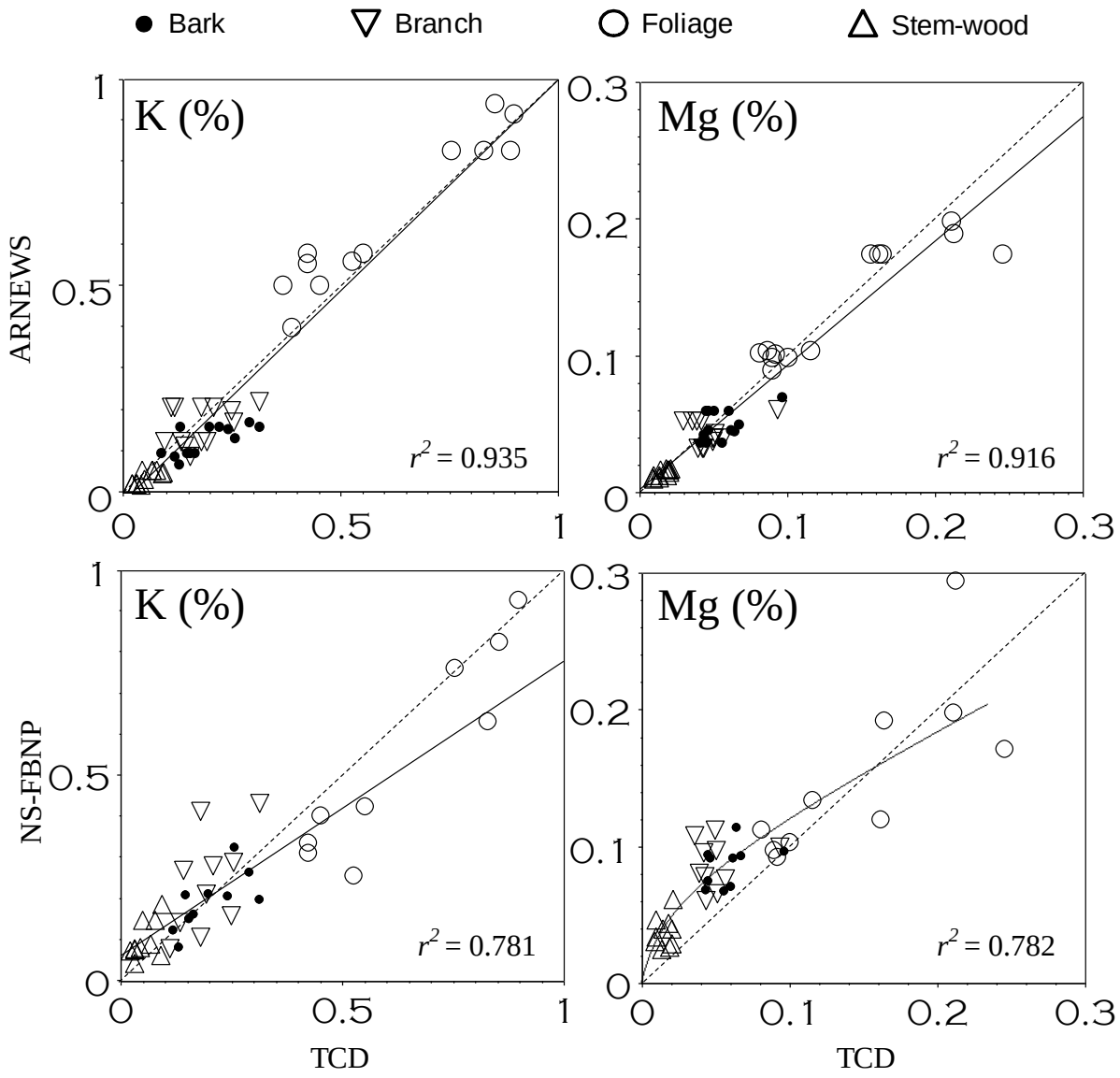


Figure 5.6. Comparing the potassium and magnesium concentrations (%) for the NS-FBNP and ARNEWS datasets. The dashed lines represent a 1:1 ratio; r^2 is the adjusted indication of fit between variables.

Table 5.4. Comparing the NS-FBNP and ARNEWS datsets with the TCD dataset by nutrient (N, K, Ca, Mg) by way of simple linear or power regression equations (superscripts 1 and 2, respectively); r^2 is the adjusted indication of fit between variables; *n* is the sample number fitting (all $P < 0.001$).

		a	*b*	r^2	*n*
N	ARNEWS[1]	-0.069	1.07	0.968	52
	NS-FBNP[2]	1.411	0.76	0.910	40
Ca	ARNEWS[1]	0.086	0.85	0.729	52
	NS-FBNP[2]	0.612	0.52	0.687	40
K	ARNEWS[1]	-0.024	1.02	0.935	52
	NS-FBNP[1]	0.062	0.72	0.781	40
Mg	ARNEWS[1]	0.002	0.91	0.916	52
	NS-FBNP[2]	0.479	0.60	0.782	40

[1]Regression equation follows a linear function: ($y = ax + b$)
[2]Regression equation follows a power function: ($y = a x^b$)

NS-FBNP Validation

In order to identify if the elevated concentrations within the NS-FBNP dataset were attributed to localized phenomenon within Nova Scotia, the TCD, ARNEWS and NS-FBNP datasets were compared a 4th tree biomass compartment macronutrient study by Freedman *et al.,* (1982). The Freedman study was conducted within central Nova Scotia, for 10 commercial tree species (Balsam Fir, White Spruce, Black Spruce, Red Spruce, Red Maple, Sugar Maple, Yellow Birch, White Birch, Large-tooth Aspen, Trembling Aspen). Using a series of simple linear regression analyses, each of the original three data sources were related to the Freedman dataset for: (i) the combined compartment and nutrient concentrations; (ii) the combined compartments, by nutrient. Scatterplots illustrating the regression analyses relating the NS-FBNP, ARNEWS and Freedman datasets to the TCD for the combined biomass compartment nutrient

concentrations are illustrated in Figure 5.7, and the corresponding regression equations are shown in Table 5.5. The results of the regression analyses using the indication of fit for the three data sources as they relate to the TCD follow that Freedman > ARNEWS > NS-FBNP. Further investigation comparing the Freedman study to the three original datasources, by nutrient, are shown in Table 5.6, the results of which illustrate the same sequence for each nutrient. It is therefore assumed that the elevated NS-FBNP nutrient concentrations are not attributed to localized phenomenon, as would be reflected by similar findings within the Freedman study.

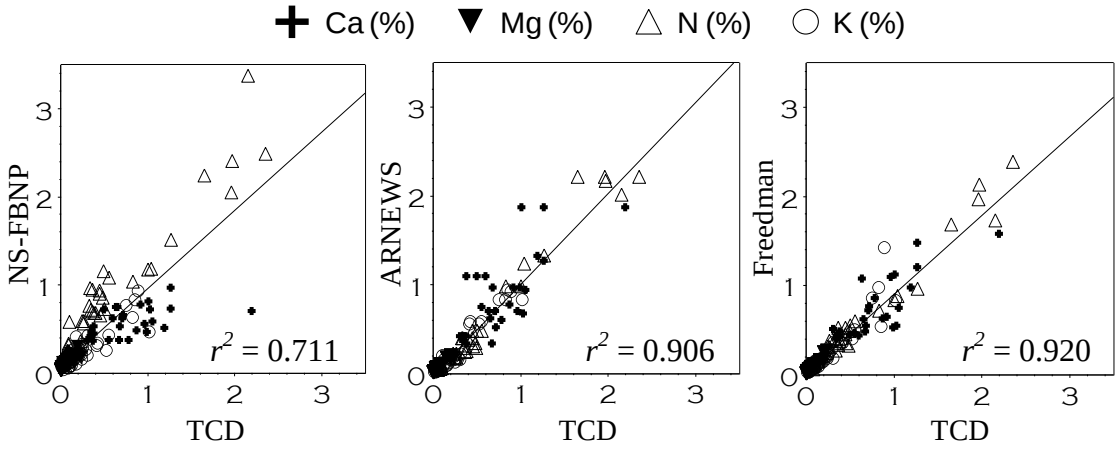


Figure 5.7. Comparing total nutrient concentrations (N, K, Mg, Ca) for the NS-FBNP, ARNEWS and Freedman datasets in relation to the TCD dataset (see Table 5.4); r^2 is the adjusted indication of fit between variables.

Table 5.5. Relating the total nutrients (%) of NS-FBNP, ARNEWS and Freedman datasets to the TCD dataset through simple linear regression (y = a + b x); r^2 is the adjusted indication of fit between variables; *n* is the sample number fitting (all $P < 0.001$).

Data Source	*a*	*b*	r^2	*n*
NS-FBNP	0.077	0.887	0.711	144
ARNEWS	-0.015	1.023	0.906	144
Freedman	0.014	0.886	0.920	144

Table 5.6. Relating NS-FBNP, ARNEWS and TCD datsets by nutrient (N, K, Ca, Mg) as they relate to the Freedman dataset through simple linear regression (y = a + bx); r^2 is the adjusted indication of fit between variables; *n* is the sample number fitting (all $P < 0.001$).

Tissue	Nutrient	*a*	*b*	r^2	*n*
NS-FBNP	N	0.258	1.13	0.865	36
	K	0.089	0.65	0.796	36
	Ca	0.218	0.44	0.607	36
	Mg	0.040	0.71	0.599	36
ARNEWS	N	-0.068	1.13	0.952	36
	K	0.030	0.86	0.814	36
	Ca	0.066	1.09	0.693	36
	Mg	0.004	0.84	0.817	36
TCD	N	0.018	0.93	0.969	36
	K	-0.023	1.04	0.849	36
	Ca	0.067	0.75	0.812	36
	Mg	0.005	0.95	0.925	36

Relationships between Nutrients

The N, K, Mg concentrations were strongly correlated with one another across the four nutrient compartments and across the three datasets as shown by the nutrient to-nutrient regression results in Table 5.7, and by the corresponding scatterplots in figures 5.8 and 5.9. In contrast, Ca was generally poorly correlated to N, K, and Mg. Further investigations revealed that:

1. stem-wood Ca concentrations were generally well correlated to the stem-wood N, K, and Mg ($r^2 \geq 0.613$; Figure 5.9; Table 5.8);

2. foliar Ca concentrations were strongly correlated with the foliar N, K, and Mg concentrations ($r^2 \geq 0.748$);

3. the bark and branch Ca concentrations were poorly correlated with the N, K, and Mg concentrations, with highest values reflective of the foliar Ca concentrations, and lowest values reflective of the stem-wood Ca concentrations. Altogether, the foliar and stem-wood Ca concentrations therefore serve as upper and lower limits of the Ca concentrations in branch and bark tissues, as shown in Table 5.9.

Table 5.7. Relating the paired nutrient ratios among N, K, Ca, Mg, as they relate to one another for the combined TCD, ARNEWS, NS-FBNP datasources through simple linear regression (y = a + bx); r^2 is the adjusted indication of fit between variables; *n* is the sample number fitting (*P* < 0.001 unless assigned *, which indicates *P* = 0.003).

	a	*b*	r^2	*n*
N / Mg	-0.169	11.93	0.885	155
K / Mg	-0.043	4.32	0.841	155
N / K	0.016	2.51	0.866	155
Ca / N	0.456	0.17	0.057	155*
Ca / K	0.045	0.45	0.058	155*
Ca / Mg	0.375	2.75	0.095	155

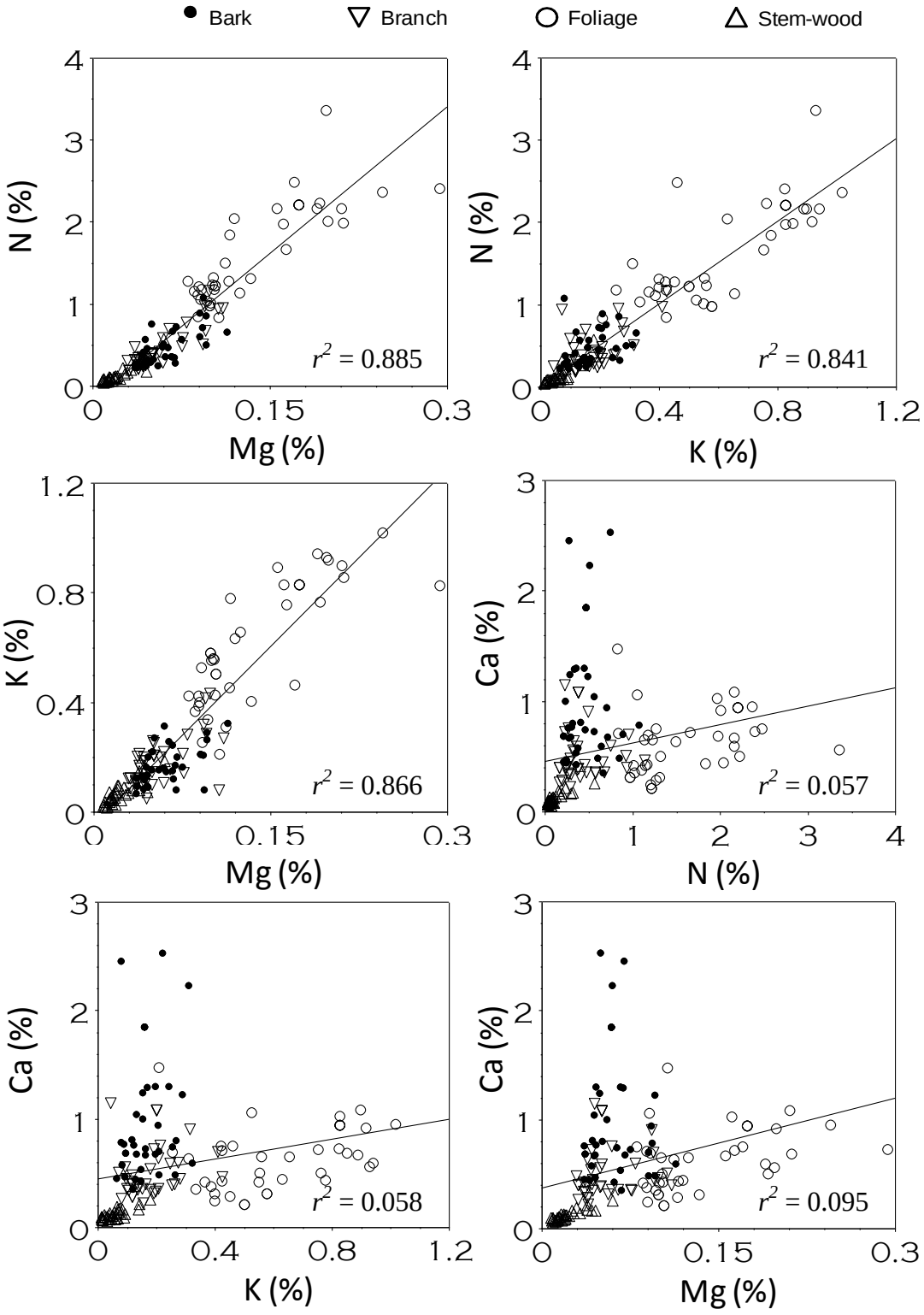


Figure 5.8. Comparing how N, K, Mg and Ca relate to one another across all three datasets, by tree compartment, through simple linear regression analysis (y = a + bx); r^2 is the adjusted indication of fit between variables.

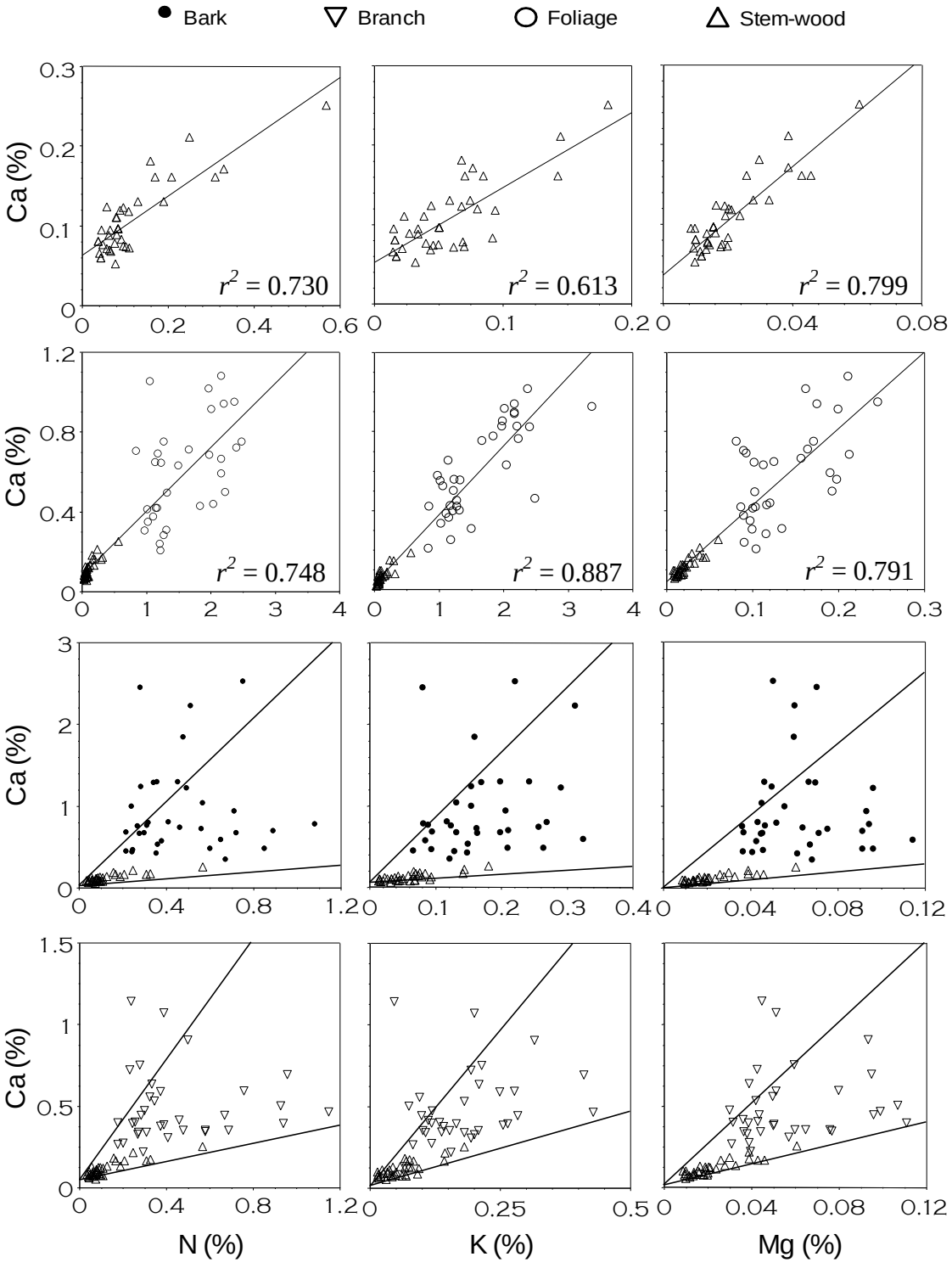


Figure 5.9. Relating N, K, and Mg concentrations to the Ca concentrations (%), by tree compartment for the combined datasets, using simple linear regression equations (y = a + bx) for stem-wood and foliage, and capturing 85% for the Ca data within the bark and branches using linear envelopes.

Table 5.8. Relating the Ca concentrations to the N, K and Mg concentrations in foliage and stem-wood for the combined datasources (TCD, ARNEWS, NS-FBNP), by simple linear regression (y = a + bx); r^2 is the adjusted indication of fit between variables; *n* is the sample number fitting ($P < 0.001$).

Tissue		*a*	*b*	r^2	*n*
Stem-wood	N	0.064	0.367	0.730	33
	K	0.053	0.939	0.613	33
	Mg	0.036	3.413	0.799	33
Foliage + Stem-wood	N	0.082	0.320	0.748	68
	K	0.031	0.349	0.887	67
	Mg	0.040	3.881	0.791	64

Table 5.9. Determing the 85% upper and lower envelope limits of the Ca concentrations to the N, K and Mg concentrations in bark and branches for the combined datasources (TCD, ARNEWS, NS-FBNP) by simple linear regression (y = a + bx); *n* is the sample number, and *% Cap* details the percentage of data points captured within the envelope.

Nutrient	Tissue(s)	Envelope Limits	*a*	*b*	*n*	% Cap
N	Bark + Stem-wood	Upper	0.03	4.30	67	97
		Lower	0.03	0.35		
	Branch + Stem-wood	Upper	0.04	1.85	68	91
		Lower	0.04	0.28		
K	Bark + Stem-wood	Upper	0.05	8.00	67	87
		Lower	0.05	0.50		
	Branch + Stem-wood	Upper	0.02	3.80	66	86
		Lower	0.02	0.90		
Mg	Bark + Stem-wood	Upper	0.01	22.00	67	90
		Lower	0.01	2.50		
	Branch + Stem-wood	Upper	0.01	12.50	66	91
		Lower	0.01	3.20		

Nutrient Concentration Lookup-Tables

Based on the results of the various regression analyses conducted within this chapter, the TCD dataset was chosen as the source of biomass compartment nutrient concentrations for the Nova Scotia Biomass Decision Support Tool (Tables 5.10 - 5.13), for the following reasons:

1. TCD represents a wide range of species, and is based on a larger per-species sample size than what is the case for the ARNEWS or NS-FBNP datasets;

2. There is greater consistency within the TCD with regard to the four tree biomass compartments than the ARNEWS or NS-FBNP datasets;

3. TCD allows for regional searching.

Table 5.10. TCD bark nutrient concentrations (%) for the 16 tree species of this study.

	Bark Concentrations (%)			
Species	**N**	**K**	**Ca**	**Mg**
BE	0.750	0.220	2.808	0.050
BF	0.462	0.257	0.739	0.064
BS	0.240	0.154	0.997	0.056
EC	0.280	0.080	2.450	0.070
EH	0.267	0.152	0.737	0.030
JP	0.245	0.128	0.440	0.041
PO	0.450	0.263	1.204	0.105
RM	0.433	0.198	1.302	0.047
RP	0.310	0.088	0.775	0.046
RS	0.277	0.164	0.669	0.045
SM	0.511	0.312	2.228	0.060
TL	0.318	0.269	0.798	0.052
WB	0.364	0.120	0.685	0.041
WP	0.354	0.147	0.422	0.061
WS	0.356	0.242	1.295	0.067
YB	0.567	0.124	1.028	0.042

Table 5.11. TCD stem-wood nutrient concentrations (%) for the 16 tree species of this study.

Stem-wood Concentrations (%)				
Species	**N**	**K**	**Ca**	**Mg**
BE	0.110	0.070	0.072	0.020
BF	0.092	0.092	0.082	0.020
BS	0.063	0.034	0.087	0.014
EC	0.078	0.032	0.052	0.010
EH	0.077	0.087	0.070	0.011
JP	0.068	0.044	0.068	0.014
PO	0.130	1.119	0.224	0.034
RM	0.089	0.080	0.112	0.020
RP	0.082	0.024	0.109	0.019
RS	0.064	0.022	0.069	0.010
SM	0.098	0.069	0.130	0.020
TL	0.059	0.062	0.070	0.018
WB	0.092	0.514	0.078	0.019
WP	0.078	0.032	0.052	0.010
WS	0.065	0.034	0.094	0.010
YB	0.103	0.043	0.070	0.016

Table 5.12. TCD branch nutrient concentrations (%) for the 16 tree species of this study.

Branch Concentrations (%)				
Species	**N**	**K**	**Ca**	**Mg**
BE	0.300	0.120	0.470	0.030
BF	0.392	0.257	0.381	0.050
BS	0.259	0.135	0.400	0.043
EC	0.240	0.047	1.140	0.045
EH	0.285	0.100	0.441	0.044
JP	0.295	0.156	0.217	0.040
PO	0.505	0.273	0.974	0.116
RM	0.309	0.170	0.466	0.042
RP	0.329	0.096	0.549	0.049
RS	0.274	0.183	0.338	0.044
SM	0.337	0.210	0.631	0.039
TL	0.272	0.201	0.325	0.038
WB	0.391	0.159	0.441	0.053
WP	0.409	0.195	0.303	0.057
WS	0.375	0.250	0.585	0.051
YB	0.460	0.113	0.413	0.036

Table 5.13. TCD foliage nutrient concentrations (%) for the 16 tree species of this study.

	Foliage Concentrations (%)			
Species	**N**	**K**	**Ca**	**Mg**
BE	2.164	0.890	0.666	0.156
BF	1.275	0.422	0.750	0.081
BS	0.837	0.424	0.705	0.089
EC	0.830	0.210	1.470	0.107
EH	1.157	0.657	0.642	0.125
JP	1.112	0.386	0.376	0.089
PO	2.114	0.781	1.060	0.208
RM	1.696	0.683	0.764	0.204
RP	1.150	0.364	0.420	0.088
RS	1.019	0.545	0.408	0.097
SM	1.949	0.755	0.934	0.154
TL	1.834	0.778	0.429	0.116
WB	1.917	0.865	0.722	0.225
WP	1.278	0.447	0.283	0.115
WS	1.053	0.525	1.053	0.092
YB	2.349	1.024	0.962	0.256

DISCUSSION

Sampling

The comparatively high nutrient concentrations associated with the NS-FBNP for bark, branch and stem-wood compartments are in part related to differences in sampling procedure. Both the ARNEWS and TCD bark and wood samples were taken from tree boles, whereas the NS-FBNP bark and wood samples were taken from twigs (to represent small-sized branches), and medium sized branches (diameter ~5cm or slightly larger, to represent live stem wood), respectively. Typically, as shown, tree stump nutrient concentrations are smaller than branch concentrations, branch concentrations are smaller than twig concentrations, and twig concentrations are smaller than foliage concentrations, for all four nutrients. A similar trend was observed by Maliondo *et al.,* (1990).

Although the ARNEWS dataset was generally in agreement with the TCD, a number of concentrations fell outside the TCD range. This may be attributed to the nation-wide ARNEWS averages, which account for a wide range of site characteristics that would not be reflected within the TCD. Moayeri (2001) stated that noticeable differences in tree species nutrient concentrations were observed between regions, which supports the use of local tree chemistry data in order to minimize the potential variability attributed to site conditions (see Augusto *et al.,* 2008). Furthermore, the species groupings by Moayeri (2001) may not necessarily reflect the variation of all the nutrient concentrations across the species within the suggested groups. For example, Red Pine and White Pine have similar N, K and Mg concentrations across all four tree compartments, but differ with respect to their Ca concentrations (Figure 5.4). A study conducted by Arthur *et al.* (1999) suggested that both Sugar Maple and Beech contained higher concentrations of Ca and Mg when compared to other northeastern deciduous tree species. Hence, grouping tree species is not advisable, and species-specific nutrient concentrations per biomass compartment is prefereable, especially if this information is available, as summarized in Tables 5.10 - 5.13.

Tree Nutrition

The strong and mostly linear relationships between the N, K and Mg concentrations across the four tree compartments suggest that uptake of these nutrients occurs according to physiological determined uptake ratios. This similarity simplifies the modeling of N, K, and Mg uptake in general terms: once the uptake or concentration of one of these elements is determined, the other elements can be estimated using the

appropriate nutrient ratios. This also applies to Ca, but only with respect to Ca in stem-wood and foliage. Bark and branch Ca concentrations tend to be scattered between the foliar and stem-wood Ca (Figure 5.9). In this regard, Boucher (1999) found that bark may act as a nutrient reserve, particularly during leaf abscission and senescence. Additionally, Whittaker and Woodwell (1968) found that Ca concentrations exceeded other nutrients within forest plots sampled on calcareous parent material, suggesting that site and related variations in Ca availability influence the degree to which Ca is taken up by vegetation. This may in part explain the high Ca values for species such as Eastern White Cedar, which inhabit calcareous sites, or occur on sites that receive Ca-rich groundwater seepage (Johnston, 1990). In general, increased uptake of Ca with increasing Ca availability within the soil is common, and this is referred to as "luxury consumption" (Chapman, 1967). Luxury consumption occurs when plants assimilate nutrient above their optimally and essentially ratio-fixed ranges, which can lead to toxic responses (Figure 5.10). In contrast, nutrient deficiencies occur when one or more of the required nutrients are not optimally available for uptake, which may lead to visual or non-visual plant symptoms such as leaf discoloration and reduced growth. Based on the diagrams in Figures 5.8 and 5.9, it would appear that the average N, K and Mg concentrations are essentially ratio-fixed, and therefore reflect optimal nutrient uptake, with bark and branch Ca somewhat exceptional. For modelling purposes, it is also of interest to note that all the species tend to follow the same trends across the four compartments.

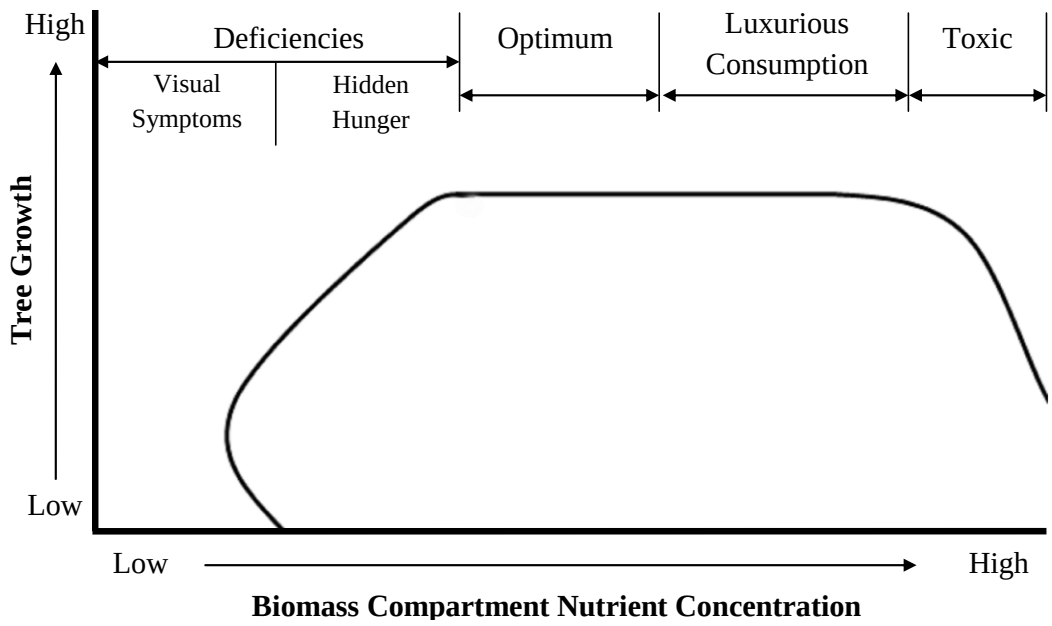


Figure 5.10. The hypothetical relationhsip between biomass compartment nutrient concentrations and tree growth, adapted from Chapman, 1967.

CONCLUSION

Examination of three datasets (TCD, ARNEWS, NS-FBNP) led to the adoption of the TCD lookup tables for N, K, Mg and Ca concentrations, by tree compartment (foliage, branch, bark and stem-wood), for dominant tree species (n = 17; Tables 5.10 - 5.13) and secondary tree species (n = 23; Appendix VI) within the Nova Scotia forest inventory. In general there was good correspondance between tree nutrient concentrations across species and biomass compartments, by dataset. Variations in sampling procedures and locality, however, likely contribute to some of the variation between the nutrient correlations between datasets. The N, K, Mg and Ca concentrations were remarkably consistent across the four biomass compartments, with the exception of Ca in bark and branches, where the Ca concentrations could either be as high as foliar Ca or as low as stem-wood Ca.

LITERATURE CITED

ARNEWS CD-ROM. (2000). *Forest Watershed Research Center. Faculty of Forestry and Environmental Management, UNB.* Fredericton, NB.

Arthur, M., Siccama, T., & Yanai, R. (1999). Calcium and magnesium in wood of northern hardwood forest species: relations to site characteristics. *Canadian Journal of Forest Research, 29*, 339-346.

Augusto, L., Meredieu, C., Bert, D., Trichet, P., Porte, A., & Bosc, A. (2008). Improving models of forest nutrient export with equations that predict the nutrient concentration of tree compartments. *Annals of Forest Science, 65*, 463-477.

Boucher, P. (1999). *Base-cation immobilization in the stem of some hardwoods of southern Quebec (MSc Thesis).* Montreal, QC.: McGill University.

Case, B., Banfield, E., Keys, K., & Arp, P. (1996). *ARNEWS plot, nutrients in vegetation and soils. Preliminary report for critical load assessments (unpublished manuscript).* Fredericton, NB.: Faculty of Forestry and Environmental Management, UNB.

Chapman, H. (1967). Plant analysis values suggestive of nutrient status of selected crops. In *Soil testing and plant analysis. II.* (pp. 77-92). Madison, WI: Soil Science Society of America. Special Publication Series No. 2.

D'Eon, S., Magasi, L., Lachance, D., & DesRochers, P. *1994.* ARNEWS: Canada's national forest health monitoring plot network. Manual on establishment and monitoring (revised). Chalk River, ON: Natural Resources Canada, Canadian Forest Service, Petawawa National Forestry Institute.

Freedman, B., Duinker, P., Barclay, H., Morash, R., & Prager, U. (1982). *Forest Biomass and Nutrient Studies in Central Nova Scotia.* Fredericton, N.B.: Maritime Forest Research Centre, Canadian Forest Service.

Freedman, B., Morash, R., & Hanson, A. (1981). Biomass and Nutrient Removals by Conventional and Whole-tree Clear-cutting of a Red Spruce - Balsam Fir Stand in Central Nova Scotia. *Canadian Journal of Forest Research, 11*, 249-257.

Johnston, W. (1990). Northern white-cedar (Thuja occidentalis L.). In R. Burns, & B. Honkala, *Silvics of North America: Vol. 1. Conifers* (pp. 260-280). Washington, D.C: USDA, Forest Service.

Keys, K., & Arp, P. (2009). Nova Scotia Forest Biomass Nutrient Project. *Unpublished*.

Maliondo, S., Mahendrappa, M., & van Raalte, G. (1990). *Distribution of biomass and nutrients in some New Brunswick forest stands: possible implications of whole-tree harvesting.* Fredericton, NB.: Forestry Canada, Maritime Region.

Mann, L., Johnson, D., West, D., Cole, D., Hornbeck, J., Martin, C., et al. (1988). Effects of whole-tree and stem-only clearcutting on postharvest hydrologic losses, nutrient capital and regrowth. *Forest Science, 34*, 412-428.

Mckeague, J. (Editor). (1978). *Manual of soil sampling and methods of analysis (2nd Ed).* Ottawa, ON.: Canadian Society of Soil Science.

Microsoft Access. (2002). *Office XP Professional and Developer* [Computer Software]. Microsoft Corporation.

Moayeri, M. (2000). *Mass Balance related sustainability of forest biomass production: Concepts and Applications (PhD Thesis).* Fredericton, NB.: University of New Brunswick.

Ouimet, R., Arp, P., Watmough, S., Aherne, J., & Demerchant, I. (2006). Determination and mapping of critical loads of acidity and exceedances for upland forest soils in Eastern Canada. *Water, Air and Soil Pollution, 172*, 57-66.

Pardo, L., Robin-Abbott, M., Duarte, N., & Miller, E. (2004). *Tree Chemistry Database (Version 1.0).* Newton Square, PA.: USDA, Forest Service.

Statview v5.0. (1998). Cary, NC: SAS Institute Inc. [Computer Software].

Whittaker, R., & Woodwell, G. (1968). Dimension and production relations of trees and shrubs in the Brookhaven forest, New York. *Journal of Ecology, 56*, 1-25.

CHAPTER 6

SPATIAL AND ASPATIAL REVIEW OF NOVA SCOTIA PHYSICAL & CHEMICAL SOIL PROPERTIES

INTRODUCTION

In 1934, the Nova Scotia Department of Agriculture and the Canada Department of Agriculture initiated a series of county-by-county soil surveys across Nova Scotia, to increase the capacity for agricultural planning (see Stobbe & McKeague, 1978). Surveys consisted of chemical and physical soil properties related to crop management, as well as detailed mapping of uniform soil series. At the provincial scale, various inconsistencies between sampling and mapping procedures between counties have resulted in misalignment of soil mapping units, and missing properties for a number of soil series. In order to relate the accumulation, retention and cycling of nutrients between trees and soils within the Biomass Decision Support Tool, a complete listing of soil physical and chemical properties was established, as well as province-wide geospatial representation of each soil property. The following chapter describes the methods used to develop a complete database and spatial coverage of Nova Scotia soil series by means of: (i) development of a soil inference system using a series of pedotransfer functions to predict missing soil properties from available data; (ii) alignment of geospatial county soil layers with the provincial boundary, as well as mapped wetland and water features; (iii) spatial assignment of soil series classifiers for complete series coverage; (iv) prediction of upland-lowland soil boundaries based on cartographic depth-to-water mapping with $10m^2$ resolution, validated using digital elevation models and aerial photography.

ASPATIAL METHODS

A database of physical and chemical soil properties (Table 6.1) was compiled from the 15 Nova Scotia county soil survey reports (Appendix VII). Within a Microsoft Excel (2007) spreadsheet, soil properties were recorded for each soil series (n = 102), by horizon. The final database contained over 1350 soil horizons, although initial review indicated a large amount of missing attributes. A soil inference system was developed using the methods described by McBratney *et al.,* (2002), to obtain a complete database of soil characteristics. Within the inference system, a series of pedotransfer functions were developed using various regression analyses and descriptive statistics. All pedotransfer functions were realized within the Statview statistical package (v.5.0; 1998).

Table 6.1 Physical and chemical soil properties tallied within the Nova Scotia soil database.

	Soil Property	Unit
Physical	Horizon description	N/A
	Horizon Depth	cm
	Coarse Fragment content	%
	Rooting Depth	cm
	Loss-on-Ignition	%
	Organic Matter content	%
	Sand content	%
	Silt content	%
	Clay content	%
	Bulk Density	$g\ cm^{-3}$
Chemical	Organic Carbon content	%
	K^+ concentration	me $100g^{-1}$
	Ca^{2+} concentration	me $100g^{-1}$
	Mg^{2+} concentration	me $100g^{-1}$
	Total Nitrogen content	%
	Cation Exchange Capacity	me $100g^{-1}$
	Base Saturation	%

Mineral Soil Texture

Although mineral soil texture descriptions were generally complete within the database, not all soil series records contained quantitative texture values. Missing fractions of sand, silt and clay were determined using the horizon descriptions in conjunction with the average sand, silt and clay contents for each texture class as described within the soil texture triangle (Agriculture Canada, 1974; Table 6.2).

Table 6.2. Average sand, silt and clay content for the missing soil texture classes within the Nova Scotia Soil Inference System, 2009.

	Average Content (%)		
Soil texture	Sand	Silt	Clay
Clay Loam	32.5	33.5	34.0
Loam	37.5	45.0	17.5
Loamy Sand	77.5	15.0	7.5
Organic Matter	0.0	0.0	0.0
Sand	92.5	2.5	5.0
Sandy Clay Loam	62.5	10.0	27.5
Sandy Loam	65.0	25.0	10.0
Silty Clay Loam	10.0	56.0	34.0
Silty Loam	25.0	61.0	14.0

A number of records within the database contained sand, silt and clay fractions that, in combination, either exceeded or fell below 100%. Each record was prorated in order that the combined sand, silt and clay contents equalled 100%, such that:

$$X_f^a = \frac{X_f}{\left(Sand_f + Silt_f + Clay_f\right)} 100 \qquad (6.1)$$

where X_f represents the fractions of *Sand*, *Silt* or *Clay* within the mineral soil, and superscript *a* denotes the amended fraction of *X*.

Coarse Fragment Content

Missing coarse fragment contents were established using the following methods, ranked by priority:

1. Soil horizon coarse fragment descriptions were referenced to numerical values within the Soil Sampling Field Manual (Day, 1983; n = 62).

2. Soil horizons that included gravel (%) within the texture assignments were assumed to have a coarse fragment content equal to that of gravel (n = 24).

3. The few remaining missing values were amended using average coarse fragment contents of the same soil series, by horizon (n = 9).

Loss-on-Ignition, Organic Matter and Organic Carbon Contents

The majority of soil horizons contained a combination of organic carbon (*Carbon*), loss-on-ignition (*LOI*), or soil organic matter (*OM*) contents, but rarely all three. In order to develop a complete listing of these attributes, pedotransfer functions were established using a series of regression analyses to relate each of these characteristics to one another. Missing values for *LOI* were first estimated using carbon as the predictive variable (Eq. 6.2; r^2 = 0.987; n = 821; P < 0.001). Conversely, carbon was estimated using the published *LOI* values as the predictive variable (Eq. 6.3; r^2 = 0.982; n = 592; P < 0.001). The complete listing of organic carbon values were then used to predict organic matter contents for both mineral soil (*MIN*; Eq. 6.4; r^2 = 0.990; n = 169; P < 0.001) and organic layers (*LFH*; Eq. 6.5; r^2 = 0.990; n = 21; P < 0.001).

$$LOI = 2.467 + 1.685\,Carbon \qquad (6.2)$$

$$Carbon = -0.511 + 0.626\,LOI - 1.917\log(LOI) \quad (6.3)$$

$$OM_{MIN} = 1.837\,Carbon_{MIN} \quad (6.4)$$

$$OM_{LFH} = 1.841\,Carbon_{LFH} \quad (6.5)$$

A number of soil horizons within the database contained no organic carbon, loss-on-ignition, or organic matter contents (n = 275). In order to populate these fields, each soil horizon was divided into 1 of 14 categories based on horizon descriptions (Day, 1983). Box plots were established for each horizon category, illustrating the range of organic carbon contents (Figure 6.1; Table 6.3). Mean contents were used to populate the missing carbon values, resulting in a complete listing of organic carbon for each soil horizon. Missing organic matter and LOI contents were then populated following equations 6.4 - 6.5, and 6.2, respectively.

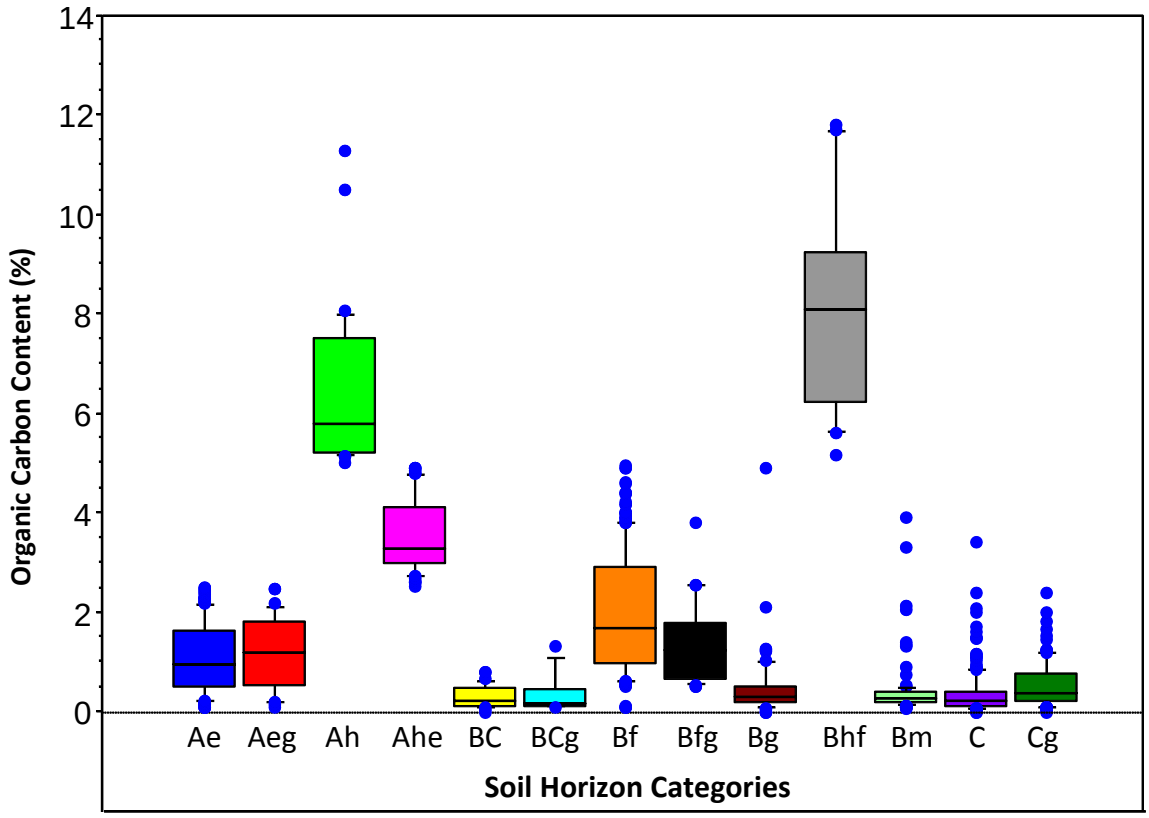


Figure 6.1. Box plots illustrating the range of organic carbon contents (%) for each of the 13 mineral soil horizons within the Nova Scotia Soil Inference System. Box plots show the 10th, 50th, and 90th percentiles, and outliers below the 10th and above the 90th percentiles.

Table 6.3. Descriptive statistics of organic carbon contents (%) in each of the soil horizon categories, including the LFH layer, within the Nova Scotia Soil Inference System.

Soil Horizon	Organic Carbon Content (%)					
	Mean	Std. Error	Minimum	Maximum	Count	# Missing
Ae	1.089	0.052	0.08	2.50	180	39
Aeg	1.173	0.128	0.10	2.48	34	8
Ah	6.389	0.278	5.00	11.28	32	7
Ahe	3.546	0.096	2.52	4.90	57	0
BC	0.298	0.038	0.00	0.80	35	7
BCg	0.377	0.113	0.10	1.31	12	1
Bf	1.982	0.083	0.09	4.96	214	25
Bfg	1.361	0.133	0.50	3.80	34	49
Bg	0.499	0.092	0.00	4.90	58	8
Bhf	8.201	0.540	5.16	11.81	16	19
Bm	0.411	0.052	0.07	3.90	110	4
C	0.363	0.032	0.00	3.40	196	34
Cg	0.553	0.048	0.00	2.40	96	27
LFH	36.478	0.889	18.26	55.51	108	47

Total Nitrogen

Missing soil nitrogen (*N*; *n* = 921) was determined for each mineral soil layer (*A*, *B*, and *C*) using both simple and multiple regression analyses. The highest correlation was found to be with organic carbon contents for both the A layer (Eq. 6.6; r^2 = 0.835; *n* = 261; *P* < 0.001) and B layer (Eq. 6.7; r^2 = 0.848; *n* = 381; *P* < 0.001), whereas the C layer was found to correlate best with both organic carbon and silt contents (*SILT*; Eq. 6.8; r^2 = 0.806; *n* = 230; *P* < 0.001). Scatter-plots illustrating the regression analyses for each mineral soil layer are shown in Figure 6.2. Total nitrogen contents within the LFH layer were found to correlate poorly to all other compiled soil properties ($r^2 \leq 0.30$). In order to populate missing LFH values, each soil series was categorized by landform, and box plots were established to illustrate the range of total nitrogen content (%), by landform (Figure 6.3; Table 6.4). Mean contents were used to populate the missing LFH nitrogen fields (*n* = 49).

$$N_A = 0.025 + 0.05\,Carbon \tag{6.6}$$

$$N_B = 0.025 + 0.043\,Carbon \tag{6.7}$$

$$N_C = 0.001\,SILT + 0.055\,Carbon \tag{6.8}$$

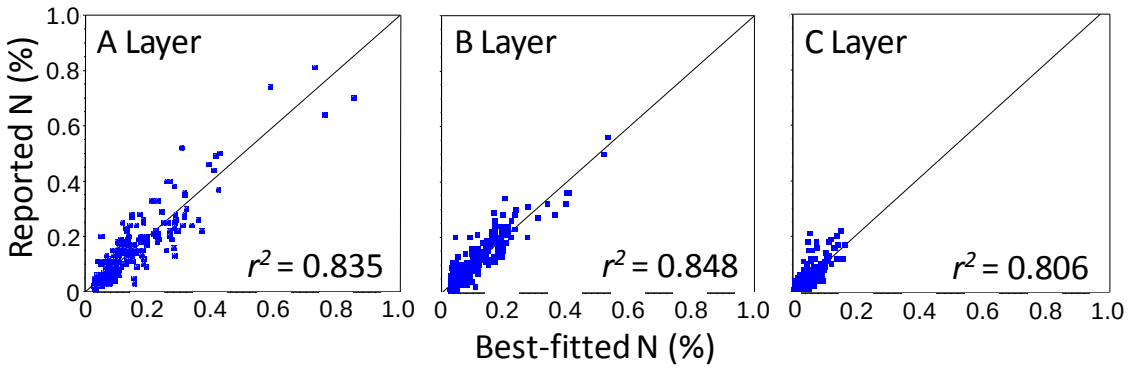


Figure 6.2. Reported nitrogen contents (%) for the A, B and C horizons versus best-fitted values (Eq. 6.6 - 6.8) within the Nova Scotia Soil Inference System. r^2 is the adjusted indication of fit between variables.

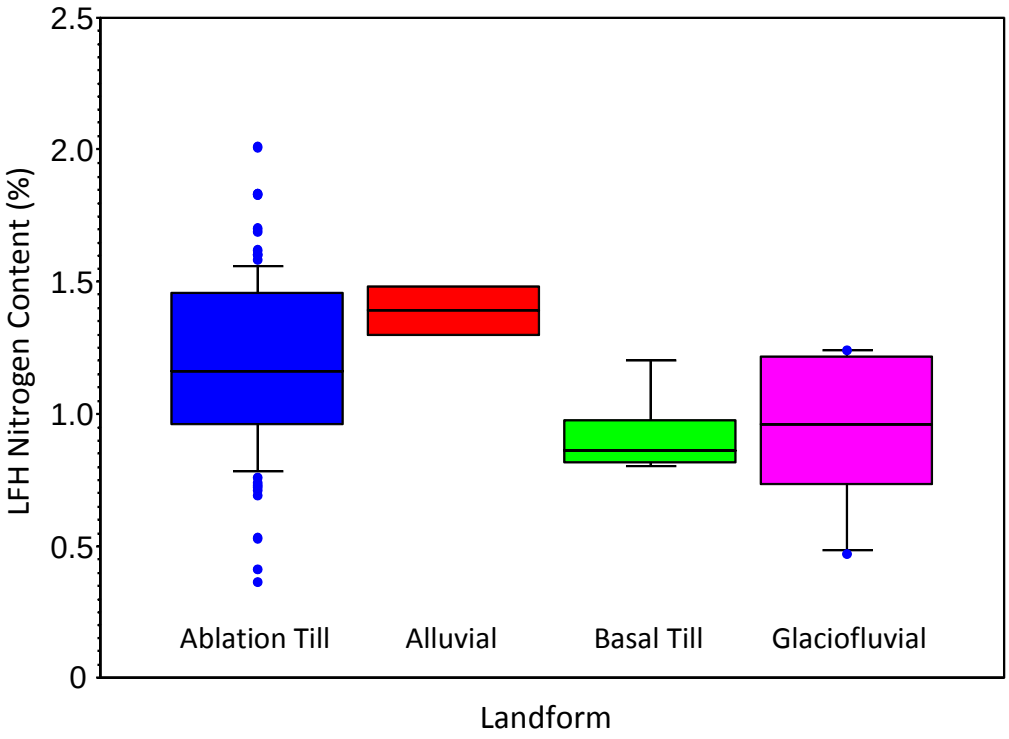


Figure 6.3. Box plots illustrating the range of LFH nitrogen contents (%) by landform within the Nova Scotia Soil Inference System. Box plots show the 10th, 50th, and 90th percentiles, and outliers below the 10th and above the 90th percentiles.

Table 6.4. Descriptive statistics of total LFH nitrogen contents (%), by landform within the Nova Scotia Soil Inference System.

	Total LFH Nitrogen (%)					
Landform	Mean	Std. Error	Minimum	Maximum	Count	# Missing
Ablation Till	1.180	0.034	0.36	2.01	90	43
Alluvial	1.390	0.090	1.30	1.48	2	0
Basal Till	0.916	0.073	0.80	1.20	5	4
Glaciofluvial	0.937	0.100	0.47	1.24	9	2

Cation Exchange Capacity

The cation exchange capacity (*CEC*) refers to the sum of exchangeable acid cations (H^+, Al^{3+}) and base cations (Ca^{2+}, Mg^{2+}, K^+, Na^+). Exchangeable Na^+, however, was almost entirely absent from the soil surveys, as it is not a growth-limiting nutrient.

Additionally, Na^+ tends to be highly mobile, very soluble, and readily leached from soils (Henderson *et al.,* 1977; Jordan *et al.,* 1986). Hence, any potential contributions of exchangeable Na^+ to the CEC were assumed to be negligible. Missing CEC fields (n = 922) were determined using the following methods, ranked by priority:

1. Where possible, CEC was calculated by summing the available base and acid cation concentrations (me $100g^{-1}$, n = 75), such that:

$$CEC = Ca^{2+} + Mg^{2+} + K^{+} + Al^{3+} + H^{+} \quad (6.9)$$

2. Soil horizons that did not have exchangeable acid cation concentrations (n = 374) were calculated using the sum of the exchangeable base-cation concentrations (*BC*; me $100g^{-1}$) and base saturation (*BS*; %), such that:

$$CEC = \frac{BC}{\left(BS/100\right)} \quad (6.10)$$

3. All remaining CEC values that could not be directly calculated using equations 6.9 and 6.10 were determined through a series of regression analyses for each soil layer. *A* layers were found to correlate best with organic matter (*OM*) and clay (*CLAY*) contents (Eq. 6.11; r^2 = 0.881; n = 81; P < 0.001), *B* layers correlated best with the combination of loss-on-ignition, silt, exchangeable Mg^{2+} (*Mg*) and nitrogen contents (Eq. 6.12; r^2 = 0.802; n = 207; P < 0.001), *C* layers correlated best using loss-on-ignition, silt and exchangeable Ca^{2+} (*Ca*; Eq. 6.13; r^2 = 0.881; n = 119; P < 0.001), and LFH was found to correlate best using only organic matter contents (Eq. 6.14; r^2 = 0.819; n = 66; P < 0.001). Scatter-plots illustrating the regression analyses for each mineral soil layer are shown in Figure 6.4.

$$CEC_A = 1.139\,OM + 0.272\,CLAY \quad (6.11)$$

$$CEC_B = 0.837\,LOI + 0.064\,SILT + 2.917\,Mg - 4.766\,N \quad (6.12)$$

$$CEC_C = 0.826\,LOI + 0.068\,SILT + 1.085\,Ca \quad (6.13)$$

$$CEC_{LFH} = -49.334 + 1.653\,OM \quad (6.14)$$

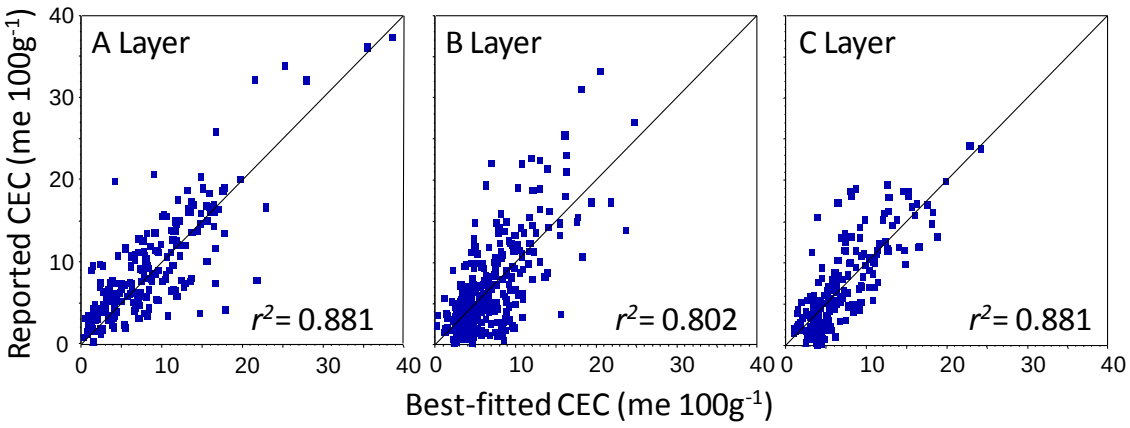


Figure 6.4. Reported CEC (me 100g^{-1}) values of the A, B and C layers versus best-fitted values (Eq. 6.11 - 6.13) within the Nova Scotia Soil Inference System. r^2 is the adjusted indication of fit between variables.

Exchangeable Base Cations

Initial review of the exchangeable base-cation concentrations were found to correlate poorly with all other compiled soil properties ($r^2 \leq 0.42$). In order to populate the missing base-cation fields, box plots were established using the soil horizon categories described previously, illustrating the range of exchangeable base-cation concentrations for Ca^{2+} (Figure 6.5; Table 6.5), Mg^{2+} (Figure 6.6; Table 6.6), and K^+ (Figure 6.7; Table 6.7). Mean contents were used to populate missing exchangeable base-cation concentrations, resulting in a complete listing of base-cation contents for each soil series.

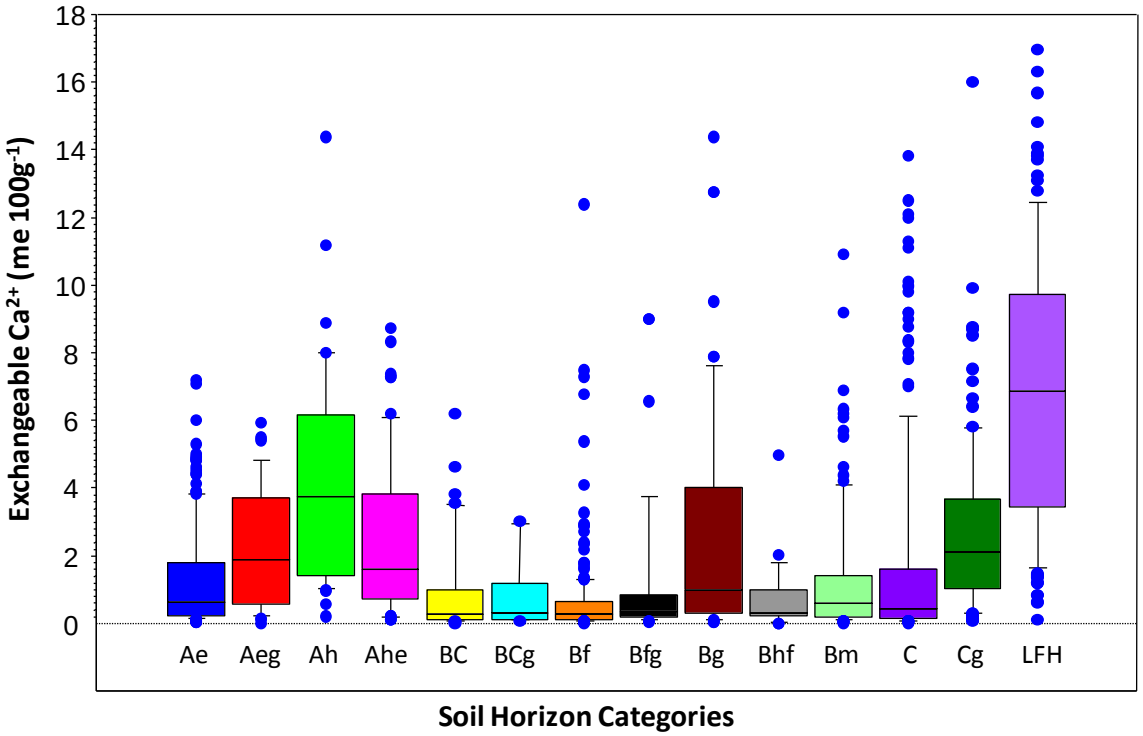


Figure 6.5. Box plots illustrating the range of exchangeable Ca^{2+} (me $100g^{-1}$), by soil horizon within the Nova Scotia Soil Inference System. Box plots show the 10th, 50th, and 90th percentiles, and outliers below the 10th and above the 90th percentiles.

Table 6.5. Descriptive statistics for exchangeable Ca^{2+} (me $100g^{-1}$), by soil horizon, within the Nova Scotia Soil Inference System.

	Exchangeable Ca^{2+} (me $100g^{-1}$)						
Soil Horizon	Mean	Std. Dev.	Std. Error	Count	Minimum	Maximum	# Missing
Ae	1.278	1.508	0.111	184	0.020	7.200	35
Aeg	2.224	1.822	0.313	34	0.000	5.940	8
Ah	4.282	3.265	0.544	36	0.200	14.360	3
Ahe	2.542	2.385	0.316	57	0.120	8.720	0
BC	0.895	1.388	0.214	42	0.000	6.200	0
BCg	0.870	1.041	0.289	13	0.080	3.010	0
Bf	0.654	1.298	0.086	227	0.000	12.400	12
Bfg	1.254	2.324	0.399	34	0.030	9.000	49
Bg	2.626	3.471	0.452	59	0.030	14.360	7
Bhf	0.749	1.090	0.232	22	0.000	4.970	13
Bm	1.356	1.989	0.190	110	0.000	10.900	4
C	1.772	2.942	0.202	212	0.000	13.800	18
Cg	2.700	2.528	0.254	99	0.080	16.000	24
LFH	6.807	4.007	0.374	115	0.110	16.950	40

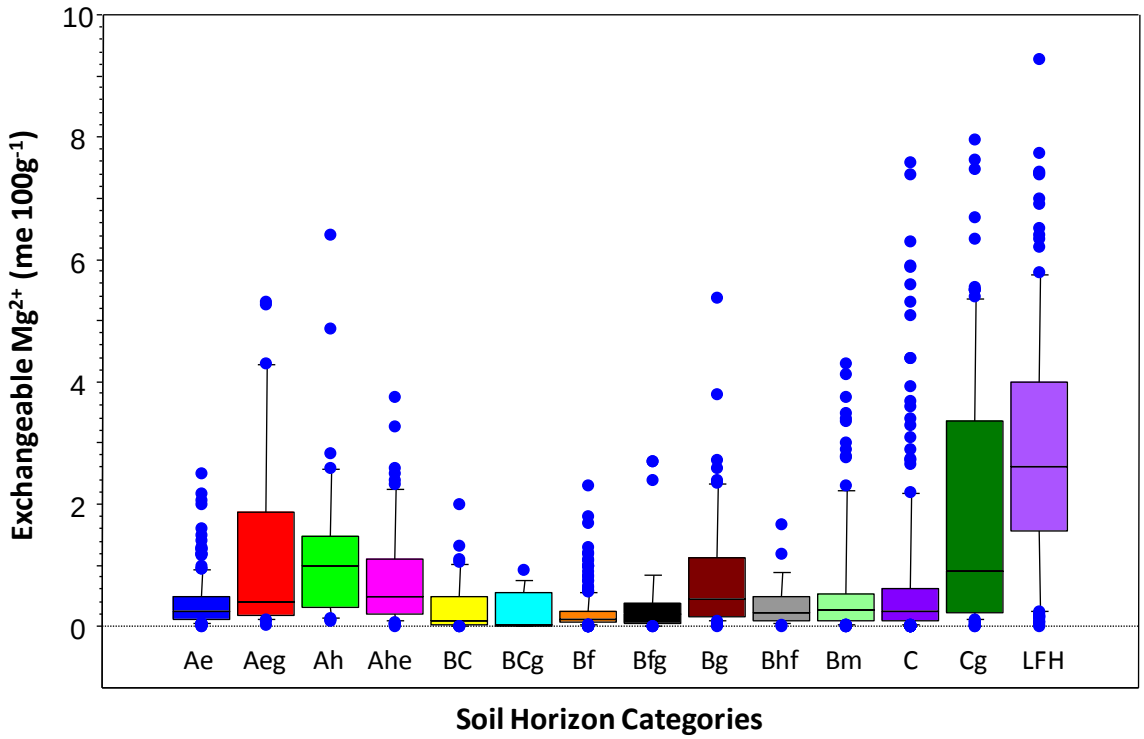


Figure 6.6. Box plots illustrating the range of exchangeable Mg^{2+} (me $100g^{-1}$), by soil horizon within the Nova Scotia Soil Inference System. Box plots show the 10th, 50th, and 90th percentiles, and outliers below the 10th and above the 90th percentiles.

Table 6.6. Descriptive statistics of exchangeable Mg^{2+} (me $100g^{-1}$), by soil horizon within the Nova Scotia Soil Inference System.

	Exchangeable Mg^{2+} (me $100g^{-1}$)						
Soil Horizon	Mean	Std. Dev.	Std. Error	Count	Minimum	Maximum	# Missing
Ae	0.397	0.428	0.032	184	0.000	2.500	35
Aeg	1.310	1.640	0.285	33	0.040	5.300	9
Ah	1.208	1.330	0.219	37	0.090	6.400	2
Ahe	0.812	0.856	0.113	57	0.000	3.750	0
BC	0.296	0.436	0.067	42	0.000	2.000	0
BCg	0.252	0.326	0.090	13	0.000	0.920	0
Bf	0.232	0.318	0.021	224	0.000	2.300	15
Bfg	0.411	0.715	0.123	34	0.000	0.271	49
Bg	0.886	1.026	0.134	59	0.000	5.380	7
Bhf	0.348	0.405	0.086	22	0.000	1.670	13
Bm	0.651	0.989	0.094	110	0.000	4.300	4
C	0.745	1.364	0.094	211	0.000	7.600	19
Cg	1.932	2.143	0.216	98	0.010	7.970	25
LFH	2.855	1.984	0.182	119	0.010	9.280	36

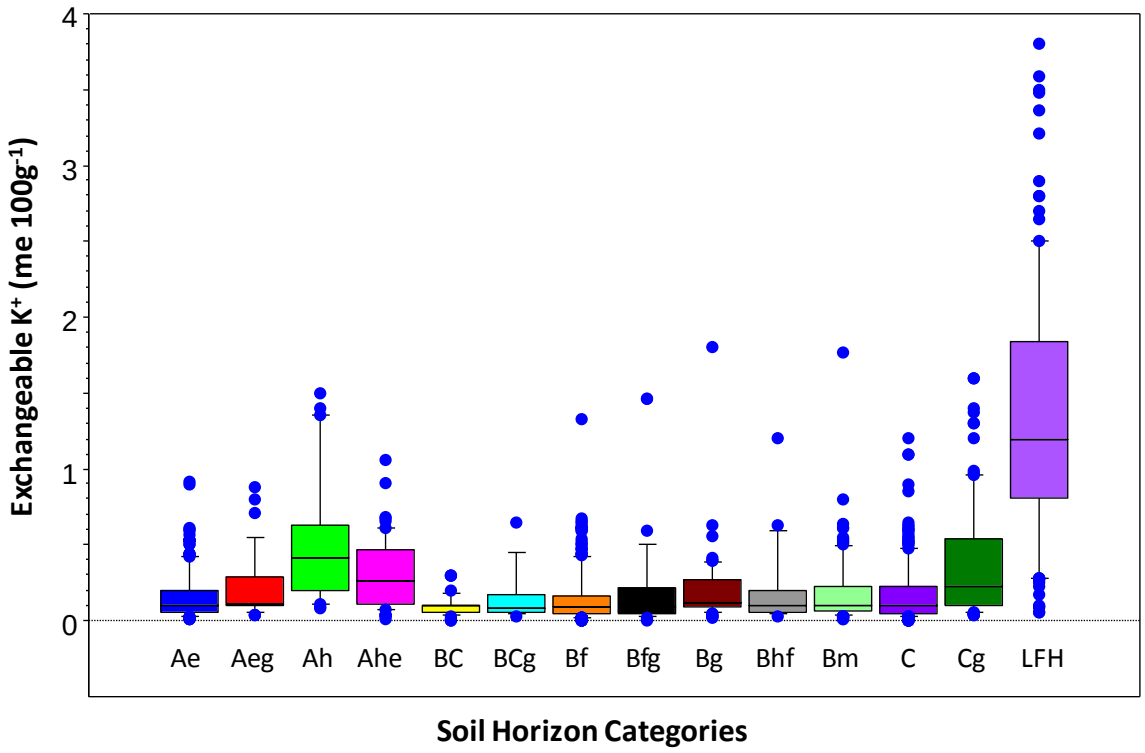


Figure 6.7. Box plots illustrating the range of exchangeable K^+ (me $100g^{-1}$), by soil horizon within the Nova Scotia Soil Inference System. Box plots show the 10^{th}, 50^{th}, and 90^{th} percentiles, and outliers below the 10^{th} and above the 90^{th} percentiles.

Table 6.7. Descriptive statistics of exchangeable K^+ (me $100g^{-1}$), by soil horizon within the Nova Scotia Soil Inference System.

	Exchangeable K^+ (me $100g^{-1}$)						
Soil Horizon	Mean	Std. Dev.	Std. Error	Count	Minimum	Maximum	# Missing
Ae	0.162	0.165	0.012	179	0.010	0.920	40
Aeg	0.220	0.218	0.037	34	0.040	0.880	8
Ah	0.546	0.424	0.073	34	0.080	1.500	5
Ahe	0.306	0.232	0.031	56	0.010	1.060	1
BC	0.100	0.070	0.011	42	0.000	0.300	0
BCg	0.165	0.185	0.051	13	0.030	0.650	0
Bf	0.152	0.178	0.012	227	0.000	1.330	12
Bfg	0.223	0.344	0.059	34	0.000	1.460	49
Bg	0.205	0.249	0.032	59	0.020	1.800	7
Bhf	0.210	0.274	0.058	22	0.030	1.200	13
Bm	0.188	0.225	0.022	109	0.010	1.770	5
C	0.180	0.206	0.014	208	0.000	1.200	22
Cg	0.386	0.390	0.039	98	0.040	1.600	25
LFH	1.358	0.848	0.079	116	0.060	3.800	39

Base Saturation

Using the complete listing of CEC values, missing base saturation (%) was calculated using the amended CEC's and the sum of soil base cations (*BC*; eq ha^{-1} yr^{-1}), by setting:

$$BS = \frac{BC}{CEC} 100 \tag{6.15}$$

Rooted Depth

In addition to the absolute soil depth (cm), soil horizons supporting vegetation were recorded either as a "Yes" or "No", to reflect rooting within each soil horizon. When this information was not directly available, rooting was determined using the detailed soil horizon descriptions. Soil horizons classified as "firm" or "very firm" were assumed to not support root growth, whereas horizons that were "slightly firm", "friable" or "very friable" were assumed to support root growth, unless the horizon was below one which did not support rooting. Additionally, all hardpan and gleyed soil horizons were assumed to not support rooting unless specifically identified as doing so.

Bulk Density

An additional set of pedotransfer functions were included within the soil inference system to determine soil bulk density (*Db*), which was not consistently recorded among the soil surveys. Functions were taken from the equations developed by Balland *et al.*, (2008), which were formulated specifically for New Brunswick and Nova Scotia soils. Mineral soil bulk density (Db_{min}) was calculated as:

$$Db_{\min} = \frac{1.23 + \left(Dp_{soil} - 1.23 - 0.75\, Sand_f\right)\left(1 - \exp\left(-0.0106\, Depth\right)\right)}{1 + 6.83\, OM_f} \tag{6.16}$$

where *Depth* refers to soil horizon midpoint depth in cm (*C* horizons without a lower depth value had 20 cm added to the horizon surface value), $Sand_f$ and OM_f refer to the fraction of sand and organic matter, respectively, prorated from the total sand, silt, clay and organic matter content, such that:

$$X_f^a = \frac{X_f}{\left(Sand_f + Silt_f + Clay_f + OM_f\right)} 100 \tag{6.17}$$

where *X* refers to either sand or organic matter, subscript *f* denotes the fraction of *X*, and superscript *a* denotes the amended fraction of *X*. Finally, Dp_{soil} refers to the soil particle density in g cm^{-3}, calculated as:

$$Dp_{soil} = \frac{1}{\left(\frac{OM_f}{D_{OM}} + \frac{1 - OM_f}{D_{MIN}}\right)} \tag{6.18}$$

where D_{OM} is the average organic matter density, set at 1.3g cm^{-3}, and D_{MIN} is the average density for most silicate and carbonate minerals, set as 2.65g cm^{-3}. Similarly, *LFH* bulk density was calculated as:

$$Db_{LFH} = \frac{1.23 + \left(Dp_{soil} - 1.23\right)\left(1 - \exp\left(-0.0106\, Depth\right)\right)}{1 + 6.83\, OM_f} \tag{6.19}$$

Final Soil Model Inputs

Using the various pedotransfer functions described above, a complete listing of Nova Scotia soil properties was completed for each soil series, by horizon. A weighted average was calculated for each soil variable, by soil layer, using the corresponding bulk density and rooted soil depth, for each soil series, i.e.:

$$X_Y = \frac{\left[\sum_{i=1}^{4}\left\langle X_Y^i \; Depth \; Db\right\rangle\right]}{\left(Depth \; Db\right)} \tag{6.20}$$

where X refers to one of the 102 soil series', subscript Y denotes the soil physical or chemical properties, the superscript i specifies one of the 4 soil layers (*A*, *B*, *C* and *LFH*), *Depth* refers to the rooted soil depth (cm) and *Db* refers to the soil bulk density (g cm^{-3}). Additionally, the final CEC values were converted to total cation exchange sites (*CES*; eq ha^{-1}), and the exchangeable base cations were converted to fractions for use within the Biomass Decision Support Tool, such that:

$$CES = CEC \; Db \; Depth \, 10^3 \tag{6.21}$$

and

$$X_f = \frac{X}{BC} \tag{6.22}$$

respectively, where X refers to one of the base-cation contents (Ca^{2+}, Mg^{2+}, K^{+}), subscript f denotes the fraction of X, and *BC* is the sum of the base cations.

SPATIAL METHODS

Spatial Alignment

Nova Scotia geospatial soil data was obtained from The National Soil Database, maintained by the Canadian Soil Information Systems (CANsis) branch of Agriculture and Agri-food Canada (2002). The geospatial soil series were delineated from the hand-drawn maps of the original soil surveyors, resulting in relatively low spatial accuracy (see Moore *et al.,* 1993). In order to repair this, each county soil layer was aligned with the georeferenced provincial boundary (NSDNR, 2006a), mapped water bodies (NSDNR, 2006b) and wetlands (NSDNR, 2000). All datasets were realized within ArcMap 9.3.1 (ESRI, 2009), unless stated otherwise. The following describes the alignment steps taken in the order of completion:

1. The 20 county soil layers were combined using the Merge tool.

2. Using the provincial boundary polygon layer, all soil polygons were deleted using the Erase tool, resulting in a layer of sliver polygons outside the provincial boundary (Figure 6.8-a). All outside sliver polygons were deleted.

3. The county soil layer was used to erase (Erase tool) the provincial boundary layer resulting in a series of isolated slivers inside the provincial boundary (Figure 6.8-b). All inside slivers were incorporated into adjacent soil polygons using the Eliminate tool (by longest shared boundary).

4. Overlap between soil polygons occurred for several counties, which when merged together created additional polygons (Figure 6.9). Overlapping polygons were selected and intersected (Intersect tool) with a 10x10m polyline grid using the Create

Fishnet tool. The resulting features were converted to individual polygons using the Multipart-To-Singlepart tool. The individual sliver polygons were then incorporated into adjacent soil polygons using the Eliminate tool (by longest shared boundary).

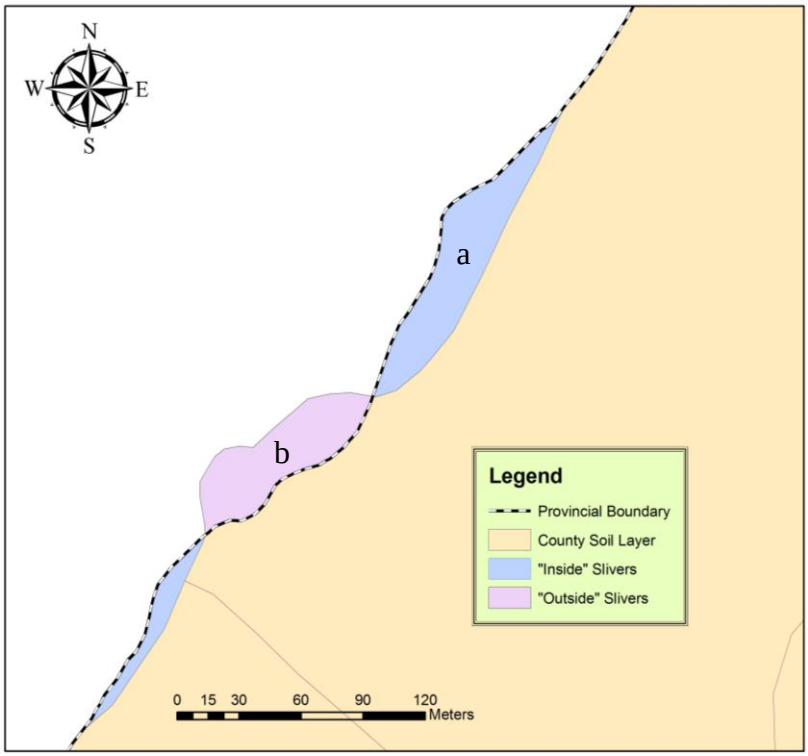


Figure 6.8. Example illustration showing the two forms of disalignment within the soil county layers, both as slivers "inside" the provincial boundary (a), and "outside" the provincial boundary (b).

5. The provincial water layer was overlaid on the provincial soil layer, showing a high degree of geospatial discordance both in detail and extent with the soil layer water features (Figure 6.10). The provincial water layer was used to erase (Erase tool) the soil layer, and any remaining water polygons within the soil layer were converted to individual polygons using the Multipart-To-Singlepart tool. All water sliver polygons were then incorporated into adjacent soil polygons using the Eliminate tool (by length).

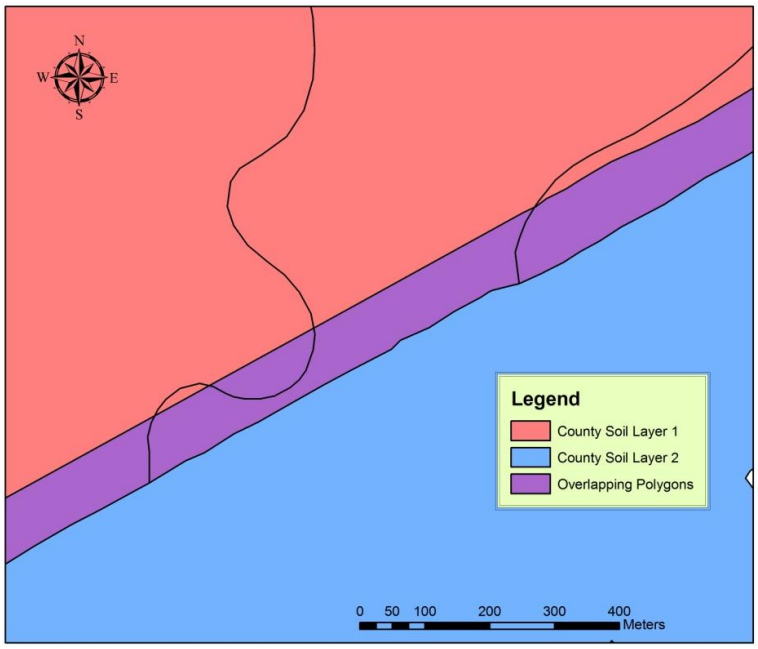


Figure 6.9. Example illustration showing the overlap of soil polygons between county soil layer borders.

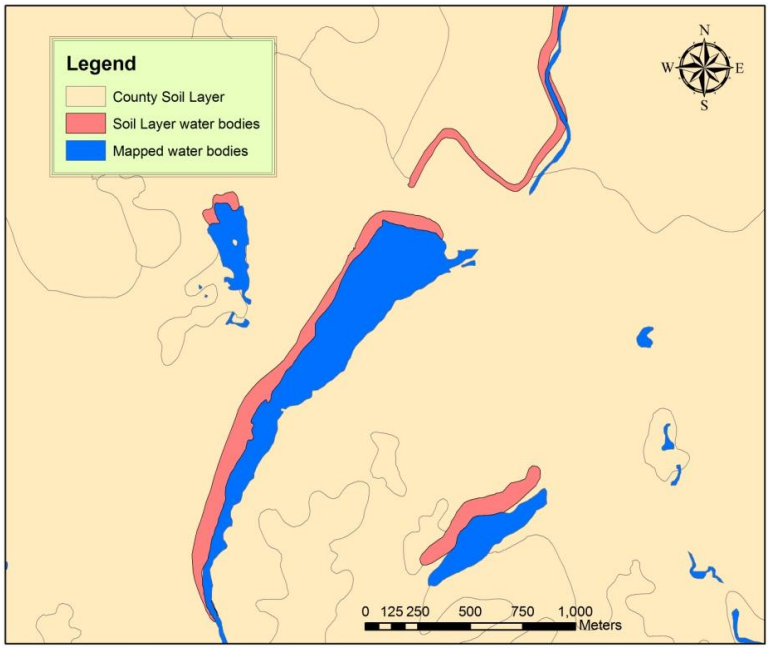


Figure 6.10. Example illustration showing the spatial inaccuracy of the county soil layers water bodies, both in detail (such as islands and shorelines), as well as actual extent of the water bodies.

6. The same procedures as described in Step 5 were completed using the provincial wetlands layer. All wetland sliver polygons with Castley, Rossignol, Dufferin or Saltmarsh soil series classifiers were incorporated into adjacent polygons using the Eliminate tool.

7. Steps 5 and 6 resulted in numerous island polygons, incorrectly classified as water or wetlands. All island polygons were given a unique ID and assigned the soil attributes from the nearest mainland soil polygon using the Nearest Feature Analysis Tool (Fox, 1998) in Arcview 3.3 (ESRI, 2002).

Soil Attribute Amendments

Assigning the aspatially-defined physical and chemical soil characteristics across Nova Scotia required numerous methods. The following section describes the steps taken to allow for complete soil physical and chemical coverage across Nova Scotia.

1. All attribute fields within the geospatial soil layer were deleted with the exception of MUGROUP (defining the county), MAPUNIT (defining the soil series) and SOILTYPE (defining non-soil landforms).

2. A new field, SOILNAME, was created and assigned with soil series or non-soil landform classifiers. Soil series summary codes from the MAPUNIT field were used to fill in the soil series classifiers. These classifiers were validated with the hardcopy survey maps, for each county.

3. The non-soil landform code descriptions within the SOILTYPE field were taken from the "linkage.txt" files associated with each county geospatial layer. SOILNAME attributes were appended as follows:

    a. SOILTYPE ZRL = bedrock substrate, and were inputted as "Rockland" in the SOILNAME attribute column.

    b. SOILTYPE "ZCB" = tidal beaches, and were inputted as "Beach" in the SOILNAME attribute column.

    c. SOILTYPE "ZMT" = mine tailings, and were inputted as "Mine_Tail" in the SOILNAME attribute column.

    d. SOILTYPE "ZNS" = non-surveyed areas, and were inputted as "NoSurvey" in the SOILNAME attribute column.

    e. SOILTYPE "ZER" = eroded areas, and were inputted as "Eroded" in the SOILNAME attribute column.

4. A number of soil series represented within the CANsis geospatial soil layer did not have corresponding physical or chemical characteristics associated with them within the soil survey reports. Surrogate values were used by averaging characteristics from similar or associated soil series, based on soil parent material, all of which were suggested by Kevin Keys, (RPF, P.Ag.; Personal communication, 2011):

    a) Arichat: Average of Thom and Mira characteristics.

    b) Pitman: Average of Yarmouth, Deerfield, Mersey and Liverpool characteristics.

    c) Comeau: Used Digby characteristics.

    d) Meteghan: Used Digby characteristics. Personal communication

    e) Seely: Average of Kentville and Annapolis characteristics.

    f) LaHave: Used Medway characteristics.

g) Bridgeville: Used Cumberland characteristics.

h) Cherryfield: Used Cumberland characteristics.

i) Mossman: Used Cumberland characteristics.

5. The Rough Mountain Land classifier (RML), represented a large portion of Cape Breton that was never surveyed for physical or chemical characteristics. RML is described as being similar overall to the Thom/Mira/Arichat series associations, depending on drainage conditions (Kevin Keys, RPF, P.Ag.; Personal communication, 2011). Using the cartographic depth-to-water mapping tool (DTW; Murphy *et al.*, 2009), RML soils were assigned into 1 of 3 categories:

   a) RML_1 = Well drained (>100cm DTW) - Average of Thom and Gibraltar characteristics.

   b) RML_2 = Imperfectly drained (25- to 100-cm DTW) - Mira characteristics.

   c) RML_3 = Poorly drained (<25cm DTW) - Arichat characteristics.

6. The Rockland soil series, which are distributed throughout mainland Nova Scotia, were assigned physical and chemical characteristics depending on the underlying bedrock substrate. Rockland soil series were assigned to 1 of 3 categories using the bedrock geology classifiers from the Ecological Land Classification for Nova Scotia (NSDNR, 2005):

   a) Rockland_1 = granitic and granodioritic substrate - average of Gibraltar, Bayswater and Aspotogan characteristics.

   b) Rockland _2 = quartzite, slate or greywacke substrate - average of Halifax, Danesville and Aspotogan characteristics.

c) Rockland _3 = mafic substrate - average of Rossway, Roxville and Tiddsville characteristics.

Upland - Lowland Soil Delineation

Since the original soil surveys were not designed to provide high-resolution soil mapping units for stand-level forest management (see Peterson *et al.,* 1991), the previously delineated alluvial soil borders were found to not match those observed from aerial photographs (see Long *et al.,* 1991). In order to increase the geospatial accuracy between upland-lowland soil boundaries across the province, a terrain analysis procedure was developed using the cartographic depth-to-water (DTW) mapping tool (Murphy *et al.,* 2011). Terrain analysis has been used extensively to enhance existing choropleth maps for finer resolution of soil formation processes and landform delineation across landscapes (Moore *et al.,* 1993). Using digital elevation models (DEM) in conjunction with aerial photograph validation (Hengl & Rossiter, 2003), the relationships between soils and the surrounding environment can be inferred for any point on the landscape (Zhu *et al.,* 2001).

Using a 1000-ha flow accumulation, a DTW raster was created without the use of mapped water features. The output grid was converted into a series of polygons and all mapped water bodies connected to the 1000-ha flow accumulation were selected and exported as a new shapefile. The DTW was then re-run using the newly exported water body layer. The resulting grid was classified to 1-m DTW and converted to a polygon feature. All exported water-body polygons that were not connected to the DTW flow channels were selected and removed, as it is assumed that they are outside of an alluvial deposit. The resulting layer was given a 10m buffer to account for the DEM resolution

(10m), and the original water body and wetland layers were then used to erase the underlying DTW polygons.

A systematic cross-referencing between the flow accumulation, current water, wetlands and DTW (at 40- and 100-ha) revealed that >90% of meandering watercourses were included within the predicted alluvial floodplains, excluding smaller watercourses and wetlands. Additionally, the extent of alluvial floodplains was validated using digital elevation and aerial photography, the results of which suggest that the predicted geospatial extent of alluvial floodplains is at least as accurate as photo-interpreted delineations. Although many upland wetlands (i.e. bogs) were found to be associated with alluvial deposits, as was evident from meander scars, these sites were not included in the final output. Although these sites may have been floodplains historically, they are categorized as organic soils, and are assumed to no longer be associated with alluvial deposits (Brinson, 1993).

LITERATURE CITED

Agriculture and Agri-food Canada. (2002). *Soil Survey Data for Nova Scotia*. Retrieved 8 10, 2009, from National Soil DataBase: http://sis.agr.gc.ca/cansis/nsdb/detailed/ns/zipfiles.html

Agriculture Canada. (1974). *A system of soil classification for Canada.* Ottawa: Canada Department of Agriculture.

Balland, V., Pollacco, J., & Arp, P. (2008). Modeling soil hydraulic properties for a wide range of soil conditions. *Ecological Modelling, 219*, 300-316.

Brinson, M. (1993). Changes in the functioning of wetlands along environmental gradients. *Wetlands, 13*, 65-74.

Day, J. (1983). *The Canadian Soil Information System (CanSIS) manual for describing soils in the field.* Ottawa: Land Resources Institute, Agriculture Canada.

ESRI: Environmental Systems Research Institute. (2009). *Arcmap (Version 9.3).* [Computer Software]. Redlands, California.

ESRI: Environmental Systems Research Institute. (2002). *Arcview (Version 3.3).* [Computer Software]. Redlands, California.

Fox, T. (2002). *Nearest Feature Analysis Tool* [Computer Software]. For use within Arcview v3.3.

Hengl, T., & Rossiter, D. (2003). Supervised Landform Classification to Enhance and Replace Photo-Interpretation in Semi-Detailed Soil Survey. *Soil Science Society of America Journal, 67,* 1810-1822.

Long, D., DeGloria, S., & Galbraith, J. (1991). Use of the global positioning system in soil survey. *Journal of Soil and Water Conservation, 46,* 293-297.

McBratney, A., Minasny, B., Cattle, S., & Vervoort, R. (2002). From pedotransfer functions to soil inference systems. *Geoderma, 109,* 41-73.

Microsoft Excel. (2007). *Microsoft Office Professional Plus Edition* [Computer Software]. Microsoft Corporation.

Moore, I., Gessler, P., Nielson, G., & Peterson, G. (1993). Soil attribute prediction using terrain analysis. *Soil Science Society of America Journal, 57,* 443-452.

Murphy, P., Ogilvie, J., & Arp, P. (2009). Topographic modelling of soil moisture conditions: a comparison and verification of two models. *European Journal of Soil Science, 60,* 94-109.

Murphy, P., Ogilvie, J., Meng, F., White, B., Bhatti, J., & Arp, P. (2011). Modelling and mapping topographic variations in forest soils at high resolution: A case study. *Ecological Modelling, 222,* 2314-2332.

NSDNR. (2000). *Nova Scotia Wetland Vegetation and Classification Inventory.* Kentville, N.S: Nova Scotia Department of Natural Resources, Wildlife branch.

NSDNR. (2006a). *Nova Scotia Provincial Boundary.* Truro, N.S: Nova Scotia Department of Natural Resources.

NSDNR. (2006b). *Nova Scotia Mapped Water Features Inventory.* Truro, N.S: Nova Scotia Department of Natural Resources.

NSDNR. (2005). Ecological Land Classification for Nova Scotia. DNR 2001-01 v2. Nova Scotia Dept. of Natural Resources. (Digital Data). Website: http://gis2.gov.ns.ca/website/nselcmap/viewer.htm.

Peterson, C. (1991). Precision GPS navigation for improving agricultural productivity. *GPS World, 2*, 38-44.

Statview V5.0. (1998). Cary, NC: SAS Institute Inc. [Computer Software].

Stobbe, P., & McKeague, J. (1978). *History of Soil Survey in Canada, 1914-1975.* Ottawa: Canada Department of Agriculture, Research Branch.

Zhu, Z., Hudson, B., Burt, J., Lubich, K., & Simonson, D. (2001). Soil Mapping Using GIS, Expert Knowledge, and Fuzzy Logic. *Soil Science Society of America Journal, 65*, 1463-1472.

CHAPTER 7

MASS BALANCE: PRIMARY ELEMENT INPUT AND EXPORT METHODOLOGY

INTRODUCTION

This chapter details how primary N, S, K, Ca and Mg inputs and exports are quantified within the Nova Scotia Biomass Decision Support Tool. The primary inputs refer to wet and dry atmospheric deposition and soil weathering, while the primary outputs refer to harvest exports and soil leaching. Also quantified are: (i) the extent of site-specific nutrient deficits, when primary harvest exports exceed the primary nutrient inputs, and (ii) the rate of site-specific base-cation depletion, when harvest exports and acid-rain induced base-cation leaching exceed primary base-cation inputs. The harvest export formulation deals with estimating stand-level biomass compartment fractions and nutrient concentrations within bark, branches, stem-wood and foliage, for four harvest scenarios, (no harvest, stem-only, whole-tree brown and whole-tree green; see chapter 4). The forest biomass and nutrient capitals under each scenario are used to estimate and map the nutrient sustainability for each upland stand within the Nova Scotia Forest Inventory, according to current stand conditions, i.e., harvestable biomass, stand composition, soil type, and expected rates of atmospheric element inputs.

PARENT MATERIAL WEATHERING

Aspatial Methods

The rate of chemical weathering of parent material was determined using the simple and readily GIS-applied "Clay Content" method (Sverdrup *et al.*, 1990; de Vries

et al., 1993; Jeffries & Ouimet, 2004), which calculates the total rate of weathering within the soil matrix based on soil mineralogy, depth, texture, and mean annual soil temperature. This method was evaluated by Whitfield *et al.,* (2006), and yielded similar results for Nova Scotia forest soils in reference to catchment- and soil profile-based methods to estimate local soil weathering rates. The "Clay Content" method was applied across Nova Scotia using the database of the Nova Scotia bedrock mineralogy (Appendix VIII), and assigning each lithology group to one of 4 classes of soil chemical weathering:

Class 1 represents acidic substrates such as those comprised of sand, gravel, granites, quartzite, gneiss, and coarse textured schist, shale, greywacke and glacial tills.

Class 2 represents intermediate substrates such as granodiorite, loess, fluvial and marine sediments, and moderate-fine textured schist, shale, greywacke and glacial tills.

Class 3 represents basic substrates such as gabbro, basalt, dolomite and volcanic deposits.

Class 4 represents calcareous substrates such as limestone, marl and gypsum.

Soils derived from sediments such as alluvial or marine floodplains were assigned to Class 3 in order to represent their generally mixed lithology and elevated nutrient inputs (Chapter 6). All non-glacial till weathering class overrides are shown in Appendix IX as suggested by Kevin Keys (RPF, P.Ag.; Personal communication, 2010). Peatlands and other lowland/wetland soils were mapped separately, but were not included within the weathering functions. Forested wetlands are not considered within the Biomass Decision Support Tool due to complications, which would require local assessments of (i) additional primary nutrient inputs on account of upland and groundwater seepage, or (ii) lack thereof as in ombrotrophic bogs and poor soil drainage conditions.

The rate of soil weathering was estimated for each lithology class in base eq ha^{-1} m^{-1} of mineral soil following the methods described by deVries, (1991):

$$Class\,1 = 56.7\,Clay - 0.32\,Clay^2 \quad (7.1)$$

$$Class\,2 = 500 + 53.6\,Clay - 0.18\,Clay^2 \quad (7.2)$$

$$Class\,3 = 500 + 59.2\,Clay \quad (7.3)$$

$$Class\,4 = 1500 + 59.2\,Clay \quad (7.4)$$

where *Clay* refers to the clay fraction of the mineral soil. This was followed by accounting for local differences in soil depth, density, temperature, organic matter and coarse fragment content within the rooted soil matrix such that:

$$BC_{we}^{0} = Db\,Depth\left(1-\frac{CF}{100}\right)EXP\left(\left(\frac{A}{(2.6+273)}\right)-\left(\frac{A}{(273+Tann)}\right)\right)\left(\frac{ClassX}{100}\right)\left(1-\frac{OM}{100}\right) \quad (7.5)$$

where *Db* is the soil bulk density (g cm^{-3}), *Depth* is the soil rooting space depth (cm), *CF* is the soil coarse fragment content (%), *A* is the Arrhenius pre-exponential factor (3600 J mol^{-1} °C^{-1}; Sverdrup, 1990), the constant 273 is the conversion from Celsius to Kelvin, 2.6 is a reference temperature for northern climates (°C; de Vries, 1991), *Tann* is the mean annual air temperature (°C), *ClassX* refers to the parent material class weathering estimations (Eq. 7.1 - 7.4), and *OM* is the soil organic matter content (%). From this, the rate of weathering for each base-cation (eq ha^{-1} yr^{-1}) can be calculated under the assumption that the weathering of each base-cation is equal to the relative concentration of each within the soil, i.e.:

$$X_{we} = 0.7 X_f \; BC_w^0 \tag{7.6}$$

where X refers to one of the base-cation elements (Ca, Mg, K), X_f refers to the fraction of X within the soil matrix (Eq. 6.22), subscript *we* denotes the contribution of X to the total weathering rate, and 0.7 assumes that the contribution of weathering from Na^+, which is not accounted for, is roughly 30% of the total weathering (Umweltbundesamt, 2004; Whitfield *et al.,* 2006). Using the results from Eq. 7.6, total base-cation weathering equivalents (BC_{we}) for use within the critical loads functions (Eq 2.1 - 2.2) are set as:

$$BC_{we} = Ca_{we} + Mg_{we} + K_{we} \tag{7.7}$$

Spatial Methods

All spatial methods were realized within Arcmap 9.3.1 (ESRI, 2009).

Soil Weathering Classes

Spatial distribution of bedrock was derived from the Biophysical Land Classification for Nova Scotia (NSDLF, 1986), whereas spatial assignment of weathering functions (Eq. 7.1 - 7.4) to soil parent materials was based on bedrock fertility classes within the Nova Scotia forest ecosystem classification (Keys *et al.,* 2007). Spatial alignment with the provincial boundary followed the same methodology as the geospatial soil layer (Chapter 6). To ensure the final bedrock layer only represented upland topography (weathering classes 1-4), the updated substrate layer was erased with the provincial wetland and water polygon layers. Any remaining sliver polygons with either no weathering class, or weathering class 0, were intersected with a 10x10m Fishnet

(Xtools Pro, 2010) and eliminated into adjacent polygons. The final layer consisted of complete georeferenced weathering class coverage across the province, spatially aligned with the provincial boundary, wetlands and water features (Figure 7.1).

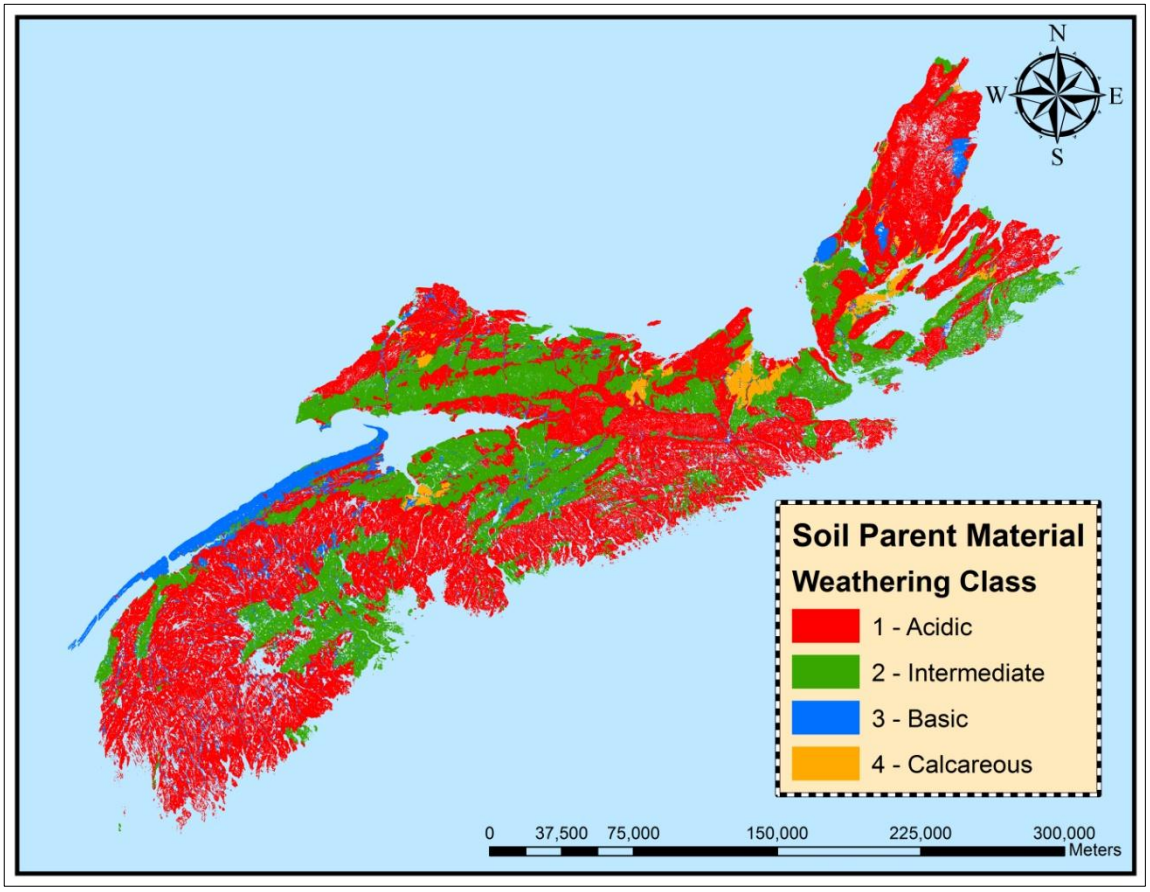


Figure 7.1. Spatial distribution of the four upland soil parent material weathering classes across Nova Scotia.

Mean Annual Temperature

In order to correct for the effect of temperature within the total rate of weathering equation (Eq. 7.5), average annual temperature (*Tann*) was georeferenced across Nova Scotia based on a 10km^2 point grid. Daily maximum and minimum temperatures (°C) were acquired from Agriculture and Agri-food Canada (2009), summarized from

Environment Canada's National Climate Archive (Canadian Daily Climate Data, 2004-2008) for the Canadian landmass south of 60°N. The daily temperature values were averaged annually, by month, for each point coordinate across Nova Scotia. A provincial temperature raster layer was interpolated from the point grid using the Tension Spline interpolation method (Franke, 1982; Figure 7.2).

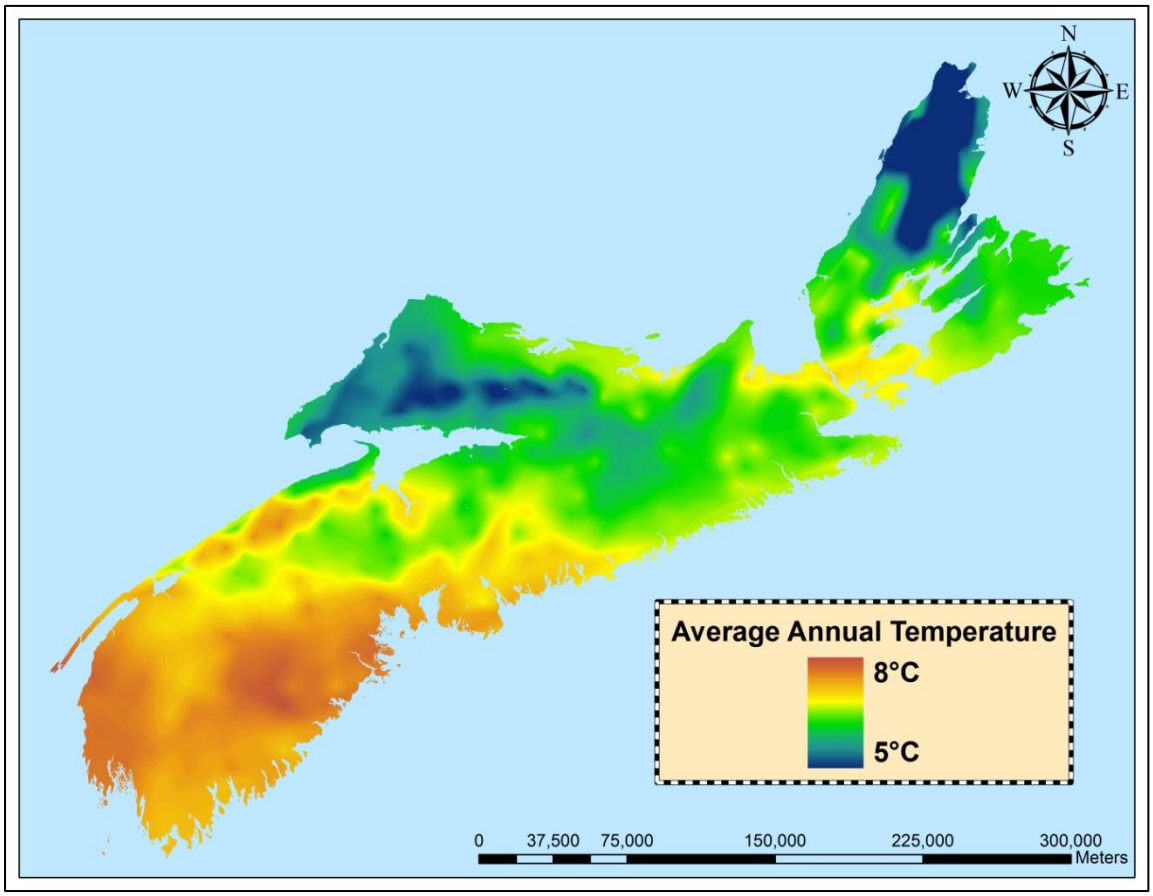


Figure 7.2. Average annual temperature across Nova Scotia based on Environment Canada's National Climate Archive, Canadian Daily Climate Data, averaged across 2004-2008 and interpolated using the Tension Spline method (Franke, 1982).

ATMOSPHERIC DEPOSITION

Atmospheric wet deposition data was taken from the National Atmospheric Chemistry Database and Analysis System (NATChem), of the Meteorological Service of Canada (see Meteorological Service of Canada, 2005). Daily ion concentrations (eq ha^{-1} yr^{-1}) were sampled by both the Canadian Air Pollution Monitoring Network (1984-2008) and the Nova Scotia Precipitation Study Network (1996-2007). Ion concentrations of base cations (K^+, Ca^{2+}, Mg^{2+}; Figures 7.3 - 7.5 respectively) and acid compounds (NH_4^+, SO_4^{2-}, SO_x, NO_3^-), were summarized by Ro and Vet (2002) as point grids ($50km^2$ resolution), which were geospatially interpolated into raster format using the kriging method (Royle *et al.,* 1981). Acid compound rasters were further summarized into total wet deposition of N ($NH_4^+ + NO_3^-$; Figure 7.6) and S ($SO_4^{2-} + SO_x$; Figure 7.7) using ArcGIS Spatial Analyst (ESRI, 2009).

Dry deposition was accounted for through a series of element-specific multipliers, established using dry deposition estimates of K^+, Ca^{2+}, Mg^{2+}, NH_4^+, SO_4^{2-} and NO_3^-, sampled at Cape Forchu, Nova Scotia (Yanni, 1996). Deposition samples were collected between May - October, 1992, and analyzed monthly using a dry deposition sampler. Deposition concentrations were multiplied by the capture-section area of the sampler, and prorated to annual deposition rates (eq ha^{-1} yr^{-1}). Multipliers were calculated as the ratio of dry to wet deposition rates for each element, with the exception of NO_3^- and NH_4^+, which were combined to represent total dry N deposition (Table 7.1). Total deposition of base cations (BC_{dep}) and acid compounds (N_{dep}, S_{dep}) were used within the critical loads and exceedance equations (Eq. 2.1 - 2.2 and Eq. 2.3, respectively), where:

$$BC_{dep} = Ca_{dep} + Mg_{dep} + K_{dep} \tag{7.8}$$

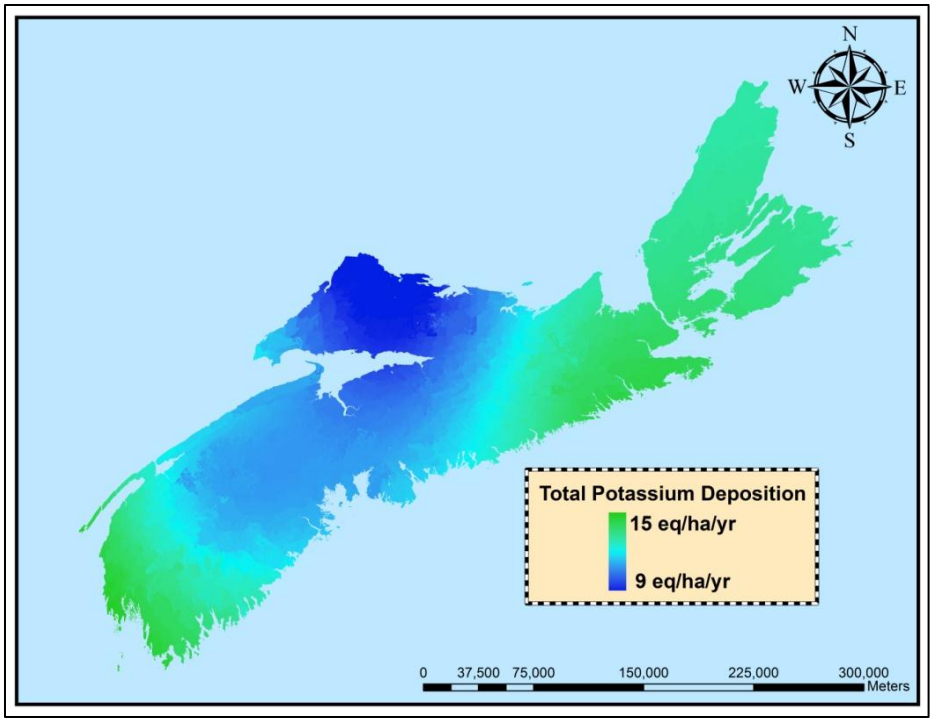


Figure 7.3. Potassium (K^+) wet deposition across Nova Scotia based on the National Atmospheric Chemistry Database and Analysis System dataset.

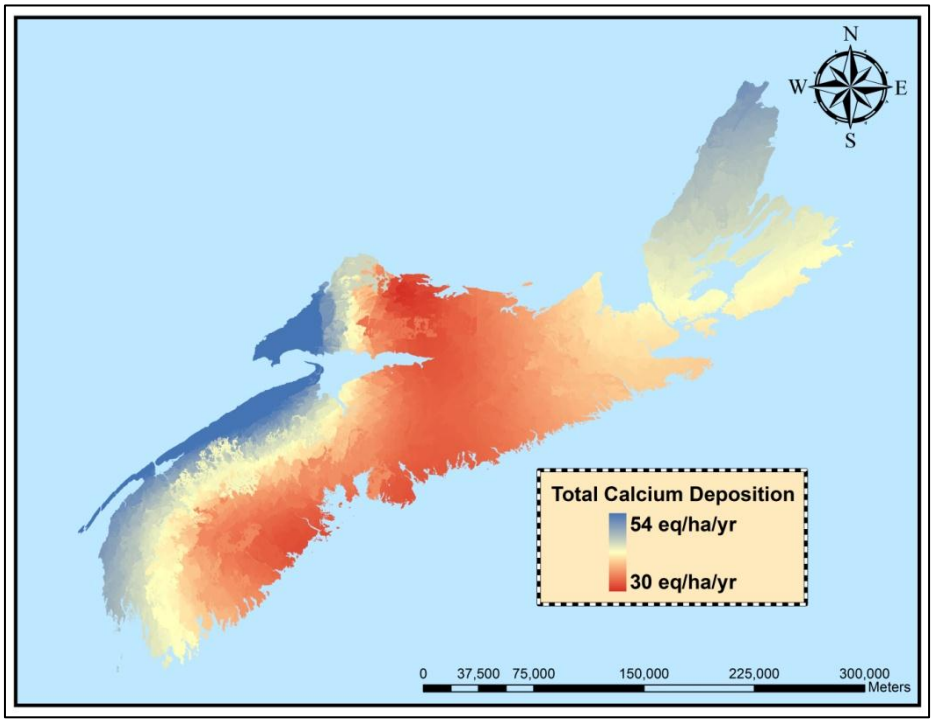


Figure 7.4. Calcium (Ca^{2+}) wet deposition across Nova Scotia based on the National Atmospheric Chemistry Database and Analysis System dataset.

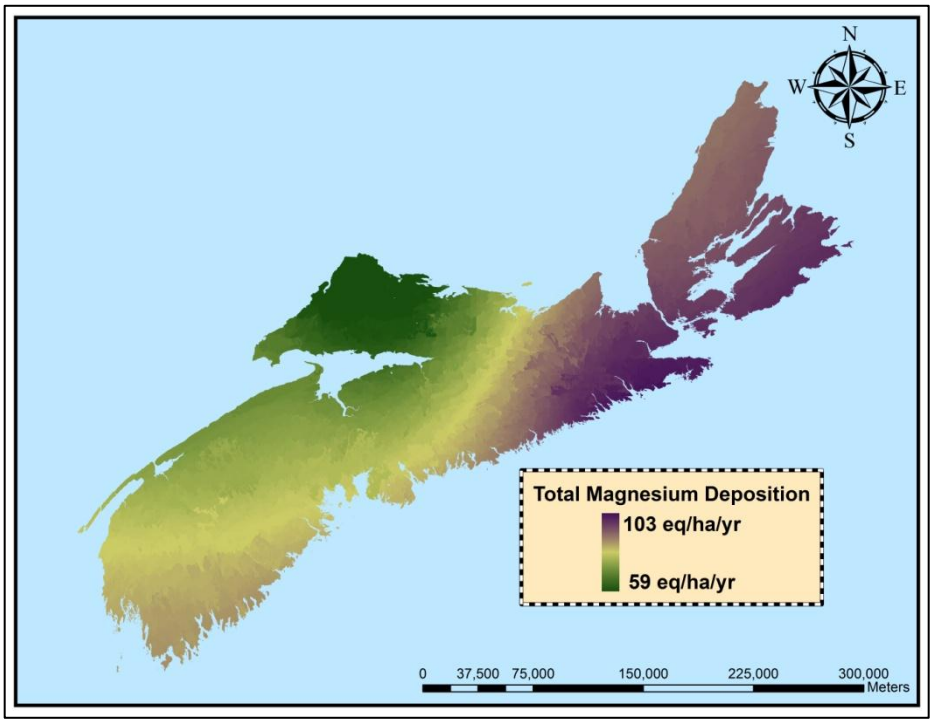


Figure 7.5. Magnesium (Mg^{2+}) wet deposition across Nova Scotia based on the National Atmospheric Chemistry Database and Analysis System dataset.

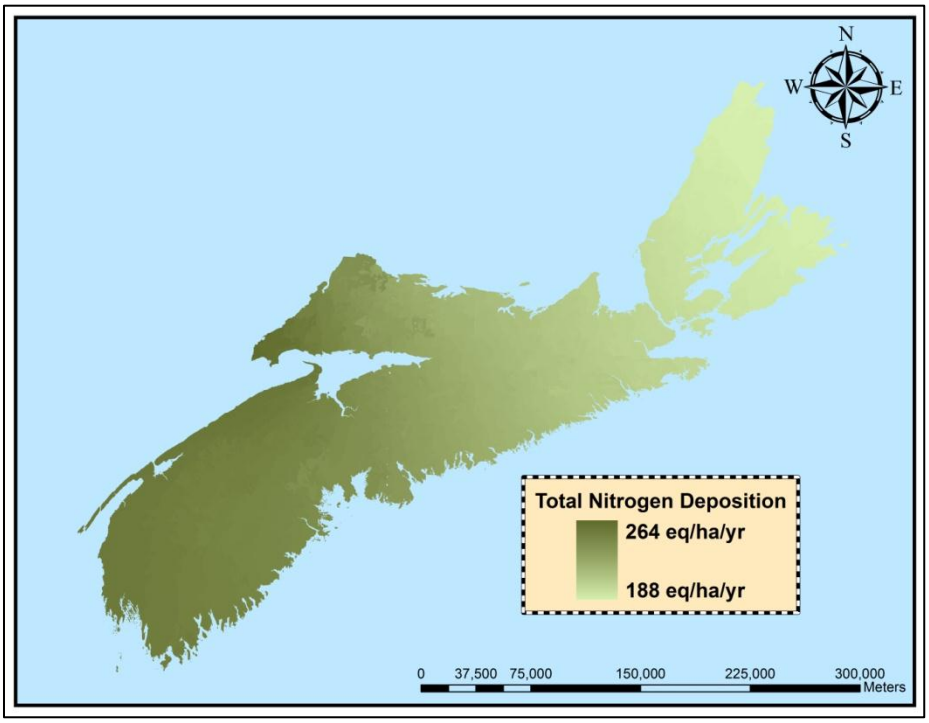


Figure 7.6. Total nitrogen (NH_4^+ & NO_3^-) wet deposition across Nova Scotia based on the National Atmospheric Chemistry Database and Analysis System dataset.

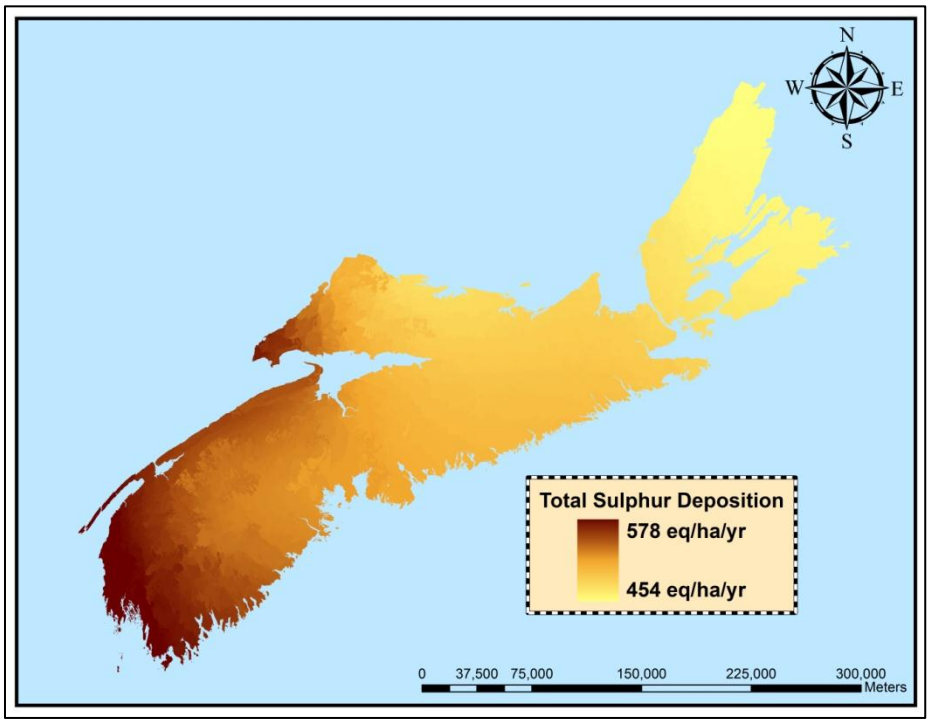


Figure 7.7. Total sulphur (SO_4^{2-} & SO_x) wet deposition across Nova Scotia based on the National Atmospheric Chemistry Database and Analysis System dataset.

Table 7.1. Multipliers representing dry deposition across Nova Scotia for base cations and acid compounds, adapted from Yanni (1996).

Dry Deposition Mulitplier	
Ca^{2+}	1.1600
Mg^{2+}	1.2906
K^{+}	1.1837
S	1.0480
N	1.1253

BIOMASS HARVESTING

Harvestable forest biomass compartments (Chapter 4) and related nutrient exports (Chapter 5) were estimated for stem-only (*SO*), full-tree brown (*FTb*) and full-tree green (*FTg*) harvest scenarios. Harvestable biomass compartments were calculated per stand for each harvest scenario (*M*; tonnes ha^{-1}) as follows:

$$M_{SO} = \sum_{i=1}^{4} \begin{bmatrix} \left(D_i V_i\right) Wood_i^f + \\ \left(D_i V_i\right) Bark_i^f \end{bmatrix} \tag{7.9}$$

$$M_{FTb} = \sum_{i=1}^{4} \begin{bmatrix} \left(D_i V_i\right) Wood_i^f + \\ \left(D_i V_i\right) Bark_i^f + \\ \left(D_i V_i\right) Branch_i^f \end{bmatrix} \tag{7.10}$$

$$M_{FTg} = \sum_{i=1}^{4} \begin{bmatrix} \left(D_i V_i\right) Wood_i^f + \\ \left(D_i V_i\right) Bark_i^f + \\ \left(D_i V_i\right) Branch_i^f + \\ \left(D_i V_i\right) Foliage_i^f \end{bmatrix} \tag{7.11}$$

where subscript *i* denotes one of the 4 primary tree species, with corresponding compositions (%), *D* is the species-specific stem densities taken from Gonzalez (1990), *V* is the total merchantable volume that each species comprises within the stand (m^3 ha^{-1}), and superscript *f* denotes the generated fractions for each biomass compartment (*wood*, *bark*, *branch* and *foliage*; Eq. 4.1; Lambert *et al.*, 2005). Nutrient exports, expressed as (eq ha^{-1}) were obtained from:

$$X_{SO} = 1000 X_{g/eq} \sum_{i=1}^{4} \begin{bmatrix} \left(D_i V_i\right)\left(Wood_i^f \left[X\right]_i^{Wood}\right) + \\ \left(D_i V_i\right)\left(Bark_i^f \left[X\right]_i^{Bark}\right) \end{bmatrix} \tag{7.12}$$

$$X_{FTb} = 1000 X_{g/eq} \sum_{i=1}^{4} \begin{bmatrix} \left(D_i V_i\right)\left(Wood_i^f \left[X\right]_i^{Wood}\right) + \\ \left(D_i V_i\right)\left(Bark_i^f \left[X\right]_i^{Bark}\right) + \\ \left(D_i V_i\right)\left(Branch_i^f \left[X\right]_i^{Branch}\right) \end{bmatrix} \tag{7.13}$$

$$X_{FTg} = 1000 X_{g/eq} \sum_{i=1}^{4} \left[\begin{array}{l} (D_i V_i)\left(Wood_i^f \left[X\right]_i^{Wood}\right) + \\ (D_i V_i)\left(Bark_i^f \left[X\right]_i^{Bark}\right) + \\ (D_i V_i)\left(Branch_i^f \left[X\right]_i^{Branch}\right) + \\ (D_i V_i)\left(Foliage_i^f \left[X\right]_i^{Foliage}\right) \end{array} \right] \quad (7.14)$$

where X refers to one of the 4 nutrients (N, Ca, Mg, K), the subscript *g/eq* denotes the equivalent weight of element X (N =14, Ca = 20, Mg = 12.2, K = 39.1; g eq^{-1}). Total uptake of base cations (BC_{up}) and nitrogen (N_{up}) for use within the critical load functions (Eq. 2.2 - 2.3) were obtained by setting:

$$BC_{up} = (Ca_{HS} + Mg_{HS} + K_{HS}) / Age \quad (7.15)$$

$$N_{up} = N_{HS} / Age \quad (7.16)$$

where the subscript *HS* denotes one of the harvest scenario outputs from Eq. 7.23 - 7.25 (*SO*, *FTb* or *FTg*, respectively), and *Age* is the stand age. All uptake equations are expressed in eq ha^{-1} yr^{-1}.

Nutrient Deficiencies

Nutrient deficiencies refer to the difference between the amount of nutrient inputs and the amount of nutrient exported from the forest site on account of harvesting. A positive value signifies an excess of nutrient on site after biomass removal, whereas a negative value signifies that biomass removal has taken more nutrients than what the site can replenish according to the current atmospheric deposition and soil weathering estimates. For nitrogen, where parent material weathering is not a factor, the equation is set as:

$$N_{def} = N_{dep} - N_{up} \tag{7.17}$$

whereas for base-cation deficiencies, weathering is incorporated, such that:

$$X_{def} = X_{dep} + X_{we} - X_{up} \tag{7.18}$$

All deficiencies are expressed in eq ha^{-1} yr^{-1}.

BASE-CATION LEACHING

The base-cation leaching rate for upland soils was estimated from the law of mass action and charge conservation, such that the acid-base-cation exchange is set as:

$$K_{exch} = \frac{CES - BC + \Delta x}{BC - \Delta x} \frac{BC_{le,CL} + \Delta x}{AC_{le,CL} - \Delta x} \tag{7.19}$$

where K_{exch} is the cation exchange ratio, set at 10 in order to reflect the adsorption preference of soil surfaces for acid cations such as H^+ and Al^{3+} over the adsorption of the competing base cations such as K^+, Na^+, Ca^{2+}, and Mg^{2+} (NEG-ECP, 2001; Nasr *et al.*, 2010; Paul Arp, PhD, Personal communication); *CES* refers to the sum of soil cation exchange sites (eq ha^{-1}); *BC* is the sum of the exchangeable soil base cations (eq ha^{-1}); Δx is the annual exchange of acid to base cations (leaching or accumulation) that shifts base saturation from the current state (*BS*) to the final state (BS_f); $BC_{le,CL}$ and $AC_{le,CL}$ are the critical base-cation and acid-cation leaching rates under a zero base-cation depletion critical load scenario ($\Delta x = 0$), respectively, given by:

$$BC_{le,CL} = BC_{dep} + BC_{we} \tag{7.20}$$

$$AC_{le,CL} = \frac{1}{K_{exch}} \frac{CES - BS_{CL}}{BS_{CL}} BC_{le,CL} \tag{7.21}$$

where BS_{CL} is the critical base saturation level, which under the requirement of no further base-cation depletion, is set to the current base saturation level of the soil. In order to calculate the actual rate of base-cation depletion, Δx is solved for:

$$\Delta x \approx -1\left(\frac{100\,(BS - BS_f)}{BS\ BS_f\ \left(K_{exch} - 1 + 100/BS\right)} BC_{le,CL} \right) \tag{7.22}$$

where BS_f refers to the final concentration of soil base cations (%), given by:

$$BS_f = \frac{100}{1 + K_{exch} \dfrac{\max(0, EXC + AC_{le,CL})}{BC_{le,CL}}} \tag{7.23}$$

where *EXC* refers to the critical load exceedance, which is set to account for nutrient uptake in order to include the impacts of harvest induced deficiencies, as:

$$EXC = \left(N_{dep} + S_{dep}\right) - BC_{dep} + BC_{we} - BC_{up} + N_{up} + AC_{le,CL} \tag{7.24}$$

The depletion of each base-cation element (X_{dpl}) is assumed to be proportional to the portion of that element on the base-cation exchange sites, i.e.:

$$X_{dpl} = X_f \Delta x \tag{7.25}$$

A positive value signifies an accumulation whereas a negative value signifies a base-cation depletion, all of which are expressed in eq ha^{-1} yr^{-1}. The rate of base-cation leaching from the soil is given by:

$$BC_{le} = BC_{le,CL} + \Delta x \tag{7.26}$$

and the corresponding leaching rate for each base-cation element is given by:

$$X_{le} = X_f\ BC_{le} \tag{7.27}$$

Total base-cation losses (X_{loss}) from a site, with and without harvesting are given by:

$$X_{loss} = X_{dep} + X_{we} - X_{up} + X_{dpl} \tag{7.28}$$

HARVEST OPERABILITY AND SUSTAINABLE MAI

Using the base-cation leaching functions (Eq. 7.22) as well as base-cation and nitrogen deficiency functions (Eq. 7.17 - 7.18), operability of each harvest scenario is determined by way of the Sprengel-Liebig Law of the Minimum (see Chapter 2). Sustainability of each harvest scenario is calculated based on deficiencies alone, as well as the combination of deficiencies and leaching, respectively, given by:

$$\min\left[N_{def}^{Export}, Ca_{def}^{Export}, Mg_{def}^{Export}, K_{def}^{Export} \right] \tag{7.29}$$

$$\min\left[N_{dpl+def}^{Export}, Ca_{dpl+def}^{Export}, Mg_{dpl+def}^{Export}, K_{dpl+def}^{Export} \right] \tag{7.30}$$

where the minimum value represents the growth-limiting nutrient within the stand. Each harvest scenario is considered sustainable only if the minimum value is > 0, which signifies that base-cation inputs exceed the amount leached, and that there are no nutrient deficiencies. Although each harvest scenario assumes 100% removal of the tissues represented (i.e. clear-cut), a sustainable rate of harvesting is also calculated using a sustainable annual stem biomass increment (*SBMI*), obtained from:

(i) the estimated rates of nutrient supply based on atmospheric deposition and soil weathering ($X_{dep} + X_{we}$), where X refers to N, K, Mg, or Ca,

(ii) the mass-weighted nutrient concentration per harvested biomass, denoted by $[X_{Export}]$ (eq tonne^{-1}),

(iii) estimating *SBMI* by harvest scenario and by nutrient element, i.e.,

$$SBMI_X^{Export} = (X_{dep} + X_{we}) / \left[X_{Export} \right] \tag{7.31}$$

(iv) choosing the minimum of $SBMI_X^{Export}$ among the harvest-specific *SBMI* estimates for N, K, Mg or Ca, i.e.,

$$SBMI^{Export} = \min(SBMI_N^{Export}, SBMI_K^{Export}, SBMI_{Mg}^{Export}, SBMI_{Ca}^{Export}) \tag{7.32}$$

A sustainable rate of harvesting (MAI_{sus}; m^3 ha^{-1} yr^{-1}) is then generated for each stand according to tree species compositions and stem density per tree species (D), such that:

$$MAI_{sus} = \sum_{i=1}^{4} \frac{SBMI_i^{Export}}{D_i} \tag{7.33}$$

LITERATURE CITED

Agriculture and Agri-food Canada. (2009). *Daily 10km Grid Climate Dataset for Canada, 2004-2008 (ANUSPLIN Raster Grid).* Government of Canada.

Data East Soft, LLC. (2010). *XTools Pro for ArcGIS desktop (v7.1.0)* [Computer Software].

de Vries, W. (1991). *Methodologies for the assessment and mapping of critical loads and of the impact of abatement strategies on forest soils.* Wageningen (The Netherlands): The Winand Staring Centre, Agricultural Research Department.

de Vries, W., Posch, M., Reinds, G., & Kamari, J. (1993). *Critical Loads and their Exceedance on Forest Soils in Europe.* Wageningen (The Netherlands): DLO, The Winand Staring Centre.

Dise, N., & Wright, R. (1995). Nitrogen leaching from European forests in relation to nitrogen deposition. *Forest Ecology and Management, 71*, 153-161.

ESRI: Environmental Systems Research Institute. (2009). *Arcmap (Version 9.3.1).* [Computer Software]. Redlands, California.

Franke, R. (1982). Smooth Interpolation of Scattered Data by Local Thin Plate Splines. *Computation & Mathamatics with Applications, 8*, 237–281.

Gonzalez, J. (1990). *Wood density of Canadian tree species.* Edmonton, Alberta: Forestry Canada, Northwest Region, North Forestry Centre.

Jeffries, D., & Ouimet, R. (2004). Critical Loads: are the being exceeded? In *Canadian acid deposition science assessment.* Downs-view, Ontario: Meteorological Service of Canada, Environment Canada.

Keys, K., Neilly, P., Quigley, E., & Stewart, B. (2007). *Field Manual for Forest Ecosystem Classification in Nova Scotia.* Truro, Nova Scotia: Manual FOR 2007-1. Ecosystem Management Group, Forestry Division, Nova Scotia Department of Natural Resources. 95pp.

Lambert, M., Ung, C., & Raulier, F. (2005). Canadian national tree aboveground biomass equations. *Canadian Journal of Forest Research, 35*, 1996-2018.

Meteorological Service of Canada. (2005). Chapter 3: Atmospheric Response to Past Emission Control Programs. In Meteorological Service of Canada, *Canadian acid deposition science assessment, 2004.* Downsview, ON.

Nasr, M., Castonguay, M., Ogilvie, J., Raymond, B., & Arp, P. (2010). Modelling and mapping critical loads and exceedances for the Georgia Basin, British Columbia, using a zero base-cation depletion criterion. *Journal of Limnology, 69*, 181-192.

NEG-ECP. (2001). *CRITICAL LOAD OF SULPHUR AND NITROGEN ASSESSMENT AND MAPPING PROTOCOL FOR UPLAND FORESTS.* Halifax, Canada: New England Governors and eastern Canadian Premiers Environmental Task Group, Acid Rain Action Plan.

NSDLF. (1986). Biophysical Land Classification for Nova Scotia. Truro, NS: Nova Scotia Dept. of Lands and Forests, Forestry Division. (Maps and Digital Data).

Ro, C., & Vet, R. (2002). *Analyzed data fields from the National Atmospheric Chemistry Database (NAtChem) and Analysis Facility.* Toronto, Ontario: Air Quality Research Branch, Meteorological Service of Canada, Environment Canada.

Royle, A., Clausen, F., & Frederiksen, P. (1981). Practical Universal Kriging and Automatic Contouring. *Geoprocessing, 1*, 377-394.

Sverdrup, H. (1990). *The kinetics of base-cation release due to chemical weathering.* Sweden: Lund University Press.

Umweltbundesamt. (2004). *Manual on methodologies and criteria for modelling and mapping critical loads and levels and air pollution effects, risks and trends.* Berlin: Umweltbundesamt.

Whitfield, C., Watmough, S., Aherne, J., & Dillon, P. (2006). A comparison of weathering rates for acid-sensitive catchments in Nova Scotia, Canada and their impacts on critical load calculations. *Geoderma, 136*, 899-911.

Yanni, S. (1996). *Hydrogeochemical assessment of water in forested watersheds at Kejimkujik National Park: Discharge rates, chemical composition, and ion fluxes (MScF Thesis).* Fredericton, New Brunswick: University of New Brunswick.

CHAPTER 8

BIOMASS DECISION SUPPORT TOOL SPECIFICATIONS

INTRODUCTION

The biomass decision support tool (BDST) is a dual model package containing both a spatial and aspatial sustainability model in order to simulate the impacts of biomass harvesting and soil acidification on long-term soil nutrient balances and forest growth. A steady-state approach is used to determine the input/output mass balance of forest nutrients based on averaged annual data. This approach allows for the estimation of sustainable biomass production across the landscape using site-specific nutrient supplies in relation to nutrient demands of the existing vegetation. The spatial model is designed to allow visualization of harvest and acid deposition impacts across the landscape, based on generalized harvest scenarios, whereas the aspatial model allows for user defined harvest prescriptions, and the ability to change inputs based on field verified data. The following chapter will present the various model specifications and components used to predict biomass harvest sustainability and quantify nutrient balances in response to harvesting and acid deposition.

MODEL COMPONENTS

Ecounit Layer

In order to run the BDSC, a geospatial ecounit layer was established in which the model calls upon the various environmental attributes associated with parent material weathering, soil, climate and atmospheric deposition. Within Arcmap 9.3.1 (ESRI, 2009),

the soil and substrate weathering polygon layers were intersected into a single layer. In order to incorporate the wet deposition and temperature grids, a series of zonal statistics were performed using ArcGIS Spatial Analyst (ESRI, 2009). An area-weighted average of wet S, N, K^+, Ca^{2+} and Mg^{2+} deposition, as well as average annual temperature, were calculated for each unique soil-substrate polygon. The resulting layer contained over 98,000 polygons, containing complete soil, substrate weathering, atmospheric deposition and temperature coverage.

Biomass Lookup Table

A biomass compartment and nutrient concentration lookup table was established as an external model input to allow the user the ability to update biomass compartment and nutrient concentration parameters, as new information becomes available. The lookup table includes the species- and biomass compartment-specific parameter values (Chapter 4), and corresponding nutrient concentrations (Chapter 5) for each of the 40 tree species within the Nova Scotia forest inventory (see Appendix X).

Forest Inventory

A geospatial forest inventory layer is used to initialize the BDST species-specific biomass and nutrient uptake calculations. The forest inventory is an external input to the model in order to allow the user to update forest characteristics as data becomes available, as well as define the scale in which to run the model, from individual stands, to entire provincial inventories. At a minimum, the model depends on the following stand-level forest inventory attributes:

a) Total merchantable volume (m^3 ha^{-1});

b) Average stem diameter (cm);

c) Average age (years);

d) Tree species composition (up to 4 levels; %)

BDST MODEL STRUCTURE

Spatial Model

The Environmental Systems Research Institute (ESRI) spatial modelling interface (ModelBuilder; Arcmap 9.3.1) allows for automated processing of both pre-existing spatial tools, as well as user developed tools, by way of the VB.NET (Microsoft Visual Studio) scripting environment. The BDST was structured as a linear, process-oriented model, in which each model process is dependent on the output of the previous process. Four primary sub-models are used within the BDST (Figure 8.1):

1. Parent material weathering sub-model, which estimates the annual rate of base-cation release within soils;

2. Critical loads and exceedances sub-model, which estimates the soil critical acid load and related exceedances caused by acid deposition;

3. Sustainable productivity model, which calculates biomass harvest sustainability based on site-specific nutrient availability and related tree species-specific nutrient demand;

4. Nutrient leaching and depletion sub-model, which estimates the rate of nutrient leaching caused by acid deposition, as well as harvest-induced base-cation depletions.

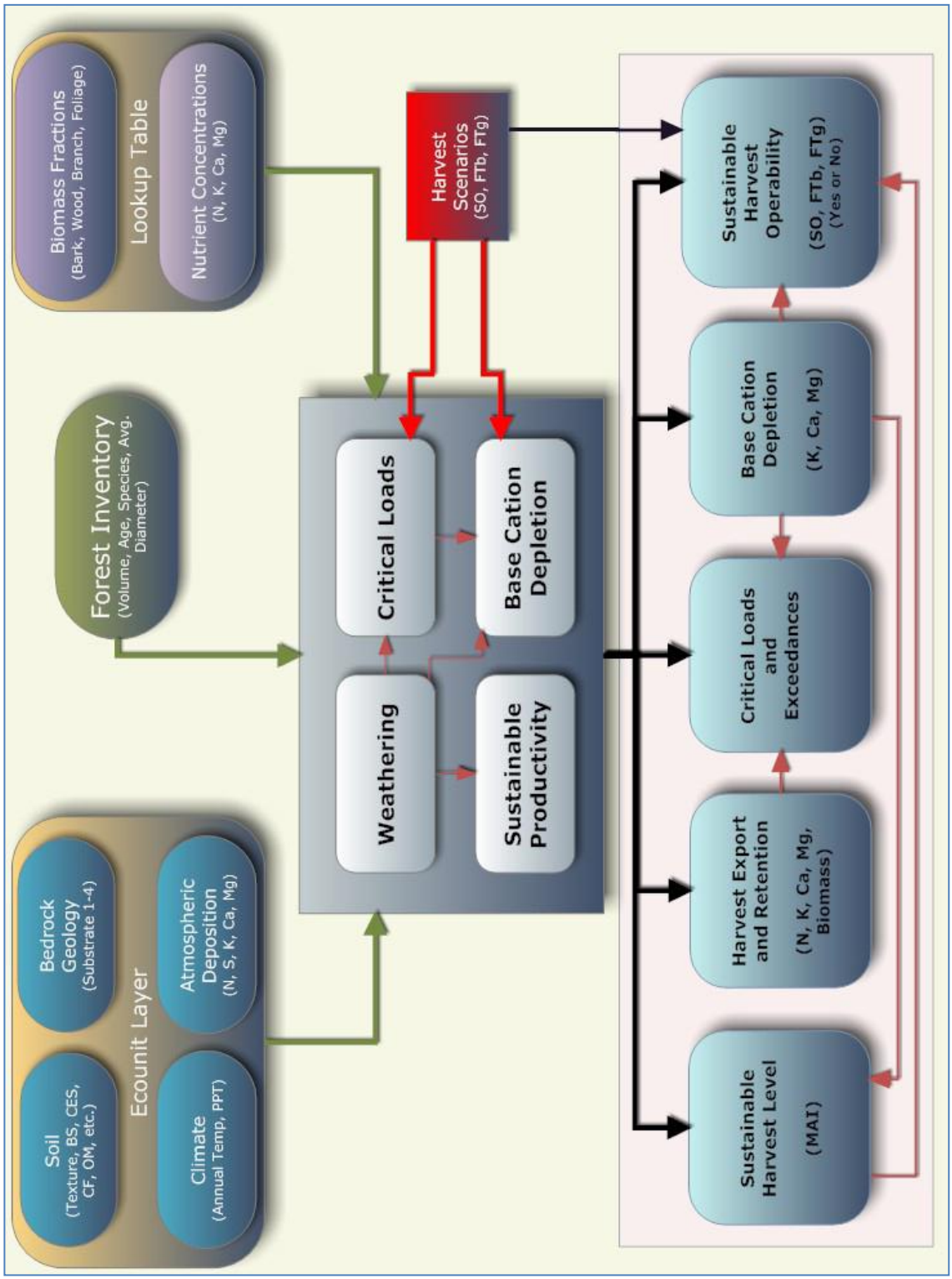


Figure 8.1. Model structure and the relationships between inputs, sub-models, and outputs for the Biomass Decision Support Tool.

Aspatial Model

The aspatial model is an individual stand calculator, constructed within a Microsoft Excel (2007) spreadsheet. The aspatial model replicates all components and sub-models within the spatial model, but allows the ability to manipulate the various forest, soil, climate, atmospheric deposition and substrate weathering characteristics, in order to:

a) Update site characteristics based on field verified data;
b) Allow for user designed harvest prescriptions to assess sustainability;
c) Allow for scenario based sustainability modelling and sensitivity analysis.

The aspatial model is initialized by selecting an individual stand from the forest inventory within ArcGIS. The tool calculates an area-weighted average of each ecounit characteristic for the selected stand, and exports the results as an ASCII file for import into MS Excel.

BDST Model Specifications

The following section lists the BDST spatial and aspatial model specifications as they relate to site-specific input variables, model outputs, potential model scenarios, model validation and modelling platforms.

Model Inputs

Soil Characteristics

- Rooted depth (cm)
- Bulk density (g cm^{-3})

- Total cation exchange sites (CES; eq ha^{-1})
- Base saturation (%)
- Coarse fragment content (%)
- Clay fraction (% of mineral soil)
- Organic carbon content (%)
- Organic matter content (%)
- Nitrogen content (%)
- Exchangeable K^{+}, Ca^{2+}, Mg^{2+} (% of CES)

Atmospheric Deposition & Climate

- Wet and dry atmospheric deposition for K, Ca, Mg, N and S (eq ha^{-1} yr^{-1})
- Average Annual Temperature (°C)

Bedrock Geology

- Soil parent material substrate (1 - acidic, 2 - intermediate, 3- basic, 4 - calcareous)

Forest Vegetation

- Stand composition (4 major tree species; %)
- Total merchantable volume (m^3 ha^{-1})
- Stand age (years)
- Average softwood and hardwood diameter (DBH; cm)
- Species specific biomass compartment parameters
- Species specific nutrient concentrations per biomass compartment (mg kg^{-1})

Model Outputs

- Total biomass removed (tonnes ha^{-1})
- Total biomass remaining on site (tonnes ha^{-1})
- Harvest operability (with and without base cation depletion; Yes or No)

- Base-cation leaching (eq ha^{-1} yr^{-1})
- Sustainable harvest rate (with and without base cation depletion; m^3 ha^{-1} yr^{-1})
- Critical acid loads and exceedances (eq ha^{-1} yr^{-1})
- Primary growth limiting nutrients (N, K, Ca or Mg)

Potential Model Scenarios

- Emission control scenarios
- Climate change scenarios
- Site productivity scenarios
- Harvest sustainability scenarios

Model Validation

- Published soil leachate fluxes for N, K, Ca and Mg
- Published critical load and exceedance estimations

Model Platforms

- ArcGIS 9.3.1, ModelBuilder (Spatial)
- Microsoft Excel 2007 (Aspatial)

LITERATURE CITED

ESRI: Environmental Systems Research Institute. (2009). *Arcmap (Version 9.3).* [Computer Software]. Redlands, California.

Microsoft Excel. (2007). *Microsoft Office Professional Plus Edition* [Computer Software]. Microsoft Corporation.

CHAPTER 9

GENERATED RESULTS, VALIDATION AND SENSITIVITY ANALYSES

INTRODUCTION

Due to confidentiality concerns with Nova Scotia forest inventory data, discussion of analysis results is mainly limited to aspatial summaries of sub-model outputs. However, detailed results are provided for Kejimkujik National Park, including results of selected model sensitivity analyses.

PROVINCIAL RESULTS AND VALIDATION

Parent Material Weathering

Across Nova Scotia, weathering rates ranged between 84 - 6017 eq ha^{-1} yr^{-1}, with a mean value of 376 eq ha^{-1} yr^{-1} (Table 9.1). Within the acidic substrate class, the maximum rate of weathering exceeded that of the intermediate class, which is attributed to the diversity of soil conditions across the acidic substrate class, as they relate to soil depth, and clay fractions. Mean weathering rates followed an acidic < intermediate < basic < calcareous sequence, as expected.

Estimated weathering rates were considerably higher than previously reported by Whitfield *et al.,* (2006), using the Clay Content method (30 - 130 eq ha^{-1} yr^{-1}), although sites within this study were restricted to 5 acid-sensitive catchments within Nova Scotia. Conversely, base-cation weathering estimates from Li & McNulty (2007), using the same approach, ranged from 225 to 2250 eq ha^{-1} yr^{-1} for acidic, intermediate and basic substrate classes. Similarly, Arp *et al.,* (1996) found that base-cation weathering rates

ranged between 131 - 2478 eq ha^{-1} yr^{-1} for acidic, intermediate and basic substrates within southern Ontario. The model estimates also fall within the range of the mineralogy dependent PROFILE weathering estimates from Ouimet *et al.*, (2001), for acidic and intermediate substrates across Quebec (70 - 2960 eq ha^{-1} yr^{-1}), and from Koseva *et al.*, (2010), for acidic, intermediate and basic substrates across Canada (142 - 2119 eq ha^{-1} yr^{-1}). The maximum weathering rates within the basic substrate class do not reflect those found within other studies, although the highest values are restricted to two soil series, which are characterized by a rooted depth >1m (i.e. Annapolis and Seely soils). Aside from these, the ranges of basic substrate weathering rates (213 - 1697 eq ha-1 yr-1) are comparable to the ranges discussed previously. No base-cation weathering rates for calcareous substrates could be found for comparison.

Table 9.1. Descriptive statistics for base-cation weathering rates (eq ha^{-1} yr^{-1}), by substrate acidity class, across Nova Scotia.

	Weathering Rate Estimates (eq ha^{-1} yr^{-1})				
Substrate Class	**Mean**	**Std. Dev.**	**Min**	**Max**	**Count**
1 - Acidic	287	103.3	84	2260	369065
2 - Intermediate	388	91.2	188	1032	543381
3 - Basic	740	348.9	213	3787	53421
4 - Calcareous	842	298.9	530	6017	14248
Combined Classes	376	173.2	84	6017	980115

Critical Acid Loads and Exceedances

Critical acid loads ranged between 0 and 5819 eq ha^{-1} yr^{-1}, with the highest critical load within the no harvest scenario (Table 9.2). Mean critical acid loads followed that CL no harvest > CL stem-only > CL full-tree brown < CL full-tree green, across Nova Scotia. For each harvesting scenario, the minimum critical acid load = 0, which suggests there are stands within the province which would be subject to harvest-induced nutrient losses, without the added strain of soil acidification. These nutrient deficient stands primarily occur within acidic substrates, although they are also present within intermediate and basic substrates due to the presence of nutrient demanding tree species in conjunction with low weathering and atmospheric nutrient inputs.

Table 9.2. Descriptive statistics for critical acid loads (eq ha^{-1} yr^{-1}), by harvest scenario, across Nova Scotia.

	Critical Acid Loads (eq ha^{-1} yr^{-1})				
Harvest Scenario	Mean	Std. Dev.	Std. Error	Min	Max
No harvest	692	256	0.37	124	5819
Stem-Only	638	275	0.37	0	5609
Full-tree Brown	622	277	0.37	0	5606
Full-tree Green	640	276	0.37	0	5608

Critical Acid load exceedances ranged from -4755 to 877 eq ha^{-1} yr^{-1}, following the opposite sequence as the critical loads, where EXC no harvest < EXC stem-only < EXC full-tree brown > EXC full-tree green (Table 9.3). The minimum exceedances under each scenario are within stands located on calcareous substrates, whereas the maximum exceedances generally occur on acidic substrates, as expected. The increase in critical loads and subsequent decrease in exceedances between the full-tree brown and full-tree

green harvest scenarios is a result of the change in the base-cation - nitrogen uptake ratio. This ratio is lowest for the full-tree green harvest scenario because of the high amount of foliar nitrogen uptake and subsequent N exports through harvesting.

Table 9.3. Descriptive statistics for critical acid load exceedances (eq ha^{-1} yr^{-1}), by harvest scenario, across Nova Scotia.

	Critical Acid Load Exceedance (eq ha^{-1} yr^{-1})				
Harvest Scenario	Mean	Std. Dev.	Std. Error	Min	Max
No harvest	95	283	0.38	-4755	726
Stem-Only	149	283	0.38	-4745	872
Full-tree Brown	165	284	0.38	-4743	877
Full-tree Green	148	283	0.38	-4745	877

The projected median critical load under the no harvest scenario (617 eq ha^{-1} yr^{-1}) is ~24% lower than the previously reported median critical load for Nova Scotia (817 eq ha^{-1} $yr^{-}1$; Ouimet *et al.,* 2006). Similarly, the median critical load exceedance (128 eq ha^{-1} yr^{-1}) is 48% higher than previously reported (-135 eq ha^{-1} yr^{-1}). The current area mapped in exceedance is 73% of the forested area across Nova Scotia as compared to the previously reported 40%. The differences in median critical loads and exceedances for Nova Scotia is attributed to (i) the Ouimet *et al.,* (2006) study using coarse filter soil weathering estimates based on bedrock geology only, whereas the current approach takes into account detailed soil information in combination with bedrock geology, including soil series-specific rooted depths and clay fractions; (ii) the current approach used a zero base-cation depletion scenario (i.e. $AC_{le,CL}$ = current soil base saturation; Chapter 2) to determine an acceptable level of base-cation losses, whereas the previous approach used critical molar base-cation/Al ratio and gibbsite dissolution parameters, both of which are highly speculative (Bosman *et al.,* 2001). The previous approach also assumes these parameters are static across all eastern Canadian soils, whereas the zero base-cation

depletion scenario allows for soil-series specific base saturation levels, for finer resolution of critical acid load estimates.

Base-cation Depletions

Mean base-cation depletions across Nova Scotia ranged between -82 and -138 eq ha^{-1} yr^{-1}, with the severest mean depletion rates occurring under the full-tree brown harvest scenario (Table 9.4). The 10% decrease in depletion rates between the full-tree brown and full-tree green harvest scenarios is a result of the increased N uptake from foliage compartments, as stated previously. Under a no harvest scenario, base-cation depletion rates follow that acidic > intermediate > basic > calcareous substrates, as expected. Base-cation accumulations are predicted for each harvest scenario, but are generally restricted to calcareous substrates (Max = 4267 - 4358 eq ha^{-1} yr^{-1}).

Table 9.4. Descriptive statistics for base-cation depletions (eq ha^{-1} yr^{-1}), by harvest scenario, across Nova Scotia.

	Base Cation Depletion (eq ha^{-1} yr^{-1})				
Harvest Scenario	Mean	Std. Dev.	Std. Error	Min	Max
No harvest	-82	213	0.29	-798	4267
Stem-Only	-125	214	0.29	-931	4358
Full-tree Brown	-138	215	0.29	-955	4355
Full-tree Green	-124	214	0.29	-955	4357

Predicted base-cation leachate estimates (Chapter 7; Eq. 7.26) were compared to stream and lake base-cation ion budgets as described by Yanni *et al.*, (2000), for 7 sites within Kejimkujik National Park (Figure 9.1). Base-cation leachate rates were averaged for each forested stand within 200m of the study site flow channels, by harvest scenario, in order to capture all direct upland leachate influences.

Mean base-cation leachate rates were comparable to the mean observed leachate rate, with only a 4% increase between the no harvest scenario and the observed leachate estimate (Table 9.5). The trend among harvest scenarios follows that of base-cation depletions, where no harvest < stem-only < full-tree brown > full-tree green.

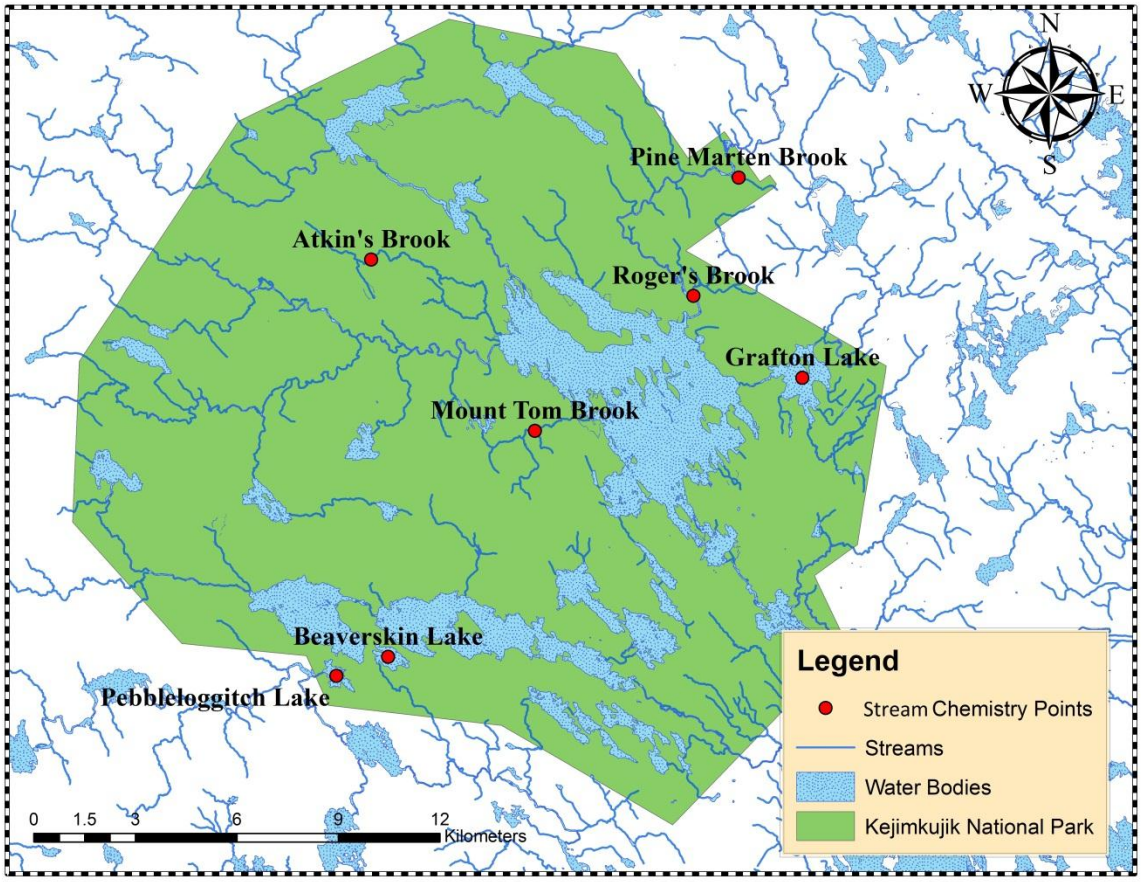


Figure 9.1. Stream chemistry study areas in relation to mapped water features within the Kejimkujik National Park boundaries.

Table 9.5. Descriptive statistics for observed base-cation leachate estimates (Yanni *et al.*, 2000; eq ha^{-1} yr^{-1}) and predicted base cation leachate estimates for the no harvest, stem-only, full-tree brown and full--tree green harvest scenarios, across Kejimkujik National Park, Nova Scotia.

	Base-cation Leachate Estimates (eq ha^{-1} yr^{-1})				
	Mean	Std. Dev.	Std. Error	Min	Max
Yanni *et al.,* (2000)	582	187	71	402	895
No Harvest	609	139	53	487	839
Stem-only	644	145	55	520	878
Full-tree Brown	654	147	56	527	887
Full-tree Green	632	143	54	512	859

Sustainable Operability

Generally, model results suggest that basic substrates supporting tolerant hardwood communities have a higher rate of potential nutrient deficiencies then acidic substrates dominated by conifer or intolerant hardwood communities. Although this appears counterintuitive due to the nutrient rich soils within these areas, the phenomenon has also been observed by Mroz *et al.,* (1985), who suggested that the greatest impact from full-tree harvesting of northern hardwood communities was found on sites with high nutrient capitals, and not within poor quality (acidic) areas. This has been attributed to northern hardwood species having a higher nutrient demand (Chapter 5), as well as deeper root networks than conifers (Schroth *et al.*, 2007).

Across Nova Scotia, growth limiting nutrients generally followed a Ca > K > N sequence for all harvest scenarios, both with and without base cation depletions. Mg was not deficient under any harvest scenario, which is attributed to the low Mg demand by trees, relative to Ca, K and N. The elevated Ca depletion estimates, which are prevalent throughout eastern North America (Federer *et al.,* 1989; Huntington *et al.,* 2000;

Lawrence *et al.*, 1997; Yanai *et al.*, 2005), are a result of Ca generally being the dominant base-cation within soils across Nova Scotia, thus more susceptible to depletion. N deficiencies range between 1 and 5% across the province, increasing from the stem-only to full-tree green harvest scenarios. This is a result of the high N concentrations in tree foliage compartments, and subsequent high N exports under a full-tree green harvest scenario.

KEJIMKUJIK SPATIAL RESULTS

Detailed results of the various model outputs are provided for Kejimkujik National Park, including results of selected model sensitivity analyses. As this thesis primarily focuses on developing a framework for establishing a biogeochemical sustainability model, the author makes no claim as to the accuracy of the predicted outputs. Output accuracy is dependent on the accuracy of the various input variables, which are potentially limited due to various spatial resolutions amongst the input data sources (see chapter 7). It is therefore recommended that all variables be reviewed when implementing stand specific analysis and harvest scenario design, and that improved input data layers be used as they become available.

Kejimkujik National Park is located within south-western Nova Scotia, encompassing an area roughly 377-km^2. The park is dominated by acidic substrate in the west, intermediate substrate in the east, and basic substrates throughout floodplain zones (Figure 9.2). The forest is dominated by conifers and intolerant hardwoods, with scattered pockets of tolerant hardwood communities throughout (Figure 9.3).

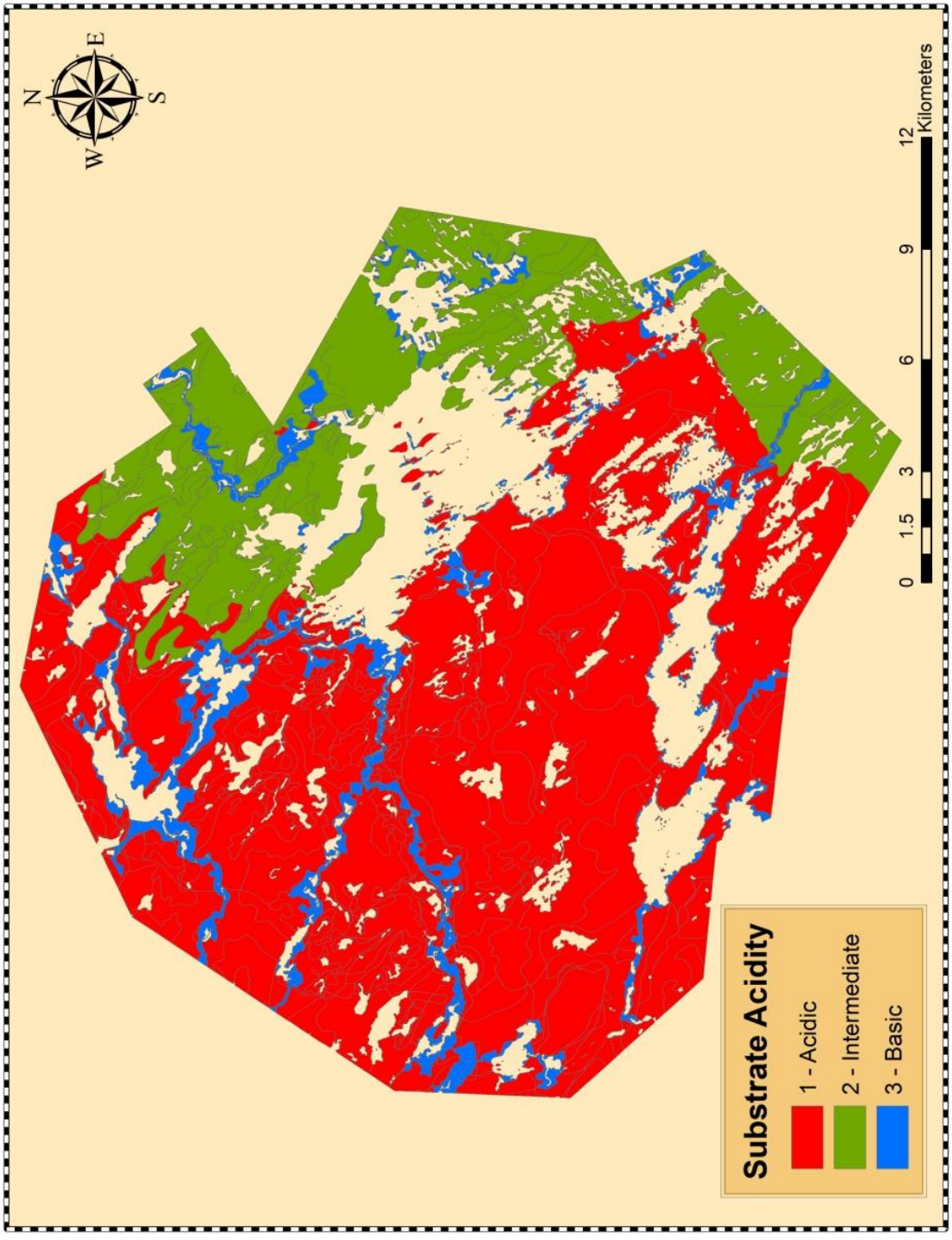


Figure 9.2. Substrate acidity classification for Kejimkujik National Park.

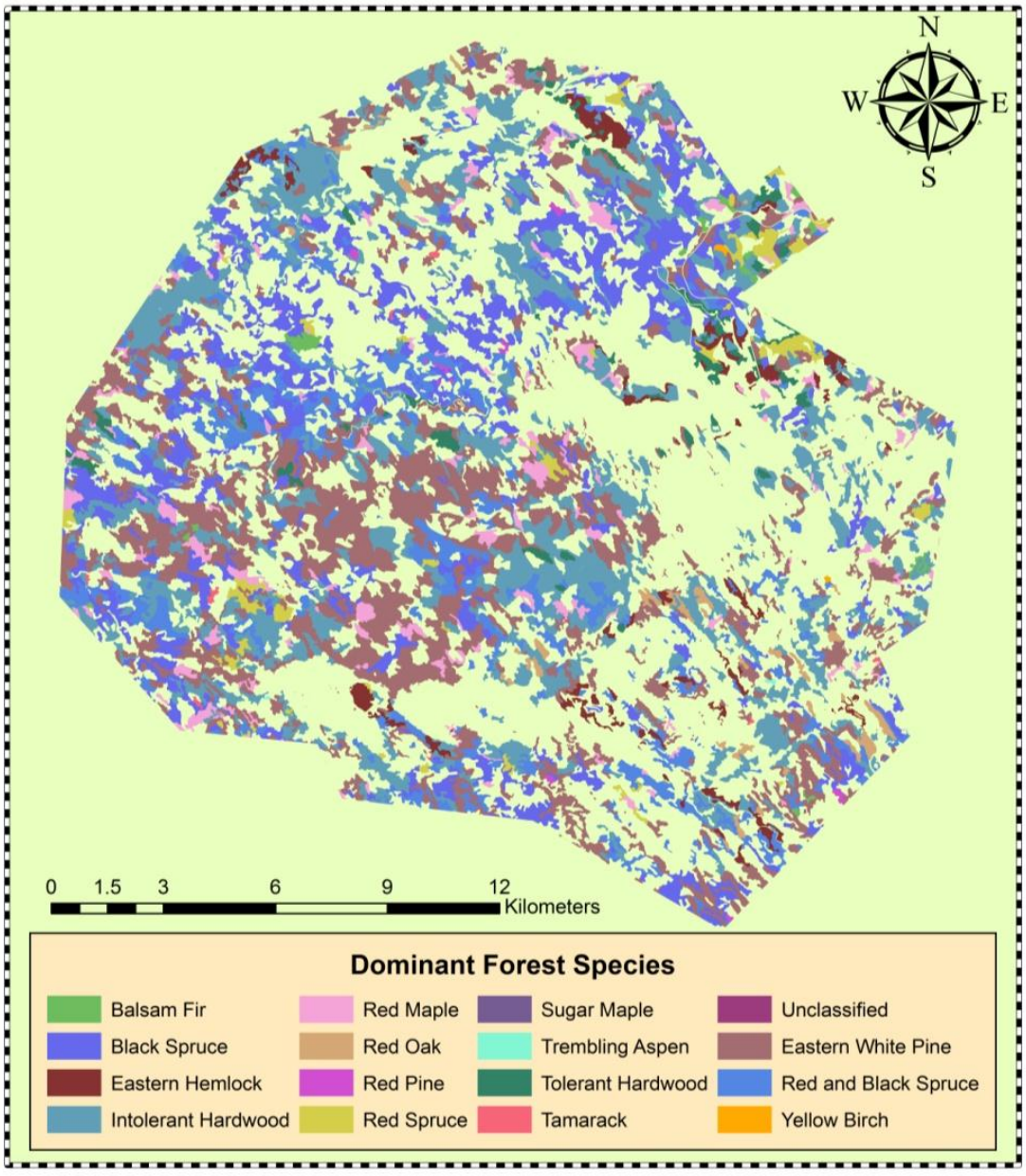


Figure 9.3. Dominant forest tree species across Kejimkujik National Park.

Parent Material Weathering

The estimated parent material weathering rates (Chapter 7) ranged from 128 to 780 eq ha^{-1} yr^{-1}, with a mean weathering rate of 398 eq ha^{-1} yr^{-1} (Figure 9.4; Table 9.6). Within the acidic substrate class, weathering rates would be as much as 661 eq ha^{-1} yr^{-1},

whereas intermediate substrates would have weathering rates within the 75th - 90th percentiles of the acidic substrate range. The intermediate substrate class was represented by relatively uniform glacial till parent material with a fairly narrow range of soil weathering rates (333 - 496 eq ha^{-1} yr^{-1}). The basic substrate class comprised of uniform alluvial soil (i.e., Cumberland series), had the highest and narrowest weathering estimates at 767 - 779 eq ha^{-1} yr^{-1} (Figure 9.5).

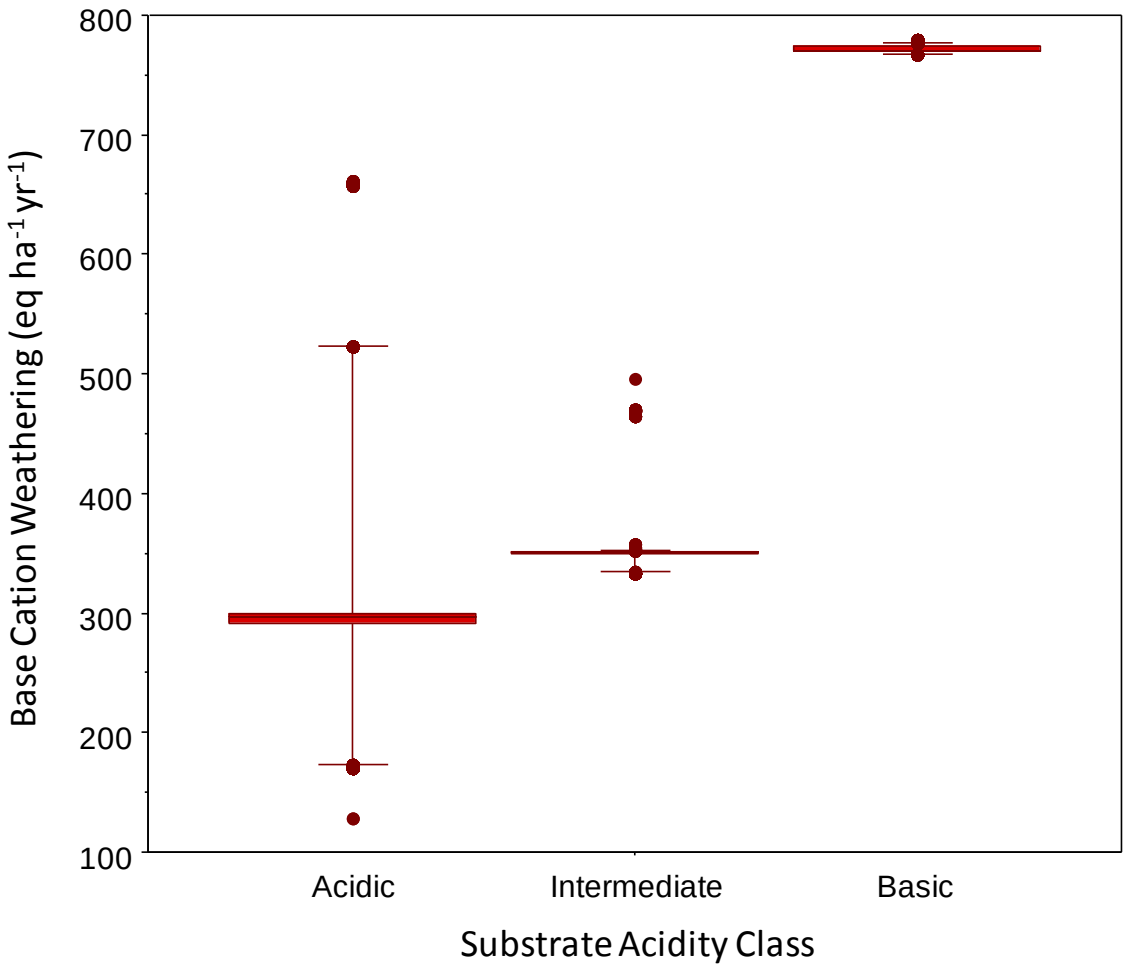


Figure 9.4. Box plots illustrating the range of base-cation weathering rates (eq ha^{-1} yr^{-1}), by substrate acidity class, across Kejimkujik National Park. Box plots show the 10th, 50th, and 90th percentiles, and outliers below the 10th and above the 90th percentiles.

Table 9.6. Descriptive statistics for base-cation weathering rates (eq ha^{-1} yr^{-1}), by substrate acidity class, across Kejimkujik National Park, Nova Scotia.

	Weathering Rate Estimates (eq ha^{-1} yr^{-1})					
Substrate Class	**Mean**	**Std. Dev.**	**Std. Error**	**Min**	**Max**	**Count**
1 - Acidic	309	124	1.78	128	661	4841
2 - Intermediate	357	31	0.83	333	496	1394
3 - Basic	772	3	0.93	767	780	1310
Combined Classes	398	199	2.29	128	780	7545

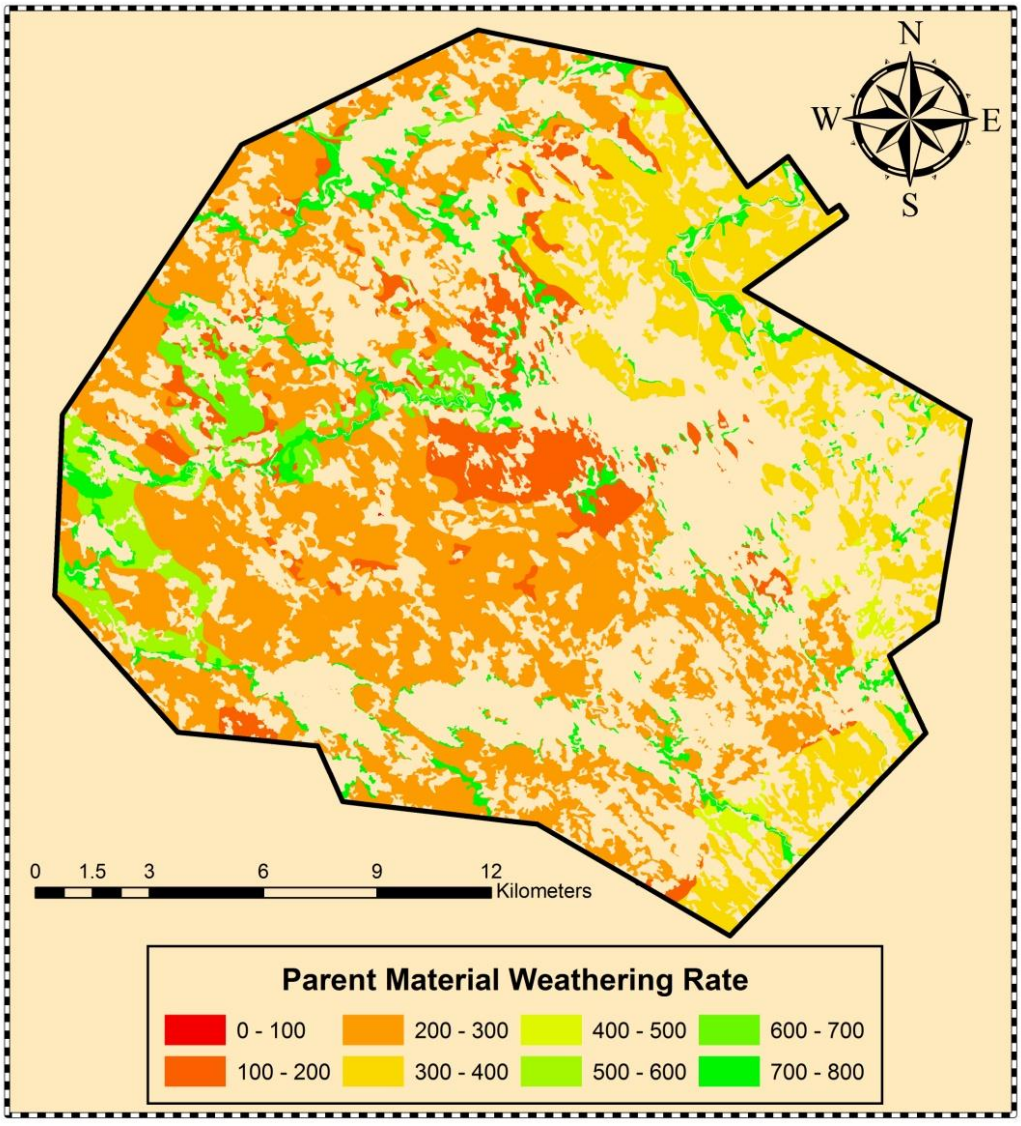


Figure 9.5. Spatial illustration of parent material weathering rates (eq ha^{-1} yr^{-1}) across Kejimkujik National Park.

Critical Acid Loads and Exceedances

The baseline critical acid loads (no harvest scenario) across Kejimkujik Park ranged between 354 - 1110 eq ha^{-1} yr^{-1}, with a mean value of 676 eq ha^{-1} yr^{-1} (Figure 9.6; Table 9.7). The lowest critical loads were located in open bedrock substrates containing shallow soils (i.e. Rockland series), whereas the highest critical loads were found on the alluvial Cumberland soil (Figure 9.7). The biomass harvest scenarios modified the general critical load trends such that CL no-harvest > CL stem-only > CL full-tree brown, but that CL full-tree brown < CL full-tree green due to the corresponding changes in the expected base-cation - nitrogen uptake ratio.

The baseline critical acid load exceedances across Kejimkujik Park varied from -282 to 809 eq ha^{-1} yr^{-1}, with a mean value of 158 eq ha^{-1} yr^{-1} (Figure 9.8; Table 9.8). As to be expected, the harvest scenario exceedance trend followed the critical acid load trend in the opposite way, such that EXC no-harvest < EXC stem-only < EXC full-tree brown, but that EXC full-tree brown > EXC full-tree green. Although all values between the 25^{th} and 50^{th} percentile suggest positive exceedances of acid deposition, there are negative exceedances as well throughout Kejimkujik Park (i.e. no soil acidification), particularly within forest stands on Cumberland soil (Figure 9.9).

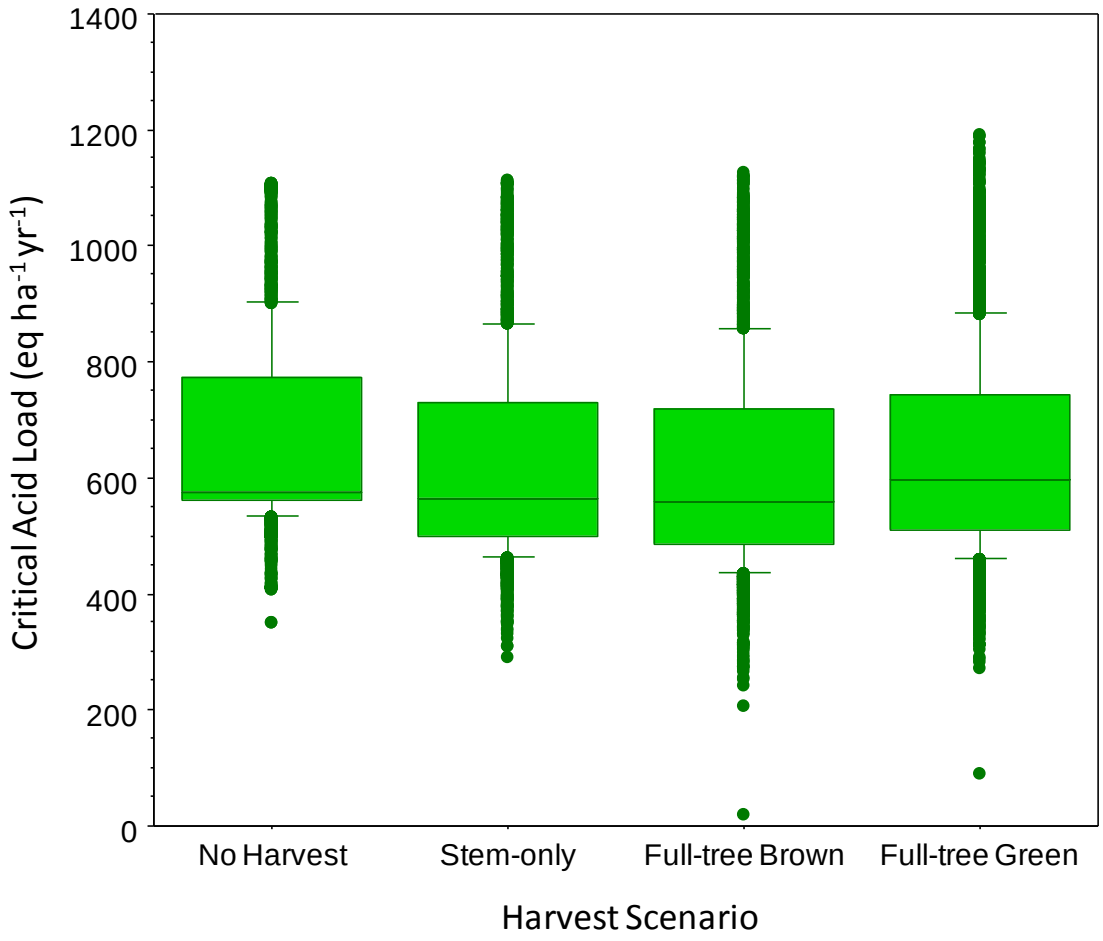


Figure 9.6. Box plots illustrating the range of critical acid loads (eq ha^{-1} yr^{-1}), by harvest scenario across Kejimkujik National Park. Box plots show the 10^{th}, 50^{th}, and 90^{th} percentiles, and outliers below the 10^{th} and above the 90^{th} percentiles.

Table 9.7. Descriptive statistics for critical acid loads (eq ha^{-1} yr^{-1}), by harvest scenario, across Kejimkujik National Park, Nova Scotia.

	Critical Acid Load Estimates (eq ha^{-1} yr^{-1})					
Harvest Scenario	**Mean**	**Std. Dev.**	**Std. Error**	**Min**	**Max**	**Count**
No Harvest	676	165	2.72	354	1111	3678
Stem-Only	627	167	2.75	294	1116	3678
Full-tree Brown	612	171	2.82	21	1127	3678
Full-tree Green	639	172	2.83	93	1194	3678

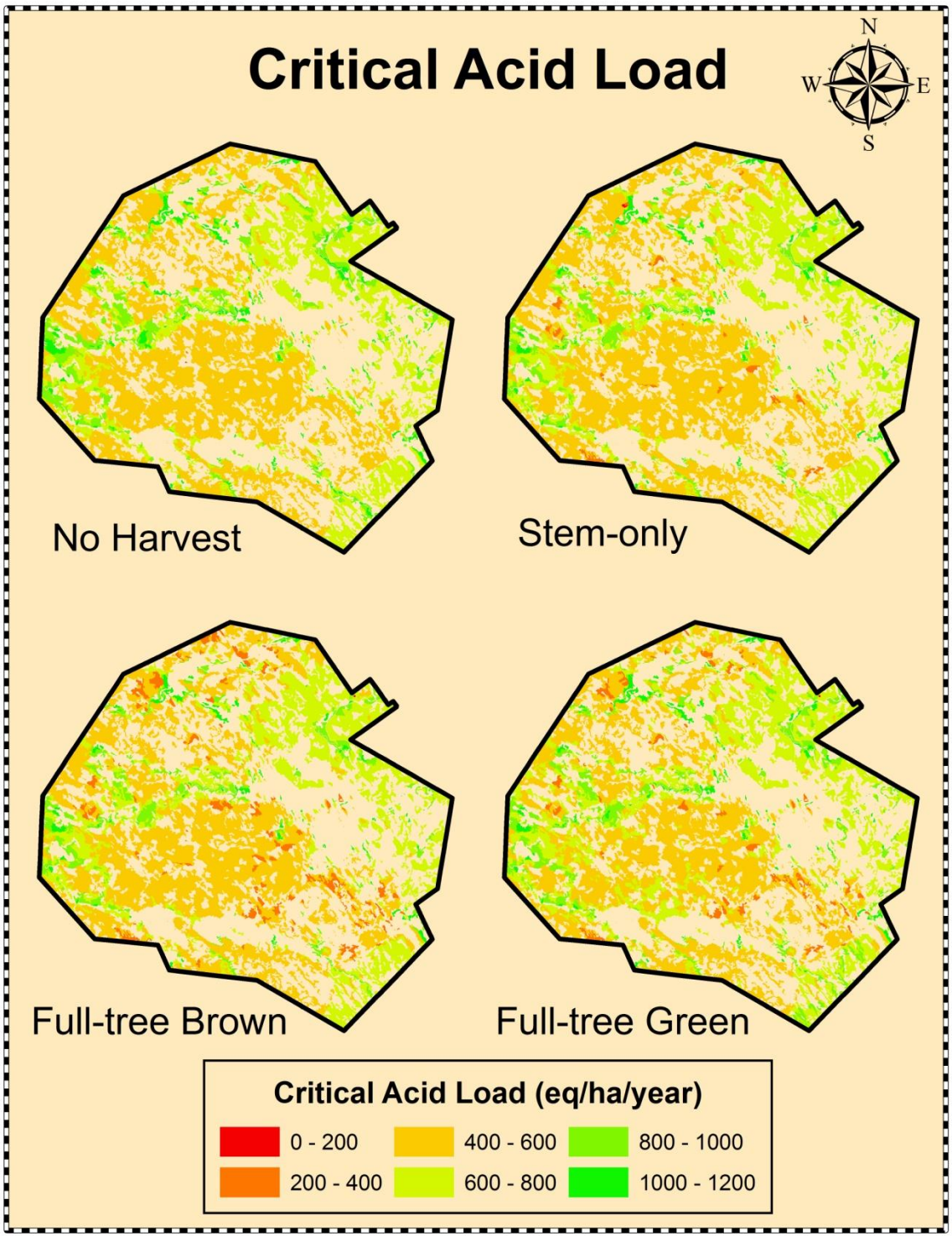


Figure 9.7. Spatial illustration of critical acid load estimations (eq ha^{-1} yr^{-1}) for each harvest scenario, within Kejimkujik National Park, Nova Scotia.

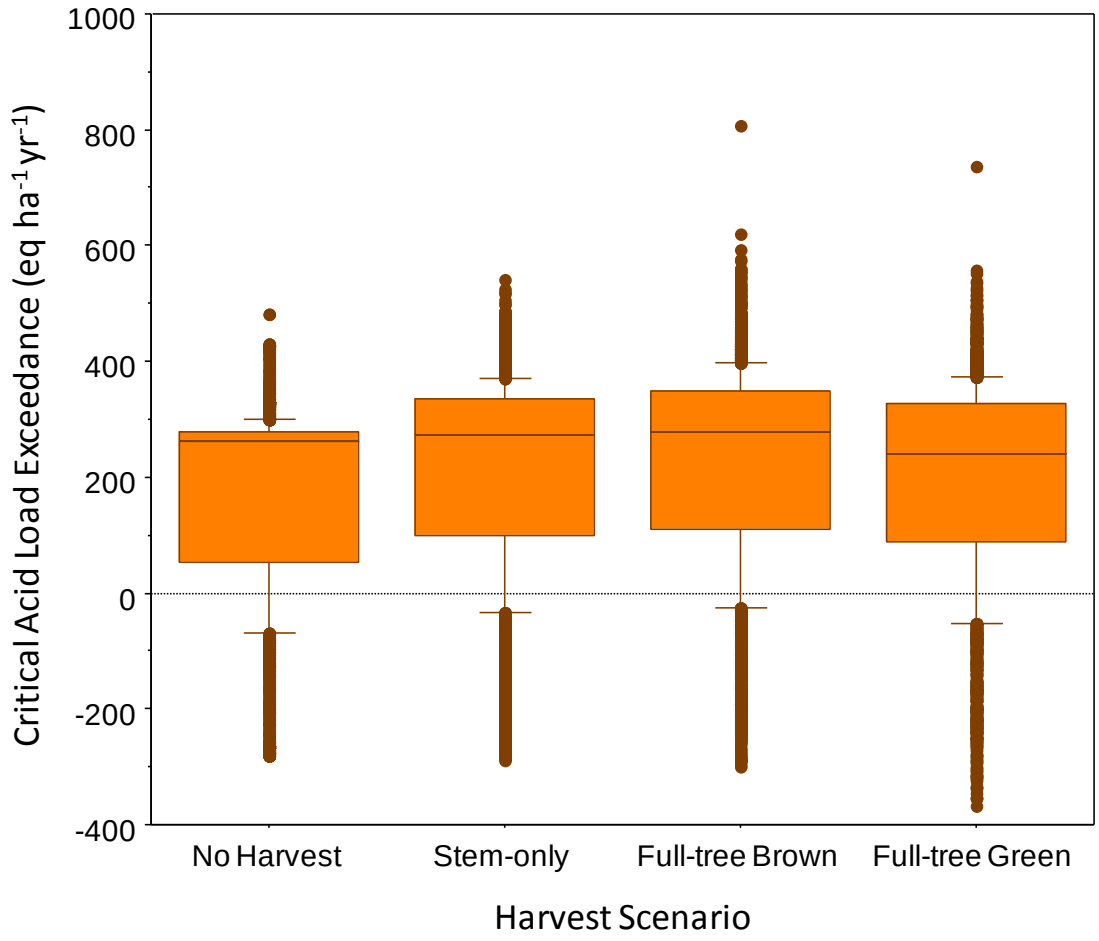


Figure 9.8. Box plots illustrating the range of critical acid load exceedances (eq ha^{-1} yr^{-1}), by harvest scenario across Kejimkujik National Park. Box plots show the 10^{th}, 50^{th}, and 90^{th} percentiles, and outliers below the 10^{th} and above the 90^{th} percentiles.

Table 9.8. Descriptive statistics for critical acid load exceedances (eq ha^{-1} yr^{-1}), by harvest scenario, across Kejimkujik National Park, Nova Scotia.

	Critical Acid Load Exceedance Estimates (eq ha^{-1} yr^{-1})					
Harvest Scenario	**Mean**	**Std. Dev.**	**Std. Error**	**Min**	**Max**	**Count**
No Harvest	158	166	2.74	-282	481	3678
Stem-Only	207	168	2.77	-289	543	3678
Full-tree Brown	222	172	2.84	-301	809	3678
Full-tree Green	195	173	2.85	-367	737	3678

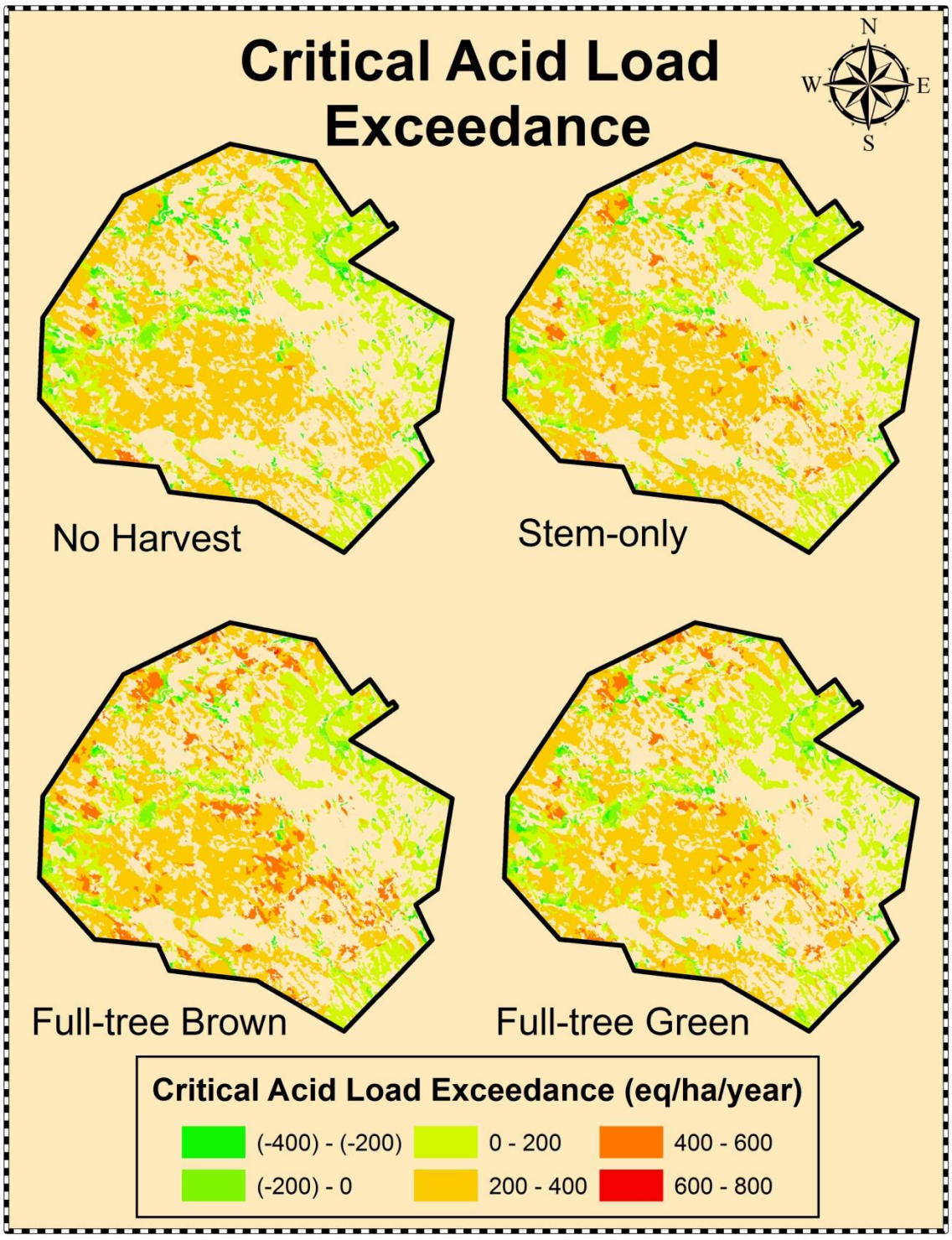


Figure 9.9. Spatial illustration of critical acid load exceedance estimations (eq ha^{-1} yr^{-1}) for each harvest scenario, within Kejimkujik National Park, Nova Scotia.

Base-cation Depletion

Base-cation depletion rates under the no harvest scenario ranged from -390 to 238 eq ha^{-1} yr^{-1} across Kejimkujik park, with a average depletion rate of -123 eq ha^{-1} yr^{-1} (Figure 9.10; Table 9.9). The relationship between base-cation depletion and critical load exceedances across Kejimkujik Park is somewhat linear, and therefore the trend between harvest scenarios follows the same sequence as critical load exceedances (no harvest < stem-only < full-tree brown > full-tree green). The severest depletions are predicted to occur within stands over acidic substrates, although there is variation within this substrate class related to soil conditions and species compositions. Although the majority of stands are predicted to experience base-cation depletions, even under a full-tree green harvest scenario, all outliers above the 90^{th} percentile are predicted to experience base-cation accumulations. Base-cation accumulations are generally limited to stands located on basic substrates (Figure 9.11).

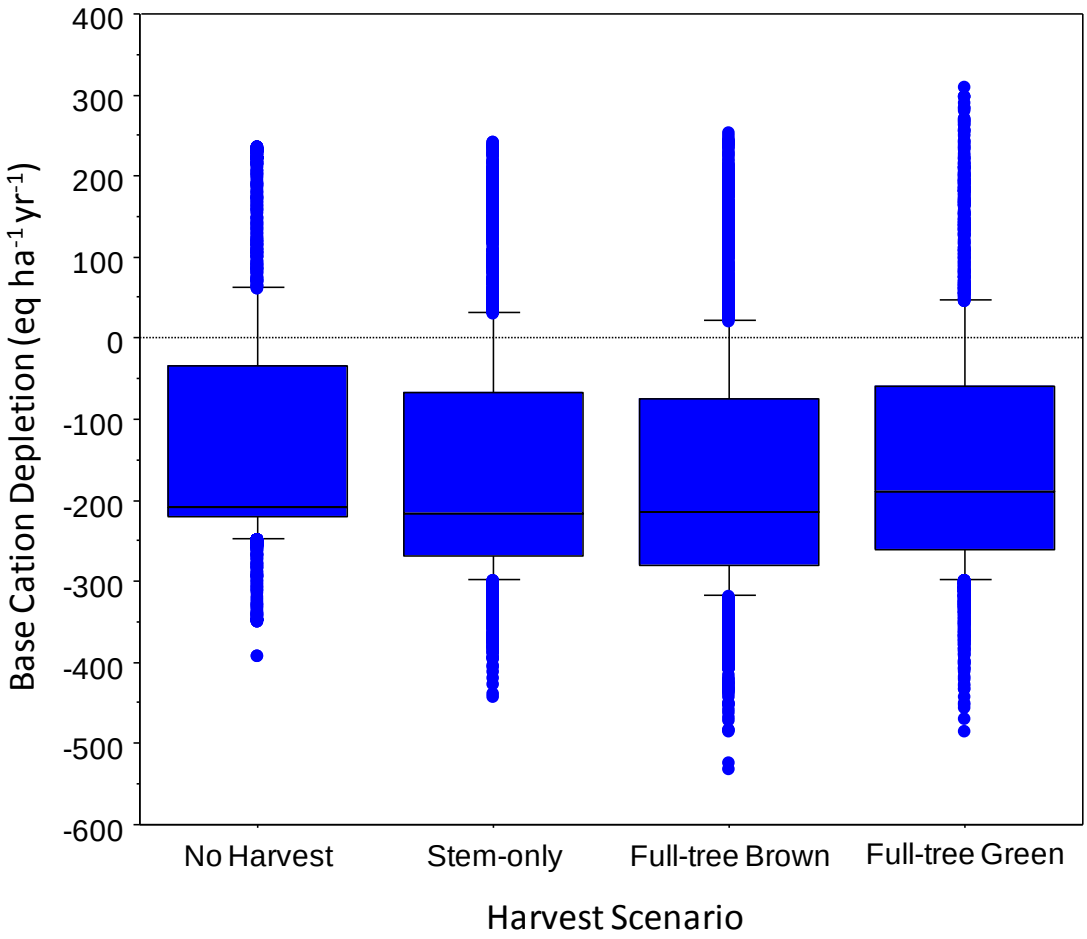


Figure 9.10. Box plots illustrating the range of base-cation depletions (eq ha^{-1} yr^{-1}), by harvest scenario across Kejimkujik National Park. Box plots show the 10^{th}, 50^{th}, and 90^{th} percentiles, and outliers below the 10^{th} and above the 90^{th} percentiles.

Table 9.9. Descriptive statistics for base-cation depletions (eq ha^{-1} yr^{-1}), by harvest scenario, across Kejimkujik National Park, Nova Scotia.

	Base Cation Depletion Estimates (eq ha^{-1} yr^{-1})					
Harvest Scenario	**Mean**	**Std. Dev.**	**Std. Error**	**Min**	**Max**	**Count**
No Harvest	-123	136	2.25	-390	238	3678
Stem-Only	-161	138	2.28	-440	244	3678
Full-tree Brown	-172	142	2.34	-531	254	3678
Full-tree Green	-151	142	2.34	-484	310	3678

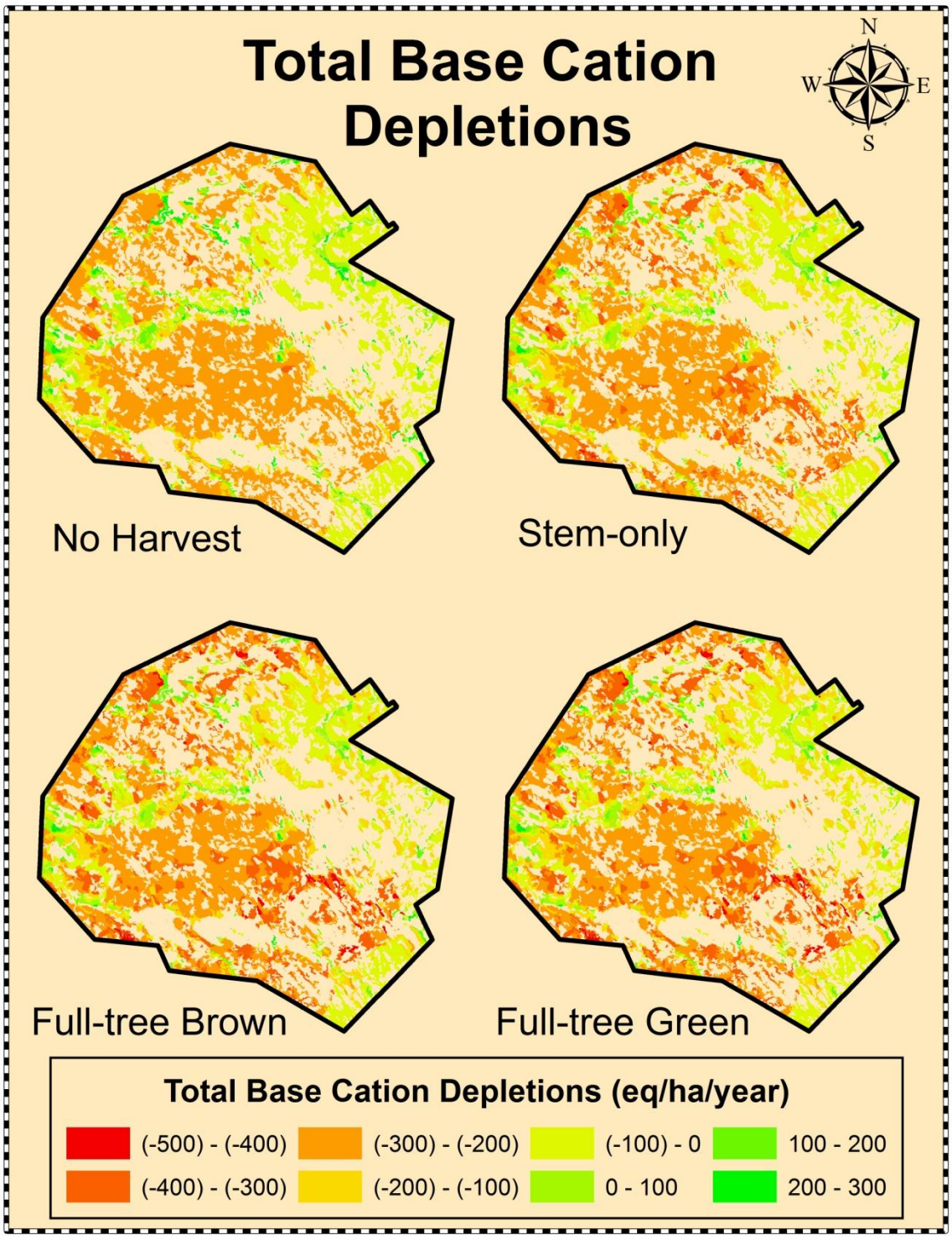


Figure 9.11. Spatial illustration of base-cation depletion estimations (eq ha^{-1} yr^{-1}) for each harvest scenario, within Kejimkujik National Park, Nova Scotia.

Sustainable Operability

Clear-cut Harvest Operability Calculator

Clear-cut harvest operability was examined by harvest scenario, with and without potential base-cation depletions. Under a deficiency-based, stem-only clear-cut scenario, 85% of Kejimkujik Park is predicted as being sustainable assuming current inventory conditions, complete removal of biomass compartments, and no adjustments in management to account for potential nutrient deficiencies (Figure 9.12). The amount of area that can be sustainably harvested follows that stem-only > full-tree brown > full-tree green. Between the stem-only and full-tree brown scenarios, a 33% decrease in operable area is predicted, following an additional 16% decrease towards the full-tree green scenario. As expected, the complete removal of nutrient-rich branch and foliage biomass compartments adds an additional strain on the sites capacity to replenish nutrients, particularly within soils that have low weathering rates. Generally, operable stands are dominated by conifers, whereas stands predicted to undergo nutrient deficiencies are dominated by tolerant and intolerant hardwoods. With the addition of base-cation depletions, operable area decreased to 42% for the stem-only scenario, 27% for the full-tree brown scenario, and 19% for the full-tree green scenario (Figure 9.13). The trend follows the same sequence as the deficiency-alone scenarios, although the relative decrease in operable area from the stem-only to full-tree green scenarios is considerably lower. Spatially, harvest operability under deficiencies alone is generally related to stand-specific nutrient supplies and demands. In contrast, harvest operability constraints due to harvest-induced nutrient deficiencies coupled with base-cation depletion are more

widespread, and basically coincide with the geospatial distribution of the acidic substrates (Figure 9.14).

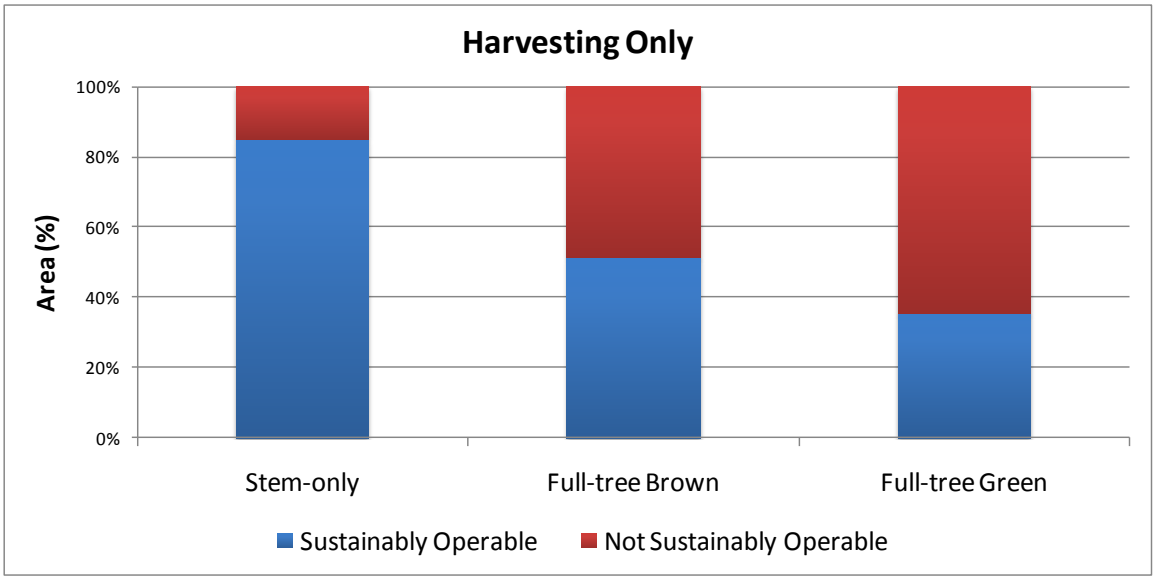


Figure 9.12. Deficiency-based area (%) predicted to be sustainably and not sustainably clear-cut harvested, across Kejimkujik National Park under the stem-only, full-tree brown and full-tree green harvest scenarios.

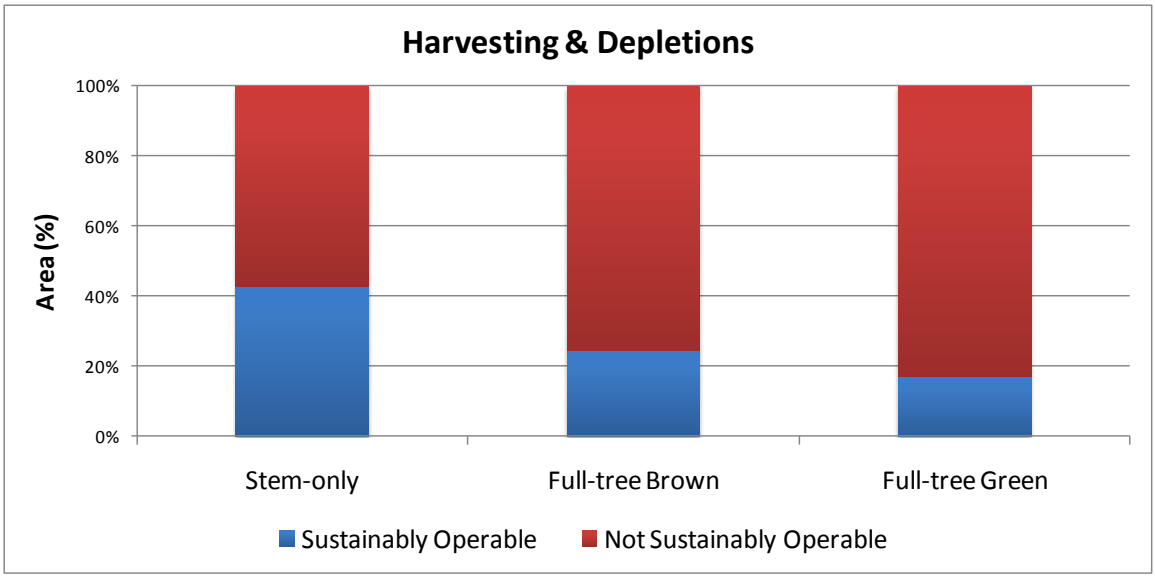


Figure 9.13. Deficiency- and depletion-based area (%) predicted to be sustainably and not sustainably clear-cut harvested, across Kejimkujik National Park under the stem-only, full-tree brown and full-tree green harvest scenarios.

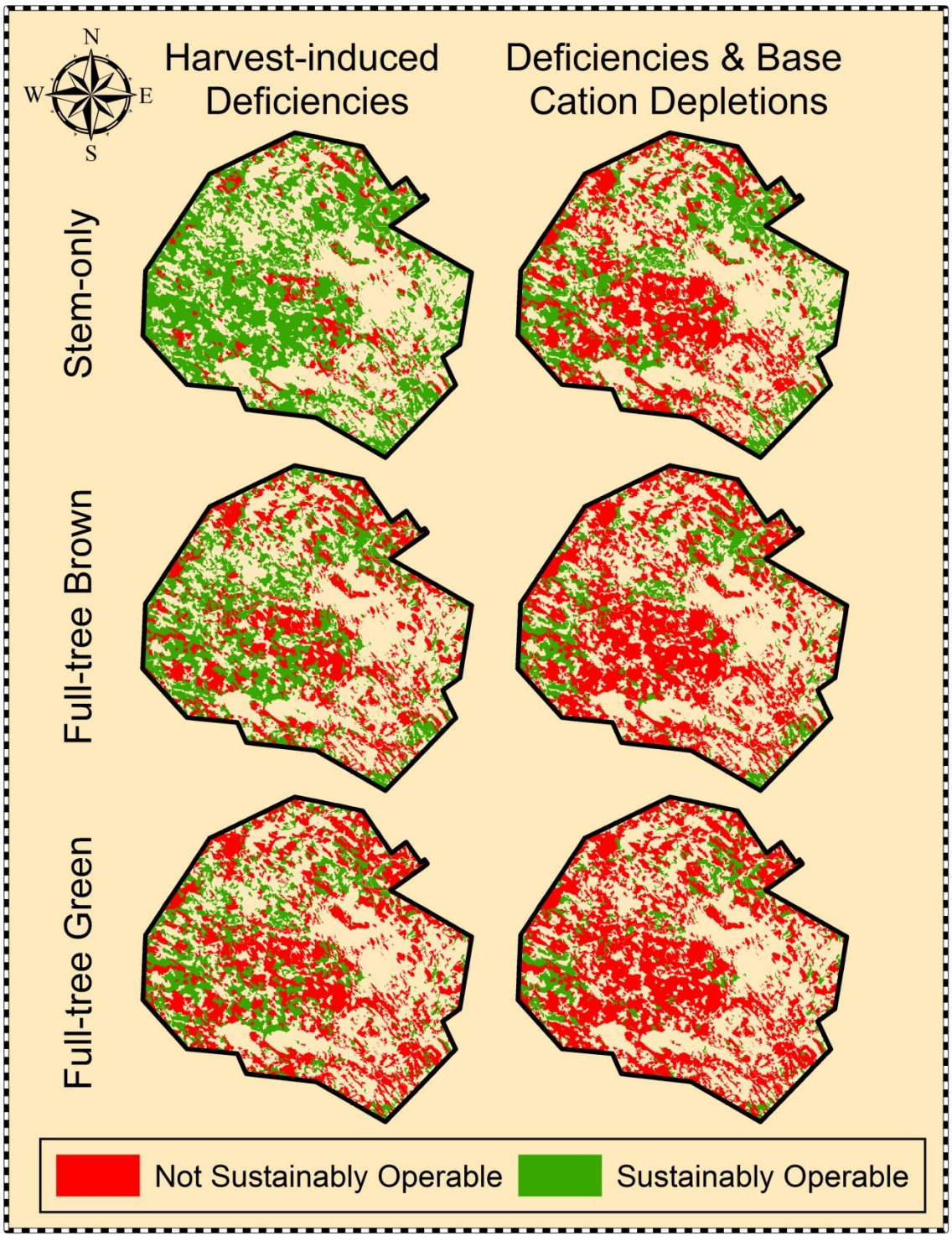


Figure 9.14. Spatial illustration of the clear-cut operability calculator outputs for each harvest scenario, with and without base cation depletions, across Kejimkujik National Park, Nova Scotia.

Growth Limiting Nutrient Assessment

Across Kejimkujik National Park, Ca is found to be the dominant growth limiting nutrient for biomass harvesting in this particular area, with and without the extra burden of base-cation depletion considered. For example, 10% of stands would be Ca-limited, while 5% would be K-limited, under a stem-only deficiency scenario (Figure 9.15). When base-cation depletion is considered as well, the amount of Ca-limited area increases substantially, regardless of harvest scenario (Figure 9.16). This is a result of the high percentage of exchangeable soil Ca relative to the corresponding K and Mg values, thereby making Ca more susceptible to base-cation depletion. Spatially, K- and N-deficiencies are predicted to occur throughout Kejimkujik Park, regardless of substrate acidity, whereas Ca deficiencies are generally limited to acidic substrates (Figure 9.17). Under the full-tree green scenarios, elevated N limitations are also predicted, especially for conifer stands with White Pine as the dominant species. Mg limitations are not predicted anywhere within Kejimkujik Park, which is due to the low Mg demand by tree species, and the subsequently low rates of Mg exports with all three harvest scenarios.

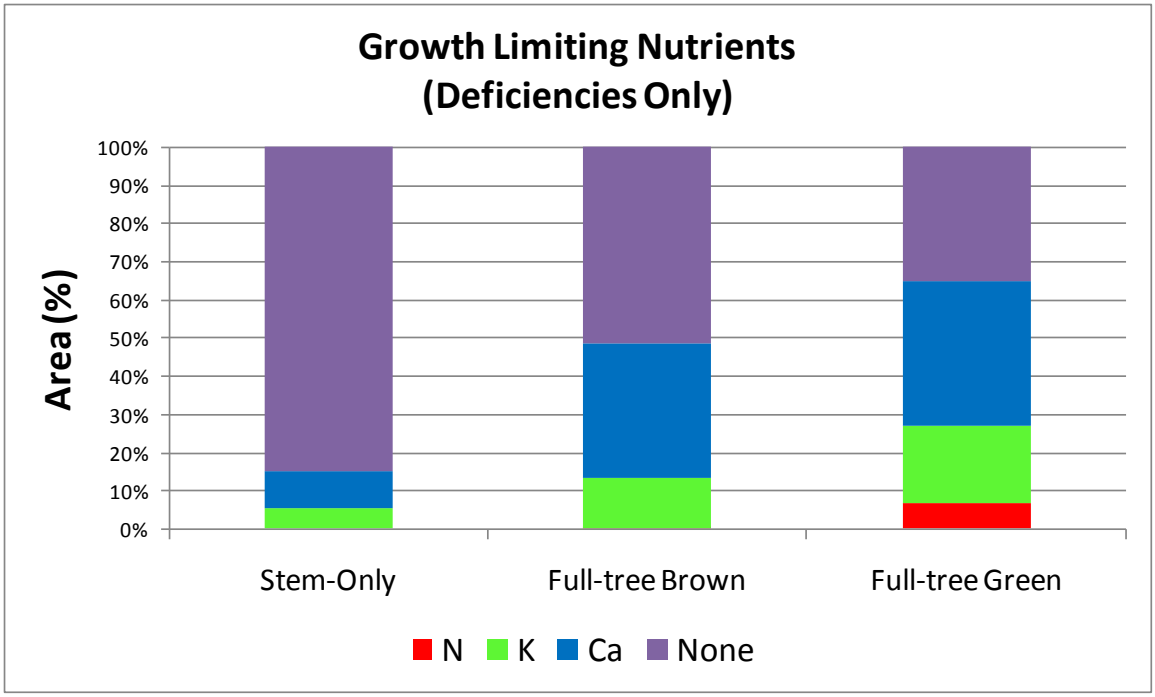


Figure 9.15. Deficiency-based area (%) predicted to be N, K or Ca limited across Kejimkujik National Park under the stem-only, full-tree brown and full-tree green harvest scenarios.

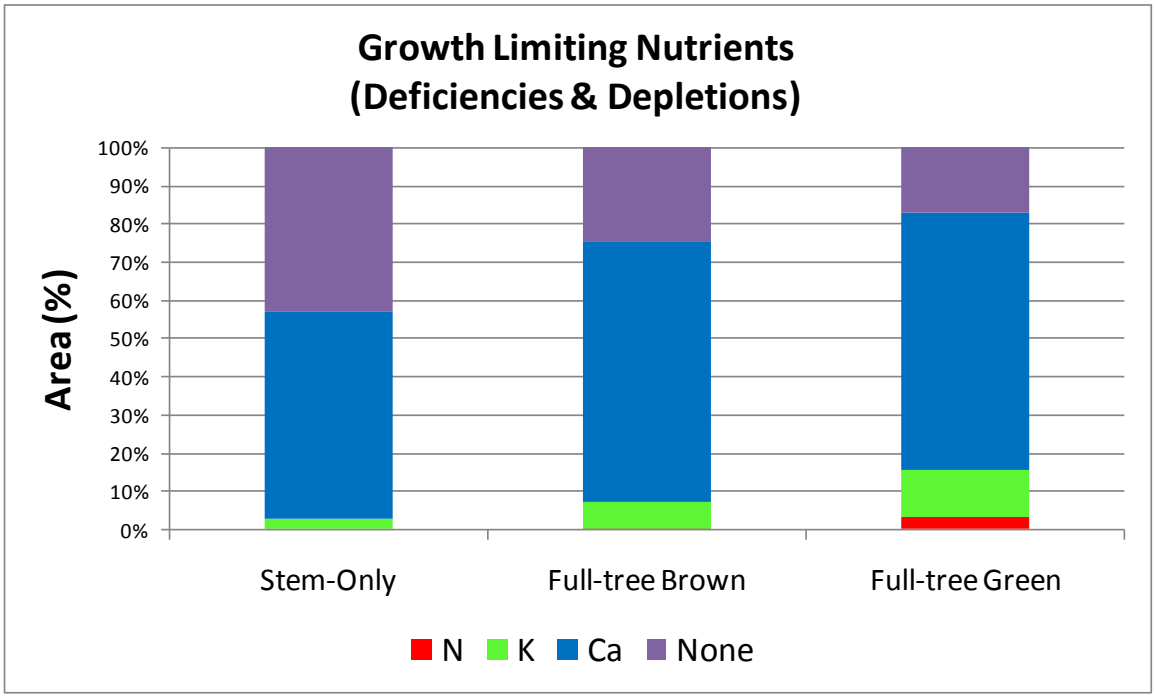


Figure 9.16. Deficiency- and depletion-based area (%) predicted to be N, K or Ca limited across Kejimkujik National Park under the stem-only, full-tree brown and full-tree green harvest scenarios.

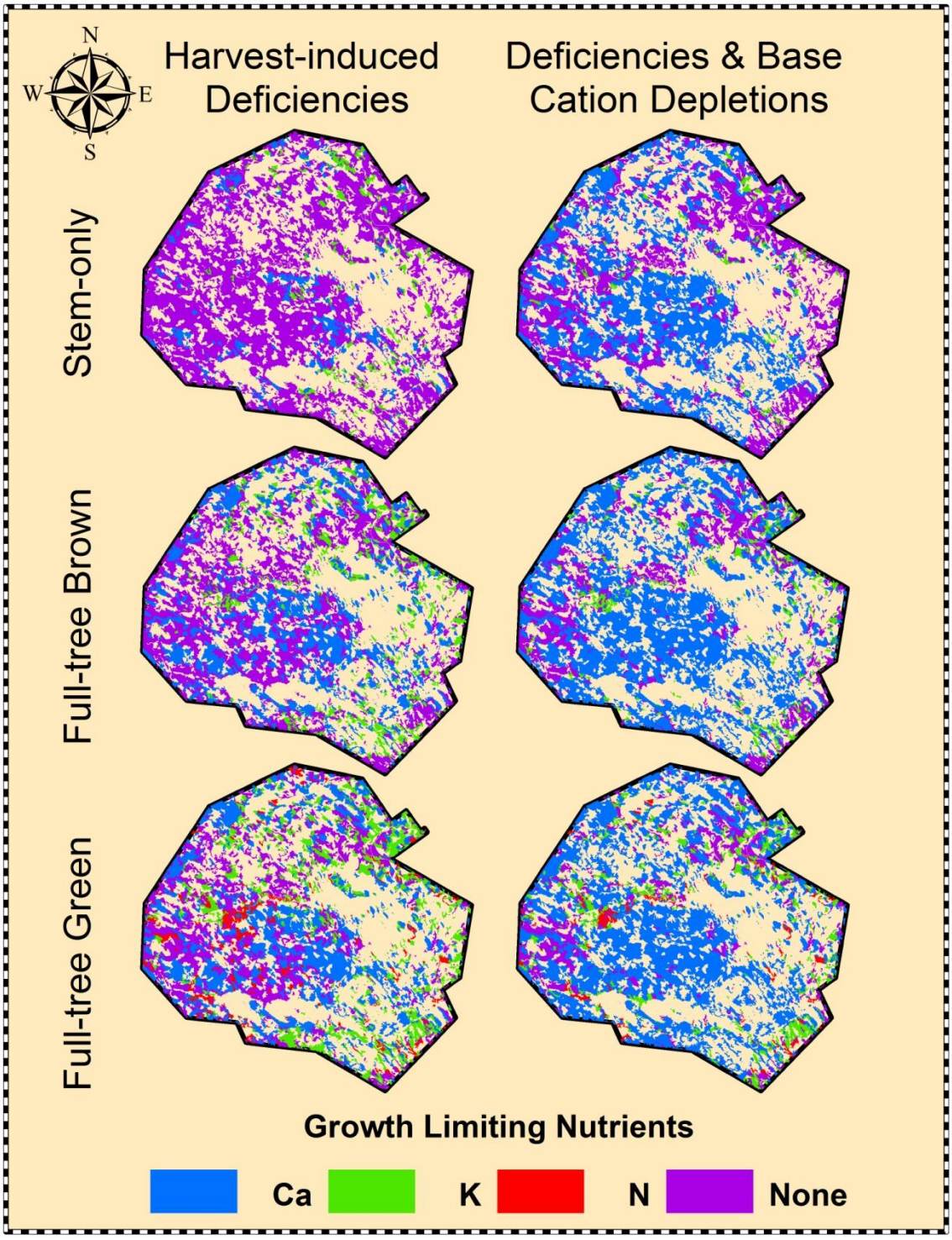


Figure 9.17. Spatial illustration of growth limiting nutrients for each harvest scenario, with and without base cation depletions, across Kejimkujik National Park, Nova Scotia.

Sustainable Harvest Rate Predictions

Sustainable rates for biomass harvesting without accounting for potential base-cation depletion losses were estimated in terms of wood volume units, ranging from 1.3 to 10 m^3 ha^{-1} yr^{-1} across Kejimkujik Park, with an average of 4.7 m^3 ha^{-1} yr^{-1} (Figure 9.18; Table 9.10). Accounting for potential base-cation depletion would decrease the mean value to 2.8 m^3 ha^{-1} yr^{-1}, drop the lower limit to 0 m^3 ha^{-1} yr^{-1}, but maintain the high limit at 9.8 m^3 ha^{-1} yr^{-1}. Sustainable harvest rates >8 m^3 ha^{-1} yr^{-1} would be mostly associated with high volume conifer stands dominated by White Pine, while sustainable harvest rates <3 m^3 ha^{-1} yr^{-1} would generally be restricted to nutrient demanding tolerant and intolerant hardwood stands. Stands with the largest sustainable harvest rates are almost exclusively found on acidic substrates (Figure 9.19) which generally support nutrient-efficient conifers as the dominant vegetation. With base-cation depletion, however, sustainable harvest rates are estimated to significantly drop on these substrates. Forest stands growing on soil substrates with high acid-buffering capacity are, in comparison, less sensitive to base-cation depletion, as to be expected.

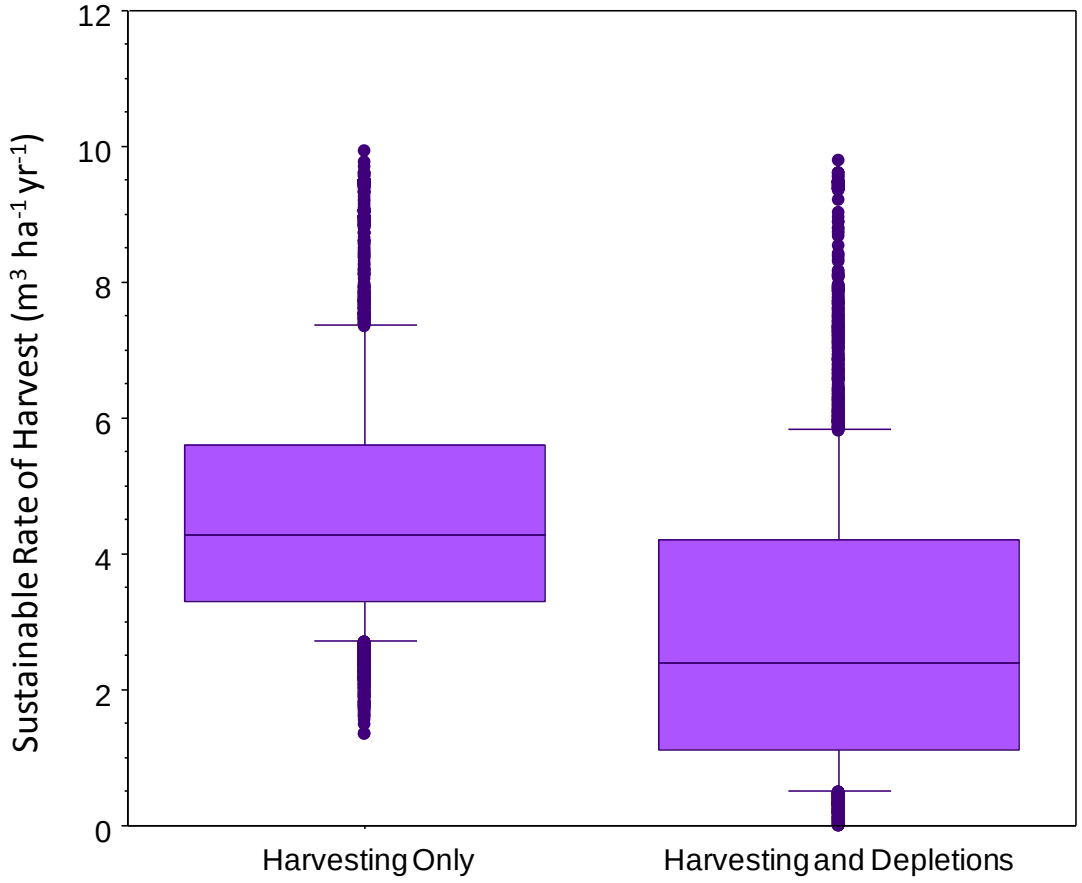


Figure 9.18 Box plots illustrating the range of sustainable harvest rates (m^3 ha^{-1} yr^{-1}), for harvesting with and without base-cation depletions, across Kejimkujik National Park. Box plots show the 10^{th}, 50^{th}, and 90^{th} percentiles, and outliers below the 10^{th} and above the 90^{th} percentiles.

Table 9.10. Descriptive statistics for sustainable harvest rates (m^3 ha^{-1} yr^{-1}), with and without base - cation depletion, across Kejimkujik National Park, Nova Scotia.

	Sustainable Harvesting Rates (m^3 ha^{-1} yr^{-1})					
	Mean	**Std. Dev.**	**Std. Error**	**Min**	**Max**	**Count**
Harvesting Only	4.67	1.84	0.03	1.378	9.953	3678
Harvest & Depletions	2.81	2.13	0.04	0	9.822	3678

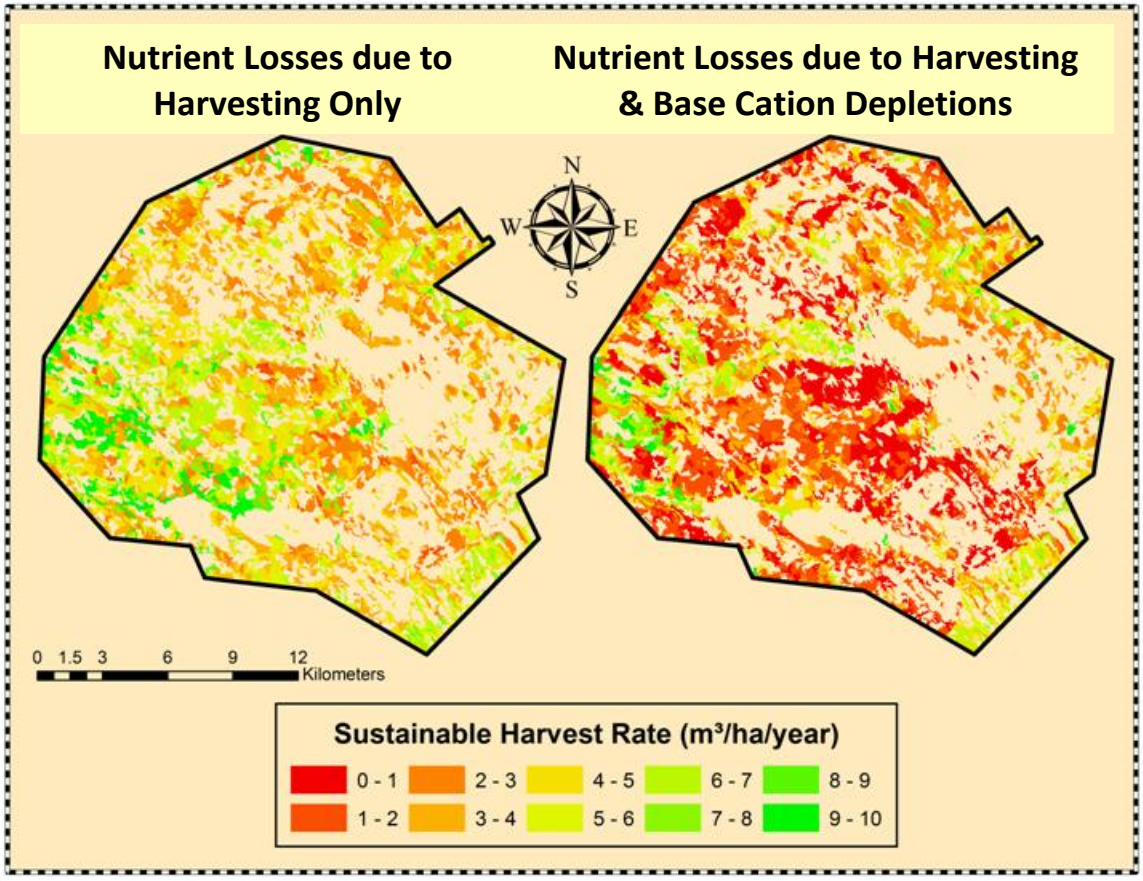


Figure 9.19. Spatial illustration of predicted sustainable harvest rates across Kejimkujik National Park for harvesting with and without base-cation depletions.

SENSITIVITY ANALYSES

The variation of inputs within the weathering sub-model, critical loads and exceedances sub-model, base-cation depletion sub-model and sustainable operability sub-model were analysed under 6 sensitivity scenarios in order to evaluate model output uncertainties. In order to compare results, sensitivity analyses are restricted to Kejimkujik National park.

Sensitivity Scenarios

1. Substrate acidity classes were increased by 1 with the exception of calcareous substrates, to evaluate the impacts of elevated base-cation inputs on base-cation depletions, critical loads and exceedances and sustainable operability.

2. Average annual temperature was increased by 1°C and 4.5°C, based on minimum and maximum Global Circulation Model (GCM) climate change predictions (see Iverson & Prasad, 1998), in order to evaluate the impacts on parent material weathering.

3. Soil depth was increased by 25cm, and decreased by 25cm (minimum value of 0cm which simulates no vegetation), in order to evaluate the impacts on parent material weathering.

4. To mimic currently occurring reductions in industrial and urban emissions, atmospheric S and N deposition rates were decreased by a factor of 1.7 and 1.6, respectively (Aherne *et al.,* 2010), to evaluate the impact of these reductions on critical load exceedances, base-cation depletions, and sustainable operability. For comparison, the S and N deposition rates were increased by the same factors as well.

5. The K_{exch} constant of 10, which represents the preference of the cation exchange sites for acid cations over base cations, was set at 5 and 15 to determine how the change in the K_{exch} value would affect the calculated rates for base-cation depletions.

6. Also examined were the harvestable forest biomass projections by changing the DBH-based projections from 40 to 20 and 60 cm.

Sensitivity Results

1) Substrate Acidity Class

Increasing the soil weathering class by 1 resulted in a 37, 41, 42 and 40% increase in mean critical acid loads across Kejimkujik Park for the no harvest, stem-only, full-tree brown and full-tree green harvest scenarios, respectively (Table 9.11). The elevated critical loads are attributed to the increased base-cation inputs, particularly within the previously classed intermediate and basic substrates. The relative increase in base cations from the acidic to intermediate class would be restricted by the small variation in intermediate class weathering rates (Figure 9.4). As a result of the elevated critical acid loads, there was a proportional decrease in critical acid load exceedances, for each harvest scenario (Table 9.12). Increasing the soil weathering class by 1 would result in mean base-cation accumulations for each harvest scenario (Table 9.13), with an average change of 168, 129, 120 and 124% for the no harvest, stem-only, full-tree brown and full-tree green scenarios, respectively. The elevated base-cation inputs would increase the soil acid buffering capacity, which results in: (i) decreased base-cation depletion within the previously classed acidic substrates (Min = -324 eq ha^{-1} yr^{-1}); (ii) increased base-cation accumulations within the basic substrates (Max = 961 eq ha^{-1} yr^{-1}).

Table 9.11. Descriptive statistics for critical acid loads under baseline and increased substrate acidity class estimates (eq ha^{-1} yr^{-1}), by harvest scenario, across Kejimkujik National Park, Nova Scotia.

	Critical Acid Load (eq ha^{-1} yr^{-1})					
	Senst. Scenario	Mean	Std. Dev.	Std. Error	Min	Max
No harvest	Baseline	676	165	2.72	354	1111
	Acidity Class +1	929	296	4.89	436	1884
Stem-Only	Baseline	627	167	2.75	294	1116
	Acidity Class +1	881	298	4.91	393	1886
Full-tree Brown	Baseline	612	171	2.82	21	1127
	Acidity Class +1	866	300	4.95	56	1898
Full-tree Green	Baseline	639	172	2.83	93	1194
	Acidity Class +1	893	301	4.96	127	1964

Table 9.12. Descriptive statistics for critical acid load exceedances under baseline and increased substrate acidity class estimates (eq ha^{-1} yr^{-1}), by harvest scenario, across Kejimkujik National Park, Nova Scotia.

	Critical Load Exceedances (eq ha^{-1} yr^{-1})					
	Senst. Scenario	Mean	Std. Dev.	Std. Error	Min	Max
No harvest	Baseline	158	166	2.74	-282	481
	Acidity Class +1	-95	296	4.89	-1055	400
Stem-Only	Baseline	207	168	2.77	-289	543
	Acidity Class +1	-47	298	4.91	-1059	443
Full-tree Brown	Baseline	222	172	2.84	-301	809
	Acidity Class +1	-32	300	4.95	-1071	774
Full-tree Green	Baseline	195	173	2.85	-367	737
	Acidity Class +1	-59	301	4.96	-1138	703

Table 9.13. Descriptive statistics for base-cation depletions under baseline and increased substrate acidity class estimates (eq ha^{-1} yr^{-1}), by harvest scenario, across Kejimkujik National Park, Nova Scotia.

		Base Cation Depletion (eq ha^{-1} yr^{-1})				
	Senst. Scenario	Mean	Std. Dev.	Std. Error	Min	Max
No harvest	Baseline	-123	136	2.25	-390	238
	Acidity Class +1	84	250	4.13	-324	891
Stem-Only	Baseline	-161	138	2.28	-440	244
	Acidity Class +1	46	250	4.13	-359	894
Full-tree Brown	Baseline	-172	142	2.34	-531	254
	Acidity Class +1	34	252	4.15	-508	904
Full-tree Green	Baseline	-151	142	2.34	-484	310
	Acidity Class +1	56	253	4.17	-462	961

Mean sustainable harvest rates increased by 28% and 102% when considering the nutrient exports due to harvesting with and without base-cation depletion, respectively (Table 9.14). Although mean sustainable harvest levels across the four harvest scenarios would generally increase due to the elevated base-cation inputs on the more easily weathered soil substrates, trees remain susceptible to N deficiencies. It is of interest to note that increasing the soil weatherability by one class does not always lead to sustainable harvest levels >0. This was noted to occur within stands located on intermediate substrate (Min = 0).

Table 9.14. Descriptive statistics for sustainable harvest rates under baseline and increased substrate acidity class estimates (m^3 ha^{-1} yr^{-1}) for harvesting, with and without base cation-depletion, across Kejimkujik National Park, Nova Scotia.

		Sustainable MAI (m^3 ha^{-1} yr^{-1})				
	Senst. Scenario	Mean	Std. Dev.	Std. Error	Min	Max
Harvesting Only	Baseline	4.67	1.84	0.03	1.38	9.95
	Acidity Class +1	5.96	2.02	0.03	1.71	10.81
Harvesting & Depletion	Baseline	2.81	2.13	0.03	0	9.82
	Acidity Class +1	5.67	2.29	0.04	0	10.90

2) Average Annual Temperature

Increasing the annual average temperature by 1°C and 4.5°C resulted in a 5 and 23% increase in mean parent material weathering rates, respectively (Table 9.15). The linear relationship between parent material weathering and temperature is such that for every 1°C increase, there would be a subsequent 5% increase in weathering rates, regardless of soil weathering class.

Table 9.15. Descriptive statistics for parent material weathering (eq ha^{-1} yr^{-1}) under the baseline, 1°C increase in average annual temperature, and 4.5°C increase in average annual temperature estimates, across Kejimkujik National Park, Nova Scotia.

Parent Material Weathering (eq ha^{-1} yr^{-1})					
Senst. Scenario	Mean	Std. Dev.	Std. Error	Min	Max
Baseline	398	199	2.29	128	780
Temp +1°C	417	208	2.4	134	816
Temp +4.5°C	488	244	2.81	157	955

3) Soil Rooting Depth

Increasing the soil rooting depth by 25cm resulted in a 55% increase in mean parent material weathering rates, whereas a 25cm decrease in soil rooting depth resulted in a 55% decrease in mean parent material weathering rates (Table 9.16). Although this appears to be a linear relationship, the sensitivity and baseline scenario is not a 1:1 situation due to factors such as organic matter and coarse fragment contents also influencing parent material weathering rates. This emphasizes the importance of using site-specific soils data for stand level analysis.

Table 9.16. Descriptive statistics for parent material weathering (eq ha^{-1} yr^{-1}) under baseline, 25cm increase in soil rooting depth, and 25cm decrease in soil rooting depth estimates, across Kejimkujik National Park, Nova Scotia.

Parent Material Weathering (eq ha^{-1} yr^{-1})					
Senst. Scenario	Mean	Std. Dev.	Std. Error	Min	Max
Baseline	398	199	2.29	128	780
Depth +25cm	617	303	3.49	262	1212
Depth -25cm	179	99	1.14	0	381.2

4) Atmospheric S and N Deposition

Decreasing the atmospheric acid deposition rates for S and N resulted in a 211, 161, 150 and 171% decrease in mean critical load exceedances for the no harvest, stem-only, full-tree brown and full-tree green harvest scenarios, respectively (Table 9.17). Conversely, increasing S and N deposition resulted in a 352, 269, 250 and 285% increase in mean critical load exceedances for each respective harvest scenario. The elevated exceedances under the increased acid deposition scenario are a result of the critical load values remaining the same regardless of acid deposition. With the decrease in acid deposition by a factor of 1.7 and 1.6 for S and N, respectively, the number of sites subject to positive exceedances under the no harvest scenario would drop from 3149 to 107, or 97% of the forested area.

Table 9.17. Descriptive statistics for critical acid load exceedances (eq ha^{-1} yr^{-1}) under baseline, decreased acid deposition and increased acid deposition estimates, for each harvest scenario, across Kejimkujik National Park, Nova Scotia.

	Critical Acid Load Exceedance (eq ha^{-1} yr^{-1})					
	Senst. Scenario	Mean	Std. Dev.	Std. Error	Min	Max
No harvest	Baseline	158	166	2.74	-282	481
	Acid Decrease	-175	166	2.73	-613	148
	Acid Increase	714	167	2.76	270	1038
Stem-Only	Baseline	207	168	2.77	-289	543
	Acid Decrease	-126	168	2.76	-619	208
	Acid Increase	763	169	2.79	262	1100
Full-tree Brown	Baseline	222	172	2.84	-301	809
	Acid Decrease	-111	172	2.83	-631	477
	Acid Increase	778	173	2.86	250	1362
Full-tree Green	Baseline	195	173	2.85	-367	737
	Acid Decrease	-138	172	2.84	-698	406
	Acid Increase	751	174	2.86	183	1290

Decreased acid deposition rates are predicted to result in mean base-cation accumulations throughout Kejimkujik Park, with a mean decrease in depletions by 211, 161, 151 and 172% for the no harvest, stem-only, full-tree brown and full-tree green harvest scenarios, respectively (Table 9.18). Increased acid deposition would increase the depletion rates by 353, 270, 252 and 287% for each respective harvest scenario. With increased acid deposition, all stands within Kejimkujik Park are predicted to experience base-cation depletions, with the severest depletions occurring on the most acidic substrates, as to be expected (Min = -987).

Table 9.18. Descriptive statistics for base-cation depletions (eq ha^{-1} yr^{-1}) under baseline, decreased acid deposition and increased acid deposition estimates, for each harvest scenario, across Kejimkujik National Park, Nova Scotia.

		Base Cation Depletion (eq ha^{-1} yr^{-1})				
	Senst. Scenario	Mean	Std. Dev.	Std. Error	Min	Max
No harvest	Baseline	-123	136	2.25	-390	238
	Acid Decrease	137	136	2.24	-120	518
	Acid Increase	-557	148	2.44	-842	-228
Stem-Only	Baseline	-161	138	2.28	-440	244
	Acid Decrease	99	137	2.27	-169	523
	Acid Increase	-595	151	1.48	-901	-221
Full-tree Brown	Baseline	-172	142	2.34	-531	254
	Acid Decrease	88	141	2.32	-313	533
	Acid Increase	-606	154	2.54	-987	-211
Full-tree Green	Baseline	-151	142	2.34	-484	310
	Acid Decrease	109	141	2.34	-267	589
	Acid Increase	-585	153	2.53	-933	-155

With decreased acid deposition rates, mean sustainable harvest rates would decrease by 9% for the harvesting only scenario, whereas a 56% increase is predicted for the harvesting with base-cation depletion scenario (Table 9.19). This somewhat contradictory result refers to (i) stands becoming more N-limited due to decreasing N deposition, and (ii) stands becoming less base-cation limited due to decreasing rates of base-cation depletion. Mean sustainable harvest rates would generally increase by <1% if base-cation depletion were not an issue, but would otherwise drop by 83%, and the critical load exceedances would increase accordingly.

Table 9.19. Descriptive statistics for sustainable harvest rates under baseline, decreased acid deposition and increased acid deposition estimates (m^3 ha^{-1} yr^{-1}) for harvesting, with and without base-cation depletion, across Kejimkujik National Park, Nova Scotia.

	Sustainable MAI (m^3 ha^{-1} yr^{-1})					
	Senst. Scenario	Mean	Std. Dev.	Std. Error	Min	Max
Harvesting Only	Baseline	4.67	1.84	0.03	1.38	9.95
	Acid Decrease	4.27	1.18	0.02	1.38	6.81
	Acid Increase	4.69	1.90	0.03	1.38	14.13
Harvesting & Depletion	Baseline	2.81	2.13	0.03	0.00	9.82
	Acid Decrease	4.37	1.27	0.02	0.75	6.81
	Acid Increase	0.48	1.20	0.02	0.00	7.25

5) K-exchange Ratio

A decrease in the K-exchange ratio from 10 to 5 resulted in a 91, 73, 69 and 77% decrease in mean base-cation depletion rates for the no harvest, stem-only, full-tree brown and full-tree green harvest scenarios, respectively (Table 9.20). Conversely, increasing the K-exchange ratio to 15 resulted in a 40, 33, 31 and 34% increase in base-cation depletion rates. A K-exchange ratio of 5 suggests that the affinity of acid cations is only 5 times greater than that of base cations. This equates to increased base-cation adsorption on the exchange sites, and therefore restricts the amount of base cations in solution relative to the acid cations. The K-exchange ratio of 15 has the opposite effect, forcing more base cations to remain in solution, thereby leading to higher rates of base-cation depletion. In general, K-exchange decreases in soils with increasing organic matter content towards 2, but increases towards 10 with increasing soil depth in correlation with the decreasing organic matter in that direction (Paul Arp, PhD, Personal communication). This indicates that pure mineral surfaces have a greater affinity for H^+ and Al^{3+} cations than base cations, and this is also consistent with the trend of increasing free Al content

with increasing soil depth, whereby surface –adsorbed Al^{3+} ions gradually change into surface bound Al oxides / hydroxides. In general, the choice of K-exchange = 10 is consistent with the notion of base-cation depletion via base-cation losses from the rooted portion of the soil into the subsoil and beyond.

Table 9.20. Descriptive statistics for base-cation depletions (eq ha^{-1} yr^{-1}) under baseline, K-exchange ratio of 5 and K-exchange ratio of 15 estimates, for each harvest scenario, across Kejimkujik National Park, Nova Scotia.

	Base Cation Depletion (eq ha^{-1} yr^{-1})					
	Senst. Scenario	Mean	Std. Dev.	Std. Error	Min	Max
No harvest	Baseline	-123	136	2.25	-390	238
	K Exchange = 5	-11	137	2.27	-282	332
	K Exchange = 15	-173	136	2.25	-436	200
Stem-Only	Baseline	-161	138	2.28	-440	244
	K Exchange = 5	-43	140	2.30	-316	337
	K Exchange = 15	-214	138	2.28	-493	206
Full-tree Brown	Baseline	-172	142	2.34	-531	254
	K Exchange = 5	-53	142	2.35	-389	345
	K Exchange = 15	-226	142	2.34	-616	217
Full-tree Green	Baseline	-151	142	2.34	-484	310
	K Exchange = 5	-35	142	2.24	-342	394
	K Exchange = 15	-203	142	2.35	-612	276

6) Mature DBH

Decreasing the mature DBH from 40cm to 20cm resulted in a 3 and 4% decrease in mean sustainable harvest rates for harvesting with and without depletion, respectively (Table 9.21). An increase to 60cm DBH resulted in a 2 and 3% increase in sustainable harvest rates with and without depletion, respectively. These relatively small changes are due to the trends in biomass compartment fractions (Chapter 4), which generally level off at 20cm DBH.

Table 9.21. Descriptive statistics for sustainable harvest rates under baseline, 20cm DBH and 60cm DBH estimates (m^3 ha^{-1} yr^{-1}) for harvesting, with and without base-cation depletion, across Kejimkujik National Park, Nova Scotia.

		Sustainable MAI (m^3 ha^{-1} yr^{-1})				
	Senst. Scenario	Mean	Std. Dev.	Std. Error	Min	Max
Harvesting Only	Baseline	4.67	1.84	0.03	1.38	9.95
	20cm DBH	4.52	1.80	0.03	1.30	9.73
	60cm DBH	4.75	1.86	0.03	1.42	10.08
Harvesting & Depletion	Baseline	2.81	2.13	0.03	0.00	9.82
	20cm DBH	2.70	2.10	0.03	0.00	9.51
	60cm DBH	2.89	2.15	0.03	0.00	10.00

LITERATURE CITED

Aherne, J., Mongeon, A., & Watmough, S. (2010). Temporal and spatial trends in precipitation chemistry in the Georgia Basin, British Columbia. *Journal of Limnology, 69*, 4-10.

Arp, P., Oja, T., & Marsh, M. (1996). Calculating critical S and N loads and current exceedances for upland forests in southern Ontario. *Canadian Journal of Forest Research, 26*, 696-709.

Bosman, B., Remacle, J., & Carnol, M. (2001). Element removal in harvested tree biomass: scenarios for critical loads in Wallonia, South Belgium. *Water, Air, and Soil Pollution, 1*, 153-167.

Federer, C., Hornbeck, J., Tritton, L., Martin, C., Pierce, R., & Smith, C. (1989). Long-term depletion of calcium and other nutrients in eastern U.S. forests. *Environmental Management, 13*, 593-601.

Huntington, T., Hooper, R., Johnson, C., Aulenbach, B., Cappellato, R., & Blum, A. (2000). Calcium Depletion in a Southeastern United States Forest Ecosystem. *Soil Science of America Journal, 64*, 1845-1858.

Iverson, L., & Prasad, A. (1998). Predicting the abundance of 80 tree species following climate change in the eastern United States. *Ecological Monographs, 68*, 465-485.

Koseva, I., Watmough, S., & Aherne, J. (2010). Estimating base-cation weathering rates in Canadian forest soils using a simple texture-based model. *Biogeochemistry, 101*, 183-196.

Lawrence, G., David, M., Bailey, S., & Shortle, W. (1997). Assessment of soil calcium status in red spruce forests in the northeastern United States. *Biogeochemistry, 38*, 19-39.

Li, H., & McNulty, S. (2007). Uncertainty analysis on simple mass balance model to calculate critical loads for soil acidity. *Environmental Pollution, 149*, 315-326.

Lorimer, C. (2001). Historical and ecological roles of disturbance in eastern North American forests: 9,000 years of change. *Wildlife Society Bulletin, 29*, 425-439.

Mroz, G., Jurgenson, M., & Frederick, D. (1985). Soil nutrient changes following whole tree harvesting on three northern hardwood sites. *Soil Science Society of America Journal, 49*, 1552-1557.

Ouimet, R., Arp, P., Watmough, S., Aherne, J., & Demerchant, I. (2006). Determination and mapping of critical loads of acidity and exceedances for upland forest soils in Eastern Canada. *Water, Air and Soil Pollution, 172*, 57-66.

Ouimet, R., Duchesne, L., Houle, D., & Arp, P. (2001). Critical loads and exceedances of acid deposition and associated forest growth in the northern hardwood and boreal coniferous forests in Quebec, Canada. *Water, Air, and Soil Pollution, 1*, 119-134.

Schroth, A., Friedland, A., & Bostick, B. (2007). Macronutrient Depletion and Redistribution in Soils under Conifer and Northern Hardwood Forests. *Soil Science Society of America Journal, 71*, 457-468.

Whitfield, C., Watmough, S., Aherne, J., & Dillon, P. (2006a). A comparison of weathering rates for acid-sensitive catchments in Nova Scotia, Canada and their impacts on critical load calculations. *Geoderma, 136*, 899-911.

Yanai, R., Blum, J., Hamburg, S., Arthur, M., Nezat, C., & Siccama, T. (2005). New Insights into Calcium Depletion in Northeastern Forests. *Journal of Forestry*, 14-20.

Yanni, S., K, K., Clair, T., & Arp, P. (2000). Fog and acidification impacts on ion budgets of basins in Nova Scotia, Canada. *Journal of the American Water Resources Association, 36*, 619-631.

CHAPTER 10

THESIS SUMMARY, ORIGINAL CONTRIBUTIONS, RECOMMENDATIONS AND CONCLUSION

THESIS SUMMARY

A method was established to assess nutrient-related sustainability of biomass harvesting across the province of Nova Scotia using current data layers informing about forest inventory (stand cover type, species composition, age and stand volume), soils (Canadian Soil Classification System, by soil series), climate (mean annual temperature), atmospheric deposition (N, S, Ca, Mg, K) and geological substrate according to local bedrock type. This was accomplished by:

1. Defining the conceptual background and reviewing the published literature concerning biogeochemical cycling of nutrients as they relate to long-term forest harvest sustainability (Chapter 2);

2. Reviewing published stem-biomass equations based on stem diameter at breast height, and presenting an alternative method of predicting wood-density correct stem biomass using traditional volume estimates (Chapter 3);

3. Projecting compartment-specific biomass (bark, stem-wood, branch and foliage) per tree species, based on (i) wood-density correct stem biomass estimates from Chapter 3, and (ii) species- and compartment-specific biomass partitioning coefficients (Chapter 4);

4. Reviewing and comparing published tree chemistry datasets, and developing a lookup table for the N, K, Ca and Mg concentrations per biomass compartment (Chapter 5);

5. Compiling and analyzing chemical and physical soil characteristics pertinent to assessing soil-based nutrient availabilities, such as soil rooting depth, texture (sand, silt and clay content), bulk density, organic matter content, coarse fragment content, cation exchange capacity and base saturation, as well as ensuring complete geospatial coverage for each characteristic across all Nova Scotia soil units (Chapter 6);

6. Developing the GIS-based Biomass Decision Support Tool to quantify, model and map stand-level harvest sustainability to avoid incurring N, Ca, Mg, K deficiencies due to over-harvesting, and within the context of environmental base-cation depletion (Chapter 7);

7. Presenting the Biomass Decision Support Tool's spatial and aspatial structures and components in order to (i) develop outputs for landscape-level visualization, and (ii) probe the inner workings of the model at the stand level, by way of a dynamically linked spread-sheet calculator (Chapter 8);

8. Analyzing the Biomass Decision Support Tool modelling and mapping results, with attention to model sensitivity, and model validation (Chapter 9).

ORIGINAL CONTRIBUTION

This thesis establishes a GIS-based biogeochemical framework for quantifying the long-term, stand-level sustainability of forest biomass harvesting, based on the mass balance (supply vs. demand) of primary, growth-limiting macronutrients (N, Ca, Mg, K). Several original contributions were needed to develop the framework, such as:

1. Establishing a method to estimate species-specific stem biomass projections across a broad range of diameter classes which are also consistent with well-established wood density expectations (Chapter 3);

2. Deriving compartment-specific biomass estimates for foliage, branches, bark and stem-wood from corrected stem biomass projections for all tree species across Nova Scotia (Chapter 4);

3. Applying the Sprengel-Liebig Law of the Minimum to determine nutrient sustainable harvest levels within the GIS-based forest inventory context, as well as establishing nutrient ratios as they relate to uptake by tree for modelling purposes.

4. Developing and using pedotransfer functions to ensure that the existing soil database for Nova Scotia is complete for deriving nutrient-sustainable forest biomass harvest levels across the province (Chapter 6);

5. Using the cartographic depth-to-water mapping method to redraw all upland-lowland soil boundaries across Nova Scotia, and to ensure that this information is also consistent with all flow channels, coast lines (lakes, ocean, as well as inland and off-shore islands), and the current spatial wetland inventory (Chapter 6);

6. Establishing a method to predict long-term sustainable harvest rates using current nutrient input-output mass balance procedures (Chapter 7);

7. Calculating critical acid loads and exceedances across Nova Scotia using a species-specific nutrient uptake and export approach, under a no base-cation depletion scenario (Chapter 7);

8. Assessing the sustainability of biomass harvesting based on 3 generalized scenarios (stem-only, full-tree brown, full-tree green) assuming complete removal (clear-cut) of each corresponding biomass compartment (Chapter 7);

9. Establishing a method to estimate stand-level base-cation depletions and relating these depletions to forest biomass harvest sustainability (Chapter 7);

10. Developing an aspatial sustainability model which allows the user to (i) inspect single spatial model stand outputs at a time, (ii) determine sustainable harvest rates based on user-defined harvest prescriptions, and (iii) make adjustments to model variables as needed, based on field verified data where conditions require additional attention (Chapter 8).

RECOMMENDATIONS

The BDST is an open framework model that, theoretically, can be applied to any jurisdiction, assuming the necessary input data is available. Although model outputs were determined using the best data currently available, the various spatial resolutions of the input data sources may not capture enough accuracy to allow stand level harvest analysis and design for management purposes. It is therefore recommended that all variables be

reviewed for stand specific analysis, and that improved data layers be incorporated into the BDST as they become available. Additionally, various assumptions and limitations were required in order to simplify the simulation of natural processes that pertain to nutrient accumulation, uptake, depletion, and harvesting. The following section details recommendations regarding the various model assumptions and limitations expressed throughout this thesis.

1. The wood-density corrected stem biomass projections should be extended to all species for which diameter-based biomass equations have been reported, as it is evident that these statistically-derived equations overestimate stem biomass for DBH >40cm, and are also density incorrect when DBH is quite small, i.e. < 5 cm (Neumann & Jandl, 2005; Jenkins *et al.*, 2003).

2. The relationship between nutrient concentrations and tree age should be further investigated. Within the BDST, all nutrient- and compartment-specific concentrations are assumed to remain static regardless of age, but this can be adjusted by converting the simple look-up tables by nutrient, species and tree compartment into age-dependent concentration functions (see Augusto *et al.*, 2008).

3. The relationship between nutrient uptake and nutrient availability within the soil requires further investigation. Within the BDST it is assumed that nutrient uptake is fixed at set rates for ideal mean annual biomass growth. In nature, nutrient uptake likely diminishes as nutrient availability decreases, and this would

especially be the case once primary macronutrient sources become exhausted (Lajtha, 1994).

4. While the N, K, and Mg concentrations are highly correlated to one another across species and tree compartments, this is not the case for Ca (Chapter 4). This element is known to be less mobile within plant tissues (Likens *et al.*, 1998), and therefore accumulates more easily in woody biomass than N and K, particularly for deciduous species (Arthur *et al.*, 1999). To what extent the apparent luxurious consumption of Ca is beneficial to tree growth remains to be explored from a physiological perspective. From an ecological perspective, luxurious consumption is of general benefit by facilitating overall on-site Ca retention, thereby stemming site-specific losses due to base-cation depletion and subsequent soil leaching. Excessive forest biomass harvesting, however, would negate these positive effects to some extent.

5. The current method of accounting for dry deposition assumes a fixed ratio between dry and wet deposition for N and base cations. In reality, dry deposition rates of atmospheric constituents are highly dependent on the absence or presence of the forest cover (hardwoods or conifers), and canopy roughness in particular (Lovett, 1994). The current dry deposition estimates most likely do not reflect the rate of actual dry deposition across Nova Scotia, which would be dictated by the geospatial distribution of forest cover and soil types (see Wesely, 1967; Wesely & Hicks, 2000).

6. Quantifying processes such as N fixation (Cleveland *et al.,* 1999), immobilisation (Berntson & Aber, 2000) and nitrification (Vitousek *et al.,* 1982) require special attention. Within the above model, it is assumed that all N is either subject to uptake, or subject to nitrate leaching. Net immobilization of N by soil organic matter together with N fixation is assumed to be negligible (Nasr *et al.,* 2010; Chapter 2). At present, these processes are not readily quantified because there is insufficient information to do so across the many site- and species-specific conditions and related upland-to-lowland N conversion and transformation gradients.

7. The acid cation - base-cation exchange ratio (K_{exch}) is currently set at 10 in order to reflect the overall preference of soil surfaces for acid cation (H^+, Al^{3+}) over base-cation (Ca^{2+}, Mg^{2+}, K^+) adsorption. The choice of K_{exch} = 10 is currently based on an as of yet unpublished ion-exchange experimentation within soil layers derived from podsolic and brunisolic soils (Paul Arp, personal communication). In reality, the acid-base-cation exchange is a complex phenomenon, which would depend on the relative concentrations of each ion pair (e.g., H^+-Ca^{2+}, Mg^{2+}-Ca^{2+}, Al^{3+}-K^+, etc.) within the soil, as well as soil pH, and clay and organic matter contents. A number of methods for determining soil exchange ratios for quantifying ion-pair exchange processes have been developed (see Kerr, 1928; Vanselow, 1932; Gapon, 1933). It is, however, beyond the scope of this work to compare the simple approach as proposed above with the more detailed literature approaches. In addition, the literature approaches remain ambivalent when applied to complex and highly variable organo-mineral surfaces

within the soil matrix, as these surfaces change from the forest floor and the varying types of soil mineral layers from the podsolic, to the brunisolic and regosolic. It is therefore suggested that a blanket approach for determining soil series-specific cation exchange ratios be investigated, as they relate to soil pH and/or mineral soil clay fractions.

8. The model should be expanded to include phosphorus (P). Information on the primary inputs and losses of P from forest soils is not readily available, while atmospheric deposition rates are generally very low (Anderson & Downing, 2006). However, while P is considered to be a macronutrient (Karl, 2000), overall annual uptake requirements are quite low relative to N, K, Ca and Mg (Gradowski & Thomas, 2006). In comparison, accumulated P pools are relatively large in forest soils on account of Al and Fe mitigated P retention (Cross & Schlesinger, 1995) and the required amounts for P uptake by the forest vegetation appears to be mobilized through mycorrhizal action (Bolan, 1991).

9. Also of general interest is the quantification of sodium (Na^+). While this element is not a growth dependent nutrient, it contributes to soil acid buffering as part of the soil weathering process, accounting for ~30% of total base-cation weathering (Whitfield *et al.*, 2006). Typically, Na uptake by vegetation is low (Peterson & Rolfe, 1982), and Na^+ tends to be readily leached within forest soils (Jordan *et al.*, 1986).

CONCLUSION

The Biomass Decision Support Tool framework allows for assessment of nutrient-related sustainability of forest operations across wide environmental gradients. Stand-level nutrient budgets are calculated using various geospatial inputs, ultimately allowing for use within a forest management context. The suite of tools were primarily developed for:

i. determining which of the primary macronutrients (N, Ca, Mg, K) will likely become growth-limiting under specific harvest practices;

ii. calculating additional nutrient losses that may occur on top of potential harvest deficits due to atmospheric acid deposition and subsequent base-cation depletion;

iii. relating the demand-supply relationship to a sustainable rate of biomass harvesting based on site-specific nutrient budgets.

LITERATURE CITED

Anderson, K., & Downing, J. (2006). Dry and wet atmospheric deposition of nitrogen, phosphorus and silicon in an agricultural region. *Water, Air, and Soil Pollution, 176*, 351-374.

Arthur, M., Siccama, T., & Yanai, R. (1999). Calcium and magnesium in wood of northern hardwood forest species: relations to site characteristics. *Canadian Journal of Forest Research, 29*, 339-346.

Augusto, L., Meredieu, C., Bert, D., Trichet, P., Porte, A., & Bosc, A. (2008). Improving models of forest nutrient export with equations that predict the nutrient concentration of tree compartments. *Annals of Forest Science, 65*, 463-477.

Berntson, G., & Aber, J. (2000). Fast nitrate immobilization in N saturated temperate forest soils. *Soil Biology and Biochemistry, 32*, 151-156.

Bolan, N. (1991). A critical review on the role of mycorrhizal fungi in the uptake of phosphorus by plants. *Plant and Soil, 134*, 189-207.

Cleveland, C., Townsend, A., Schimel, D., Fisher, H., Howarth, R., Hedin, L., *et al.* (1999). Global patterns of terrestrial biological nitrogen (N_2) fixation in natural ecosystems. *Global Biogeochemical Cycles, 13*, 623-645.

Cross, A., & Schlesinger, W. (1995). A literature review and evaluation of the. Hedley fractionation: Applications to the biogeochemical cycle of soil phosphorus in natural ecosystems. *Geoderma, 64*, 197-214.

Gapon, E. (1933). On the theory of exchange adsorption in soils. *Journal of General Chemistry U.S.S.R, 3*, 144-152.

Gradowski, T., & Thomas, S. (2006). Phosphorus limitation of sugar maple growth in central Ontario. *Forest Ecology and Management, 226*, 104-109.

Jenkins, J., Chojnacky, D., Heath, L., & Birdsey, R. (2003). National-Scale Biomass Estimators for United States Tree Species. *Forest Science, 49*, 12-35(24).

Jordan, T., Correll, D., Peterjohn, W., & Weller, D. (1986). Nutrient flux in a landscape: the Rhode River Watershed and recieving waters. In D. Correll, *Watershed Research Perspectives* (pp. 57-75). D.C.: Smithsonian Institute Press.

Karl, D. (2000). Phosphorus, the staff of life. *Nature, 406*, 31-32.

Kerr, H. (1928). The nature of base exchange and soil acidity. *Journal of American Society of Agronomy, 20*, 309-316.

Lajtha, K. (1994). Nutrient uptake in eastern deciduous tree seedlings. *Plant and Soil, 160*, 193-199.

Likens, G., Driscoll, C., Buso, D., Siccama, T., Johnson, C., Lovett, G., et al. (1998). The biogeochemistry of calcium at Hubbard Brook. *Biogeochemistry, 41*, 89-173.

Lovett, G. (1994). Atmospheric Deposition of Nutrients and Pollutants in North America: An Ecological Perspective. *Ecological Applications, 4*, 630-650.

Nasr, M., Castonguay, M., Ogilvie, J., Raymond, B., & Arp, P. (2010). Modelling and mapping critical loads and exceedances for the Georgia Basin, British Columbia, using a zero base-cation depletion criterion. *Journal of Limnology, 69*, 181-192.

Neumann, M., & Jandl, R. (2005). Derivation of locally valid estimators of the aboveground biomass of Norway spruce. *European Journal of Forest Research, 124*, 125-131.

Peterson, D., & Rolfe, G. (1982). Nutrient Dynamics of Herbaceous Vegetation in Upland and Floodplain Forest Communities. *American Midland Naturalist, 107*, 325-339.

Vanselow, A. (1932). Equilibria of the base exchange reactions of bentonites, permutites, soil colloids and zeolites. *Soil Science, 33*, 95-113.

Vitousek, P., Gosz, J., Grier, C., Melillo, J., & Reiners, W. (1982). A comparitive analysis of potential nitrification and nitrate mobility in forest ecosystems. *Ecological Monographs, 52*, 155-177.

Wesely, M. (1967). Parameterization of surface resistances to gaseous dry deposition in regional-scale numerical models. *Atmospheric Environment, 23*, 1293-1304.

Wesely, M., & Hicks, B. (2000). A review of the current status of knowledge on dry deposition. *Atmospheric Environment, 34*, 2261-2282.

Whitfield, C., Watmough, S., Aherne, J., & Dillon, P. (2006a). A comparison of weathering rates for acid-sensitive catchments in Nova Scotia, Canada and their impacts on critical load calculations. *Geoderma, 136*, 899-911.

APPENDIX (I)

COMMON NAME, LATIN NAME AND SPECIES CODE FOR TREE SPECIES WITHIN THE NOVA SCOTIA FOREST INVENTORY

Common Name	Latin Name	Species Code
Austrian Pine	*Pinus nigra*	AP
Ash (Black and White)	*Fraxinus nigra / americana*	AS
Black Cherry	*Prunus serotina*	BC
Beech	*Fagus grandifolia*	BE
Balsam Fir	*Abies balsamea*	BF
Balsam Poplar	*Populus balsamifera*	BP
Black Spruce	*Picea mariana*	BS
Douglas Fir	*Pseudotsuga menziesii*	DF
Eastern White Cedar	*Thuja occidentalis*	EC
Eastern Hemlock	*Tsuga canadensis*	EH
European Larch	*Larix decidua*	EL
Gray Birch	*Betula populifolia*	GB
Intolerant Hardwood (RM, WB)	N/A	IH
Ironwood	*Ostrya virginiana*	IW
Japanese Larch	*Larix kaempferi*	JL
Jack Pine	*Pinus banksiana*	JP
Norway Spruce	*Picea abies*	NS
Other Hardwood	N/A	OH
Other Softwood	N/A	OS
Aspen - Large Tooth and Trembling	*Populus grandidentata / tremuloides*	PO or TA
Red Maple	*Acer rubrum*	RM
Red Oak	*Quercus rubra*	RO
Red Pine	*Pinus resinosa*	RP
Red Spruce	*Picea rubens*	RS
Sugar Maple	*Acer saccharum*	SM
Scots Pine	*Pinus sylvestris*	SP
Sitka Spruce	*Picea sitchensis*	SS
Tolerant Hardwood (SM, YB, BE, RO)	N/A	TH
Eastern Larch	*Larix laricina*	TL
Unclassified Species	N/A	UC
Unclassified Hardwood	N/A	UH
Unclassified Species	N/A	US
White Birch	*Betula papyrifera*	WB
White Elm	*Ulmus americana*	WE
Western Larch	*Larix occidentalis*	WL
White Pine	*Pinus strobus*	WP
White Spruce	*Picea glauca*	WS
Hybrid Larch	N/A	XL
Red and Black Spruce (Mixed stand)	N/A	XS
Yellow Birch	*Betula alleghaniensis*	YB

APPENDIX (II)

KER'S SPECIES-SPECIFIC BIOMASS COMPARTMENT PARAMETERS

(γ; Ker, 1980a, 1980b)

	Stem wood			Bark			Branch			Foliage			Total			Stem		
	γ_1	γ_2	c	γ_1	γ_2	c	γ_1	γ_2	c	γ_1	γ_2	c	γ_1	γ_2	C	γ_1	γ_2	c
BE	-2.0961	2.2956	1.01	-4.1698	2.1154	1.03	-3.5982	2.3708	1.13	-3.7607	1.6303	1.06	-1.6309	2.2538	1.01	-1.9797	2.2809	1.01
BF	-3.2027	2.4228	1.02	-4.4204	2.2391	1.06	-2.6293	1.7793	1.05	-2.7854	1.6737	1.05	-1.8337	2.1283	1.03	-2.9476	2.3932	1.02
BS	-3.2073	2.4743	1.01	-4.3913	2.1815	1.02	-2.7616	1.9421	1.04	-2.5387	1.7206	1.05	-1.7823	2.1777	1.02	-2.9601	2.4321	1.01
EH	-2.9095	2.3570	1.01	-4.2813	2.2660	1.03	-2.8376	1.9157	1.05	-3.0924	1.6829	1.04	-1.8223	2.1536	1.01	-2.6855	2.3418	1.01
TL	-3.0695	2.5050	1.01	-4.0854	2.0868	1.01	-4.0294	2.1727	1.06	-5.0986	1.9790	1.11	-2.3583	2.3572	1.01	-2.7985	2.4472	1.01
EC	-2.9565	2.2804	1.01	-4.6633	2.2228	1.02	-1.0525	1.0295	1.05	-1.5063	0.9629	1.04	-2.1643	2.1439	1.01	-2.7842	2.2706	1.01
WP	-3.5128	2.5979	1.03	-4.1854	2.1781	1.05	-2.6466	1.7086	1.08	-2.0241	1.6296	1.07	-1.8221	2.1420	1.03	-3.1855	2.5360	1.03
JP	-3.2143	2.5578	1.01	-3.9655	1.9916	1.01	-4.0101	2.2443	1.06	-4.2862	2.0512	1.08	-2.2136	2.3291	1.01	-2.9216	2.4883	1.01
RM	-2.5475	2.3795	1.02	-3.8218	2.1419	1.03	-4.0186	2.3506	1.06	-4.0486	1.6529	1.04	-2.0274	2.3199	1.01	-2.3065	2.3418	1.02
RP	-3.1049	2.4418	1.00	-4.1568	2.0701	1.01	-4.8438	2.4631	1.07	-4.4257	2.1220	1.04	-2.4684	2.3503	1.01	-2.8368	2.3892	1.00
RS	-3.2073	2.4743	1.01	-4.3913	2.1815	1.02	-2.7616	1.9421	1.04	-2.5387	1.7206	1.05	-1.7823	2.1777	1.02	-2.9601	2.4321	1.01
SM	-2.2792	2.3869	1.01	-3.8804	2.2684	1.03	-4.0484	2.3841	1.11	-4.1703	1.6990	1.04	-1.8329	2.3376	1.01	-2.0675	2.3603	1.01
TA	-3.1729	2.5325	1.01	-4.2765	2.4007	1.03	-4.9158	2.5992	1.09	-4.6192	1.8405	1.06	-2.6224	2.4827	1.01	-2.8857	2.5046	1.01
WA	-2.3689	2.3903	1.01	-3.9236	2.1762	1.03	-3.4591	2.1935	1.05	-4.1177	1.6932	1.04	-1.8740	2.3213	1.01	-2.1858	2.3649	1.01
WB	-2.7623	2.4931	1.01	-3.9298	2.2795	1.01	-4.4464	2.5073	1.11	-4.2579	1.8735	1.06	-2.2308	2.4313	1.01	-2.5071	2.4594	1.01
WS	-3.3668	2.4847	1.02	-4.5138	2.1547	1.03	-3.4995	2.1368	1.06	-3.2985	1.9103	1.05	-2.2662	2.2907	1.01	-3.1114	2.4370	1.02
YB	-2.4467	2.4369	1.01	-4.0633	2.3086	1.02	-3.5521	2.3585	1.14	-4.1049	1.7241	1.07	-1.8701	2.3666	1.01	-2.2673	2.4200	1.01

APPENDIX (III)

LAMBERT'S SPECIES-SPECIFIC BIOMASS COMPARTMENT PARAMETERS

(β; Lambert *et al.*, 2005)

	Stem wood		Bark		Branch		Foliage	
	β_1	β_2	β_1	β_2	β_1	β_2	β_1	β_2
AP	0.0564	2.4465	0.0188	2.0527	0.0033	2.7515	0.0212	2.0690
AS	0.1861	2.1665	0.0406	1.9946	0.0461	2.2291	0.1106	1.2277
BC	0.3743	1.9406	0.0679	1.8377	0.0796	2.0103	0.0840	1.2319
BE	0.1478	2.2986	0.0120	2.2388	0.0370	2.3680	0.0376	1.6164
BF	0.0534	2.4030	0.0115	2.3484	0.0070	2.5406	0.0840	1.6695
BP	0.0510	2.4529	0.0297	2.1131	0.0120	2.4165	0.0276	1.6215
BS	0.0477	2.5147	0.0153	2.2429	0.0278	2.0839	0.1648	1.4143
DF	0.0619	2.3821	0.0139	2.3282	0.0217	2.2653	0.0776	1.6995
EC	0.0654	2.2121	0.0114	2.1432	0.0335	1.9367	0.0499	1.7278
EH	0.0619	2.3821	0.0139	2.3282	0.0217	2.2653	0.0776	1.6995
EL	0.0625	2.4450	0.0174	2.1109	0.0196	2.2652	0.0801	1.4875
GB	0.0720	2.3885	0.0168	2.2569	0.0088	2.5689	0.0099	1.8985
IH	Average of RM and WB Biomass							
IW	0.1929	1.9672	0.0671	1.5911	0.0278	2.1336	0.0293	1.9502
JL	0.0625	2.4450	0.0174	2.1109	0.0196	2.2652	0.0801	1.4875
JP	0.0804	2.4041	0.0184	2.0703	0.0079	2.4155	0.0389	1.7290
NS	0.0359	2.5775	0.0116	2.3022	0.0283	2.0823	0.1601	1.4670
OH	0.0871	2.3702	0.0241	2.1969	0.0167	2.4807	0.0390	1.6229
OS	0.0648	2.3927	0.0162	2.1959	0.0156	2.2916	0.0861	1.6261
PO	0.0605	2.4750	0.0168	2.3949	0.0080	2.5214	0.0261	1.6304
RM	0.1014	2.3448	0.0291	2.0893	0.0175	2.4846	0.0515	1.5198
RO	0.1754	2.1616	0.0381	2.0991	0.0085	2.7790	0.0373	1.6740
RP	0.0564	2.4465	0.0188	2.0527	0.0033	2.7515	0.0212	2.0690
RS	0.0989	2.2814	0.0220	2.0908	0.0005	3.2750	0.0066	2.4213
SM	0.1315	2.3129	0.0631	1.9241	0.0330	2.3741	0.0393	1.6930
SP	0.0804	2.4041	0.0184	2.0703	0.0079	2.4155	0.0389	1.7290
SS	0.0989	2.2814	0.0220	2.0908	0.0005	3.2750	0.0066	2.4213
TH	Average of SM, BE, YB and RO Biomass							
TL	0.0625	2.4450	0.0174	2.1109	0.0196	2.2652	0.0801	1.4875
UC	0.0787	2.3702	0.0185	2.2159	0.0230	2.2678	0.0767	1.5720
UH	0.0871	2.3702	0.0241	2.1969	0.0167	2.4807	0.0390	1.6229
US	0.0648	2.3927	0.0162	2.1959	0.0156	2.2916	0.0861	1.6261
WB	0.0593	2.5026	0.0135	2.4053	0.0135	2.5532	0.0546	1.6351
WE	0.0402	2.5804	0.0073	2.4859	0.0401	2.1826	0.0750	1.3436
WL	0.0625	2.4450	0.0174	2.1109	0.0196	2.2652	0.0801	1.4875
WP	0.0997	2.2709	0.0192	2.2038	0.0056	2.6011	0.0284	1.9375
WS	0.0359	2.5775	0.0116	2.3022	0.0283	2.0823	0.1601	1.4670
XL	0.0625	2.4450	0.0174	2.1109	0.0196	2.2652	0.0801	1.4875
XS	Average of RS and BS Biomass							
YB	0.1932	2.1569	0.0192	2.2475	0.0305	2.4044	0.1119	1.3973

As suggested by Lambert *et al.*, (2005), UH and OH were calculated using "Hardwood" parameters, US and OS were calculated using "Softwood" parameters, UC was calculated using "All" parameters

APPENDIX (IV)

SPECIES-SPECIFIC STEM-WOOD DENSITIES

(Gonzalez, 1990)

Species	Density (ovendry; tonnes/m3)	Data source
AP	0.419	Same as RP
AS	0.650	Jessome, 1977
BC	0.623	Jessome, 1977
BE	0.705	Jessome, 1977
BF	0.367	Jessome, 1977
BP	0.416	Jessome, 1977
BS	0.445	Jessome, 1977
DF	0.524	Gohre, 1955
EC	0.308	Jessome, 1977
EH	0.447	Jessome, 1977
EL	0.544	Same as TL
GB	0.588	Same as WB
IH	0.587	Average (WB, RM)
IW	0.786	Jessome, 1977
JL	0.544	Same as TL
JP	0.454	Jessome, 1977
NS	0.393	Same as WS
OH	0.617	Average of all hardwoods
OS	0.417	Average of all softwoods
RM	0.586	Jessome, 1977
RO	0.655	Jessome, 1977
RP	0.419	Hejja, 1986
RS	0.425	Jessome, 1977
SM	0.702	Jessome, 1977
SP	0.454	Same as JP
SS	0.417	Hejja, 1986
TA	0.424	Jessome, 1977
TH	0.678	Average (BE, SM, RO, YB)
TL	0.544	Jessome, 1977
UC	0.526	Average of all species
UH	0.617	Same as OH
US	0.417	Same as OS
WB	0.588	Jessome, 1977
WE	0.617	Jessome, 1977
WL	0.640	Jessome, 1977
WP	0.365	Hejja, 1986
WS	0.393	Jessome, 1977
XL	0.544	Same as TL
XS	0.435	Average (BS, RS)
YB	0.649	Jessome, 1977

APPENDIX (V)

TREE CHEMISTRY DATABASE SEARCH CRITERIA

(Pardo *et al.*, 2004)

Average N, K, Ca and Mg concentrations in foliage, branch, bark and stem-wood compartments of 16 tree species (BF, BS, RS, TL, EH, EC, WP, RP, JP, RM, SM, BE, YP, WB, WS, and PO) were obtained. The results were limited so that only values from healthy trees, of all ages, within north-eastern United States and eastern Canada were returned.

Microsoft Access query:

1) Tables selected: **Nutrients**, **Site**, and **Species**.

2) From **Species**, *Species_Name* was selected.

3) From **Site**, *Forest_Health* and *Region*.

4)From **Nutrients**, *Bark_N_%, Bark_K_%, Bark_Ca_%, Bark_Mg_%, Bole_N_%, Bole_K_%, Bole_Ca_%, Bole_Mg_%, Branch_N_%, Branch_K_%, Branch_Ca_%, Branch_Mg_%, Foliage_N_%, Foliage_K_%, Foliage_Ca_%,* and *Foliage_Mg_%*.

5) All species stated above were entered in criteria row of **Species**, *Species_Name*.

6) In the criteria row of **Site** *Forest_Health*, "<>1" was entered which selects for all stands other than those declining in forest health.

7) In the criteria row of **Site** *Region*, "*eastern Canada", "central Canada", "northeast", "mid Atlantic",* and "*north central"* were selected.

Results were exported into Excel and summarized in Pivot Tables.

APPENDIX (VI)

SPECIES-SPECIFIC BIOMASS COMPARTMENT NUTRIENT CONCENTRATIONS (%) FOR THE 40 SPECIES WITHIN THE NOVA SCOTIA FOREST INVENTORY

	Bark N	Bark K	Bark Ca	Bark Mg	Branch N	Branch K	Branch Ca	Branch Mg	Foliage N	Foliage K	Foliage Ca	Foliage Mg	Bole N	Bole K	Bole Ca	Bole Mg
AP	0.3100	0.0878	0.7748	0.0459	0.3288	0.0962	0.5488	0.0493	1.1504	0.3635	0.4198	0.0877	0.0820	0.0237	0.1090	0.0193
AS	0.4332	0.1985	2.2059	0.0468	0.3092	0.1704	0.4655	0.0421	1.9555	1.2883	1.4067	0.3070	0.0885	0.0803	0.1233	0.0204
BC	0.7600	0.4800	2.6893	0.1100	0.1850	0.1688	0.1042	0.0404	2.5615	1.1000	1.1650	0.3517	0.2400	0.2600	0.0751	0.0300
BE	0.7500	0.2200	2.8080	0.0500	0.3000	0.1200	0.4700	0.0300	2.1640	0.8905	0.6664	0.1559	0.1100	0.0700	0.0716	0.0200
BF	0.4616	0.2566	0.7394	0.0636	0.3919	0.2569	0.3812	0.0505	1.2746	0.4222	0.7497	0.0806	0.0918	0.0921	0.0823	0.0204
BP	0.2267	0.1321	0.6053	0.0529	0.2543	0.1392	0.4890	0.0581	1.8000	0.7100	0.7500	0.2700	0.0654	0.0562	0.1123	0.0172
BS	0.2400	0.1542	0.9966	0.0555	0.2592	0.1352	0.3996	0.0430	0.8372	0.4238	0.7045	0.0893	0.0630	0.0342	0.0874	0.0138
DF	0.2673	0.1523	0.7368	0.0295	0.2850	0.0997	0.4410	0.0438	1.1570	0.6573	0.6415	0.1251	0.0770	0.0868	0.0704	0.0112
EC	0.2800	0.0800	2.4500	0.0700	0.2400	0.0470	1.1400	0.0450	0.8300	0.2100	1.4700	0.1070	0.0780	0.0324	0.0516	0.0101
EH	0.2673	0.1523	0.7368	0.0295	0.2850	0.0997	0.4410	0.0438	1.1570	0.6573	0.6415	0.1251	0.0770	0.0868	0.0704	0.0112
EL	0.3177	0.2687	0.7983	0.0517	0.2720	0.2007	0.3250	0.0380	1.8340	0.7783	0.4287	0.1163	0.0590	0.0623	0.0703	0.0180
GB	0.3639	0.1201	0.6846	0.0413	0.3913	0.1594	0.4413	0.0533	1.9165	0.8850	0.7222	0.2247	0.0924	0.0514	0.0775	0.0185
IH	0.3985	0.1593	0.9931	0.0441	0.3502	0.1649	0.4534	0.0477	1.8062	0.7736	0.7430	0.2144	0.0904	0.0659	0.0948	0.0195
IW	0.6080	0.2300	2.3100	0.0800	0.2560	0.1140	0.6900	0.0530	1.8357	0.8653	1.9093	0.2433	0.1200	0.2060	0.1960	0.0410
JL	0.3177	0.2687	0.7983	0.0517	0.2720	0.2007	0.3250	0.0380	1.8340	0.7783	0.4287	0.1163	0.0590	0.0623	0.0703	0.0180
JP	0.2445	0.1280	0.4404	0.0406	0.2954	0.1559	0.2171	0.0397	1.1115	0.3863	0.3763	0.0893	0.0678	0.0440	0.0676	0.0135
NS	0.3560	0.2418	1.2949	0.0666	0.3750	0.2503	0.5851	0.0514	1.0526	0.5247	1.0532	0.0919	0.0654	0.0343	0.0943	0.0101
OH	0.4843	0.2097	1.6522	0.0586	0.3366	0.1711	0.5348	0.0517	2.0060	0.8850	0.9635	0.2289	0.1109	0.0977	0.1105	0.0217
OS	0.2829	0.1600	0.6872	0.0459	0.2890	0.1572	0.3539	0.0417	1.0714	0.4548	0.5065	0.0893	0.0648	0.0432	0.0702	0.0126
PO	0.4497	0.2631	1.2038	0.1053	0.5046	0.2767	0.9736	0.1156	2.1136	0.7813	1.0599	0.2082	0.1298	0.1119	0.2239	0.0343
RM	0.4332	0.1985	1.3016	0.0468	0.3092	0.1704	0.4655	0.0421	1.6958	0.6827	0.7638	0.2041	0.0885	0.0803	0.1121	0.0204
RO	0.3958	0.1290	2.4273	0.0380	0.3696	0.2520	0.9020	0.0663	2.1250	0.9757	0.6997	0.1728	0.1257	0.1093	0.0557	0.0057
RP	0.3100	0.0878	0.7748	0.0459	0.3288	0.0962	0.5488	0.0493	1.1504	0.3635	0.4198	0.0877	0.0820	0.0237	0.1090	0.0193
RS	0.2773	0.1635	0.6685	0.0445	0.2738	0.1826	0.3381	0.0442	1.0187	0.5446	0.4084	0.0970	0.0640	0.0220	0.0690	0.0096
SM	0.5114	0.3119	2.2280	0.0600	0.3365	0.2101	0.6313	0.0390	1.9486	0.7551	0.9337	0.1537	0.0976	0.0691	0.1301	0.0198
SP	0.2445	0.1280	0.4404	0.0406	0.2954	0.1559	0.2171	0.0397	1.1115	0.3863	0.3763	0.0893	0.0678	0.0440	0.0676	0.0135
SS	0.2773	0.1635	0.6685	0.0445	0.2738	0.1826	0.3381	0.0442	1.0187	0.5446	0.4084	0.0970	0.0640	0.0220	0.0690	0.0096
TH	0.5561	0.1963	2.1229	0.0476	0.3665	0.1738	0.6041	0.0429	2.1467	0.9113	0.8155	0.1845	0.1090	0.0729	0.0819	0.0152
TL	0.3177	0.2687	0.7983	0.0517	0.2720	0.2007	0.3250	0.0380	1.8340	0.7783	0.4287	0.1163	0.0590	0.0623	0.0703	0.0180
UC	0.3834	0.1958	1.2062	0.0535	0.3176	0.1711	0.4674	0.0470	1.5904	0.6944	0.7455	0.1571	0.0866	0.0688	0.0891	0.0171
UH	0.2641	0.1642	0.7477	0.0386	0.2382	0.1456	0.3093	0.0329	1.1821	0.5052	0.4671	0.1004	0.0554	0.0410	0.0642	0.0122
US	0.2281	0.1221	0.6186	0.0391	0.2234	0.1192	0.3292	0.0365	0.9466	0.3792	0.4233	0.0852	0.0527	0.0364	0.0662	0.0114
WB	0.3639	0.1201	0.6846	0.0413	0.3913	0.1594	0.4413	0.0533	1.9165	0.8645	0.7222	0.2247	0.0924	0.0514	0.0775	0.0185
WE	0.4332	0.1985	1.3016	0.0468	0.3092	0.1704	0.4655	0.0421	1.6958	0.6827	0.7638	0.2041	0.0885	0.0803	0.1121	0.0204
WL	0.3177	0.2687	0.7983	0.0517	0.2720	0.2007	0.3250	0.0380	1.8340	0.7783	0.4287	0.1163	0.0590	0.0623	0.0703	0.0180
WP	0.3544	0.1473	0.4223	0.0613	0.4088	0.1946	0.3034	0.0573	1.2779	0.4469	0.2827	0.1154	0.0780	0.0324	0.0516	0.0101
WS	0.3560	0.2418	1.2949	0.0666	0.3750	0.2503	0.5851	0.0514	1.0526	0.5247	1.0532	0.0919	0.0654	0.0343	0.0943	0.0101
XL	0.3177	0.2687	0.7983	0.0517	0.2720	0.2007	0.3250	0.0380	1.8340	0.7783	0.4287	0.1163	0.0590	0.0623	0.0703	0.0180
XS	0.2587	0.1589	0.8326	0.0500	0.2665	0.1589	0.3689	0.0436	0.9279	0.4842	0.5564	0.0932	0.0635	0.0281	0.0782	0.0117
YB	0.5672	0.1243	1.0283	0.0423	0.4600	0.1130	0.4130	0.0363	2.3490	1.0241	0.9624	0.2558	0.1026	0.0433	0.0701	0.0155

	Comments
AP	Same as RP
AS	Same as RM
BC	Same as Pin Cherry except Bark, Stemwood and Branch Ca, Branch N, and Foliage N, Ca, Mg and K
BP	Average of TA and LTA
DF	Same as EH
EL	Same as TL
GB	Same as WB except Foliage K
IH	Average of WB and RM
JL	Same as TL
NS	Same as WS
OH	Average of all hardwood species
OS	Average of all softwood species
PO	Same as Trembling Aspen
SP	Same as JP
SS	Same as RS
TH	Average of YB, RO, SM and BE
UC	Same as OH
UH	Same as OS
US	Average of all species
WE	Same as RM
WL	Same as TL
XL	Same as TL
XS	Average of RS and BS

APPENDIX (VII)

CHRONOLOGICAL LISTING OF NOVA SCOTIA SOIL SURVEYS

Cann, D.B., Hilchey, J.D., & Smith, G.R. 1954. Soil survey of Hants County, Nova Scotia. Nova Scotia Soil Survey Report No. 5. Canadian Department of Agriculture. 65pp.

Cann, D.B. & Hilchey, J.D. 1954. Soil survey of Antigonish County, Nova Scotia. Nova Scotia Soil Survey Report No. 6. Canadian Department of Agriculture. 54pp.

Cann, D.B. & Hilchey, J.D. 1958. Soil survey of Lunenburg County, Nova Scotia. Nova Scotia Soil Survey Report No. 7. Canadian Department of Agriculture. 48pp.

Cann, D.B. & Hilchey, J.D. 1959. Soil survey of Queens County, Nova Scotia. Nova Scotia Soil Survey Report No. 8. Canadian Department of Agriculture. 48pp.

Hilchey, J.D., Cann, D.B., & MacDougall, J.I. 1960. Soil survey of Yarmouth County, Nova Scotia. Nova Scotia Soil Survey Report No. 9. Canadian Department of Agriculture. 47pp.

MacDougall, J.I., Cann, D.B., & Hilchey, J.D. 1961. Soil survey of Shelburne County, Nova Scotia. Nova Scotia Soil Survey Report No. 10. Canadian Department of Agriculture. 38pp.

Hilchey, J.D., Cann, D.B., & MacDougall, J.I. 1962. Soil survey of Digby County, Nova Scotia. Nova Scotia Soil Survey Report No. 11. Canadian Department of Agriculture. 58pp.

Cann, D.B., MacDougall, J.I., & Hilchey, J.D. 1963. Soil survey of Cape Breton Island, Nova Scotia. Nova Scotia Soil Survey Report No. 12. Canadian Department of Agriculture. 85pp.

MacDougall, J.I., Cann, D.B., & Hilchey, J.D. 1963. Soil survey of Halifax County, Nova Scotia. Nova Scotia Soil Survey Report No. 13. Canadian Department of Agriculture. 53pp.

Hilchey, J.D., Cann, D.B., & MacDougall, J.I. 1964. Soil survey of Guysborough County, Nova Scotia. Nova Scotia Soil Survey Report No. 14. Canadian Department of Agriculture. 55pp.

Cann, D.B., MacDougall, J.I., & Hilchey, J.D. 1965. Soil survey of Kings County, Nova Scotia. Nova Scotia Soil Survey Report No. 15. Canadian Department of Agriculture. 97pp.

MacDougall, J.I., & Nowl J.L. & Hilchey, J.D. 1969. Soil survey of Annapolis County, Nova Scotia. Nova Scotia Soil Survey Report No. 16. Canadian Department of Agriculture. 84pp.

Nowl J.L, & MacDougall, J.I. 1973. Soil survey of Cumberland County, Nova Scotia. Nova Scotia Soil Survey Report No. 17. Canadian Department of Agriculture. 133pp.

Webb, K.T. 1990. Soils of Pictou County, Nova Scotia. Nova Scotia Soil Survey Report No. 18. Research Branch, Agriculture Canada. 183pp.

Webb, K.T., Thompson, R.L., Beke, G.J., & Nowland, J.L. 1991. Soils of Colchester County, Nova Scotia. Nova Scotia Soil Survey Report No. 19. Research Branch, Agriculture Canada. 201pp.

APPENDIX (VIII)

NOVA SCOTIA ECOLOGICAL LAND CLASSIFICATION BEDROCK UNIT SUBSTRATE CLASSES

Bedrock Unit Code	Bedrock Unit Description	Substrate Class	Comments
SIM Acid	Acid sedimentary, igneous, metamorphic (SIM) rocks	1	Includes granites, sandstones, quartzites, conglomerates, gneisses
Acid/SS	SIM Acid rocks plus shales/slates	1 or 2	Substrate class is dependant on parent material texture; see below
Shales/Slate	Shales and slates	2	
Medium Ign	Medium igneous rocks	2	Includes diorite and andesite
Medium Ign/SS	Medium igneous rocks plus shales/slates	2	
Basic Ign	Basic igneous rocks	3	Includes basalt and gabbro
Basic Ign/SS	Basic igneous rocks plus shales/slates	3	
Marble	Marble	3	
Lime/Gyp	Limestone or gypsum	4	
Lime/Gyp/SS	Limestone or gypsum plus shales/slates	4	
Karst	Karst	4	Assumed limestone or gypsum

Acid/SS Parent Material Texture	Substrate Class
Very Coarse; Moderately Coarse; Coarse	1
Moderate; Moderately Fine; Fine; Very Fine	2

APPENDIX (IX)

LANDFORM DEPENDENT SOIL PARENT MATERIAL WEATHERING CLASSES

Soil Series	Parent Material Landform	Weathering Class
Acadia	Alluvial	3
Bridgeville	Alluvial	3
Chaswood	Alluvial	3
Chegoggin	Alluvial	3
Cherryfield	Alluvial	3
Cumberland	Alluvial	3
Mossman	Alluvial	3
Stewiacke	Alluvial	3
Avonport	Fluvial	2
Canning	Glaciofluvial	1
Cornwallis	Glaciofluvial	1
Gulliver	Glaciofluvial	3
Hebert	Glaciofluvial	1
Kingsport	Glaciofluvial	1
LaHave	Glaciofluvial	2
Medway	Glaciofluvial	1
Millar	Glaciofluvial	1
Nictaux	Glaciofluvial	1
Torbrook	Glaciofluvial	1
Truro	Glaciofluvial	1
Fash	Lacustrine	2
Lawrencetown	Lacustrine	2
Comeau	Marine	2
Digby	Marine	2
Meteghan	Marine	2

APPENDIX (X)

BIOMASS COMPARTMENT AND NUTRIENT CONCENTRATION LOOK-UP TABLE

Species	Biomass Compartment	A coefficient	B coefficient	N (mg/kg)	K (mg/kg)	Ca (mg/kg)	Mg (mg/kg)	Stem Density (tonnes/m^3)
AP	Stem-wood	0.8529	0.0231	819.67	236.69	1090.19	193.08	0.419
	Bark	0.2843	-0.3707	3100.37	877.69	7747.69	459.27	0.419
	Branch	0.0499	0.3281	3288.15	961.54	5488.46	492.50	0.419
	Foliage	0.3206	-0.3544	11504.36	3634.74	4198.16	877.37	0.419
AS	Stem-wood	0.8439	0.0164	885.00	802.60	1233.00	204.20	0.650
	Bark	0.1841	-0.1555	4331.67	1985.00	22059.00	468.33	0.650
	Branch	0.2091	0.0790	3091.82	1704.44	4655.10	421.25	0.650
	Foliage	0.5015	-0.9224	19554.55	12883.33	14066.67	3070.00	0.650
BC	Stem-wood	0.8548	0.0108	2400.00	2600.00	751.00	300.00	0.623
	Bark	0.1551	-0.0921	7600.00	4800.00	26893.00	1100.00	0.623
	Branch	0.1818	0.0805	1850.00	1688.40	1042.00	403.80	0.623
	Foliage	0.1918	-0.6979	25615.00	11000.00	11649.88	3516.67	0.623
BE	Stem-wood	0.9267	0.0036	1100.00	700.00	716.25	200.00	0.705
	Bark	0.0752	-0.0562	7500.00	2200.00	28080.00	500.00	0.705
	Branch	0.2320	0.0730	3000.00	1200.00	4700.00	300.00	0.705
	Foliage	0.2357	-0.6786	21640.00	8904.62	6663.85	1559.00	0.705
BF	Stem-wood	0.8257	0.0080	917.94	921.38	823.25	203.88	0.367
	Bark	0.1778	-0.0466	4615.88	2566.47	7394.12	636.47	0.367
	Branch	0.1082	0.1456	3919.41	2568.82	3811.76	504.71	0.367
	Foliage	0.8350	-0.7255	12745.50	4222.00	7496.50	805.50	0.367
BP	Stem-wood	0.7385	0.0409	1204.12	1061.82	1551.98	298.92	0.416
	Bark	0.4301	-0.2989	3881.10	2680.35	10281.29	879.04	0.416
	Branch	0.1738	0.0045	4560.71	2928.64	8650.52	933.21	0.416
	Foliage	0.3997	-0.7905	18000.00	7100.00	7500.00	2700.00	0.416
BS	Stem-wood	0.8172	0.0248	630.00	342.00	874.00	137.50	0.445
	Bark	0.2621	-0.2470	2400.00	1542.00	9966.00	555.00	0.445
	Branch	0.4762	-0.4060	2592.00	1352.00	3996.00	430.00	0.445
	Foliage	2.8232	-1.0756	8371.67	4238.33	7045.00	893.33	0.445
DF	Stem-wood	0.8195	0.0082	770.00	868.33	704.45	111.93	0.524
	Bark	0.1840	-0.0457	2673.33	1522.50	7367.50	295.00	0.524
	Branch	0.2873	-0.1086	2850.00	996.67	4410.00	438.33	0.524
	Foliage	1.0274	-0.6744	11570.00	6573.00	6415.00	1251.25	0.524
EC	Stem-wood	0.8555	0.0079	779.75	323.67	515.50	101.00	0.308
	Bark	0.1491	-0.0610	2800.00	800.00	24500.00	700.00	0.308
	Branch	0.4382	-0.2675	2400.00	470.00	11400.00	450.00	0.308
	Foliage	0.6528	-0.4764	8300.00	2100.00	14700.00	1070.00	0.308
EH	Stem-wood	0.8195	0.0082	770.00	868.33	704.45	111.93	0.447
	Bark	0.1840	-0.0457	2673.33	1522.50	7367.50	295.00	0.447
	Branch	0.2873	-0.1086	2850.00	996.67	4410.00	438.33	0.447
	Foliage	1.0274	-0.6744	11570.00	6573.00	6415.00	1251.25	0.447
EL	Stem-wood	0.8575	0.0210	590.00	623.33	703.33	180.00	0.544
	Bark	0.2387	-0.3156	3176.67	2686.67	7983.33	516.67	0.544
	Branch	0.2689	-0.1613	2720.00	2006.67	3250.00	380.00	0.544
	Foliage	1.0990	-0.9390	18340.00	7783.33	4286.67	1163.33	0.544
GB	Stem-wood	0.8261	0.0155	923.76	514.48	774.90	184.81	0.588
	Bark	0.1928	-0.1161	3639.09	1200.91	6846.36	413.18	0.588
	Branch	0.1010	0.1959	3912.50	1594.17	4412.50	533.33	0.588
	Foliage	0.1136	-0.4745	19165.00	8850.00	7222.33	2247.33	0.588
IH	Stem-wood	0.8324	0.0153	904.38	658.54	947.70	194.50	0.587
	Bark	0.1876	-0.1223	3985.38	1592.95	9931.04	440.76	0.587
	Branch	0.1680	0.1057	3502.16	1649.31	4533.80	477.29	0.587
	Foliage	0.5657	-0.8213	18061.55	7736.10	7429.95	2144.04	0.587
IW	Stem-wood	0.8388	0.0253	1200.00	2060.00	1960.00	410.00	0.786
	Bark	0.2918	-0.3508	6080.00	2300.00	23100.00	800.00	0.786
	Branch	0.1209	0.1917	2560.00	1140.00	6900.00	530.00	0.786
	Foliage	0.1274	0.0083	18356.67	8653.33	19093.33	2433.33	0.786
JL	Stem-wood	0.8575	0.0210	590.00	623.33	703.33	180.00	0.544
	Bark	0.2387	-0.3156	3176.67	2686.67	7983.33	516.67	0.544
	Branch	0.2689	-0.1613	2720.00	2006.67	3250.00	380.00	0.544
	Foliage	1.0990	-0.9390	18340.00	7783.33	4286.67	1163.33	0.544

JP	Stem-wood	0.8795	0.0175	678.25	440.00	676.25	135.25	0.454
	Bark	0.2013	-0.3163	2445.00	1280.00	4403.75	405.50	0.454
	Branch	0.0864	0.0289	2953.75	1558.75	2171.25	397.25	0.454
	Foliage	0.4255	-0.6576	11115.00	3862.86	3762.86	893.00	0.454
NS	Stem-wood	0.8174	0.0249	653.50	342.63	942.88	100.63	0.393
	Bark	0.2641	-0.2504	3560.00	2417.50	12948.75	666.25	0.393
	Branch	0.6443	-0.4703	3750.00	2502.86	5851.43	514.29	0.393
	Foliage	3.6451	-1.0856	10525.56	5246.67	10532.22	918.89	0.393
OH	Stem-wood	0.8102	0.0203	1168.37	1030.58	1118.82	230.36	0.617
	Bark	0.2242	-0.1530	4885.23	2258.85	16501.63	631.04	0.617
	Branch	0.1553	0.1308	3597.06	1935.60	5860.87	566.03	0.617
	Foliage	0.3628	-0.7270	20639.73	9113.51	10093.33	2373.26	0.617
OS	Stem-wood	0.8318	0.0192	647.91	431.80	701.99	125.93	0.417
	Bark	0.2080	-0.1776	2828.86	1600.03	6871.86	459.17	0.417
	Branch	0.2003	-0.0819	2889.91	1571.86	3539.43	417.22	0.417
	Foliage	1.1053	-0.7474	10713.84	4547.54	5064.68	892.70	0.417
TA	Stem-wood	0.7881	0.0136	1298.24	1118.64	2238.96	342.84	0.424
	Bark	0.2188	-0.0665	4497.19	2630.69	12037.58	1053.08	0.424
	Branch	0.1042	0.0600	5046.43	2767.29	9736.04	1156.43	0.424
	Foliage	0.3400	-0.8310	21136.12	7812.78	10599.28	2082.16	0.424
RM	Stem-wood	0.8281	0.0226	885.00	802.60	1120.50	204.20	0.586
	Bark	0.2377	-0.2329	4331.67	1985.00	13015.71	468.33	0.586
	Branch	0.1429	0.1624	3091.82	1704.44	4655.10	421.25	0.586
	Foliage	0.4206	-0.8024	16958.11	6826.88	7637.56	2040.74	0.586
RO	Stem-wood	0.8253	0.0089	1256.67	1093.33	556.67	56.67	0.655
	Bark	0.1793	-0.0536	3957.50	1290.00	24273.33	380.00	0.655
	Branch	0.0400	0.6263	3696.00	2520.00	9020.00	663.33	0.655
	Foliage	0.1755	-0.4787	21250.37	9757.14	6996.67	1727.65	0.655
RP	Stem-wood	0.8261	0.0155	819.67	236.69	1090.19	193.08	0.419
	Bark	0.1928	-0.1161	3100.37	877.69	7747.69	459.27	0.419
	Branch	0.1010	0.1959	3288.15	961.54	5488.46	492.50	0.419
	Foliage	0.1136	-0.4745	11504.36	3634.74	4198.16	877.37	0.419
RS	Stem-wood	0.8458	0.0172	640.00	220.00	690.00	96.00	0.425
	Bark	0.1881	-0.1734	2773.33	1635.00	6685.00	445.00	0.425
	Branch	0.0043	1.0108	2738.33	1825.56	3381.11	442.22	0.425
	Foliage	0.0564	0.1571	10186.88	5445.63	4083.75	970.00	0.425
SM	Stem-wood	0.7962	0.0328	976.25	691.28	1300.89	198.26	0.702
	Bark	0.3820	-0.3560	5113.75	3118.89	22280.20	600.00	0.702
	Branch	0.1998	0.0940	3365.00	2101.25	6312.50	390.00	0.702
	Foliage	0.2379	-0.5871	19485.68	7551.48	9337.07	1537.29	0.702
SP	Stem-wood	0.8795	0.0175	678.25	440.00	676.25	135.25	0.454
	Bark	0.2013	-0.3163	2445.00	1280.00	4403.75	405.50	0.454
	Branch	0.0864	0.0289	2953.75	1558.75	2171.25	397.25	0.454
	Foliage	0.4255	-0.6576	11115.00	3862.86	3762.86	893.00	0.454
SS	Stem-wood	0.8458	0.0172	640.00	220.00	690.00	96.00	0.417
	Bark	0.1881	-0.1734	2773.33	1635.00	6685.00	445.00	0.417
	Branch	0.0043	1.0108	2738.33	1825.56	3381.11	442.22	0.417
	Foliage	0.0564	0.1571	10186.88	5445.63	4083.75	970.00	0.417
TH	Stem-wood	0.8561	0.0120	1089.73	729.49	818.59	152.48	0.678
	Bark	0.1575	-0.1088	5560.81	1963.06	21229.22	475.83	0.678
	Branch	0.1190	0.2754	3665.25	1737.81	6040.63	428.96	0.678
	Foliage	0.2739	-0.6327	21466.51	9113.49	8155.47	1845.36	0.678
TL	Stem-wood	0.8575	0.0210	590.00	623.33	703.33	180.00	0.544
	Bark	0.2387	-0.3156	3176.67	2686.67	7983.33	516.67	0.544
	Branch	0.2689	-0.1613	2720.00	2006.67	3250.00	380.00	0.544
	Foliage	1.0990	-0.9390	18340.00	7783.33	4286.67	1163.33	0.544
UC	Stem-wood	0.8302	0.0168	908.14	731.19	910.40	178.14	0.526
	Bark	0.1951	-0.1375	3857.05	1929.44	11686.75	545.10	0.526
	Branch	0.2426	-0.0856	3243.49	1753.73	3539.43	491.62	0.526
	Foliage	0.8091	-0.7814	15676.78	6830.52	7579.00	1632.98	0.526
UH	Stem-wood	0.8102	0.0203	1168.37	1030.58	1118.82	230.36	0.617
	Bark	0.2242	-0.1530	4885.23	2258.85	16501.63	631.04	0.617
	Branch	0.1553	0.1308	3597.06	1935.60	5860.87	566.03	0.617
	Foliage	0.3628	-0.7270	20639.73	9113.51	10093.33	2373.26	0.617

US	Stem-wood	0.8318	0.0192	647.91	431.80	701.99	125.93	0.417
	Bark	0.2080	-0.1776	2828.86	1600.03	6871.86	459.17	0.417
	Branch	0.2003	-0.0819	2889.91	1571.86	3539.43	417.22	0.417
	Foliage	1.1053	-0.7474	10713.84	4547.54	5064.68	892.70	0.417
WB	Stem-wood	0.8234	0.0127	923.76	514.48	774.90	184.81	0.588
	Bark	0.1875	-0.0846	3639.09	1200.91	6846.36	413.18	0.588
	Branch	0.1875	0.0633	3912.50	1594.17	4412.50	533.33	0.588
	Foliage	0.7582	-0.8548	19165.00	8645.33	7222.33	2247.33	0.588
WE	Stem-wood	0.8538	0.0102	1110.00	1005.00	865.00	255.00	0.617
	Bark	0.1550	-0.0843	3265.00	2730.00	8525.00	705.00	0.617
	Branch	0.8516	-0.3876	4075.00	3090.00	7565.00	710.00	0.617
	Foliage	1.5928	-1.2266	24500.00	10250.00	13600.00	3133.33	0.617
WL	Stem-wood	0.8575	0.0210	590.00	623.33	703.33	180.00	0.544
	Bark	0.2387	-0.3156	3176.67	2686.67	7983.33	516.67	0.544
	Branch	0.2689	-0.1613	2720.00	2006.67	3250.00	380.00	0.544
	Foliage	1.0990	-0.9390	18340.00	7783.33	4286.67	1163.33	0.544
WP	Stem-wood	0.8426	0.0085	779.75	323.67	515.50	101.00	0.365
	Bark	0.1623	-0.0586	3544.00	1472.50	4222.50	612.50	0.365
	Branch	0.0473	0.3387	4087.50	1945.71	3034.29	572.86	0.365
	Foliage	0.2400	-0.3249	12779.41	4468.82	2826.67	1154.33	0.365
WS	Stem-wood	0.8174	0.0249	653.50	342.63	942.88	100.63	0.393
	Bark	0.2641	-0.2504	3560.00	2417.50	12948.75	666.25	0.393
	Branch	0.6443	-0.4703	3750.00	2502.86	5851.43	514.29	0.393
	Foliage	3.6451	-1.0856	10525.56	5246.67	10532.22	918.89	0.393
XL	Stem-wood	0.8575	0.0210	590.00	623.33	703.33	180.00	0.544
	Bark	0.2387	-0.3156	3176.67	2686.67	7983.33	516.67	0.544
	Branch	0.2689	-0.1613	2720.00	2006.67	3250.00	380.00	0.544
	Foliage	1.0990	-0.9390	18340.00	7783.33	4286.67	1163.33	0.544
XS	Stem-wood	0.8297	0.0215	635.00	281.00	782.00	116.75	0.435
	Bark	0.2265	-0.2146	2586.67	1588.50	8325.50	500.00	0.435
	Branch	0.0152	0.5888	2665.17	1588.78	3688.56	436.11	0.435
	Foliage	0.1767	-0.2362	9279.27	4841.98	5564.38	931.67	0.435
YB	Stem-wood	0.9169	-0.0090	1026.00	433.33	700.57	155.00	0.649
	Bark	0.0911	0.0816	5672.00	1243.33	10283.33	423.33	0.649
	Branch	0.1447	0.2385	4600.00	1130.00	4130.00	362.50	0.649
	Foliage	0.5310	-0.7686	23490.00	10240.71	9624.29	2557.50	0.649

VITA

Candidate's Full Name:	Joshua Daniel Noseworthy
Place and Date of Birth:	Saint John, New Brunswick, August 7, 1986
Universities Attended:	University of New Brunswick, Fredericton, Canada. Bachelor of Science in Forestry (BScF) 2007 - 2009 University of New Brunswick, Fredericton, Canada. Master of Science in Forestry (candidate) 2009 - 2011